การแยกและการวิเคราะห์ส่วนประกอบทางเคมีของสารที่ออกฤทธิ์ทางชีวภาพจากรากต้นชงโค (*Bauhinia saccocalyx* Pierre) และต้นกันเกรา (*Fagraea fragrans* Roxb.)

นางสาวสำเนียง อภิสันติยาคม

วิทยานิพนธ์นี้เป็นส่วนหนึ่งของการศึกษาตามหลักสูตรปริญญาวิทยาศาสตรดุษฎีบัณฑิต
สาขาวิชาเคมี
มหาวิทยาลัยเทคโนโลยีสุรนารี
ปีการศึกษา 2547
ISBN 974-533-373-5

ISOLATION AND IDENTIFICATION OF BIOACTIVE CHEMICAL CONSTITUENTS OF THE ROOTS OF *BAUHINIA SACCOCALYX* PIERRE AND *FAGRAEA FRAGRANS* ROXB.

Miss Samneang Apisantiyakom

A Thesis Submitted in Partial Fulfillment of the Requirements for the Degree of Doctor of Philosophy in Chemistry

Suranaree University of Technology

Academic Year 2004

ISBN 974-533-373-5

ISOLATION AND IDENTIFICATION OF BIOACTIVE CHEMICAL CONSTITUENTS OF THE ROOTS OF *BAUHINIA SACCOCALYX* PIERRE AND *FAGRAEA FRAGRANS* ROXB.

Suranaree University of Technology has approved this thesis submitted in partial fulfillment of the requirements for the Degree of Doctor of Philosophy.

Thesis Examining Committee

(Asst. Prof. Dr.Malee Tangsathitkulchai)

Chairperson

(Asst. Prof. Dr.Thanaporn Manyum)

Member (Thesis Advisor)

(Dr.Prasat Kittakoop)

Member

(Assoc. Prof. Dr.Saowanee Rattanaphani)

Member

(Dr.Pichaya Trakanrungroj)

Member

(Assoc. Prof. Dr.Sarawut Sujitjorn)

Vice Rector for Academic Affairs

(Assoc. Prof. Dr.Prasart Suebka)

Dean of Institute of Science

สำเนียง อภิสันติยาคม : การแยกและการวิเคราะห์ส่วนประกอบทางเคมีของสารที่ออกฤทธิ์ทางชีวภาพจากรากต้นชงโค (*Bauhinia saccocalyx* Pierre) และต้นกันเกรา (*Fagraea fragrans* Roxb.) (IDENTIFICATION OF BIOACTIVE CHEMICAL CONSTITUENTS OF THE ROOTS OF *BAUHINIA SACCOCALYX* PIERRE AND *FAGRAEA FRAGRANS* ROXB.) อาจารย์ที่ปรึกษา : ผู้ช่วยศาสตราจารย์ ดร.ธนพร แม่นยำ, 175 หน้า. ISBN 974-533-373-5

การแยกสารจากรากต้นชงโค (*Bauhinia saccocalyx* Pierre) สามารถแยกสารจำพวกไบเบนซิลซึ่งเป็นสารใหม่ได้ 4 ชนิด คือ บัวฮินอลเอ-ดี (**I-IV**) และสารที่มีการรายงานแล้ว 4 ชนิด ได้แก่ไบเบนซิล **V** และ **VI**, บัวฮิโนซิพินเอ (**VII**) และบัวฮิโนซิพินบี (**VIII**) โดยพบว่าบัวฮินอลเอ (**I**) มีฤทธิ์ยับยั้งการเจริญเติบโตของเซลล์มะเร็งปอด มะเร็งเต้านม และมะเร็งช่องปากอย่างมีนัยสำคัญด้วยค่าไอซี 50 เท่ากับ 3.4, 2.7 และ 4.5 ไมโครกรัมต่อมิลลิลิตรตามลำดับ บัวฮินอลบี (**II**) มีฤทธิ์ยับยั้งการเจริญเติบโตของเซลล์มะเร็งปอด (ค่าไอซี 50 เท่ากับ 1.1 ไมโครกรัมต่อมิลลิลิตร) และมะเร็งเต้านม (ค่าไอซี 50 เท่ากับ 9.7 ไมโครกรัมต่อมิลลิลิตร) แต่ไม่มีฤทธิ์ยับยั้งการเจริญเติบโตของเซลล์มะเร็งช่องปาก (ที่ระดับความเข้มข้น 20 ไมโครกรัมต่อมิลลิลิตร) ไบเบนซิล **VI** มีฤทธิ์ยับยั้งการเจริญเติบโตของเซลล์มะเร็งปอด (ค่าไอซี 50 เท่ากับ 14.1 ไมโครกรัมต่อมิลลิลิตร) และมะเร็งเต้านม (ค่าไอซี 50 เท่ากับ 4.0 ไมโครกรัมต่อมิลลิลิตร) แต่ไม่มีฤทธิ์ยับยั้ง (ที่ระดับความเข้มข้น 20 ไมโครกรัมต่อมิลลิลิตร) การเจริญเติบโตของเซลล์มะเร็งช่องปาก นอกจากนี้ สาร **I**, **II** และ **VI** ยังมีฤทธิ์ต้านเชื้อวัณโรคอย่างอ่อน ด้วยค่าเอ็มไอซีเท่ากับ 50, 25 และ 50 ไมโครกรัมต่อมิลลิลิตรตามลำดับ แต่ไม่มีฤทธิ์ (ที่ระดับความเข้มข้น 20 ไมโครกรัมต่อมิลลิลิตร) ต้านเชื้อมาลาเรียสายพันธุ์เค 1 (*Plasmodium falciparum*) โดยสาร **II** และ **VI** มีฤทธิ์ยับยั้งการเจริญเติบโตของเชื้อรา *Candia albicans* ในระดับอ่อนด้วย (ค่าไอซี 50 เท่ากับ 28.9 และ 11.7 ไมโครกรัมต่อมิลลิลิตรตามลำดับ) ในขณะที่สาร **I** ไม่มีฤทธิ์ต้านการอักเสบโดยยับยั้งการทำงานของเอนไซม์ไซโคลออกซิเจเนส 1 (COX-1) และไซโคลออกซิเจเนส 2 (COX-2) สาร **II** และ **VI** มีฤทธิ์ยับยั้งการทำงานของเอนไซม์ทั้งสองชนิดนี้ ด้วยค่าไอซี 50 ใกล้เคียงกับยาแอสไพรินซึ่งใช้เป็นสารมาตรฐานด้วย

ในส่วนของต้นกันเกรา (*Fagraea fragrans* Roxb.) สามารถแยกสารที่มีการรายงานแล้ว 4 ชนิด ได้แก่ไพนอเรซินอล (**IX**), นัวคลิดอล (**X**), เจนติโอจินอล (**XI**), และสเวอโรไซด์ (**XII**) จากส่วนของเปลือกลำต้น, ราก, ผลไม้ และลำต้นตามลำดับ โดยพบว่าสาร **IX** มีฤทธิ์ต้านเชื้อ

ปอด (ค่าไอซี 50 เท่ากับ 18.94 และ 5.06 ไมโครกรัมต่อมิลลิลิตรตามลำดับ) และมีฤทธิ์ต้านเชื้อวัณโรคอย่างอ่อน (ค่าเอ็มไอซีเท่ากับ 200 และ 50 ไมโครกรัมต่อมิลลิลิตรตามลำดับ) แต่ไม่มีฤทธิ์ยับยั้งการเจริญเติบโตของเซลล์มะเร็งเต้านมและมะเร็งช่องปาก และไม่มีฤทธิ์ต้านเชื้อมาลาเรียสายพันธุ์เค 1 (ที่ระดับความเข้มข้น 20 ไมโครกรัมต่อมิลลิลิตร) สาร **XII** มีฤทธิ์ต้านเชื้อไวรัสที่ก่อให้เกิดโรคเริม (เปอร์เซ็นต์การยับยั้งไม่น้อยกว่า 35-50% ที่ระดับไอซี 50 เท่ากับ 1.2 ± 0.3 ไมโครกรัมต่อมิลลิลิตร)

การพิสูจน์โครงสร้างทางเคมีของสารทั้ง 12 ชนิด ใช้วิธีวิเคราะห์ข้อมูลทางสเปกโทรสโกปี

สาขาวิชาเคมี
ปีการศึกษา 2547

ลายมือชื่อนักศึกษา _____
ลายมือชื่ออาจารย์ที่ปรึกษา _____
ลายมือชื่ออาจารย์ที่ปรึกษาร่วม _____
ลายมือชื่ออาจารย์ที่ปรึกษาร่วม _____

SAMNEANG APISANTIYAKOM : ISOLATION AND IDENTIFICATION OF BIOACTIVE CHEMICAL CONSTITUENTS OF THE ROOTS OF *BAUHINIA SACCOCALYX* PIERRE AND *FAGRAEA FRAGRANS* ROXB.
THESIS ADVISOR : ASST. PROF. THANAPORN MANYUM, Ph.D.
175 PP. ISBN 974-533-373-5

BAUHINIA SACCOCALYX/*FAGRAEA FRAGRANS*/BIBENZYL/CYTOTOXICITY ANTIFUNGAL/ANTIMYCOBACTERIAL

Four new bibenzyls, bauhinols A-D (**I-IV**), together with four known compounds, bibenzyls **V** and **VI**, bauhinoxepin A (**VII**), and bauhinoxepin B (**VIII**) were isolated from the roots of *Bauhinia saccocalyx*. Bauhinol A (**I**) exhibits significant cytotoxicity towards NCI-H187 (small-cell lung cancer), BC (breast cancer), and KB (oral-cavity cancer) cell lines, with IC_{50} values of 3.4, 2.7, and 4.5 μg/mL, respectively. Bauhinol B (**II**) is cytotoxic against NCI-H187 (IC_{50} = 1.1 μg/mL) and BC (IC_{50} = 9.7 μg/mL) cell lines, but inactive towards the KB cell line (at 20 μg/mL). Bibenzyl **VI** is active against NCI-H187 (IC_{50} = 14.1 μg/mL) and BC (IC_{50} = 4.0 μg/mL) cells, but inactive (at 20 μg/mL) towards the KB cell line. Compounds **I**, **II**, and **VI** show mild antimycobacterial activities, with MIC values of 50, 25, and 25 μg/mL, respectively, but are inactive (at 20 μg/mL) against K1 malarial parasite strain (*Plasmodium falciparum*). Compound **II** and **VI** also demonstrates mild antifungal activities towards *Candia albicans* (IC_{50} = 28.9 and 11.7 μg/mL, respectively). While compound **I** is inactive against cyclooxygenase 1 (COX-1) and

Four known compounds, pinoresinol (**IX**), naucledal (**X**), gentiogenal (**XI**), and sweroside (**XII**) were isolated from the stem bark, roots, fruits, and stems of *Fagraea fragrans* Roxb., respectively. Compound **IX** possesses antimalarial activity against *Plasmodium falciparum* (K1 strain), with IC_{50} value of 3.4 μg/mL, and antitubercular activity against *Mycobacterium tuberculosis* (H37Ra), with MIC value of 200 μg/mL. Compounds **X** and **XI** exhibit cytotoxicity towards NCI-H187 cell line (IC_{50} values of 18.94 and 5.06 μg/mL, respectively) and also demonstrate mild antitubercular activity (MIC = 200 and 50 μg/mL, respectively). However, compounds **X** and **XI** are inactive towards the KB and BC cell lines, and inactive against K1 malarial parasite strain (at 20 μg/mL). Compound **XII** demonstrates mild anti-HSV-1 (Herpes simplex virus type 1) activity (% inhibition ≥ 35-50% at IC_{50} = 1.2 ± 0.3 μg/mL).

Chemical structures of these isolated compounds were elucidated by analyses of spectroscopic data.

School of Chemistry

Academic Year 2004

Student's Signature Samreang. Apisantiyakom.

Advisor's Signature T. Mayuo

Co-advisor's Signature

Co-advisor's Signature J.B Brenner

ACKNOWLEDGEMENTS

I wish to thank Asst. Prof. Dr. Thanaporn Manyum and my co-advisor, Prof. Dr. John B. Bremner and Dr. Prasat Kittakoop, for their kind instructions and many helpful suggestions. I also wish to express my appreciation to Prof. Dr. Yodhathai Thebtaranonth, Assoc. Prof. Dr. Saowanee Rattanaphani, and Dr. Kanyawin Kitikara, and the thesis examining commitee for their kind guidance. A large debt of gratitude is owed to Dr. Sumalee Kamchonwongpaisan for her kind suggestions and inspiration, which led me to the success in this research.

I wish to acknowledge the National Center for Genetic Engineering and Biotechnology (BIOTEC), National Science and Technology Development Agency (NSTDA) for providing all research facilities. Special thanks are due to the BIOTEC staff, in particular, Dr. Pattama Pittayakhajonwut for chemical structure drawing, Miss Arun Glahtyou for her assistance of NMR spectroscopic service, Mr. Sutichai Intamas for MS analysis, Mr. Aibrohim Drama for *F. fragrans* IR spectral data, Miss Panarat Charoenchai for plant identification, and Mr. Somporn Palasarn for many helps, the staff of the School of Chemistry, Suranaree University of Technology, and all my friends for their care and best wishes. I also thank the Biodiversity Research and Training Program (BRT) for financial support (grant no. BRT643003) and Suranaree University of Technology for financial support for thesis research.

Finally, I am deeply indebted to my family for their encouragement, support, understanding, patience, care and love.

Samneang Apisantiyakom

CONTENTS

Page

CONTENTS (Continued)

Page

CONTENTS (Continued)

Page

CONTENTS (Continued)

Page

LIST OF TABLES

LIST OF TABLES (Continued)

Table Page

LIST OF SCHEMES AND FIGURES

Scheme Page

Figure

LIST OF SCHEMES AND FIGURES (Continued)

LIST OF SCHEMES AND FIGURES (Continued)

LIST OF SCHEMES AND FIGURES (Continued)

Scheme Page

LIST OF SCHEMES AND FIGURES (Continued)

Scheme Page

LIST OF SCHEMES AND FIGURES (Continued)

Scheme Page

LIST OF SCHEMES AND FIGURES (Continued)

Scheme Page

LIST OF ABBREVIATIONS

br	broad
c	concentration in grams per 100 milliliter
^{o}C	degree Celsius
$CDCl_3$	chloroform-d_1
CFU/mL	colony-forming unit per milliliter
CH_2Cl_2	dichloromethane
cm	centimeter
cm^{-1}	wave number unit
COSY	correlation spectroscopy
d	doublet
dd	doublet of doublets
DEPT	distortionless enhancement by polarization transfer
dq	doublet of quartets
ESI-TOF	electrospray ionization-time of flight
Fig.	figure
Figs.	figures
g	gram
g/mL	gram per milliliter
HMBC	heteronuclear multiple bond correlation
HMQC	heteronuclear multiple quantum coherence
HPLC	high performance liquid chromatography

LIST OF ABBREVIATIONS (Continued)

Hz	hertz
IC_{50}	50% inhibitory concentration
IR	infrared spectroscopy
J	coupling constant in hertz
kg	kilogram
l	length
L	liter
m	multiplet
m/z	a value of mass divided by charge
MeOH	methanol
mg	milligram
mg/kg	milligram per kilogram
MHz	megahertz
MIC	minimum inhibitory concentration
nm	nanometer
NMR	nuclear magnetic resonance spectroscopy
NOESY	nuclear overhauser effect spectroscopy
ppm	parts per million
q	quartet
qd	quartet of doublets
s	singlet
t	triplet

LIST OF ABBREVIATIONS (Continued)

td	triplet of doublets
TLC	thin-layer chromatography
UV	ultraviolet radiation
UV-Vis	ultraviolet-visible radiation
v/v	volume by volume
$[\alpha]_D^t$	specific rotation
δ	chemical shift in ppm
ε	molar absorptivity in liter per mole per centimeter
Φ	diameter
λ_{max}	maximum absorption wavelength
μCi	microcurie
μg/mL	microgram per milliliter
μL	microliter
ν_{max}	maximum absorption wavenumber

CHAPTER I

INTRODUCTION

1.1 *Bauhinia saccocalyx* Pierre

B. saccocalyx Pierre is a plant in Leguminosae-Caesalpiniodeae family. The genus *Bauhinia* is one of the largest genera in Leguminosae-Caesalpiniodeae family, and is distributed throughout most tropical and subtropical countries. It is also distributed in many parts of Thailand such as Northern: Nakorn Sawan, Nan, Phrae; Northeastern: Khon Kaen, Loei, Phetchabun, Sakon Nakhon, Udon Thani; Eastern: Chaiyaphum, Nakhon Ratchasima, Ubon Ratchathani; Central: Lop Buri, Saraburi; Southwestern: Kanchanaburi, Ratchaburi, Uthai Thani (Smitinand and Lasen, 1984).

Thirty five species of plants in the genus *Bauhinia* are found in Thailand as follows: (Smitinand, 2001)

1. *B. acuminata* L. กาแจ๊ะกูโด Ka-chae-ku-do (Malay-Narathiwat); กาหลง Kalong, ส้มเสี้ยว Som siao (Central); โยธิกา Yo thi ka (Nakhon Si Thammarat); เสี้ยวน้อย Siao noi (Chiang Mai).
2. *B. aureifolia* K. & S. S. Larsen ใบสีทอง Bai si thong, ย่านดาโอ๊ะ Yan da o (Narathiwat).

3. *B. bassacensis* Pierre ex Gagnep. เครือเขาหนัง Khruea khao nang (Lampang);
ชงโค Chong kho, โยธิกา Yo thi ka (Peninsular);
เถากระไดลิง Thao kradai ling (Southeastern)

4. *B. bidentata* Jack ชงโคป่าดอกแดง Chong kho pa dok daeng (Peninsular);
(*B. bicornuta* (Miq.) K. & S. S. Larsen) เล็บกระรอก Lep krarok (Pattani);
เล็บควายเล็ก Lep khwai lek (Yala).

5. *B. binata* Blanco แสลงพัน Salaeng phan (Chonburi).

6. *B. bracteata* (Graham ex Benth.) Baker ปอแก้ว Po-kaeo (Karen-Northern);
ปอเจี๋ยน Po chian (Northern);
ปอบุ้ง Po bung (Chiang Mai);
เสี้ยวเครือ Siao khruea (Nakhon Ratchasima);
เสี้ยวดอกขาว Siao dok khao, เสี้ยวเตี้ย Siao tia (Loei);
เสี้ยวส้ม Siao som (Uthai Thani, Sakhon Nakhon);
แสลงพัน Salaeng phan (Chonburi).

7. *B. curtisii* Prain เครือเขาแกบ Khruea khao kaep (Northeastern).

8. *B. ferruginea* Roxb. ย่านตีนควาย Yan tin khwai (Narathiwat).

9. *B. glauca* (Wall. ex Benth.) Benth.

(*B. glauca*) ชงโค Chong kho (Peninsular).

(*B. tenuiflora* (Watt ex C. B. Clarke) K. & S. S. Larsen)

คางโค Khang kho (Chantaburi);

พาซิว Pha-sio (Karen-Lampang);

เสี้ยวเครือ Siao khruea (Chiang Mai, Lampang);

เสี้ยวต้น Siao ton (Nan);

เสี้ยวป่า Siao pa (Chiang Mai).

10. *B. harmsiana* Hosseus ชงโคขี้ไก่ Chong kho khi kai (Kanchanaburi);

เสี้ยว Siao (Phrae); เสี้ยวเคือ Siao khuea (Lamphun).

11. *B. hirsuta* Weinm. วุ้งพู Wung-phu (Karen-Mae Hong Son);

เสี้ยวน้อย Siao noi (Northern).

12. *B. integrifolia* Roxb. กุกูกูด้อ Ku-ku-ku-do,

กุกูกูบา Ku-ku-ku-ba (Malay-Pattani);

ชงโคย่าน Chong kho yan (Peninsular);

ดาโอะ Da o (Narathiwat);

เถาไฟ Thao fai, โยทะกา Yo thaka (Bangkok);

ปอลิง Po ling (Surat Thani);

เล็บควายใหญ่ Lep khwai yai (Pattani).

13. *B. involucellata* Kurz แสลงพัน Salaeng phan (Kanchanaburi, Saraburi).

14. *B. lakhonensis* Gagnep. ส้มเสี้ยวเถา Som siao thao (Northeastern).

15. *B. malabarica* Roxb. คังโค Khang kho (Suphan Buri);

แดงโค Dang kho (Saraburi);

ป้าม Pam (Suai –Surin); ส้มเสี้ยว Som siao (Northern);

เสี้ยวส้ม Siao som (Nakhon Ratchasima);

เสี้ยวใหญ่ Siao yai (Prachin Buri).

16. *B. monandra* Kurz จงโค Chong kho, โยทะกา Yo thaka (Bangkok).

17. *B. nervosa* (Wall. ex Benth.) Baker เสี้ยวแก้ว Siao kaeo (General).

18. *B. ornata* Kurz กวาวขน Kwao khon, ปอมุ้ง Po mung (Chiang Mai);

var. *B. kerrii* (Gagnep.) K. & S. S. Larsen

โคคลาน Kho khlan (Prachuap Khiri Khan);

ปอมุ้ง Po mung (Chiang Mai);

เสี้ยว Siao, ชงโค Chong kho (Phrae);

เสี้ยวเครือ Siao khruea (Sukhothai);

แสลงพันแดง Salaeng phan daeng (Loei, Lop Buri).

var. *B. burmanica* K. & S. S. Larsen ปอเกี๋ยน Po kian (Northern).

19. B. *penicilliloba* Pierre ex Gagnep. เสี้ยวแดง Siao daeng (Loei).

(*B. tenuiflora* (Watt ex C. B. Clarke) K. & S. S. Laren)

20. *B. pottsii* G. Don ชิงโค Ching kho (Ranong, Surat Thani);

var. *pottsii* ชงโคดำ Chong kho dam (Trang).

var. *decipiens* (Craib) K. & S. S. Larsen ชงโค Chong kho (Trat).

var. *mollissima* (Wall. ex Prain) K. & S. S. Larsen

ชงโคไฟ Chong kho fai (Peninsular).

var. *subsessilis* (Craib) de Wit ชงโคขาว Chong kho khao (Central);

ชงโคป่า Chong kho pa (Chanthaburi);

ชั่งโค Chang kho (Trat);

ชิงโค Ching kho, ส้มเสี้ยว Som siao (Surat Thani);

ชุมโค Chum kho (Chumphon).

var. *velutina* (Wall. ex Benth.) K. & S. S. Larsen ชงโค Chong kho (Ranong).

21. *B. pulla* Craib กาหลง Kalong,

แสลงพันเถา Salaeng phan thao (Nakhon Sawan);

แสลงพัน Salaeng phan (Nakhon Ratchasima).

22. *B. purpurea* L. กะเฮอ Ka-heo,

สะเปซี Sa-pe-si (Karen-Mae Hong Son);

ชงโค Chong kho (Central);

เสี้ยวดอกแดง Siao dok daeng (Northern);

เสี้ยวหวาน Siao wan (Mae Hong Son);

23 *B. racemosa* Lam. ชงโคขี้ไก่ Chong kho khi kai (Kanchanaburi);

ชงโคนา Chong kho na,

ชงโคใบเล็ก Chong kho bai lek (Ratchaburi);

ชงโคเล็ก Chong kho lek (Saraburi);

ส้มเสี้ยว Som saio (Lampang);

เสี้ยว Saio (Northern);

เสี้ยวใหญ่ Saio yai (Prachin Buri).

24. *B. saccocalyx* Pierre คิงโค Khing kho (Nakhon Ratchasima);

ชงโค Chong kho (Chanthaburi, Nakhon Rachasima,

Suphan Buri, Uthai Thani);

ส้มเสี้ยว Som siao (Nakhon Sawan, Udon Thani);

ส้มเสี้ยวโพะ Som siao po,

ส้มดอกขาว Siao dok khao (Loei); เสี้ยวป่า Siao pa (Nan).

25. *B. scandens.* L. กระไดลิง Kradai ling (Ratchaburi);

var. *horsfieldii* (Miq.) K. & S. S. Larsen กระไดวอก Kradai wok (Northern);

โชกนุ้ย Chok-nui (Chaobon-Chaiyaphum);

มะลืมดำ Ma luem dam (Chiang Mai).

26. *B. sirindhorniae* K. & S. S. Larsen

สามสิบสองประดง Sam sip song pra dong (Nong khai);

สิรินธรวัลลี Sirinthon wanli (Bangkok).

27. *B. similis* Craib แสลงพันกระดูก Salaeng phan kraduk (Kanchanaburi).

28. *B. strychnifolia* Craib ขยัน Khayan, เครือขยัน Khruea khayan (Northern);

สยาน Sayan (Tak, Lampang);

หญ้านางแดง Ya nang daeng (Northeastern).

29. *B. strychnoidea* Prain โชคนุ้ย Chok nui (Narathiwat).

30. *B. tomentosa* L. ชงโคดอกเหลือง Chong kho dok lueang (Bangkok).

31. *B. variegata* L. เปียงพะโก Piang phako (Sukhothai);

โพะเพ่ Pho-phe (Karen-Kanchanaburi);

เสี้ยวดอกขาว Siao dok khao (Northern);

นางอั้ว Nang ua (Chiang Mai).

32. *B. viridescens* Desv. บะหมะคอหมี Ba-ma-kho-mi (Karen-Kanchanaburi);

var. *viridescens* ส้มเสี้ยวน้อย Som siao noi (Prachin Buri);

ส้มเสี้ยวใบบาง Som siao bai bang (Prachuap Khiri Khan);

เสี้ยวเคี้ยว Siao khiao (Loei);

เสี้ยวน้อย Siao noi, เสี้ยวป๊อก Siao pok (Phrae);

เสี้ยวฟ่อม Siao form (Northern).

var. *hirsuta* K. & S. S. Larsen กาหลงเขา Kalong khao (Kanchanaburi).

33. *B. wallichii* J. F. Macbr. ชงโคภูคา Chong kho phuka (Nan).

34. *B. winitii* Craib คิ้วนาง Khio nang, อรพิม Ora phim (Central).

35. *B. yunnanensis* Franch. เสี้ยวแพะ Siao phae (Lampang);

หญ้าเกล็ดปลามง Ya-klet-pla-mong (Shan-Northern).

Previous study revealed that a crude CH_2Cl_2 root extract of *B. saccocalyx* exhibits antimalarial (IC_{50} value of 5.0 μg/mL) and antimycobacterial (MIC at 25 μg/mL) activities. Two new antimycobacterial dibenzo[b,f]oxepins, bauhinoxepin A and bauhinoxepin B were previously isolated and characterized (Kittakoop, Nonpichai, Thongon, Charoenchai, and Thebtaranonth, 2004).

In the present study, compositions of minor metabolites in *B. saccocalyx* were explored. Biological activities of the metabolites isolated were also evaluated.

1.2 *Fagraea fragrans* Roxb.

F. fragrans Roxb. is a plant in the Potaliaceae family (Wongsatit, C., et al., 1996). This plant grows abundantly in Southeast Asia, for example, Singapore and Malaysia. It is known locally as Tammusu (or Temmusu). It also grows sparsely in southern and northeastern parts of Thailand, where it is called Kankrao (Central), Tamsao or Thamsao (Southern) and Man Pla (Northern and Northeastern).

There are 8 species of plants in the genus *Fagraea* found in Thailand as follows: (Smitinand, T., 2001).

1. *F. acuminatissima* Merr. ชะบาไพร Chaba phrai (Narathiwat).
2. *F. auriculata* Jack เทียนฤาษี Thian ruesi (Northern); ชะบาช้าง Chaba chang (Narathiwat).
3. *F. carnosa* Jack เนียมฤาษี Niam ruesi (Northern).
4. *F. ceilanica* Thumb. โกงกางเขา Kongkang khao (Chanthaburi); ตังติดนก Tang tit nok (Nong Khai);

นางสวรรค์ Nang sawan,

นิ้วนางสวรรค์ Nio nang sawan (Peninsular);

ฝ่ามือผี Fa-mue-phi (Mae Hong Son);

โพดา Phoda (Pattani).

5. *F. crenulata* Maingar ex C. B. Clark เนียมฤาษี Niam ruesi,

หลุมปัง Lum pang,

ลิงอกาเยาะ Li-ngo-ka-yo (Malay-Narathiwat);

หูช้าง Hu chang (Narathiwat).

6. *F. fragrans* Roxb. กันเกรา Kan krao (Central);

ตะมะซู Ta-ma-su,

ตำมูซู Tam-mu-su (Malay-Peninsular);

ตาเตรา Ta-trao (Khmer-Eastern);

ตำเสา Tam sao, ทำเสา Tham sao (Peninsular);

มันปลา Man pla (Northern, Northeastern).

7. *F. racemosa* Jack ตะเคียนเต่า Ta Khian thao (Trat);

ทุ่มบก Thum bok (Nakhon Si Thammarat);

พวาน้ำ Phawa nam (Chumphon, Pattani);

ทุ่มบก Thum bok, หว้าน้ำ Wa num (Peninsular);

ปูเละ Pu-le (Malay-Narathiwat).

8. *F. tubulosa* Blume — ชะบาป่า Chaba pa (Narathiwat);

นาฆอฮูแต Na-kho-hu-tae,

ปือนา Pue-na (Malay-Narathiwat).

F. fragrans grows in watery ground and sunny locations, but slowly. Most of them were lopped and it is almost absent from the forests of Thailand. There are not many Thais who know about this plant, especially amongst the younger generation. Furthermore, very little has been known about the chemical constituents of this plant, compared to others since 1964.

A preliminary test by thin layer chromatography [stationary phase was silica gel 60, and mobile phase was $CHCl_3$: EtOH (85 : 15 v/v)] of crude extracts from hexane, followed by chloroform and ethanol of the stem bark, roots, and leaves showed many spots that luminesced under UV at 254 nm and 366 nm. This indicates the presence of many compounds with various polarities. It may be of value to pursue, isolate and purify. Finally, this may lead to obtaining more complete information on the chemical constituents of *F. fragrans.*

So far research on 5 species of the genus *Fagraea* found in Thailand, including *F. acuminatissima* Merr., *F. carnosa* Jack, *F. ceilanica* Thumb., *F. crenulata* Maingar ex C. B. Clark, and *F. tubulosa* Blume, has not been carried out. In

the present study, *F. fragrans* Roxb. were chemically investigated, and its metabolites were also tested for biological activities.

1.3 Research objectives

1.3.1 To isolate and identify chemical constituents from the roots of *B. saccocalyx* as well as from the leaves, roots, stem bark, stems, flowers and fruits of *F. fragrans.*

1.3.2 To investigate biological activities of the isolated compounds from both *B. saccocalyx* and *F. fragrans.*

1.4 Research hypothesis

1.4.1 New bioactive compounds may be isolated from the roots of *B. saccocalyx,* as well as from the leaves, roots, stem bark, stems, flowers and fruits of *F. fragrans.*

1.4.2 The alcoholic extract from stem wood of *F. fragrans* inhibits the growth of *Plasmodium falciparum in vitro*. Therefore, the extract from the leaves, roots, and stem bark may give a positive test result.

1.4.3 Previous work on *F. fragrans* showed only the isolation of the alkaloid gentianine and of swertisin. Thus, further research may lead to the isolation of various novel alkaloids besides gentianine and other components.

1.5 Scope and limitation of the study

1.5.1 The roots of *B. saccocalyx* were collected in August, 2003, from Nakhon Sawan province, Thailand. The trees are about 20-25 feet high, and not specific in age.

1.5.2 The plant parts of *F. fragrans*, grown in Ubon Ratchathani University, Muang Srikri subdistrict of Warinchamrap district, Ubon Ratchathani province, Thailand, were used for the extraction. The trees are about 30 feet high and not specific in age. The leaves, roots, stems, and stem bark were collected in September, 2002, whereas the flowers and fruits were collected in April, 2003.

1.5.3 The biological activities of the isolated compounds from *B. saccocalyx* and *F. fragrans* were evaluated.

CHAPTER II

HISTORICAL

2.1 Botanical of *Bauhinia saccocalyx* Pierre

B. saccocalyx Pierre is a plant in Leguminosae-Caesalpiniodeae family. It is a small tree or shrub, about 15-30 feet in height. Its leaves are alternate, simple, bipartite, ovate-orbicular, light green glabrous and entire with deeply imarginate apex and 2-2.5 cm long petiole. The tip of leaf lobes is acute and the base is cordate. Axillary and 5-10 cm long inflorescence is in racemose type. Its 2.5 cm × 3.5 cm flower is imperfectly monoecious with 0.3-0.5 cm long pedicel, 5 hairy sepals each splitting into 3, 5 claw petals (0.5-0.6 cm × 1.0-1.2 cm, white, indistinct, and ovate-lanceolate), 10 stamens (white with light yellow anther), and superior ovary comprising of 1 carpel and 1 locule. Its pod is oblong, dehiscent, and woody with round seeds, about 2-3 cm in diameter (http://flora.sut.ac.th, 2004).

2.2 Ethnopharmacology of the plants in the genus *Bauhinia*

The genus *Bauhinia* is one of the largest genera in Leguminosae-Caesalpiniodeae family and is distributed throughout most tropical and subtropical countries. Information from the NAPRALERT database reveals that plants in this genus have been widely used for treatment of diseases, as well as there are many references to laboratory assays for their biological activities. However, the following information will briefly review on the biological activities of the plants in this genus.

B. racemosa Lamk. is found in tropical parts of the world and used in the indigenous system of medicine; for example, a decoction of its leaves has been used in the treatment of headache and malaria, and its bark as an astringent for diarrhea and dysentery in Indian medicine (Anjaneyulu, Raghava Reddy and Reddy,1984).

The aqueous extract of *B. megalandra* leaves is able to inhibit the intestinal glucose absorption in a concentration-dependent way and additive to phlorizine. Moreover, *B. megalandra* leaf extract drastically reduces the ^{14}C-glucose uptake by enterocyte brush border membrane vesicles. The *B. megalandra* leaf extract administrated orally, simultaneously with glucose, improves the glucose tolerance with a significant reduction of the 30-min peak. The extract does not have an effect on the glucose tolerance when glucose is administrated subcutaneously (Gonzalez-Mujica, Motta, Marquez, and Capote-Zulueta, 2003).

B. variegata Linn. is distributed almost through out India. Its powdered bark is traditionally used for tonic, and ulcers. It is also useful for the treatment of skin diseases. The roots are used as antidote to snake poison and also show anti-inflammatory activity (Yadava and Reddy, 2003). Additionally, the ethanol extract from bark of *B. variegata* L. exhibits antimalarial activity with IC_{50} value of 72 µg/mL (Simonsen, et al., 2001).

The $CHCl_3$ extract of *B. tarapotensis* Benth. leaves has been studied by the inhibition of the croton oil-induced ear edema in mice. A bioassay-guided fractionation shows an interesting anti-inflammatory activity. Additionally, the main anti-inflammatory principles of *B. tarapotensis* leaves are triterpenic acids of ursane and oleanane series (Sosa, et al., 2002).

B. forficata is widely used in Brazil folk medicine for the treatment of

Diabetes mellitus. The demonstration of the active component present in *B. forficata* is responsible for its antioxidant effect. However, the increase in hepatic glycogen deserves further investigation (Damasceno, Volpato, Calderon Ide, Aguilar, and Rudge, 2004).

B. rufescens Lam. is a small tree, widely distributed in North and West Africa. Its stem bark and root bark is used for the treatment of leprosy and different kinds of venereal diseases whereas the roots are reputed to cure fever (Dalziel, 1948). Interestingly, the CH_2Cl_2 extract of the root bark shows antifungal activity in a bioassay with the plant pathogenic fungus *Cladosporium cucumerinum* (Maillard, Recio-Iglesias, Saadou, Stoeckli-Evans, and Hostettmann, 1991).

In 1990 Iwagawa and co-workers found that the methanolic extract of the leaves of *B. japonica* has an antibacterial activity against *Escherichia coli* (Iwagawa, et al., 1990).

Furthermore, *B. candicans* Benth., which is an Argentinian medicinal plant species, has hypoglycaemic and hypocholesterolaemic properties (Iribarren and Pomilio, 1987).

2.3 The chemical constituents of the plants in the genus *Bauhinia*

Two new antimycobacterial dibenzo[b,f]oxepins, bauhinoxepin A (**1**) and bauhinoxepin B (**2**), were isolated from the roots of *B. saccocalyx* (Kittakoop, et al., 2004). Racemosol (**3**) and its derivative (**4**), as well as the bibenzyls preracemosol A (**5**) and preracemosol B (**6**) were isolated from the CH_2Cl_2 crude extract of the roots of *B. malabarica* (Kittakoop, Kirtikara, Tanticharoen, and Thebtaranonth, 2000). Racemosol A and its derivative were first isolated from *B. racemosa* and *B. rufescens*

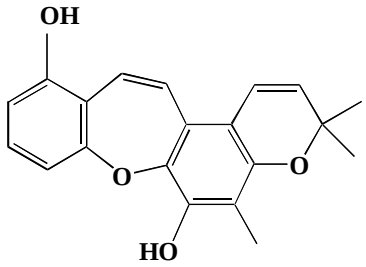

(1) Bauhinoxepin A

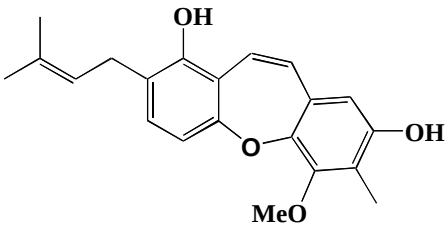

(2) Bauhinoxepin B

(Anjaneyulu, Raghava Reddy, Reddy, Cameron, and Roe, 1986; Maillard, et al., 1991). Compounds **3**-**6** exhibit moderate antimalarial activities with IC_{50} values of 0.9, 2.0, 18.0 and 3.0 µg/mL, respectively. Furthermore, compounds **3** and **4** exhibit cytotoxicity against KB (oral-cavity cancer, IC_{50} at 15.0 µg/mL for **3** and 5.6 µg/mL for **4**) and BC (breast cancer, IC_{50} at 6.1 µg/mL for **3** and 3.6 µg/mL for **4**) cell lines, while compounds **5** and **6** show no cytotoxicity (Kittakoop, et al., 2000).

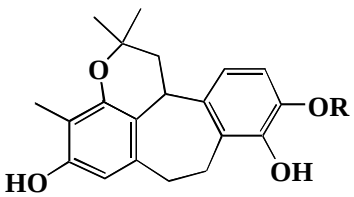

(3) Racemosol, R = Me
(4) De-*O*-methylracemosol, R = H

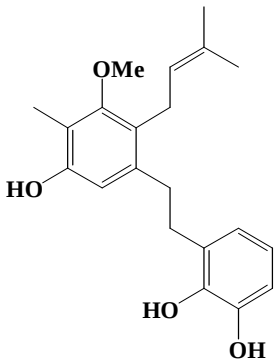

(5) Preracemosol A

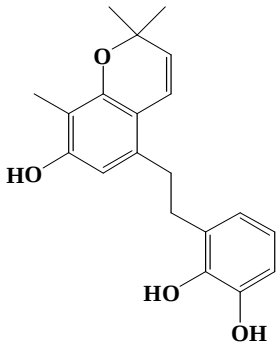

(6) Preracemosol B

In 2003, a novel flavonol glycoside 5,7,3',4'-tetrahydroxy-3-methoxy-7-*O*-*α*-L-rhamnopyranosyl(1→3)-*O*-*β*-galactopyranoside was isolated from the roots of *B. Variegata*, and shows anti-inflammatory activity (Yadava, and Reddy, 2003).

Meyre-Silva and colleagues found that the MeOH crude extract from the leaves of *B. microstachya* exhibits an anagesic activity. Thus three flavonols: afzelin (**7**), myricitrin (**8**), and quercitrin (**9**), together with gallic acid methyl ester (**10**) were isolated (Meyre-Silva, et al., 2001).

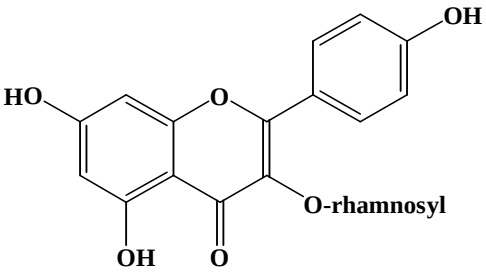

(7) Afzelin

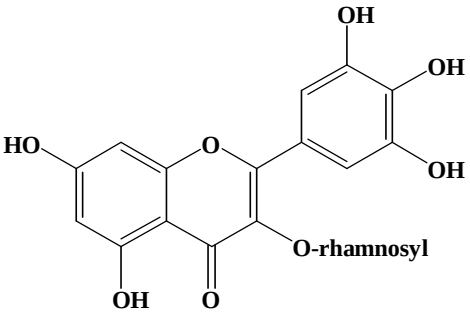

(8) Myricitrin

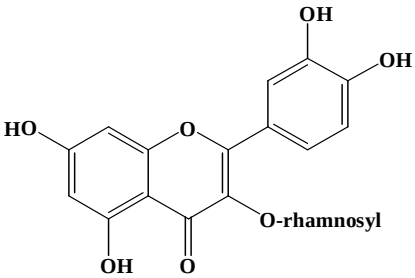

(9) Quercitrin

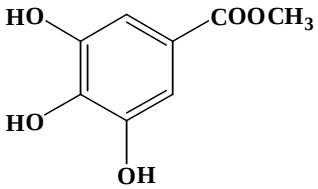

(10) Gallic acid methyl ester

Two phytoconstituents were isolated from the leaves of *B. forficata*, and have been identified as *β*-sitosterol (**11**), and kaempferol-3,7-dirhamnoside (kampferitrin, **12**) (Silva, et al., 2000).

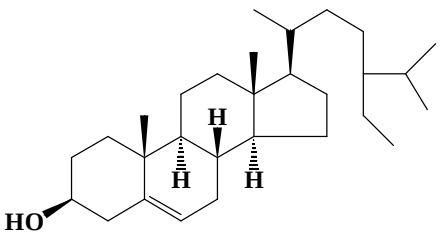

(11) β-Sitosterol

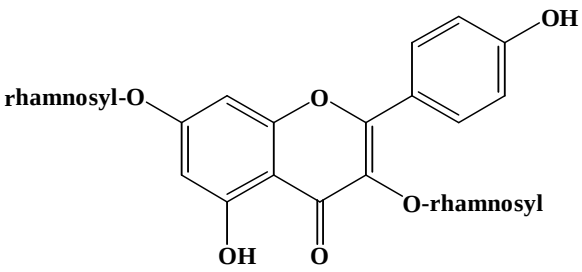

(12) Kaempferitrin

B. purpurea is a popular ornamental plant in Taiwan. In 1998, Kuo and co-workers isolated 6-(3″-oxobutyl)taxifolin (**13**), and three glycerol derivatives: 2,3-dihydroxypropyl oleate, 2,3-dihydroxypropyl linoleate, and 2,3-dihydroxypropyl 16-hydroxyhexadecanoate. However, their biological activities have not been reported (Kuo, Yeh, and Huang, 1998).

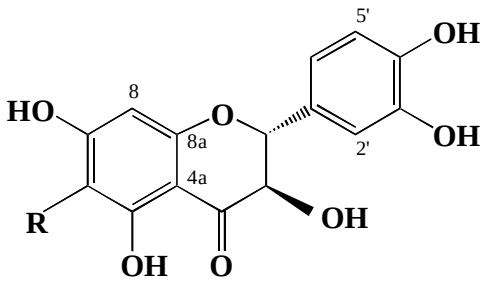

(13) 6-(3"-Oxobutyl)taxifolin R = CH_2–CH_2–C(=O)–CH_3

Tang and co-workers isolated two flavanones taxifolin (**14**) and aromadendrin (**15**) from the roots of *B. hupehana*. However, the biological activities of these two compounds have not been evaluated (Tang, Yuan, Zhang, and Zhou, 1992).

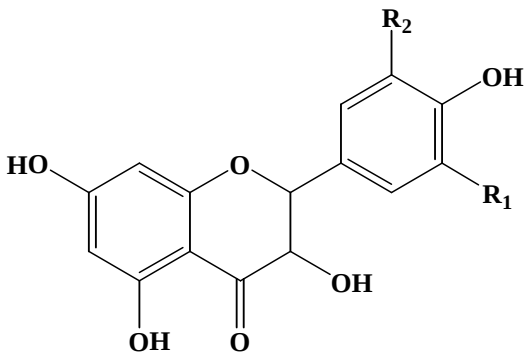

(14) Taxifolin, R_1 = OH, R_2 = H
(15) Aromadendrin, R_1 = R_2 = H

Jagdish Kumar and colleagues isolated phenolic constituents from the pods of Indian plant, *B. vahlii.*, and catechin (**16**) and mopanol (**17**) together with kaempferol

(**18**) from the flowers (Jagdish Kumar, Krupadanam, and Srimannarayana, 1990).

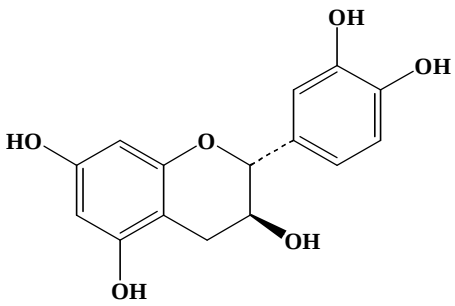

(16) Catechin

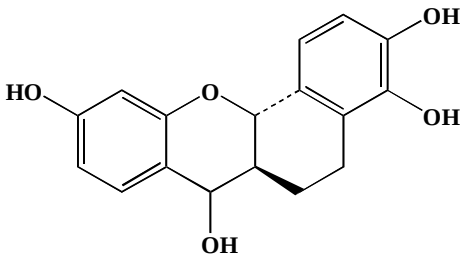

(17) Mopanol

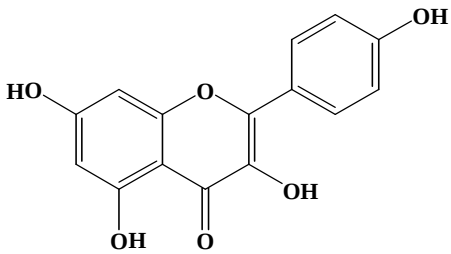

(18) Kaempferol

In 1985, Sultana and his co-workers investigated secondary metabolites from the leaves of *B. vahlii* Linn. and agathisflavone (**19**), betulinic acid (**20**), campesterol (**21**), quercetin (**22**), isoquercetrin (**23**), *β*-sitosterol (**11**), and stigmasterol (**25**) were isolated (Sultana, Ilyas, Kamil, and Shaida, 1985)

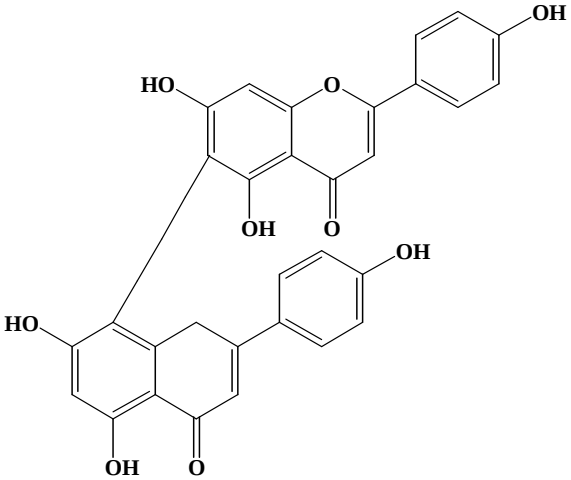

(19) Agathisflavone

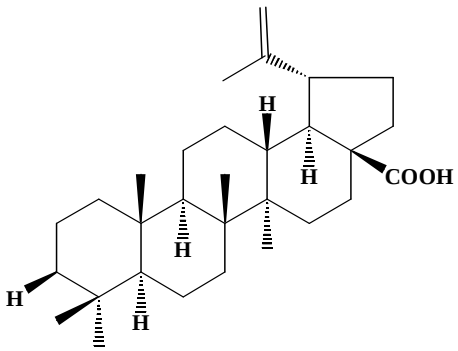

(20) Betulinic acid

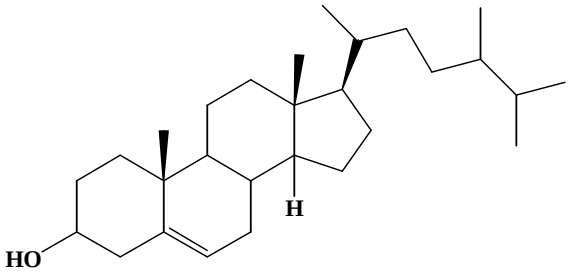

(21) Campesterol

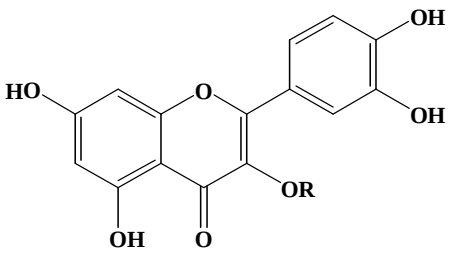

(22) Quercetin, R = H
(23) Isoquercetrin, R = glucoside
(24) Rutin, R = rhamnoglucoside

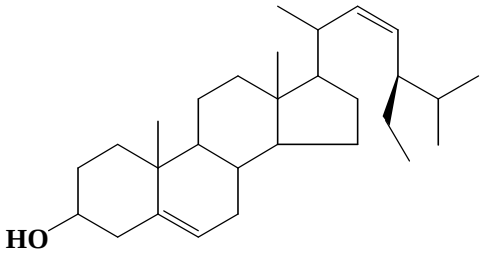

(25) Stigmasterol

B. manca is a plant cultivated throughout Costarica. The flavonoids: chrysoeriol (**26**) and 3-*O*-galloyl epi catechin (**27**) as well as flavones: luteolin-3′,5-dimethyl ester (**28**) and 2,4′-dihydroxy-4-methoxychalcone (**29**) were isolated from the stems of *B. manca* (Achenbach, Stocker, and Constenla, 1988).

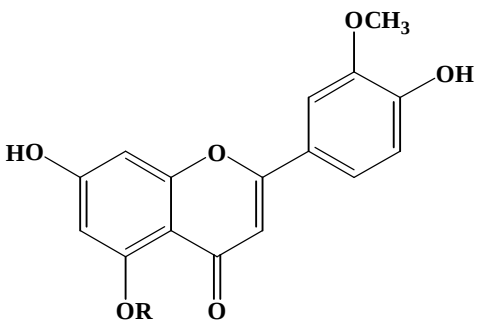

(26) Chrysoeriol, R = H
(28) Luteolin-3',5-dimethyl ester, R = Me

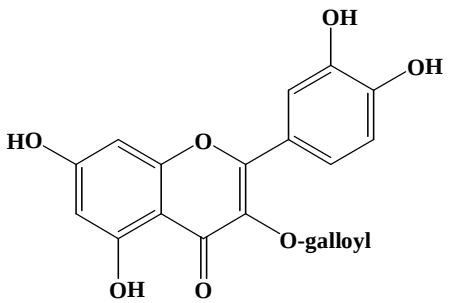

(27) 3-*O*-Galloyl epi catechin

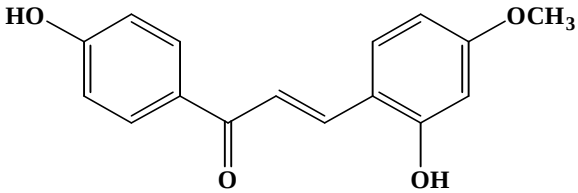

(29) 2,4'-Dihydroxy-4-methoxychalcone

Three flavonoids: quercitrin (**9**), isoquercitrin (**23**), and rutin (**24**) were isolated from the seeds of *B. malabarica* (Duret and Paris, 1977).

Anjaneyulu and co-workers isolated a new dibenzoxepin derivative, 1,7-dihydroxy-3-methoxy-2-methyldibenzo(2,3-6,7)oxepin (**30**), as well as its derivatives (**31**, **32**) and *trans*-resveratrol (**33**) from the heartwood of *B. racemosa* Lamk. (Anjaneyulu, et al., 1984). In addition, a new compound, de-*O*-methylracemosol (**4**) was first isolated from the benzene extract of its root bark (Prabhakar, Gandhidasan, Raman, Krishnasamy, and Nandudi, 1994). Furthermore, the isolation of *β*-amyrin (**34**) and *β*-sitosterol (**11**) from the stem bark of *B. racemosa* was reported (Prakash and Khosa, 1976).

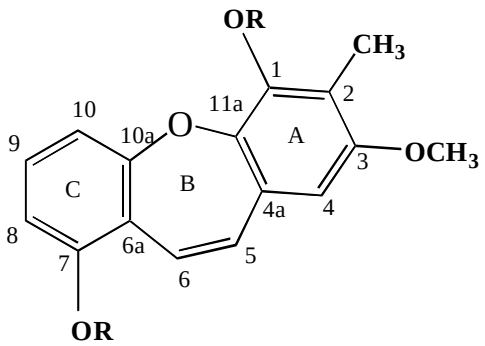

(30) R = H : 1,7-Dihydroxy-3-methoxy-2-methyldibenzo(2,3-6,7)oxepin
(31) R = Ac
(32) R = Me

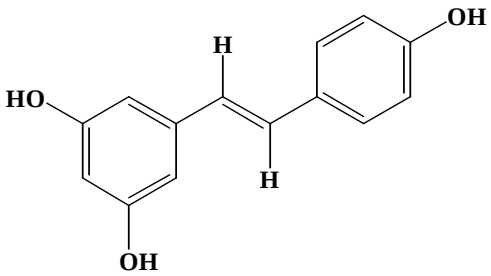

(33) *trans*-Resveratrol

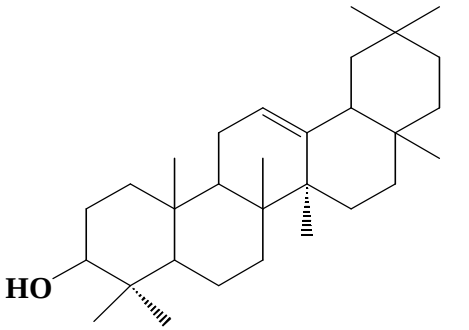

(34) β-Amyrin

A new acylated flavonol glycoside, quercetin 3-α-arabinopyranoside-2″gallate, together with quercetin (**22**), hyperin (**35**) and guaijavarin (**36**) were isolated from the leaves of *B. japonica* (Iwagawa, et al., 1990).

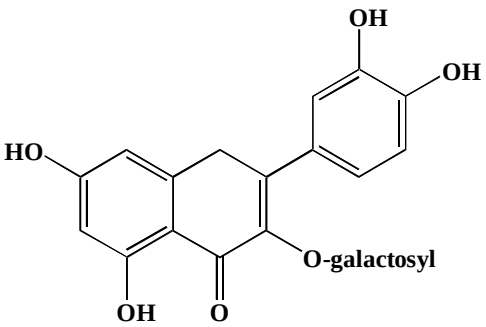

(35) Hyperin

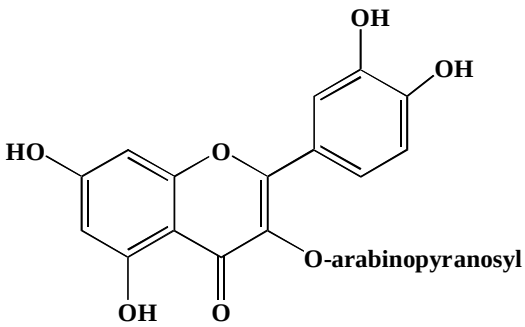

(36) Guaijavarin

In 1987, a novel steroidal glycoside sitosterol 3-*O*-α-D-xyluronofuranoside (**37**) was first isolated from the methanolic extract of the aerial parts of *B. candicans* (Iribarren and Pomilio, 1987).

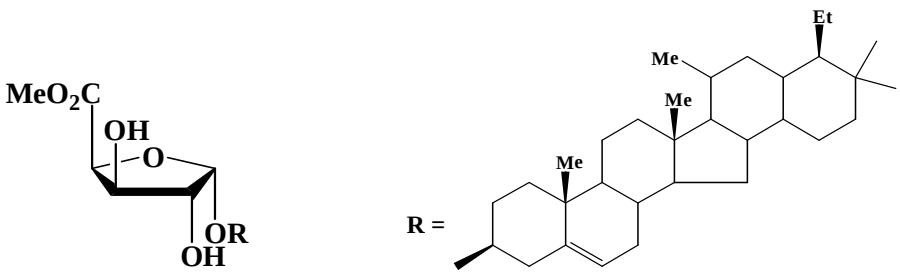

(37) Sitosterol 3-*O*-α-D-xyluronofuranoside

Four antifungal tetracyclic compounds were isolated from the CH_2Cl_2 extract of the root bark of *B. rufescens* Lam., including de-*O*-methylracemosol (**4**), 5,6-dihydro-11-methoxy-2,2,12-trimethyl-2*H*-naphtho[1,2-f][1]benzopyran-8,9-diol (**38**), 11-methoxy-2,2,12-trimethyl-2*H*-naphtho[1,2-f][1]benzopyran-8,9-diol (**39**), and 1,7,8,12b-tetrahydro-2,2,4-trimethyl-2*H*-benzo[6,7]cyclohepta[1,2,3-de][1]benzopyran-5,10,11-triol (**40**) (Maillard, Recio-Iglesias, Saadou, Stoeckli-Evans, and Hostettmann, 1991).

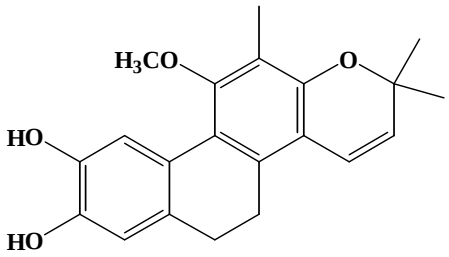

(38) 5,6-Dihydro-11-methoxy-2,2,12-trimethyl-2*H*-naphtho[1,2-f][1]-benzopyran-8, 9-diol

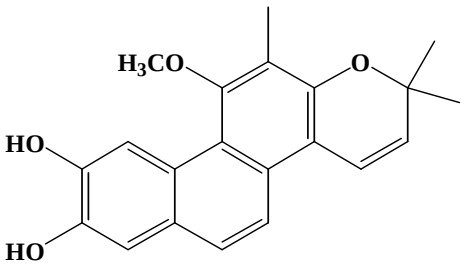

(39) 11-Methoxy-2,2,12-trimethyl-2*H*-naphtho[1,2-f][1]benzopyran-8,9-diol

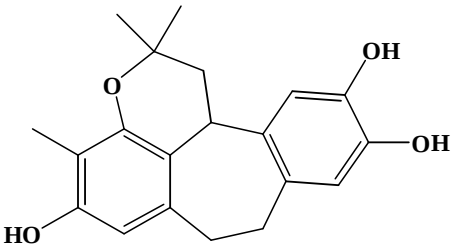

(40) 1,7,8,12b-Tetrahydro-2,2,4-trimethyl-2*H*-benzo[6,7]cyclohepta[1,2,3-de][1]benzo-pyran- 5,10,11-triol

2.4 Botanical of *Fagraea fragrans* Roxb.

F. fragrans Roxb. is a tall tree, 30-45 feet (some 100 feet) in height. Its leaves are simple, opposite, elliptic 4-6 cm wide, 8-12 cm long, thin, and coriaceous. Inflorescence is in axillary. Corymb is in the uppermost leaf-axil.

Sweet fragrant flowers appear once a year from April to May, white color at first then pale yellow. Berries, when ripe, are coral-red and broadly ellipsoid. Leaves and berries have an intense bitter taste (Wongsatit, et al., 1996).

2.5 Ethnopharmacology of the plants in the genus *Fagraea*

The *Fagraea* is a genus of trees and shrubs with various species. Most of them have been used for traditional herbal medicine in many countries around the world, especially in the rain forest countries from Southeast Asia, Australia, Pacific Islands to the African continent; for example, Thailand, Malaysia, Indonesia, Papua New Guinea, Tonga and Kenya. They have been a source of important antimalarial drugs and provided novel and effective treatments in traditional remedies (Leaman, et al., 1995).

In Malaysia and India, the roots and leaves of *F. racemosa* Jack are used for the treatment of fever and malaria (Leaman, et al., 1995). The roots are also used as a painkillers. In Indonesia, a decoction of the leaves of *F. auriculata* Jack is used as a fever medication and a rinse for mouth ulcers (Grosvenor, Gothard, Mc.William, Supriono, and Gray, 1995).

F. bodenii Wenh. is the medicinal plant of the Morobe province in Papua New Guinea. When its leaves are chewed with traditional salt, they can heal an enlarged spleen caused by malaria. *F. imperialis* is also a plant from Morobe province in Papua

New Guinea. Its bark is used for fever treatment (Holdsworth and Sakulas, 1986). In Tonga, the bark of *F. berteroana* A. Gray. is the local medicine to cure morning sickness of children (Ostraff, Anitoni, Nicholson, and Booth, 2000) and postpartum abdominal pain caused by retained blood clots in the uterus (Singh, Ikahihifo, Panuve, and Slatter, 1984).

In Malay folk medicine, a decoction of the leaves and twigs of *F. fragrans* is used for the treatment of dysentery. The bark is believed to have medicinal value for malaria (Natarajan, Wan, and Zaman, 1974). However, in Thai traditional medicine, it is believed that leaves contain antimalarial, element tonic, and antiasthmatic agents, and are externally used for mild infectious skin diseases (Wongsatit, et al., 1996), while an aqueous extract of the stems is used as a remedy for coughs (สมาคมพ่อค้ายา กรุงเทพฯ, 2521; สมาคมโรงเรียนแพทย์แผนโบราณ สำนักวัดพระเชตุพนวิมลมังคลาราม, 2521).

2.6 The chemical constituents of the plants in the genus *Fagraea*

An alkaloid gentianine (**41**) and swertiamarin (**42**) were isolated from the leaves and fruits of *F. fragrans* (Natarajan, et al., 1974; Kun-anake and Ragvatin, 1976). Previous research on pharmacological investigations of alkaloid gentianine showed that, when given orally 100 mg/kg, it produces 60% analgesia in mice. Furthermore, gentianine has no antipyretic activity nor diuretic effect in mice, no

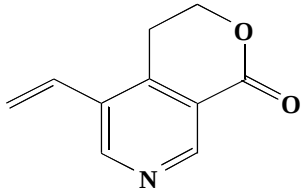

(41) Gentianine

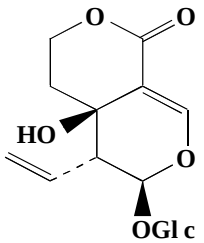

(42) Swertiamarin

hypoglycaemic activity in guinea pigs, and no cardiovascular and central nervous system effects on anesthetized cats (Wan, Macko, and Douglas, 1972).

Previous work revealed that the gentianine fails to have antimalarial activity against *Plasmodium berghei* in mice and *Entamoeba invadens* maintained in a monophasic medium (Natarajan, et al., 1974; Kun-anake and Ragvatin, 1976). However, the alcoholic extract of the wood of *F. fragrans* inhibits growth of *Plasmodium falciparum in vitro* (Wongsatit, et al., 1996), whereas the methanol extract from the hardwood of *F. fragrans* inhibits growth of two common wood-decaying fungi, *Pycnoporus sanguineus* and *Schizophyllum commune* (Hong and Mohd, 1983).

Considering previous research on plants in the genus *Fagraea*, the gentianine was isolated by using concentrated NH_3 followed by dilute HCl (Kun-anake and Ragvatin, 1976). However, the natural products isolated under strongly acidic or basic conditions are limited to the water-soluble compounds with high stability under such conditions (Cannell, 1998). Thus, extreme pH conditions of isolation should be avoided. Furthermore, other alkaloids besides gentianine might decompose and/or react under drastic conditions. Therefore, by extraction with other organic solvents such as hexane, chloroform and ethanol, other natural products may be isolated. These may include compounds with antimalarial activities.

In addition, the two new flavones; swertisin 6″-*O*-rhamnoside (**43**) and swertisin (**60**) were isolated from the leaves of *F. obovata* Wall. (Qasim, Roy, Kamil, and Ilyas, 1987).

In 1989, Cambie and associates reported that five new compounds were isolated from the heartwood of the Fijian tree *F. gracilipes* A. Gray in addition to

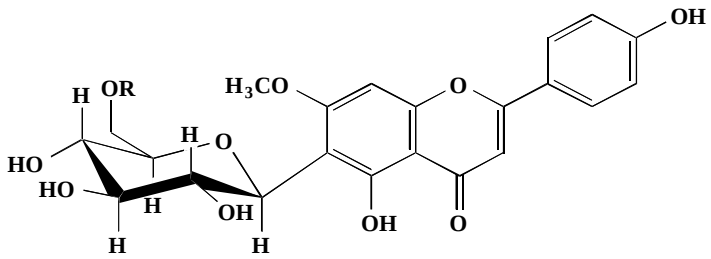

(43) Swertisin 6'' -*O*-rhamnoside, R = rhamnose

methyl caffeate (**44**), methyl *p*-coumarate (**45**), methyl sinapate (**46**), secoiridoid

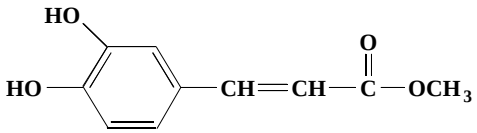

(44) Methyl caffeate

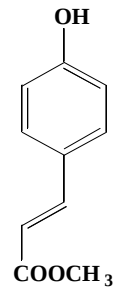

(45) Methyl *p*-coumarate

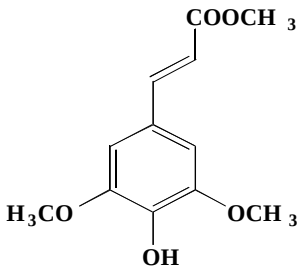

(46) Methyl sinapate

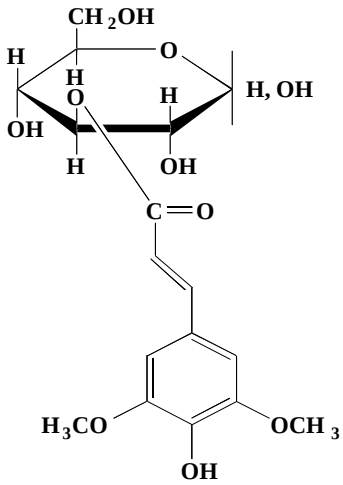

(47) 3-*O*-Sinapoyl D-glucose

glucoside sweroside (**48**)**,** 1,2;5,6-di-*O*-isopropylidene-3-*O*-sinapoyl D-glucose (**50**), and 1,2;5,6-di-*O*-isopropylidene D-glucose (**51**). The new compounds have been identified as methyl syringate α-*L*-rhamnoside (**52**), (*Z*)-5-ethylidene-3,4,5,6-

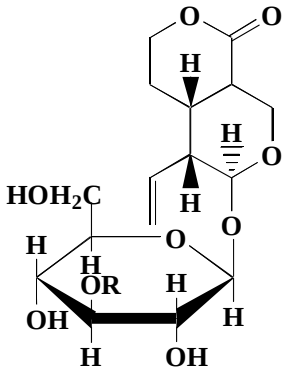

(48) Secoiridoid glucoside sweroside, R = H
(49) 3' -*O*-Sinapoyl sweroside, R = sinapoyl

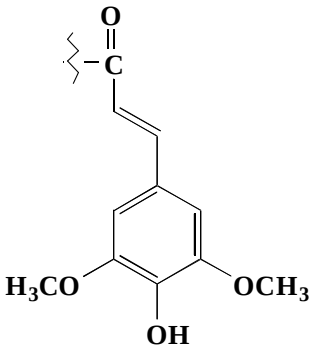

Sinapoyl group

tetrahydro-*cis*-6,8-dimethoxy-1*H*,8*H*-pyrano[3,4-*c*]pyran-1-one (**53**), (*Z*)-5-ethylidene-3,4,5,6-tetrahydro-*trans*-6,8-dimethoxy-1*H*,8*H*-pyrano[3,4-*c*]pyran-1-one (**54**), 3-*O*-sinapoyl D-glucose (**47**), and 3'-*O*-sinapoyl sweroside (**49**) by spectroscopic methods, chemical conversion and x-ray analysis (Cambie, Rickard, Lal, and Tanaka, 1990).

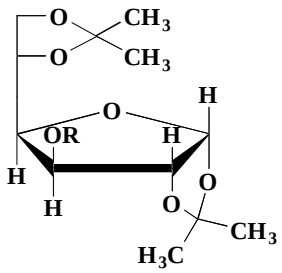

(50) 1,2;5,6-Di-*O*-isopropylidene-3-*O*-sinapoyl D-glucose, R = sinapoyl
(51) 1,2;5,6-Di-*O*-isopropylidene D-glucose, R = H

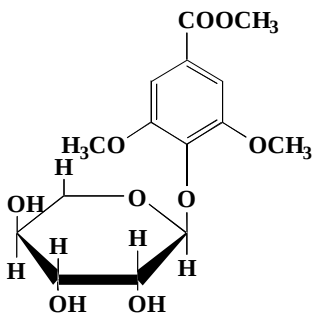

(52) Methyl syringate α-L-rhamnoside

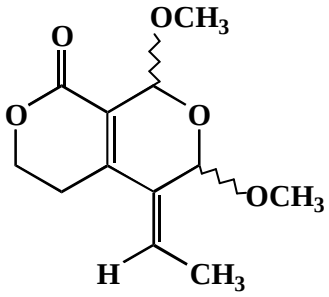

(53) (*Z*)-5-Ethylidene-3,4,5,6-tetrahydro-cis-6,8-dimethoxy-1*H*,8*H*-pyrano[3,4-c]pyran-1-one
(54) (*Z*)-5-Ethylidene-3,4,5,6-tetrahydro-trans-6,8-dimethoxy-1*H*,8*H*-pyrano[3,4-c]pyran-1-one

Consequently in 1997, Cuendet and co-workers isolated four new glucosides named blumeosides A-D (**55-58**) from the methanolic stem-bark extract of *F. blumei* G. Don. (Loganiaceae). Blumeosides A-D were accompanied by the benzyl-alcohol derivative di-*O*-methylcrenatin (**59**) the flavone *C*-glucoside swertisin (**60**), and adoxosidic acid (**61**). Moreover, blumeosides A-D inhibit bleaching of crocin induced by alkoxyl radicals. Blumeosides A and D also demonstrate scavenging properties towards the 2,2-diphenyl-1-picryl-hydrazyl (DPPH) radical in TLC autographic and spectrophotometric assays (Cuendet, Hostettmann, Potterat, and Dyatmiko, 1997).

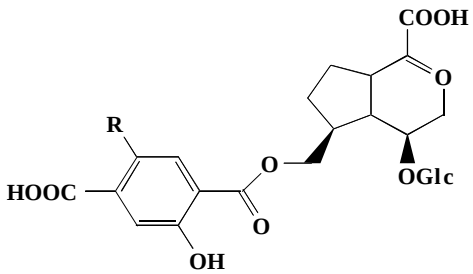

(55) Blumeoside A, R = OH
(56) Blumeoside C, R = H

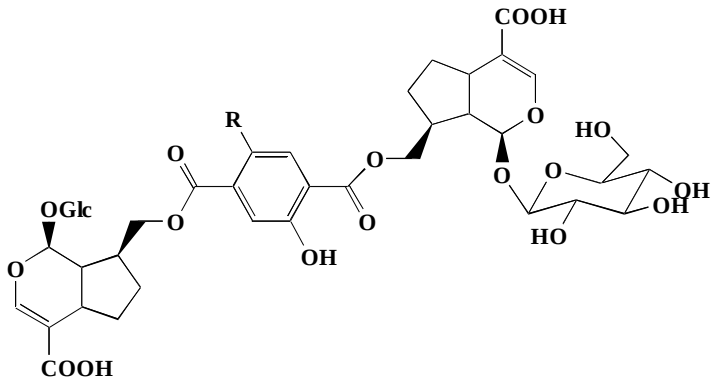

(57) Blumeoside B, R = H
(58) Blumeoside D, R = OH

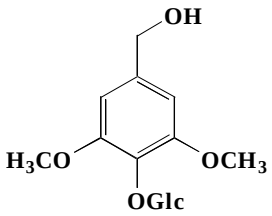

(59) Di-*O*-Methylcrenatin

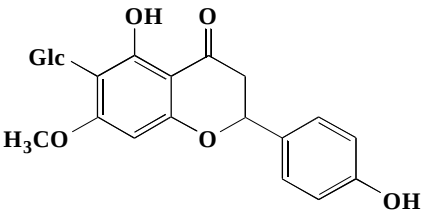

(60) Swertisin

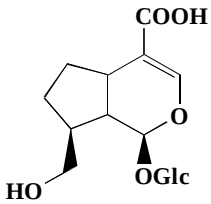

(61) Adoxosidic acid
Glc = β-D-glucopyranosyl

The results of bioactivity screening of crude extracts of plants in the genus *Fagraea* are as follows:

Leaf extract of *F. auriculata* Jack, in aqueous suspensions inhibits the growth of *Escherichia coli, Saccharomyces cerevisiae* and *Staphylococcus aureus,* but is inactive against *Fusarium oxysporum.* (Grosvenor, Supriono, and Gray, 1995).

F. obovata Wall was extracted with 50% ethanol. The crude extract of the roots shows effects on cardiovascular system. However, it fails to have antibacterial activity (against *Bacillus subtilis, Staphylococcus aureus, Salmonella typhi, Escherichia coli, Agrobacterium tumefaciens,* and *Mycobacterium tuberculosis* H37Ra), antifungal activity (against *Candida albicans, Cryptococcus neoformans, Trichophyton mentagrophytes, Microsporum canis*, and *Aspergillus niger),* and antiviral activity (against *Ranikhet disease* virus and *Vaccinia* virus) (Bhakuni, Dhar, Dhar, Dhawan, and Mehrotra, 1968).

Ethanol extract from *F. racemosa* seeds was studied for an antimutagenic assay in bacteria *Salmonella typbimurium.* It was found that the extract could strongly inhibit the mutagenic activity of 2-aminoanthracene in the presence of the Ames S-9 metabolic activation (Wall, Wani, Hughes, and Taylor, 1988).

CHAPTER III

EXPERIMENTAL

3.1 Source of Plant Materials

3.1.1 *Bauhinia saccocalyx* Pierre

The roots of *B. saccocalyx* were collected from Lad-yaow district, Nakhon Sawan province, Thailand, in August, 2003. The trees are 20-25 feet high and not examined in age.

3.1.2 *Fagraea fragrans* Roxb.

The leaves, roots, stem bark, stems, flowers and fruits of *F. fragrans* were collected from Ubon Ratchathani University, Muang Srikri subdistrict of Warinchamrap district, Ubon Ratchathani province, Thailand. The trees are about 30 feet high and not specific in age. The leaves, roots, stem bark, and stems were collected in September, 2002, whereas the flowers and fruits were collected in April, 2003.

A voucher herbarium specimen of *B. saccocalyx* Pierre (BRU 521) and *F. fragrans* Roxb.(Loganiaceae) (BRU 524) were deposited at the National Center for Genetic Engineering and Biotechnology (BIOTEC), Pathumthani province, Thailand.

3.2 Instrumentation and general techniques

3.2.1 Instrumentation

- Rotary evaporator (*Buchi B-169* Vacuum System).

- UV-Vis spectra were recorded on a *Cary-1E UV-Visible* spectrophotometer in λ_{max} (nm) and log ε.
- IR spectra were recorded on a *Bruker Vector 22* spectrophotometer in cm^{-1}.
- The ^{1}H-NMR, ^{13}C-NMR, DEPT, ^{1}H,^{1}H-COSY, NOESY, HMQC- and HMBC spectral data were performed on *Bruker DRX-400* or *Bruker AV-500* spectrometer, operating at 400 MHz (^{1}H) and 100 MHz (^{13}C), or at 500 MHz (^{1}H) and 125 MHz (^{13}C), respectively.
- Electrospray-ionization time-of-flight mass spectrometry (ESI-TOF-MS) was performed on a *Micromass- LCT* mass spectrometer.
- HPLC (*Waters 600 Controller*) was equipped with an UV photodiode array detector (*Waters 996*) and the column was C_{18} reversed phase column (*Prep Nova Pak, Waters*).
- Optical rotation was observed on *Jasco DIP-370* polarimeter.

3.2.2 General techniques

- **Analytical thin-layer chromatography (TLC)**

Technique	:	One dimension
Adsorbent	:	Silica gel 60 G F_{254} (E. Merck) precoated plate
Layer thickness	:	0.2 mm
Distance	:	5.0 cm
Temperature	:	Laboratory temperature (28-30^{o}C)
Detection	:	Ultraviolet light at wavelengths of 254 and 366 nm (Camag UV-Cabinet)

- **Gel filtration chromatography**

Gel filter : Sephadex LH-20

Packing method : Gel of Sephadex LH –20 was suspended in MeOH, left until swell adequately for 24 hours, loaded into the column, and allowed to settle properly.

Sample loading : The sample was dissolved in a small volume of 100% MeOH and applied on the top of a column.

3.3 Extraction and Isolation

Generally, the bioactive chemical components could be dissolved and extracted by non-polar solvents. Therefore, the natural product isolation of the roots of *B.* saccocalyx and the plant parts of F. *fragrans* was focused herein only on CH_2Cl_2 crude extracts.

3.3.1 Extraction and isolation of pure compounds from the roots of *B. saccocalyx*

The dried powder of the roots of *B. saccocalyx* (2.34 kg) were macerated at laboratory temperature for 48 hours with CH_2Cl_2 (8 L) and then MeOH (8 L). The filtrate was pooled and evaporated under reduced pressure to afford the corresponding CH_2Cl_2 crude extract (19.89 g) and MeOH crude extract (17.30 g).

The CH_2Cl_2 crude extract of roots was further investigated and purified by repeated Sephadex LH-20 (100% MeOH as eluent) column chromatography and HPLC (C_{18} reversed phase column) to obtain eight pure compounds.

The research procedure for the isolation of the root extract of *B. saccocalyx* is in the following diagram:

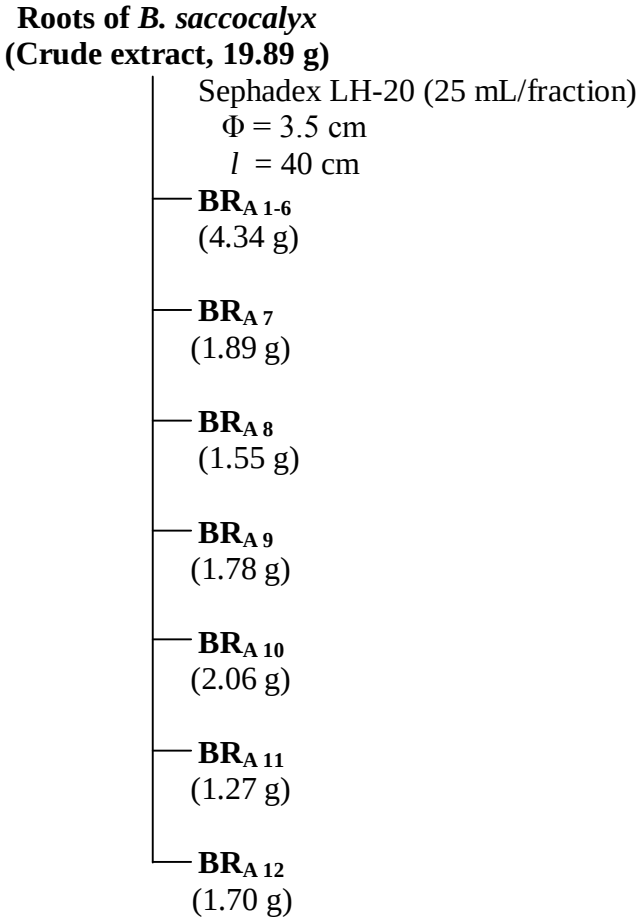

Scheme 3.1 The isolation procedure of the root extract of *B. saccocalyx*

The CH_2Cl_2 crude extract of the root of *B. saccocalyx* (19.89 g) was isolated and purified by Sephadex LH-20 (100% MeOH as eluent) to obtain 12 fractions. The ^{1}H NMR data of fractions $BR_{A\,7}$, $BR_{A\,8}$, and $BR_{A\,11}$ reveal the presence of proton signals at δ_H 7-10 ppm indicating the presence of aromatic rings. Therefore, fractions $BR_{A\,7}$, $BR_{A\,8}$, and $BR_{A\,11}$ were of interest and purified by repeated Sephadex LH-20 column chromatography and HPLC (C_{18} reversed phase column), yielding eight pure compounds. Three compounds, BR7D-4H (1.30 mg), BR7D-5H (9.20 mg),

and BR7D-6H (36.40 mg) were obtained from the fraction $BR_{A\ 7}$, three compounds, BR8D-4H (1.40 mg), BR8D-5H (42.00 mg), and BR8D-6H (13.20 mg) were obtained from the fraction $BR_{A\ 8}$, and two compounds BR11D-2H (11.90 mg) and BR11D-3H (16.20 mg) were from fraction $BR_{A\ 11}$.

The procedures for the isolation of fractions $BR_{A\ 7}$, $BR_{A\ 8}$ and $BR_{A\ 11}$ are shown in the following schemes:

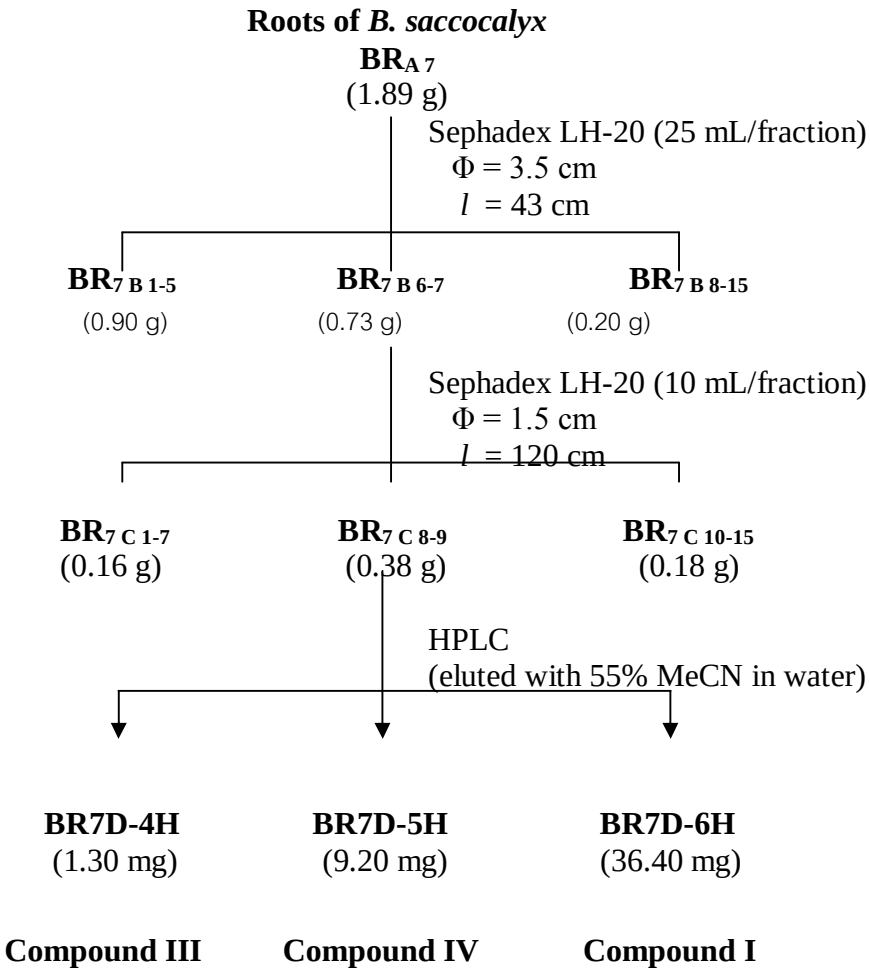

Scheme 3.2 The isolation of the fraction $BR_{A\ 7}$

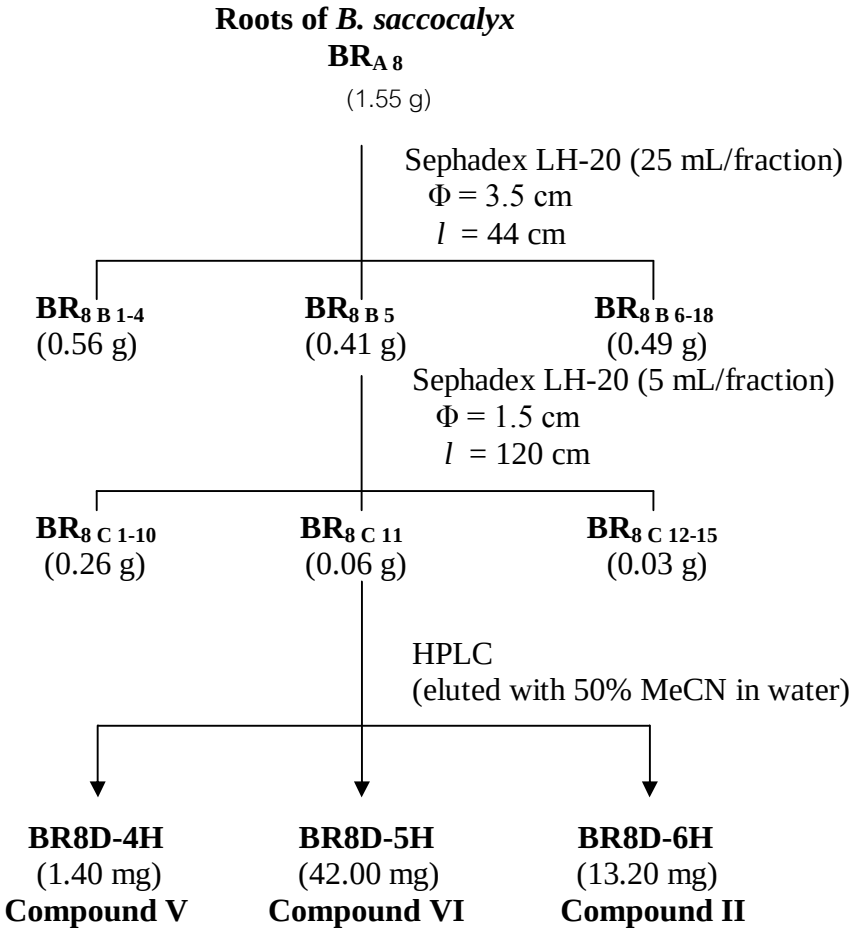

Scheme 3.3 The isolation of the fraction $BR_{A\,8}$

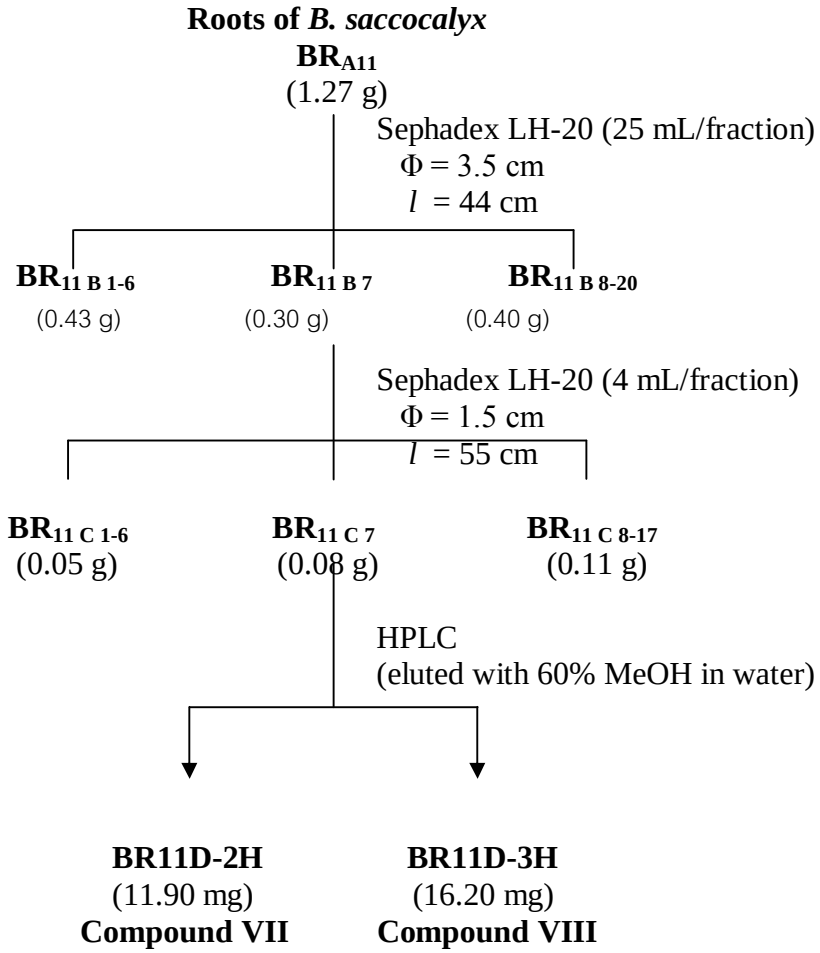

Scheme 3.4 The isolation of the fraction $BR_{A\ 11}$

3.3.2 Extraction and isolation of pure compounds from *F. fragrans*

The dried powder of leaves (5.00 kg), stem bark (2.70 kg), roots (2.90 kg), fruits (2.50 kg), stems (2.20 kg), and flowers (0.50 kg) were successively macerated at laboratory temperature for 48 hours with CH_2Cl_2 (8 L) and then MeOH (8 L). The filtrate was pooled and evaporated under reduced pressure to afford the corresponding CH_2Cl_2 crude extracts of leaves (22.54 g), stem bark (4.30 g), roots (27.36 g), fruits (6.93 g), stems (6.49 g), and flowers (8.27 g) as well as MeOH crude extracts of leaves (24.10 g), stem bark (8.03 g), roots (23.11 g), fruits (5.05 g), stems (10.09 g), and flowers (3.24 g).

Consequently, the CH_2Cl_2 crude extracts of leaves, stem bark, roots, fruits, stems and flowers were examined by ^{1}H-NMR spectral data. They all show the presence of proton signals around δ_H 7-10 ppm, revealing the molecular structure containing aromatic rings. Therefore, the CH_2Cl_2 crude extracts of leaves, stem bark, roots, fruits, stems and flowers were of interest and repeatedly purified by Sephadex LH-20 (100% MeOH as eluent). Finally by HPLC (C_{18} reversed phase column) were afforded five pure compounds. There were a pure compound from fraction FB-B7 (310.90 mg) of stem bark, a pure compound from fraction FR-F1H (16.90 mg) of roots, a pure compound from fractions FF-C7 (29.10 mg), FF-D4 (38.00 mg) and FF-D5 (43.40 mg) of fruits, a pure compound from fractions FS-E1H (28.10 mg) and FS-E2H (8.90 mg) of stems, and a pure compound from fraction FW-E2H (1.70 mg) of flowers. However, none of pure compounds were obtained from leaves (the survey of the ^{1}H-NMR spectrum of the crude extract indicated that chlorophyll is a major component in the leaf extract).

Details for the isolation of *F. fragrans* extracts are in the following diagrams:

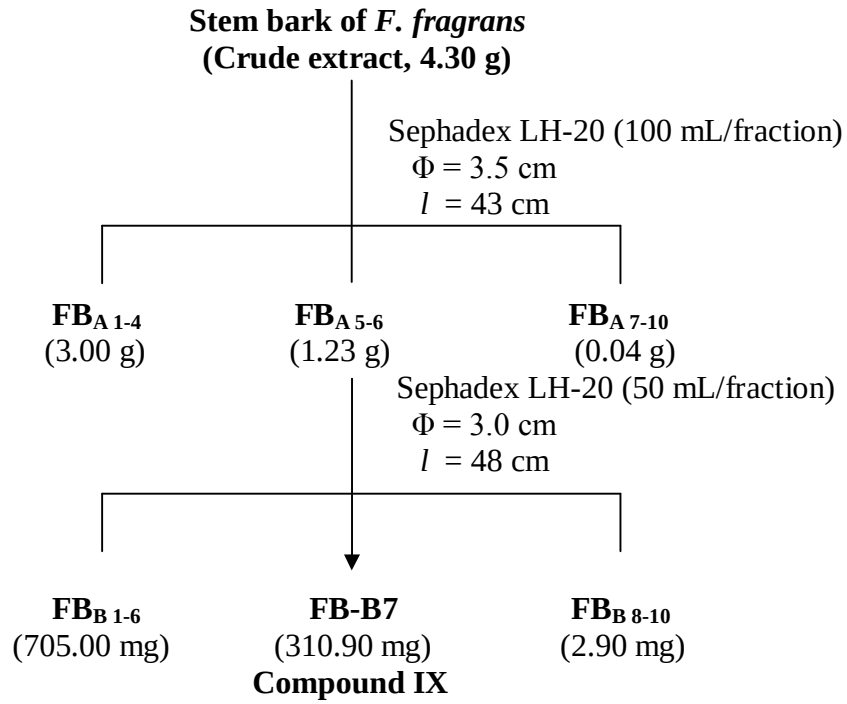

Scheme 3.5 The isolation procedure of the bark extract of *F. fragrans*

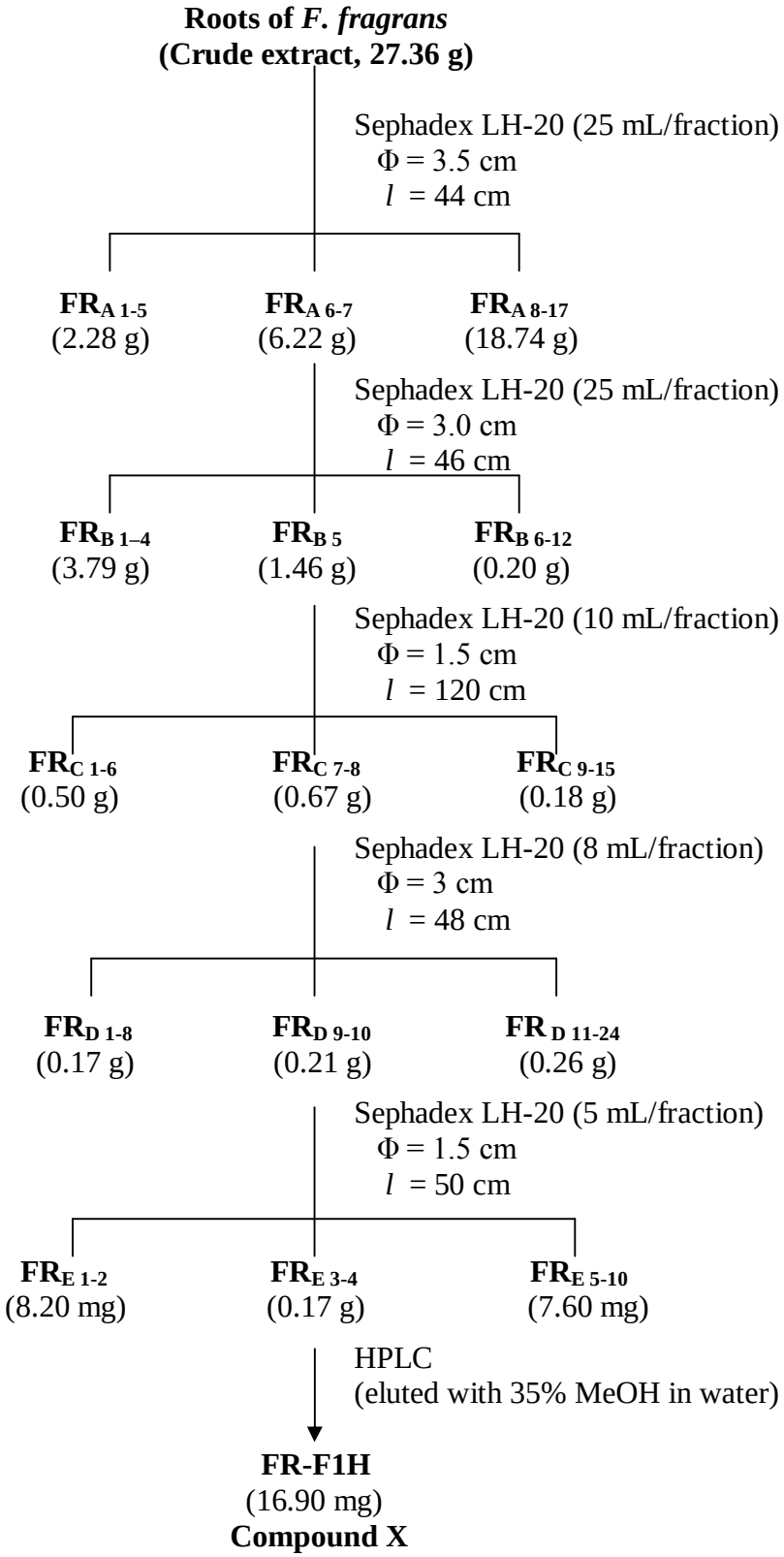

Scheme 3.6 The isolation procedure of the root extract of *F. fragrans*

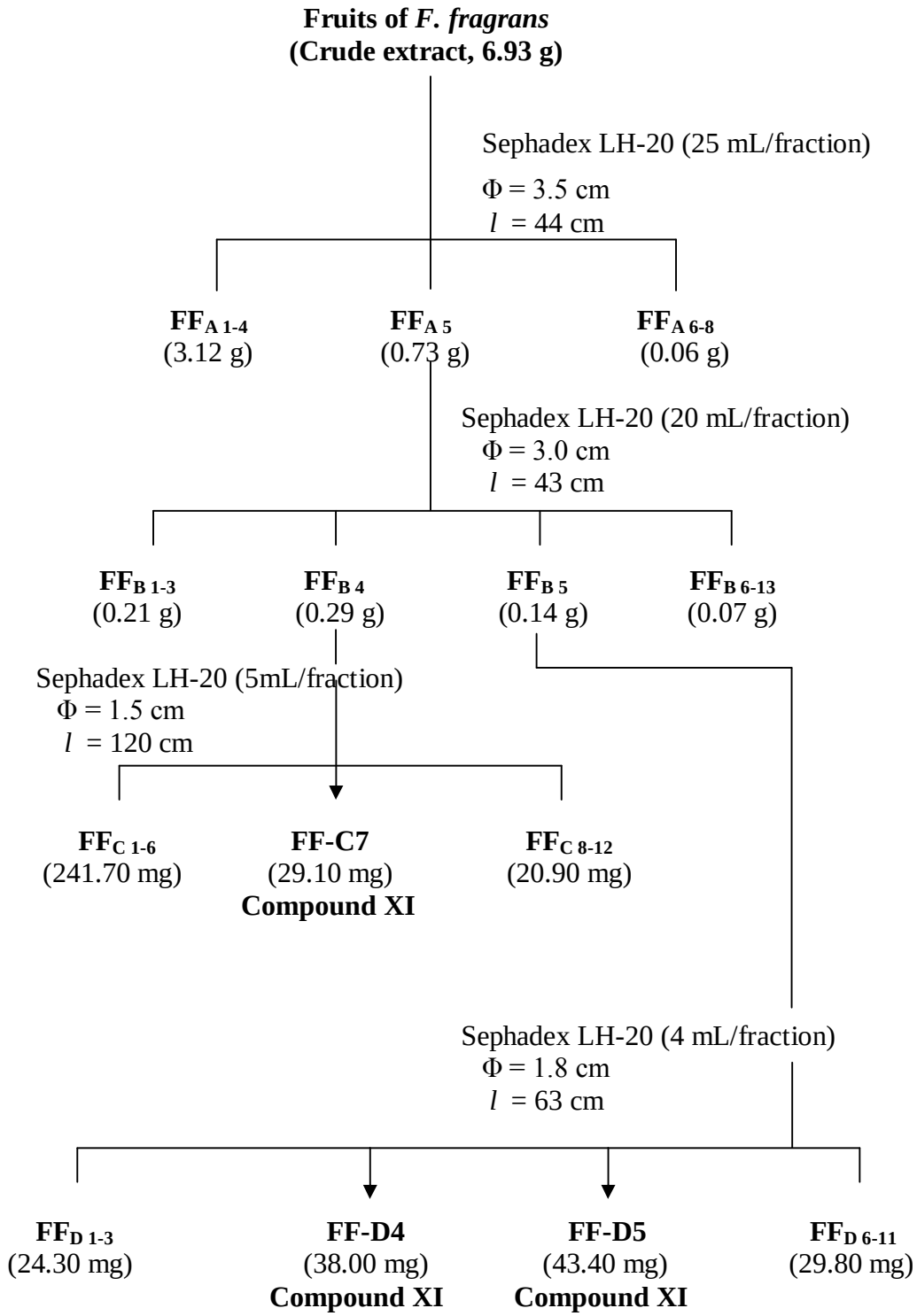

Scheme 3.7 The isolation procedure of the fruit extract of *F. fragrans*

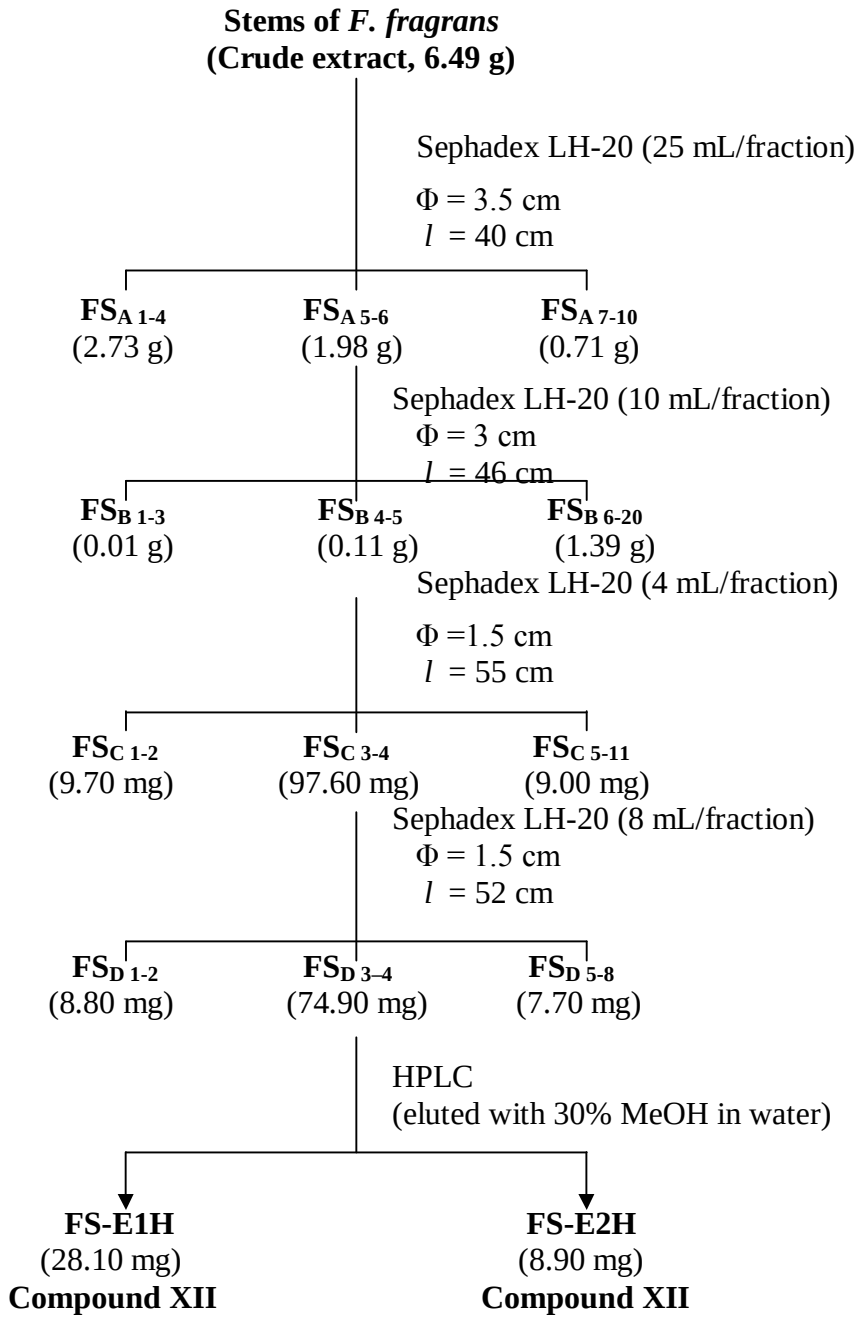

Scheme 3.8 The isolation procedure of the stem extract of *F. fragrans*

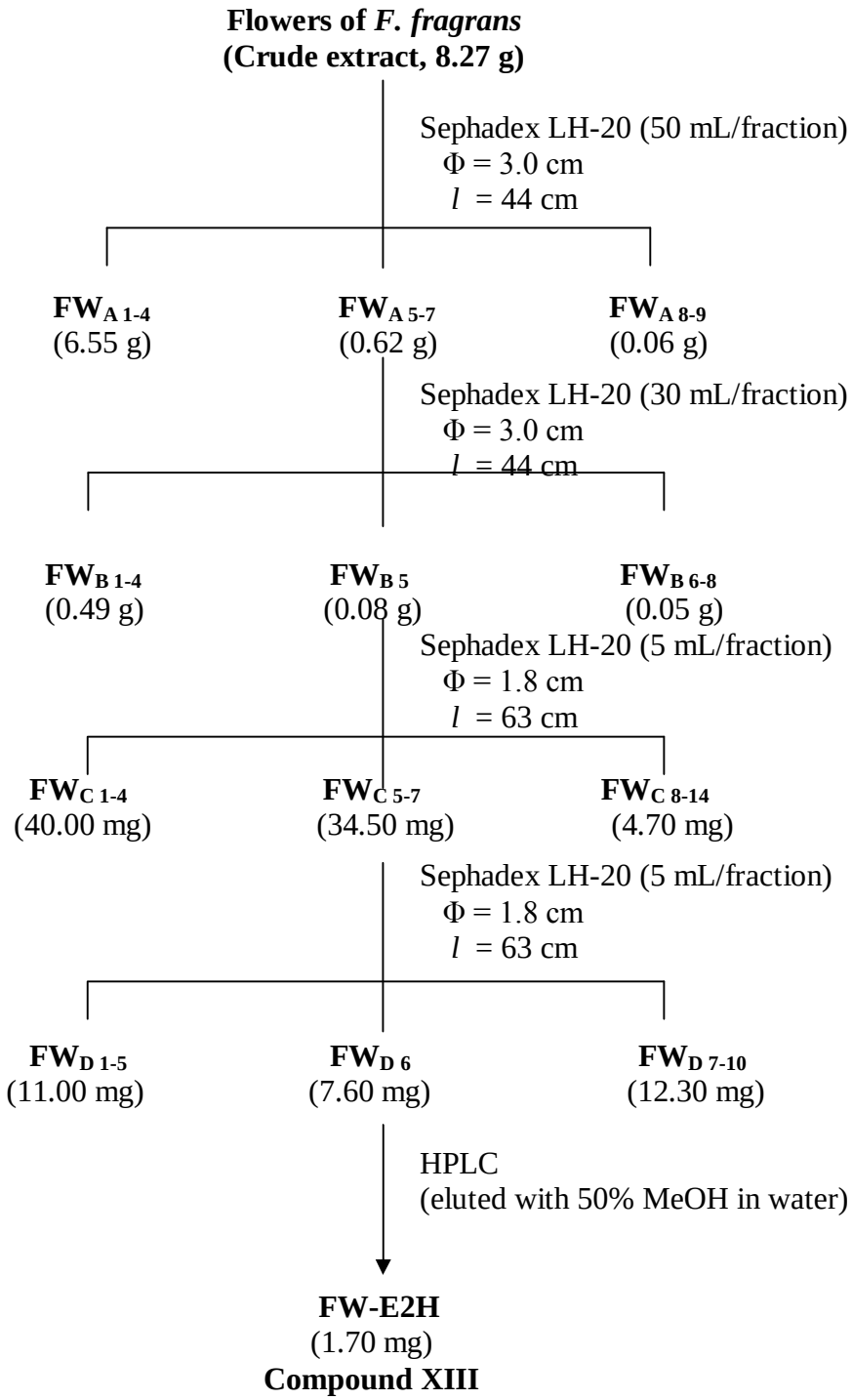

Scheme 3.9 The isolation procedure of the flower extract of *F. fragrans*

3.4 Biological activity test

All biological activities including antifungal, antimycobacterial, cytotoxic, antimalarial, and anti-inflammatory activities of the isolated compounds from both *B. saccocalyx* and *F. fragrans* were evaluated by the staff at Bioassay Laboratory, the National Center for Genetic Engineering and Biotechnology (BIOTEC), Pathumthani province, Thailand. The details for each test are as follows:

Antifungal activities were assessed against a clinical isolate of *Candida albicans* by means of a method modified from the soluble formazan assay (Hawser, Norris, Jessup, and Ghannoum, 1998). Briefly, 100 μL of 2×10^6 CFU/mL *C. albicans* in RPMI-1640 medium, containing 34.53 g/mL of 3-[*N*-morpholino]-propanesulfonic acid (MOP; Sigma, USA), was added to each well of 96-well microculture plate containing 100 μL of the tested compound diluted in 10% DMSO; *Sigma,* USA. Plates were incubated at 37^o for 4 h, before 50 μL of a solution containing 1 mg/mL of 2,3-bis-[2-methoxy-4-nitro-5-sulfonylphenyl]-5-[(phenyl-amino)carbonyl]-2*H*-tetrazolium hydroxide (XTT tetrazolium; Sigma, USA) and 0.025 mM of *N*-methylphenazolium methosulfate (PMS; Sigma, USA) were added. After an additional 4-hour incubation at 37^oC, the number of living cells was determined by measuring the absorbance of XTT formazan at 450 nm. Amphotericin B (Sigma, USA) and 10% DMSO were used as positive and negative controls, respectively. In this system, the IC_{50} value of the standard drug, amphotericin B, is 0.04 ± 0.01 μg/mL (n = 3).

Antimycobacterial activities were assayed against *Mycobacterium tuberculosis* H37Ra, using the Microplate Alamar-Blue Assay (MABA) (Collins and Franzblau, 1997). The twofold dilution technique, starting at a concentration of 200 μg/mL, was used, and the MIC value was recorded at the minimum concentration of the tested

compound inhibiting bacterial growth. The standard drugs, isoniazid (Sigma, USA) and kanamycin sulfate (Sigma, USA), used as reference compounds for the antimycobacterial assay, show MIC values of 0.040-0.090 and 2.0-5.0 μg/mL, respectively.

Cytotoxicity was determined by employing the colorimetric method described by Skehan, et al (Skehan, et al., 1990). The cell types tested are NCI-H187 (small-cell lung cancer), KB (oral-cavity cancer), BC (breast cancer), and Vero. The reference compound Ellipticine (Sigma, USA), exhibits activity towards Vero, KB, and BC cell lines, with IC_{50} values of 0.2-0.3 μg/mL.

Antimalarial activities were evaluated against the parasite *Plasmodium falciparum* (K1, multidrug-resistant strain), which was cultured continuously according to the method of Trager and Jensen (Trager and Jensen, 1976). Quantitative assessment of antimalarial activity *in vitro* was determined by the microculture radioisotope technique based upon the method described by Desjardins, et al. (Desjardins, Canfield, Haynes, and Chulay, 1979). Briefly, a mixture of 200 μL of 1.5% of erythrocytes with 1% parasitemia at the early ring stage was pre-exposed to 25 μL of the medium containing a test sample dissolved in DMSO (0.1% final concentration) for 24 hours, employing the incubation conditions described above. Subsequently, 25 μL of [^3H]hypoxanthine (Amersham, USA) in culture medium (10 μCi) was added to each well, and the plates were incubated for an additional 24 hours. Levels of incorporated radioactively labeled hypoxanthine, indicating parasite growth, were determined by means of a *TopCount* microplate scintillation counter (Packard, USA). Inhibition concentrations (IC_{50}) represent the concentrations required for 50% reduction in parasite growth. The standard sample was dihydroartemisinin (Sigma, USA).

The anti-inflammatory activity assay (cyclooxygenase 1, COX-1 and cyclooxygenase 2, COX-2) was performed by means of the radioimmunoassay method previously

described by Kirtikara et al. (Kirtikara, et al., 1998). Immortalized COX-$1^{-/-}$ and COX-$2^{-/-}$ mouse-lung fibroblast cells (prepared as described in Kirtikara, et al., 1998) were used to produce prostaglandin E_2 (PGE_2), representing COX-2 and COX-1 activity, respectively. Briefly, immortalized COX-$1^{-/-}$ and COX-$2^{-/-}$ mouse-lung fibroblast cells were plated at 1 $\times$ 10^5 cells/mL in complete Dulbelcco's Modified Eagle Medium (DMEM) containing 0.1 mM nonessential amino acids, 292 mg/mL L-glutamine, 50 mg/mL ascorbic acid, and 10% fetal bovine serum (PAA, Austria), in 96-well flat-bottomed tissue-culture plates at 83 μL/well. The cells were incubated at 37^{o}C for 72 hours in a humidified incubator with 5% CO_2. Subsequently, the cells were washed with phosphate buffer saline solution and incubated for 30 minutes in 83 μL serum-free DMEM containing test compounds. DMEM Media containing drug vehicle, DMSO (0.1%), and aspirin were used as a control for 100% COX activities and a positive control, respectively. The medium was then replaced with serum-free DMEM containing the same amount of drugs or DMSO and 20 μM of arachidonic acid (Sigma, USA), and the cells were incubated for 30 minutes. Culture supernatants were collected at the end of incubation time and assayed for PGE_2 concentrations by the radioimmunoassay method (Kirtikara, et al., 1998). The inhibition of COX activity was determined from the percent reduction of PGE_2 produced by drug-treated cells relative to PGE_2 produced by cells treated with DMSO alone. IC_{50} values of COX-1 and COX-2 were determined with the SOFTmax software (Molecular Devices, Sunnyvale, CA). Aspirin (Sigma, USA) was used as a positive control and was almost equally effective against COX-1 and COX-2. Typical IC_{50} values of aspirin for COX-1 and COX-2 are 2.06 and 3.57 μg/mL, respectively.

CHAPTER IV

RESULTS AND DISCUSSION

4.1 Compound I (bauhinol A, a new compound)

4.1.1 Structure elucidation

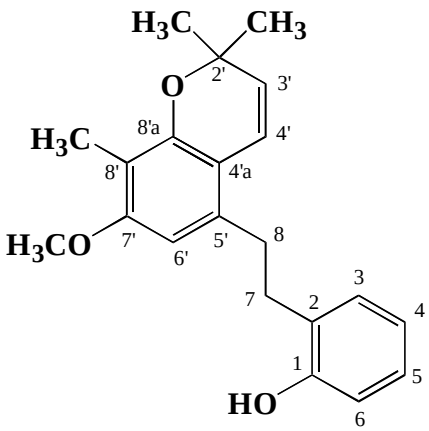

I
(Arbitrary atom numbering)

Compound **I** was obtained as brown, unstable, viscous liquid, from the root extract of *B. saccocalyx*. The exact mass at *m/z* 347.1667 ($[M + Na]^+$, 347.1623 calculated for $[C_{21}H_{24}O_3 + Na]^+$) obtained from the ESI-TOF mass spectrum (Fig. 1.1) establishes the molecular formula of **I** as $C_{21}H_{24}O_3$. The infrared spectrum (Fig. 1.2) of **I** shows absorption peaks (ν_{max}) at 3443 cm^{-1} (broad O–H stretching), 2972 cm^{-1} (C–H stretching), 1602 cm^{-1} (C=C stretching of an aromatic ring), 1455 cm^{-1} (C–H deformation of methylene group), 1132 cm^{-1} (C–O stretching), and 753 cm^{-1} (=C–H out of plane bending of a benzene ring). The UV-Vis spectrum (Fig. 1.3) of **I** shows absorption peaks (λ_{max}) at 203 and 278 nm.

The ^{1}H-NMR spectrum (Fig. 1.4) of compound **I** exhibits signals of a dimethylchromene unit [at δ_H 6.62 ppm (*d*, *J* = 9.94 Hz) for H–C-4′, 5.56 ppm (*d*, *J* = 9.95 Hz) for H–C-3′, and 1.44 ppm (*s*, 2Me) for Me–C-2′], two groups of downfield-shifted methylenes [at δ_H 2.88 ppm (*m*) for H–C-7 and 2.93 ppm (*m*) for H–C-8], a 1,2-disubstituted benzene ring [at δ_H 7.13 ppm (*dd*, *J* = 7.32 and 1.56 Hz) for H–C-3, 6.90 ppm (*td*, *J* = 7.30 and 0.90 Hz) for H–C-4, 7.12 ppm (*td*, *J* = 7.70 and 1.70 Hz) for H–C-5, and 6.76 ppm (br *d*, *J* = 7.86 Hz) for H–C-6], and two methyl groups [at δ_H 2.10 ppm (*s*) for Me–C-8′ and 3.79 ppm (*s*) for MeO–C-7′]. Further, an aromatic singlet at δ_H 6.25 ppm for H–C-6′ suggests that the benzene ring of the chromene unit is triply substituted.

The ^{13}C-NMR spectrum (Fig. 1.5) of **I** reveals 21 signals, which are classified by DEPT and HMQC spectra (Figs. 1.5 and 1.6), as seven methines, four methyls, two methylenes, and eight quaternary carbon atoms. The downfield C-1 signal at δ_C 153.72 ppm, together with the IR absorption peak at 3443 cm^{-1} (broad), indicates the presence of an oxygenated sp^2 quaternary carbon atom, while the downfield C-2′ signal at δ_C 75.33 ppm is of an oxygenated sp^3 quaternary carbon atom of a dimethylchromene unit.

The ^{1}H,^{1}H-COSY spectrum (Fig. 1.8) of **I** shows the connectivity from H–C-3 to H–C-6 in the 1,2-substituted benzene ring, and demonstrates couplings between H–C-3′ and H–C-4′ in a chromene unit, and between CH_2-7 and CH_2-8.

The HMBC spectral data (Fig. 1.7) are very informative concerning the assembly of the gross structure of **I**. The following ^{1}H,^{13}C long range correlations are observed: both H–C-3 and H–C-5 to C-1; both H–C-4 and H–C-6 to C-2; CH_2-7 to C-1, C-2, and C-3; CH_2-8 to C-4′a, C-5′, and C-6′; the 2′-Me H-atoms to C-2′ and C-3′; H–C-3′ and H–C-6′ to C-4′a; H–C-4′ to C-2′, C-5′, and C-8′a; H–C-6′ to C-8,

C-7′, and C-8′; the 7′-OMe H-atoms to C-7′; and the 8′-Me H-atoms to C-7′, C-8′ and C-8′a.

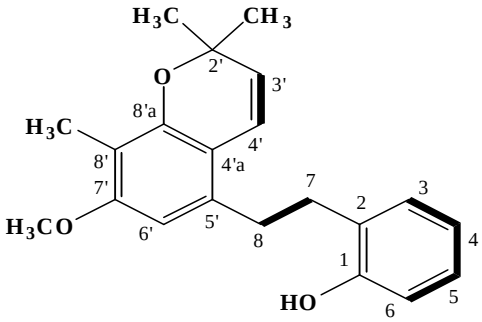

The bold lines show the connectivities from ^{1}H,^{1}H-COSY spectrum of compound I

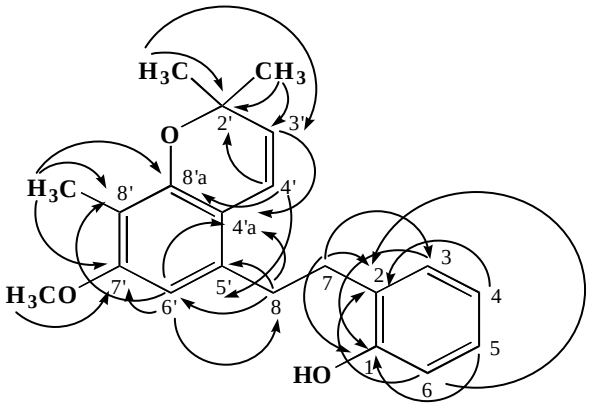

The curved arrows show HMBC correlations of compound I

The NOESY spectrum (Fig. 1.9) of **I** shows cross peaks between the 2′-Me H-atoms and H–C-3′; the 8′-Me H-atoms and the 2′-Me H-atoms; the 7′-OMe H-atoms and H–C-6′; H–C-8 and H–C-6′; and H–C-3 and H–C-7.

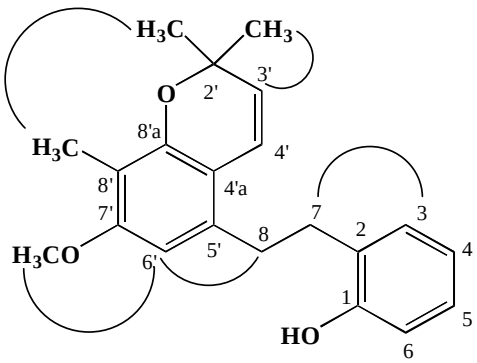

The curved lines show NOESY correlations of compound I

Based on these spectral data, **I** is identified as 2-[2-(7-methoxy-2,2,8-trimethyl-2*H*-1-benzopyran-5-yl)ethyl]phenol. The complete assignment of the H- and C-atoms for **I** is shown in Table 4.1.

Table 4.1 The ^{1}H- and ^{13}C-NMR spectral data of compound I at 500 and 125 MHz, respectively in $CDCl_3$ (*J* in Hz).

	δ (ppm)	
	^{1}H	**^{13}C**
C-1	–	153.72
C-2	–	128.04
H–C-3	7.13 (*dd*, *J* = 7.32, 1.56)	130.52
H–C-4	6.90 (*td*, *J* = 7.30, 0.90)	120.95
H–C-5	7.12 (*td*, *J* = 7.70, 1.70)	127.41
H–C-6	6.76 (*br d*, *J* = 7.86)	115.51
CH_2-7	2.88 (*m*)	32.60
CH_2-8	2.93 (*m*)	33.15
C-2′	–	75.33
H–C-3′	5.56 (*d*, *J* = 9.95)	128.30
H–C-4′	6.62 (*d*, *J* = 9.94)	119.35
C-4′a	–	113.13
C-5′	–	135.30
H–C-6′	6.25 (*s*)	104.10
C-7′	–	157.90
C-8′	–	112.30
C-8′a	–	151.90
Me–C-2′	1.44 (*s*)	27.80
Me–C-2′	1.44 (*s*)	27.80
Me–C-8′	2.10 (*s*)	8.02
MeO–C-7′	3.79 (*s*)	55.60

4.1.2 Biological activities

Compound **I** exhibits significant cytotoxicity towards NCI-H187, BC, and KB cell lines with IC_{50} values of 3.40, 2.71, and 4.48 µg/mL, respectively. It also shows mild antimycobacterial activity against *Mycobacterium tuberculosis* H37Ra with the MIC value of 50 µg/mL. However, it is inactive against the malarial parasite *in vitro*, COX-1 and COX-2 at 20 µg/mL. Further, it shows no antifungal activity against *Candida albicons* at 50 µg/mL.

4.2 Compound II (bauhinol B, a new compound)

4.2.1 Structure elucidation

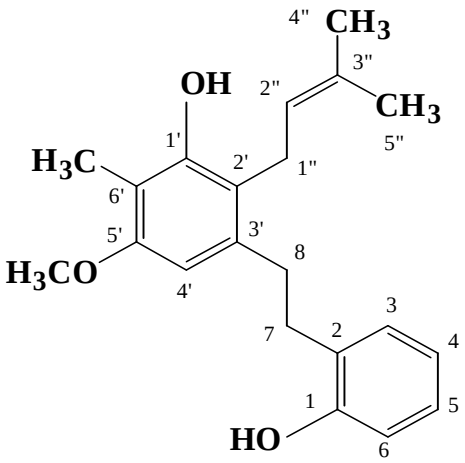

II

(Arbitrary atom numbering)

Compound **II** was obtained as brown viscous liquid from the root extract of *B. saccocalyx*. A molecular formula $C_{21}H_{26}O_3$ is established from the ESI-TOF mass spectrum (Fig. 2.1) with the exact mass at *m/z* 349.1795 ($[M + Na]^+$, 349.1780 calculated for $[C_{21}H_{26}O_3 + Na]^+$).

The infrared spectrum (Fig. 2.2) of **II** shows absorption peaks (ν_{max}) at

3417 cm^{-1} (broad, O–H stretching), 2934 cm^{-1} (C–H stretching), 1614 and 1581 cm^{-1} (C=C stretching of an aromatic ring), 1458 cm^{-1} (C–H deformation of methylene group), 1127 cm^{-1} (C–O stretching), and 743 cm^{-1} (=C–H out of plane deformation of a benzene ring). The UV-Vis spectrum of **II** (Fig. 2.3) shows absorption peaks (λ_{max}) at 206 and 274 nm.

The ^{1}H-NMR spectrum (Fig. 2.4) of **II** looks very similar to that of compound **I**, indicating that **II** is a derivative of **I**. Careful analysis of the ^{1}H-NMR spectrum reveals the replacement of the dimethyl-2*H*-1-pyran ring in **I** with a 3-methyl-but-2-enyl moiety in **II** (ring opening).

The ^{13}C-NMR spectrum (Fig. 2.5) of **II** shows 21 signals, which are classified by DEPT and HMQC spectra (Figs. 2.5 and 2.6) as six methines, three methylenes, four methyls, and eight quaternary carbon atoms. The downfield C-1 and C-1′ signals at δ_C 153.73 and 153.68 ppm, together with the IR absorption peak at 3417 cm^{-1} (broad), indicates the presence of oxygenated sp^2 quaternary carbon atoms.

The ^{1}H,^{1}H-COSY spectrum (Fig. 2.8) of **II** demonstrates couplings between H–C-2″ and CH_2-1″, allylic couplings from both Me-4″ and Me-5″ to H–C-2″, and couplings between CH_2-7 and CH_2-8, and also shows the connectivity from H–C-3 to H–C-6.

The HMBC spectral data (Fig. 2.7) of **II** shows the following correlations; H–C-3 to C-1; both H–C-4 and H–C-6 to C-2; H–C-5 to C-1 and C-3; CH_2-7 to C-1, C-3, and C-3′; CH_2-8 to C-2 and C-4′; the 6′-Me H-atoms to C-1′, C-5′ and C-6′; the 5′-OMe H-atoms to C-5′; CH_2-1″ to C-1′, C-2′, C-3′, C-2″ and C-3″; H–C-2″ to C-2′, C-4″ and C-5″; and both Me-4″ and Me-5″ to C-2″ and C-3″.

The NOESY spectrum (Fig. 2.9) of compound **II** shows cross peak

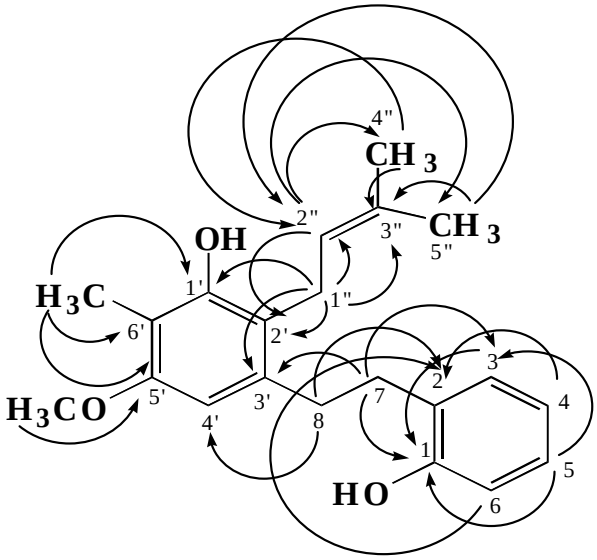

The curved arrows show HMBC correlations of compound II

between H–C-2″ and Me-4″, but none between H–C-2″ and Me-5″, and indicates the correlations of the 5′-OMe H-atoms to H–C-4′ and the 6′-Me H-atoms. Further, the NOESY spectrum also reveals the close proximity between CH_2-8 and H–C-4′; CH_2-8 and CH_2-1″; and CH_2-7 and H–C-3.

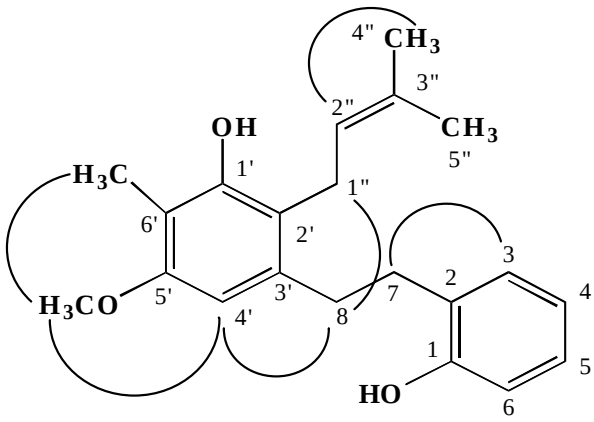

The curved lines show NOESY correlations of compound II

On the basis of these spectral data, compound **II** is a prenyl derivative

of compound **I**, and identified as 3-[2-(2-hydroxyphenyl)ethyl]-5-methoxy-6-methyl-2-(3-methylbut-2-enyl)phenol. The complete assignment of the H- and C- atoms for compound **II** is shown in Table 4.2.

Table 4.2 The ^{1}H- and ^{13}C-NMR spectral data of compound II at 500 and 125 MHz, respectively in $CDCl_3$ (*J* in Hz).

	δ (ppm)	
	^{1}H	**^{13}C**
C-1	–	153.73
C-2	–	127.90
H–C-3	7.13 (*dd*, *J* = 7.30, 1.50)	130.40
H–C-4	6.90 (*td*, *J* = 7.50, 0.90)	121.00
H–C-5	7.12 (*td*, *J* = 7.70, 1.70)	127.42
H–C-6	6.77 (br *d*, *J* = 8.00)	115.50
CH_2-7	2.86 (*m*)	32.60
CH_2-8	2.92 (*m*)	34.40
C-1′	–	153.68
C-2′	–	117.50
C-3′	–	137.81
H–C-4′	6.31 (*s*)	104.40
C-5′	–	156.60
C-6′	–	110.83
CH_2-1″	3.38 (*d*, *J* = 6.90)	25.43
H–C-2″	5.12 (*td*, *J* = 5.50, 1.20)	122.93
C-3″	–	134.44
Me-4″	1.75 (*d*, *J* = 1.10)	25.81
Me-5″	1.84 (br *s*)	17.90
Me–C-6′	2.12 (*s*)	8.20
MeO–C-5′	3.78 (*s*)	55.60

4.2.2 Biological activities

Compound **II** possesses cytotoxicity against NCI-H187 and BC cell lines with IC_{50} values of 1.08 and 9.66 µg/mL, respectively, but is inactive towards the KB cell line at 20 µg/mL. It also demonstrates mild antifungal activity with IC_{50} value of 28.94 µg/mL and mild antimycobacterial activity with MIC value of 25 µg/mL. Further, it inhibits both COX-1 and COX-2 with IC_{50} values of 9.0 and 1.3 µg/mL, respectively. However, it exhibits no antimalarial activity at 20 µg/mL.

4.3 Compound III (bauhinol C, a new compound)

4.3.1 Structure elucidation

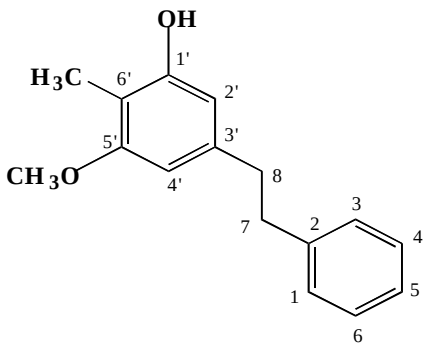

III
(Arbitrary atom numbering)

Compound **III** was obtained as brown viscous liquid from the root extract of *B. saccocalyx*. The molecular formula is assigned as $C_{16}H_{18}O_2$ by means of the ESI-TOF mass spectrometry (Fig. 3.1), which reveals the molecular ion peak at *m/z* 243.1337 ($[M + H]^+$, 243.138 calculated for $[C_{16}H_{19}O_2]^+$). The infrared spectrum (Fig. 3.2) of **III** shows absorption peaks (ν_{max}) at 3448 cm^{-1} (broad, O–H stretching), 2934 cm^{-1} (saturated C–H stretching), 1618, 1507 and 1456 cm^{-1}(C=C stretching of a benzene ring), 1420 cm^{-1} (C–H deformation of methylene group), 1112 cm^{-1} (C–O stretching of –C–OH), and 700 and 760 cm^{-1} (=C–H out of plane bending of a mono-

substituted benzene ring). The UV-Vis spectrum (Fig. 3.3) shows absorption peaks (λ_{max}) at 205 and 278 nm.

The ^{13}C-NMR spectrum (Fig. 3.5) of compound **III** shows 16 signals, which are classified by DEPT and HMQC spectra (Figs. 3.5 and 3.6), as seven methines, two methylenes, two methyls, and five quaternary carbon atoms. The downfield C-1′ signal at δ_C 154.00 ppm, together with the IR absorption peak at 3448 cm^{-1} (broad), suggests the presence of a hydroxyl group attached to an sp^2 carbon atom.

The ^{1}H- and ^{13}C-NMR resonances of CH_2 groups at δ_H 2.87 ppm and δ_C 37.87 ppm, and δ_H 2.94 ppm and δ_C 37.90 ppm show a characteristic of the bibenzyl moiety in **III**. Analyses of ^{1}H- and ^{13}C-NMR spectral data (Figs. 3.4 and 3.5) readily reveal the replacement of the 1,2-substituted benzene rings in compound **I** and compound **II** with a mono-substituted benzene ring in compound **III**. Additionally, the ^{1}H- and ^{13}C-NMR spectral data indicate the replacement of the 2′-prenyl group of compound **II** with an aromatic H-atom (δ_H 6.32 ppm, br *s*).

The HMBC spectral data (Fig. 3.7) clearly establish the gross structure of compound **III** by the correlations of H-C-1 (or H–C-3) to C-7; H–C-3 (or H–C-1) to C-5; H–C-4 to C-2; H–C-5 to C-1 and C-3; H–C-6 (or H–C-4) to C-2; CH_2-7 to C-1 (or C-3) and C-3′; CH_2-8 to C-2, C-2′ and C-4′; H–C-4′ to C-2′, C-6′, and C-8; the 5′-OMe H-atoms to C-5′; and the 6′-Me H-atoms to C-1′, C-5′, and C-6′.

The ^{1}H,^{1}H-COSY spectrum (Fig. 3.8) of compound **III** shows the correlation between H–C-2′ and H–C-4′, whose broad singlet implies *meta* coupling. The ^{1}H,^{1}H-COSY spectrum also reveals the correlation of CH_2-7 and CH_2-8, as well

as correlations among methine H-atoms of the mono-substituted benzene ring.

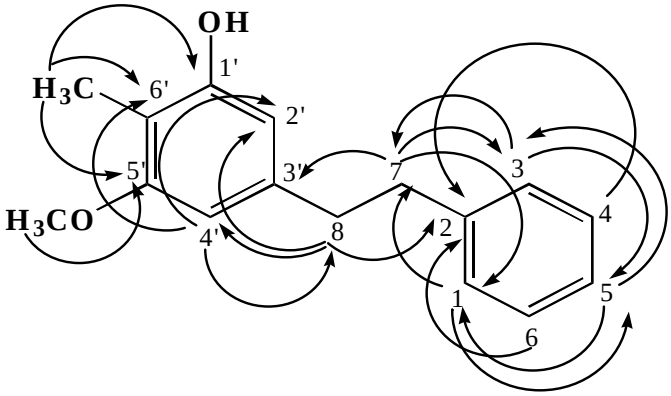

The curved arrows show HMBC correlations of compound III

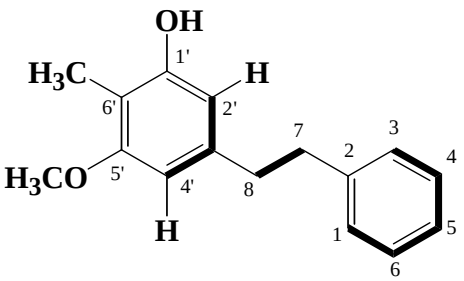

The bold lines show connectivities from ^{1}H,^{1}H-COSY spectrum of compound III

The NOESY spectrum (Fig. 3.9) exhibits cross peaks between CH_2-7 and H–C-2′; H–C-4′ and the 5′-OMe H-atoms; CH_2-8 and H–C-4′; and the 5′-OMe H-atoms and the 6′-Me H-atoms.

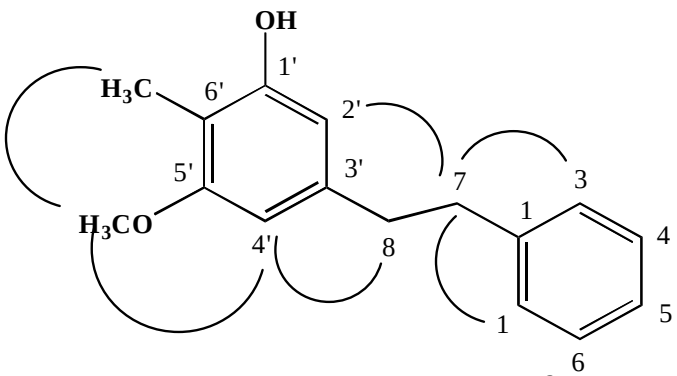

The curved lines show NOESY correlations of compound III

Based on these spectral data, compound **III** is identified as 3-methoxy-2-methyl-5-(2-phenylethyl)phenol. The complete assignment of the H- and C- atoms for **III** is shown in Table 4.3.

Table 4.3 The ^{1}H- and ^{13}C-NMR spectral data of compound III at 500 and 125 MHz, respectively in $CDCl_3$ (*J* in Hz).

	δ (ppm)	
	^{1}H	^{13}C
H–C-1	7.24 (*m*)	128.47
C-2	–	141.80
H–C-3	7.24 (*m*)	128.47
H–C-4	7.33 (*m*)	128.31
H–C-5	7.33 (*m*)	125.96
H–C-6	7.33 (*m*)	128.31
CH_2-7	2.94 (*m*)	37.90
CH_2-8	2.87 (*m*)	37.87
C-1′	–	154.00
H–C-2′	6.32 (*br s*)	103.57
C-3′	–	140.70
H–C-4′	6.36 (*br s*)	108.06
C-5′	–	158.70
C-6′	–	110.00
Me–C-6′	2.13 (*s*)	7.82
MeO–C-5′	3.82 (*s*)	55.70

4.3.2 Biological activities

The biological activities of **III** were not evaluated due to the limited amount of compound isolated.

4.4 Compound IV (bauhinol D, a new compound)

4.4.1 Structure elucidation

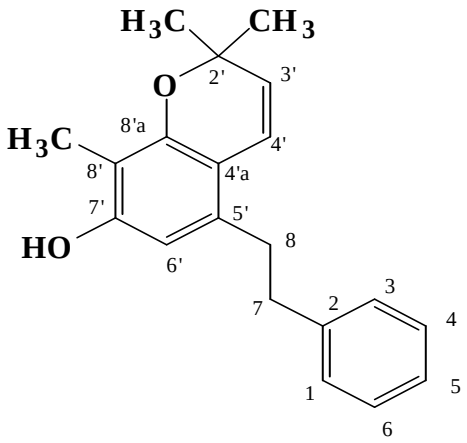

IV
(Arbitrary atom numbering)

Compound **IV** was obtained as yellow viscous liquid form the root extract of *B. saccocalyx*. Since it was not very stable in a solution, all necessary spectral data had to be collected rapidly. The pseudo-molecular ion of **IV** could not be observed in the ESI-TOF mass spectrum, possibly due to the unstable nature of the molecule. Analysis of ^{1}H- and ^{13}C-NMR, DEPT (Figs. 4.3 and 4.4) and HMQC spectral data (Fig. 4.5), as well as analogous correlation of NMR data of **IV** with those of compounds **I-III**, readily establish the molecular formula of compound **IV** as $C_{20}H_{22}O_2$.

The infrared spectrum (Fig. 4.1) of **IV** shows absorption peaks (ν_{max}) at 3444 cm^{-1} (broad O–H stretching), 2926 cm^{-1} (C–H stretching), 1603 and 1496 cm^{-1} (C=C stretching of an aromatic ring), 1455 cm^{-1} (C–H deformation of methylene group), 1419 cm^{-1} (O–H bending), 1103 cm^{-1} (C–O stretching of –C–OH), and 699 and 750 cm^{-1} (=C–H out of plane bending of a mono-substituted benzene ring). The UV-Vis spectrum (Fig. 4.2) of compound **IV** shows absorption peaks (λ_{max}) at 210, 234, 284, and 316 nm.

The ^{1}H-NMR spectrum (Fig. 4.3) of compound **IV** reveals signals of a dimethylchromene unit [at δ_H 6.45 ppm (*d*, *J* = 10.0 Hz), 5.50 ppm (*d*, *J* = 10.0 Hz), and 1.40 ppm (*s*, 2Me)], and two downfield methylene groups [at δ_H 2.82 ppm (*m*, 4H)], suggesting that compound **IV** is a (phenylethyl)-substituted dimethylchromene. An aromatic singlet at δ_H 6.17 ppm for H–C-6′ reveals the presence of the triply substituted benzene ring of the chromene unit in **IV**.

The ^{13}C-NMR spectrum (Fig. 4.4) of compound **IV** shows 20 signals, which are classified by DEPT and HMQC spectra (Figs. 4.4 and 4.5), as eight methines, two methylenes, three methyls, and seven quaternary carbon atoms. The downfield C-7′ carbon signal at δ_C 153.90 ppm, together with the IR absorption peak at 3444 cm^{-1} (broad), suggests the presence of a hydroxyl group attached to an sp^2 carbon atom. The downfield C-2′ signal at δ_C 75.40 ppm is if an oxygenated sp^3 quaternary carbon atom attached to the geminal dimethyl group of the chromene unit.

Analysis of ^{1}H- and ^{13}C-NMR spectral data reveals that compound **IV** is a desmethyl derivative of compound **I** by the replacement of the methoxy group with a hydroxyl group at C-7′ in compound **IV**. In addition, the 1,2-disubstituted benzene ring of compound **I** is replaced with a mono-substituted benzene ring in compound **IV**.

The HMBC spectral data (Fig. 4.6) readily confirm the gross structure of compound **IV** by showing the correlations of H–C-1 and H–C-3 to C-7; both H–C-4 and H–C-6 to C-2; H–C-5 to C-1 and C-3; CH_2-7 to C-1 and C-3; CH_2-8 to C-2, C-4′a, and C-6′; the 2′-Me H-atoms to C-2′, C-3′, and C-4′; H–C-3′ to C-2′ and C-4′a; H–C-6′ to C-8 and C-4′a; and the 8′-Me H-atoms to C-7′, C-8′ and C-8′a.

The ^{1}H,^{1}H-COSY spectrum (Fig. 4.7) of compound **IV** reveals

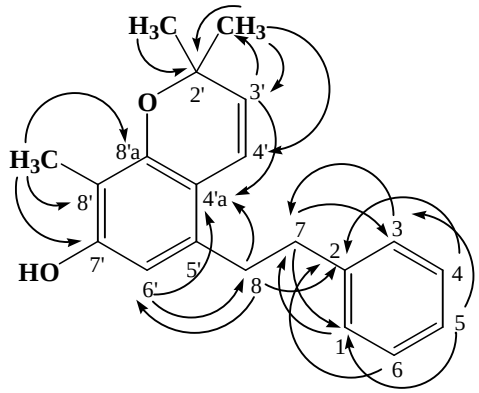

The curved arrows show HMBC correlations of compound IV

between H–C-3′ and H–C-4′ in the chromene unit; correlations between CH_2-7 and CH_2-8; and correlations among H-atoms in the mono-substituted benzene ring.

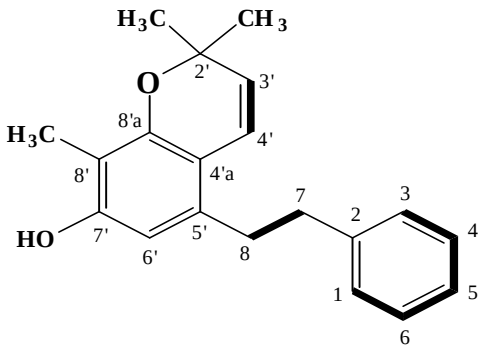

The bold lines show connectivities from ^{1}H,^{1}H-COSY spectrum of compound IV

The NOESY spectral data (Fig. 4.8) of compound **IV** show cross peaks between the 2′-geminal dimethyl H-atoms and the 8′-Me H-atoms and H–C-3′; H–C-6′ and CH_2-8; CH_2-7 and H–C-3 (or H–C-1); and CH_2-8 and H–C-4′.

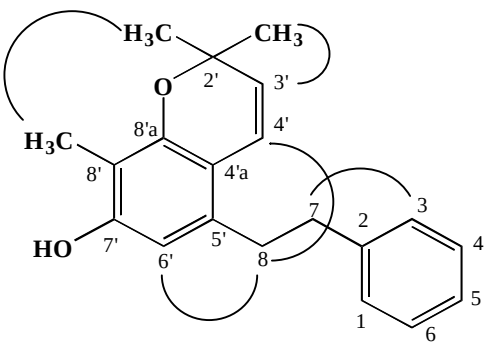

The curved lines show NOESY correlations of compound IV

On the basis of these spectral data, compound **IV** is identified as 2,2,8-trimethyl-5-(2-phenylethyl)-2*H*-1-benzopyran-7-ol. The complete assignment of the H- and C-atoms of compound **IV** is shown in Table 4.4.

Table 4.4 The ^{1}H- and ^{13}C-NMR spectral data of compound IV at 400 and 125 MHz, respectively in $CDCl_3$ (*J* in Hz).

	δ (ppm)	
	^{1}H	**^{13}C**
H–C-1	7.17 (br *d*, *J* = 6.80)	128.40
C-2	–	141.70
H–C-3	7.17 (br *d*, *J* = 6.80)	128.40
H–C-4	7.28 (*m*)	128.30
H–C-5	7.18 (*m*)	125.93
H–C-6	7.28 (*m*)	128.30
CH_2-7	2.82 (*m*)	37.50
CH_2-8	2.82 (*m*)	34.20
C-2′	–	75.40
H–C-3′	5.50 (*d*, *J* = 10.0)	127.64
H–C-4′	6.45 (*d*, *J* = 10.0)	119.20
C-4′a	–	112.60
C-5′	–	135.50
H–C-6′	6.17 (*s*)	108.00
C-7′	–	153.90
C-8′	–	109.70
C-8′a	–	152.20
Me–C-2′	1.40 (*s*)	27.70
Me–C-2′	1.40 (*s*)	27.70
Me–C-8′	2.07 (*s*)	7.70

4.4.2 Biological activities

The biological activities of compound **IV** could not be observed due to the unstable nature of the molecule.

4.5 Compound V (methyldihydropinosylvin, a known compound)

4.5.1 Structure elucidation

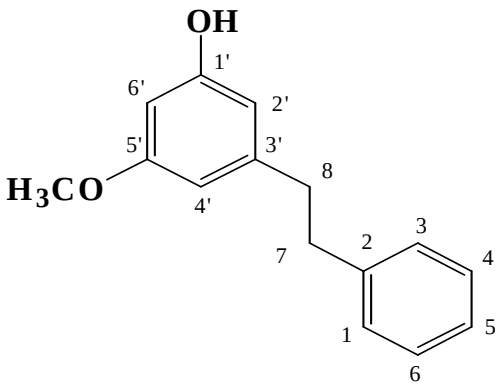

V
(Arbitrary atom numbering)

Compound **V** was obtained as pale yellow viscous liquid from the root extract of *B. saccocalyx*. The ESI-TOF-MS spectrum (Fig. 5.1) of compound **V** shows an exact mass at *m/z* 251.1047 ($[M + Na]^+$, 251.1048 calculated for $[C_{15}H_{16}O_2 + Na^+]$), establishing a molecular formula as $C_{15}H_{16}O_2$.

The infrared spectrum (Fig. 5.2) of compound **V** shows absorption peaks (ν_{max}) at 3449 cm^{-1} (broad O–H stretching), 1599 and 1497 cm^{-1} (C=C stretching of an aromatic ring), 1456 cm^{-1} (C–H deformation of methylene group), 1151 cm^{-1} (C–O stretching of –C–OH group), and 698 and 750 cm^{-1} (=C–H out of plane bending of a mono-substituted benzene ring).

The UV-Vis spectrum (Fig. 5.3) of compound **V** shows absorption peaks (λ_{max}) at 205, 229 and 280 nm.

The ^{1}H-NMR spectral data (Fig. 5.4) of compound **V** reveal signals of two adjacent methylene groups at δ_H 2.95 ppm (*m*) for CH_2-7 and 2.89 ppm (*m*) for CH_2-8, methoxy H-atoms at 3.80 ppm (*s*) for 5′-OMe, aromatic H-atoms at 6.28 ppm (*t*, *J* = 2.24 Hz) for H–C-4′, 6.29 ppm (*t*, *J* = 1.70 Hz) for H–C-6′, 6.34 ppm (*t*, *J* = 1.65 Hz) for H–C-2′, 7.22 ppm (*td*, *J* = 7.68 and 1.15 Hz) for H–C-5, 7.31 ppm (*dd*, *J* = 7.20 and 1.60 Hz) for H–C-1 and H–C-3, and 7.33 ppm (*d*, *J* = 1.50 Hz) for H–C-4 and H–C-6, respectively.

The ^{13}C-NMR spectrum (Fig. 5.5) of compound **V** shows 15 signals, which are classified by DEPT and HMQC spectra (Figs. 5.5 and 5.6), as eight methines, two methylenes, one methyl, and four quaternary carbon atoms. The downfield signals at δ_C 156.56 and 160.93 ppm indicate the presence of two oxygenated sp^2 quaternary carbon atoms, and the IR absorption peak at 3449 cm^{-1} (broad) reveals the presence of a hydroxyl group in **V**.

The ^{1}H-NMR spectrum (Fig. 5.4) of **V** reveals characteristics of bibenzyl methylenes at δ_H 2.95 ppm (*m*) for CH_2-7, and 2.89 ppm (*m*) for CH_2-8 in **V**.

The HMBC spectrum (Fig. 5.7) of compound **V** conclusively establishes the bibenzyl molecular structure, exhibiting the correlations of H–C-1 (or H–C-3) to C-5 and C-7; CH_2-7 to C-1 (or C-3) and C-3′; CH_2-8 to C-2, C-2′ and C-4′; H–C-6′ to C-2′ and C-4′; and the 5′-OMe H-atoms to C-5′.

The ^{1}H,^{1}H-COSY spectrum (Fig. 5.8) of compound **V** reveals *ortho* couplings among H–C-2′, H–C-4′, and H–C-6′; couplings among H-atoms on a mono-substituted benzene ring; and couplings between CH_2-7 and CH_2-8.

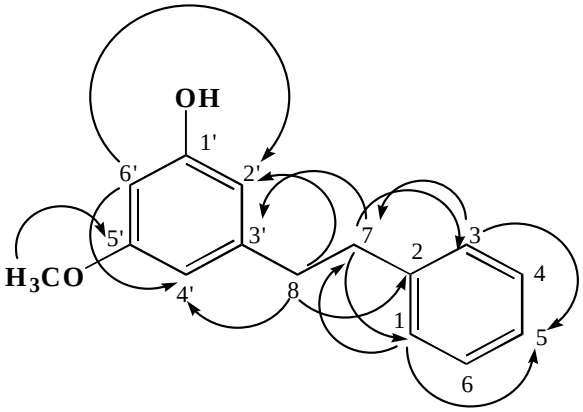

The curved arrows show HMBC correlations of compound V

From literature search, compound **V** is a known compound, identified as methyldihydropinosylvin (Hanawa, Yamada, and Nakashima, 2001), which was previously isolated from the bark of *Pinus strobus*. The ^{1}H- and ^{13}C-NMR spectral data of **V** are in good agreement with those reported in the literature (Hanawa, et al., 2001).

The ^{1}H- and ^{13}C-NMR spectral data of compound **V** and methyl-dihydropinosylvin are shown in Table 4.5.

4.5.2 Biological activities

The biological activity of compound **V** could not be evaluated, due to the limited amount of the isolated compound.

Table 4.5 The ^{1}H- and ^{13}C-NMR spectral data of compound V (at 500 and 125 MHz, respectively) and methyldihydropinosylvin in $CDCl_3$ (*J* in Hz).

	δ (ppm)			
	Compound V		**Methyldihydropinosylvin**	
	^{1}H	**^{13}C**	**^{1}H**	**^{13}C**
C-1′	–	156.56	–	159.40
H–C-2′	6.34 (*t*, J = 1.65)	106.87	6.22 (*br t*, J = 2.00)	109.00
C-3′	–	144.59	–	145.10
H–C-4′	6.28 (*t*, J = 2.24)	107.97	6.20 (*br t*, J = 1.80)	106.50
C-5′	–	160.93	–	162.20
H–C-6′	6.29 (*t*, J = 1.70)	99.10	6.16 (*t*, J = 2.10)	99.90
H–C-1	7.31 (*dd*, J = 7.20, 1.60)	128.39	7.14 (*m*)	129.50
C-2	–	141.68	–	143.10
H–C-3	7.31 (*dd*, J = 7.20,1.60)	128.39	7.14 (*m*)	129.50
H–C-4	7.33 (*d*, J = 1.50)	128.48	7.22 (*t*, J = 7.50)	129.30
H–C-5	7.22 (*td*, J = 7.68, 1.15)	126.00	7.14 (*m*)	126.80
H–C-6	7.33 (*d*, J = 1.50)	128.48	7.22 (*t*, J = 7.50)	129.30
CH_2-7	2.95 (*m*)	37.60	2.76 (*dd*, J = 9.30, 6.00)	39.30
CH_2-8	2.89 (*m*)	37.98	2.85 (*dd*, J = 9.30, 6.00)	38.90
MeO–C-5′	3.80 (*s*)	55.30	3.68 (*s*)	55.50

4.6 Compound VI (3,5-dihydroxy-2-(3-methyl-2-butenyl)bibenzyl, a known compound)

4.6.1 Structure elucidation

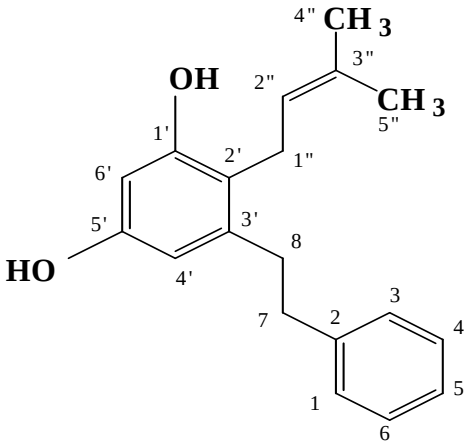

VI

(Arbitrary numbering)

Compound **VI** was obtained as brown viscous liquid from the root extract of *B. saccocalyx*. The exact mass at *m/z* 283.1706 ($[M + H]^+$, 283.1698 calculated for $[C_{19}H_{22}O_2 + H]^+$) obtained from the ESI-TOF-MS spectrum (Fig. 6.1) establishes the molecular formula of compound **VI** as $C_{19}H_{22}O_2$.

The infrared spectrum (Fig. 6.2) of compound **VI** shows absorption peaks (ν_{max}) at 3356 cm^{-1} (broad O–H stretching), 3024 cm^{-1} (C–H stretching), 1624, 1589 and 1497 cm^{-1} (C=C stretching of an aromatic ring), 1282 cm^{-1} (O–H bending), 1126 cm^{-1} (C–O stretching), and 695 and 745 cm^{-1} (=C–H out of plane deformations of a mono-substituted benzene ring). The UV-Vis spectrum (Fig. 6.3) of **VI** shows absorption peaks (λ_{max}) at 208 and 283 nm.

The ^{1}H-NMR spectral data (Fig. 6.4) of compound **VI** reveal signals of methyl groups at δ_H 1.76 ppm (*s*) for H–C-4″ and 1.82 ppm (*s*) for H–C-5″, bibenzyl

methylene groups at 2.86 ppm (*s*) for CH_2-7 and CH_2-8, a methylene group at 3.34 ppm (*d*, *J* = 6.72 Hz) for H–C-1″, a methine group at 5.12 ppm (*t*, *J* = 6.80 Hz) for H–C-2″, and aromatic H-atoms at 6.27-7.34.

Analyses of ^{13}C-NMR, DEPT (Fig. 6.5) and HMQC (Fig. 6.6) spectral data of compound **VI** reveal the presence of eight methines, three methylenes, two methyls, and six quaternary carbon atoms. The downfield C-1′ and C-5′ signals at δ_C 155.72 and 154.49 ppm, together with the IR absorption peak at 3356 cm^{-1} (broad), indicate the presence of hydroxyl groups attached to sp^2carbon atoms.

Furthermore, the ^{1}H-NMR spectral data (Figs. 6.4) show a typical set of H-atom signals for a prenyl moiety; a methylene at δ_H 3.34 ppm (*d*, *J* = 6.72 Hz) for H–C-1″, a methine at 5.12 ppm (*t*, *J* = 6.80 Hz) for H–C-2″, and methyls at 1.76 and 1.82 ppm for H–C-4″ and H–C-5″, respectively.

The ^{1}H,^{1}H-COSY spectrum (Fig. 6.8) of compound **VI** reveals the correlations between H–C-1″ and H–C-2″, as well as allylic couplings between both H–C-4″ and H–C-5″ and H–C-2″. The ^{1}H,^{1}H-COSY spectrum of compound **VI** also shows couplings between H–C-4′ and H–C-6′, between CH_2-7 and CH_2-8, and among H-atoms in a mono-substituted benzene ring.

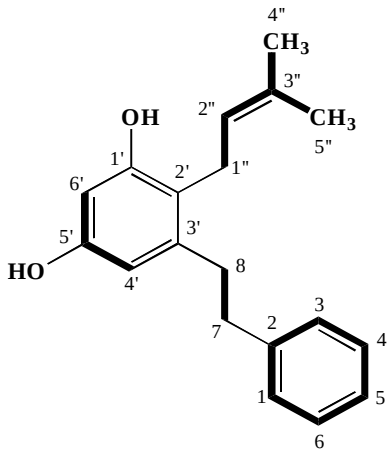

The bold lines show the connectivities from ^{1}H,^{1}H-COSY spectrum of compound VI

The HMBC spectrum (Fig. 6.7) of compound **VI** well establishes its gross structure by showing the correlations of H–C-1 (or H–C-3) to C-7; H–C-5 to C-1 and C-3; H–C-6 (or H–C-4) to C-2; CH_2-7 to C-1, C-3, and C-3′; CH_2-8 to C-2, C-2′ and C-4′; H–C-6′ to C-1′, C-2′, C-4′, and C-5′; H–C-1″ to C-3′, C-1′ and C-3″; H–C-2″ to C-2′; both H–C-4″and H–C-5″ to C-2″ and C-3″.

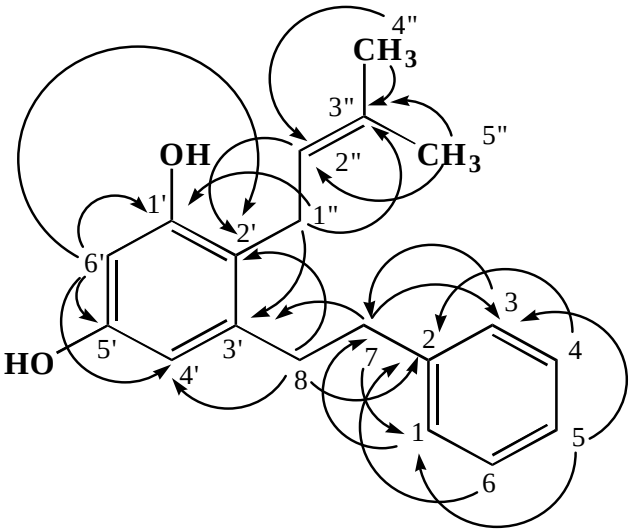

The curved arrows show HMBC correlations of compound VI

The NOESY spectrum (Fig. 6.9) of compound **VI** shows cross peaks between H–C-1 and CH_2-7; CH_2-8 and H-C-4′; H–C-4″ and H–C-5″; and H–C-4″ and H–C-2″ (but none between H–C-5″ and H-C-2″).

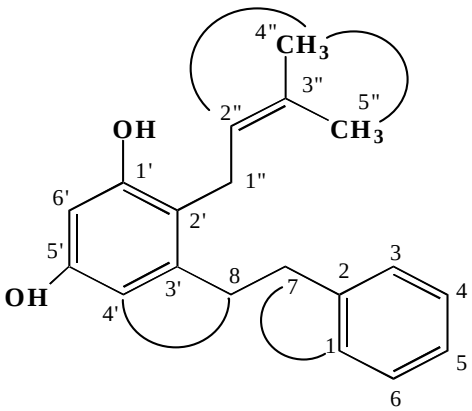

The curved lines show NOESY correlations of compound VI

On the basis of these spectral data, compound **VI** is identified as 3,5-dihydroxy-2-(3-methyl-2-butenyl)bibenzyl (Asakawa, Hashimoto, Takikawa, Tori, and Ogawa, 1991), which was previously isolated from the liverwort *Radula kojana*. The ^{1}H- and ^{13}C-NMR spectral data of compound **VI** and 3,5-dihydroxy-2-(3-methyl-2-butenyl)bibenzyl are shown in Table 4.6.

4.6.2 Biological activities

Compound **VI** exhibits cytotoxicity towards NCI-H187 and BC cell lines with IC_{50} values of 14.10 and 4.0 μg/mL, respectively, but is inactive towards the KB cell line with IC_{50} at 20 μg/mL. It also shows mild antifungal activity with IC_{50} value of 11.7 μg/mL and mild antimycobacterial activity against *Mycobacterium tuberculosis* H37Ra with MIC value of 25 μg/mL. In addition, it inhibits both COX-1 and COX-2 with IC_{50} values of 2.5 μg/mL and 1.8 μg/mL, respectively. However, it shows no antimalarial activity at 20 μg/mL.

Table 4.6 The ^{1}H- and ^{13}C-NMR spectral data of compound VI (at 500 and 125 MHz, respectively) and 3,5-dihydroxy-2-(3-methyl-2-butenyl)bibenzyl in $CDCl_3$ (*J* in Hz).

	δ (ppm)			
	Compound VI		**3,5-Dihydroxy-2-(3-methyl-2-butenyl)bibenzyl**	
	^{1}H	**^{13}C**	**^{1}H**	**^{13}C**
H–C-1	7.28 (*dt*, *J* = 7.39, 1.61)	128.46	7.17 (*m*)	128.40
C-2	–	141.77	–	141.70
H–C-3	7.28 (*dt*, *J* = 7.39, 1.61)	128.46	7.17 (*m*)	128.40
H–C-4	7.34 (*td*, *J* = 7.56, 1.55)	128.47	7.28 (*m*)	128.40
H–C-5	7.22 (*m*)	126.06	7.19 (*m*)	126.00
H–C-6	7.34 (*td*, *J* = 7.56, 1.55)	128.47	7.28 (*m*)	128.40
CH_2-7	2.86 (*s*)	37.59	2.83 (*s*)	37.50
CH_2-8	2.86 (*s*)	35.68	2.83 (*s*)	35.70
C-1′	–	155.72	–	155.70
C-2′	–	117.68	–	117.60
C-3′	–	142.17	–	142.10
H–C-4′	6.30 (*d*, *J* = 2.57)	108.95	6.26 (*d*, *J* = 2.40)	108.90
C-5′	–	154.49	–	154.40
H–C-6′	6.27 (*d*, *J* = 2.55)	101.47	6.23 (*d*, *J* = 2.40)	101.40
CH_2-1″	3.34 (*d*, *J* = 6.72)	24.94	3.28 (*d*, *J* = 6.40)	24.90
H–C-2″	5.12 (*t*, *J* = 6.80)	122.71	5.09 (*t*, *J* = 6.40)	122.60
C-3″	–	134.15	–	134.20
Me-4″	1.76 (*s*)	25.78	1.72 (*s*)	25.70
Me-5″	1.82 (*s*)	18.00	1.79 (*s*)	18.00

4.7 Compound VII (bauhinoxepin A, a known compound)

4.7.1 Structure elucidation

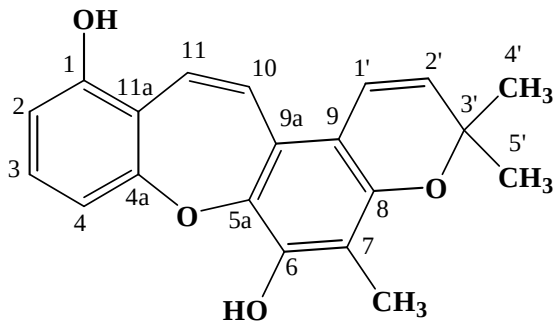

VII

(Arbitrary atom numbering)

Compound **VII** was obtained as colorless solid from the roots of *B. saccocalyx*. According to the mass and ^{1}H-NMR spectra of compound **VII** (Figs. 7.1 and 7.3), it is identified as bauhinoxepin A, which was previously isolated from the roots of *B. saccocalyx* (Kittakoop, et al., 2004). The ^{1}H-NMR spectral data of compound **VII** and bauhinoxepin A are shown in Table 4.7.

Table 4.7 The ^{1}H-NMR spectral data of compound VII and bauhinoxepin A at 500 MHz in $CDCl_3$ (*J* in Hz).

	δ (ppm)	
	Compound VII	**Bauhinoxepin A**
H–C-2	6.60 (*d*, *J* = 7.96)	6.61 (*d*, *J* = 7.90)
H–C-3	7.15 (*t*, *J* = 7.83)	7.12 (*t*, *J* = 8.10)
H–C-4	6.75 (*d*, *J* = 7.97)	6.74 (*d*, *J* = 8.00)
H–C-10	6.95 (*d*, *J* = 10.26)	6.96 (*d*, *J* = 11.70)
H–C-11	7.00 (*d*, *J* = 11.65)	7.00 (*d*, *J* = 11.70)
Me-7	2.14 (*s*)	2.14 (*s*)
H–C-1′	6.47 (*d*, *J* = 10.25)	6.49 (*d*, *J* = 10.00)
H–C-2′	5.58 (*d*, *J* = 10.00)	5.58 (*d*, *J* = 10.00)
Me-4′	1.40 (*s*)	1.41 (*s*)
Me-5′	1.40 (*s*)	1.41 (*s*)
HO–C-1	5.55 (br *s*)	5.50 (br *s*)
HO–C-6	6.15 (br *s*)	6.15 (br *s*)

4.8 Compound VIII (bauhinoxepin B, a known compound)

4.8.1 Structure elucidation

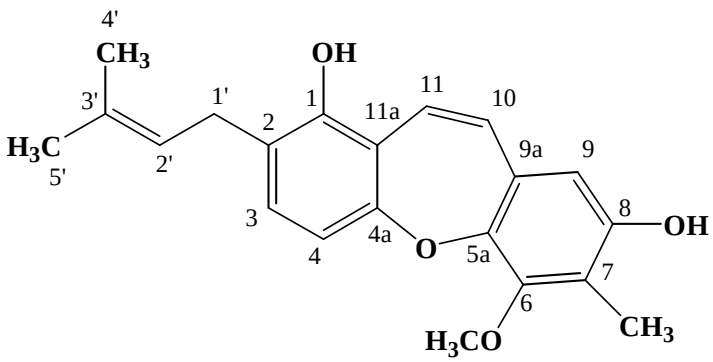

VIII
(Arbitrary atom numbering)

Compound **VIII** was obtained as colorless solid from the roots of *B. saccocalyx*. According to the mass and ^{1}H-NMR spectra of compound **VIII** (Figs. 8.1 and 8.3), it is identified as bauhinoxepin B, which was previously isolated from the roots of *B. saccocalyx* (Kittakoop, et al. 2004). The ^{1}H-NMR spectral data of compounds **VIII** and bauhinoxepin B are shown in Table 4.8.

Table 4.8 The ^{1}H-NMR spectral data of compound VIII and bauhinoxepin B at 500 and 125 MHz, respectively in $CDCl_3$ (*J* in Hz).

	δ (ppm)	
	Compound VII	**Bauhinoxepin B**
H–C-3	7.00 (*d*, *J* = 8.26)	6.99 (*d*, *J* = 8.30)
H–C-4	6.50 (*d*, *J* = 8.30)	6.50 (*d*, *J* = 8.30)
H–C-9	6.31 (*s*)	6.30 (*s*)
H–C-10	6.55 (*d*, *J* = 11.42)	6.54 (*d*, *J* = 11.50)
H–C-11	6.95 (*d*, *J* = 11.43)	6.90 (*d*, *J* = 11.50)
CH_2-1′	3.74 (*d*, *J* = 7.25)	3.73 (*d*, *J* = 7.30)
H–C-2′	5.47 (*t*, *J* = 7.30)	5.41 (br *t*, *J* = 7.30)
Me-4′	1.74 (*s*)	1.75 (*s*)
Me-5′	1.77 (*s*)	1.78 (*s*)
MeO–C-6	3.90 (*s*)	3.92 (*s*)
Me–C-7	2.20 (*s*)	2.19 (*s*)
HO–C-1	5.34 (br *s*)	5.25 (br *s*)
HO–C-8	5.13 (br *s*)	5.05 (br *s*)

4.9 Compound IX (pinoresinol, a known compound)

4.9.1 Structure elucidation

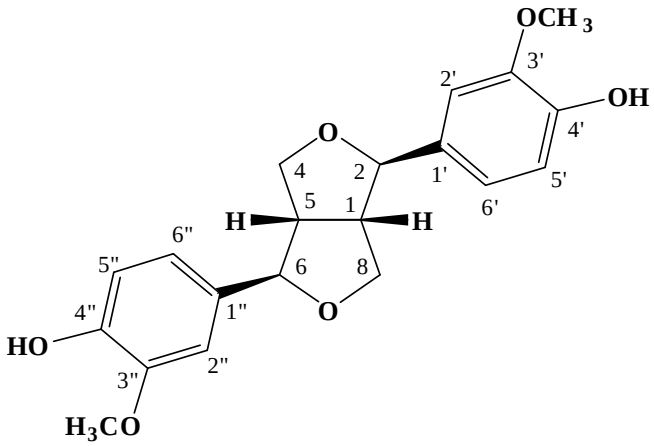

IX
(Arbitrary atom numbering)

Compound **IX** was obtained as yellow solid from the stem bark extract of *F. fragrans*. The molecular formula $C_{20}H_{22}O_6$ is established by the ESI-TOF mass spectrum (Fig. 9.1), with the exact mass at *m/z* 381.1311 $[M + Na]^+$, 381.1314 calculated for $[C_{20}H_{22}O_6 + Na]^+$).

The infrared spectrum (Fig. 9.2) of **IX** shows absorption peaks (ν_{max}) at 3406 cm^{-1} (broad O–H stretching), 1604 and 1517 cm^{-1}(C=C stretching of an aromatic ring), 1463 cm^{-1}(C–H deformation of methylene group), 1272 cm^{-1}(O–H bending), 1031 cm^{-1}(C–O stretching), and 1022 cm^{-1} and 776 cm^{-1}(O–H out of plane). The UV-Vis spectrum (Fig. 9.3) of compound **IX** exhibits absorption peaks (λ_{max}) at 205, 230, and 280 nm.

The ^{1}H- and ^{13}C-NMR spectral data of compound **IX** are not complicated. Its ^{13}C-NMR spectrum (Fig. 9.5) shows only 10 lines, while its mass from the mass spectrum indicates the presence of 20 carbon atoms in **IX**. Therefore, the molecular structure of compound **IX** is symmetrical with C-2 symmetry. The ^{1}H-

NMR spectrum (Fig. 9.4) of **IX** shows signals of a downfield methine at δ_H 3.12 ppm, an oxygenated methine at 4.75 ppm, non-equivalent methylenes at 3.80 and 4.24 ppm, a singlet methyl ether at 3.91 ppm, and three aromatic H-atoms at 6.82-6.85 ppm.

Analysis of ^{13}C-NMR and DEPT spectral data (Fig. 9.5) of compound **IX** reveals the presence of ten methines, two methylenes, two methyls, and six quaternary carbon atoms.

The ^{1}H,^{1}H-COSY spectrum (Fig. 9.8) of compound **IX** shows the correlations between H–C-1 (or H–C-5) and H–C-2 (or H–C-6); between H–C-1 (or H–C-5) and CH_2-8 (or CH_2-4); and between aromatic H-atoms: H–C-2′ (or H–C-2″) and H–C-6′ (or H–C-6″), and H–C-5′ (or H–C-5″) and H–C-6′ (or H–C-6″).

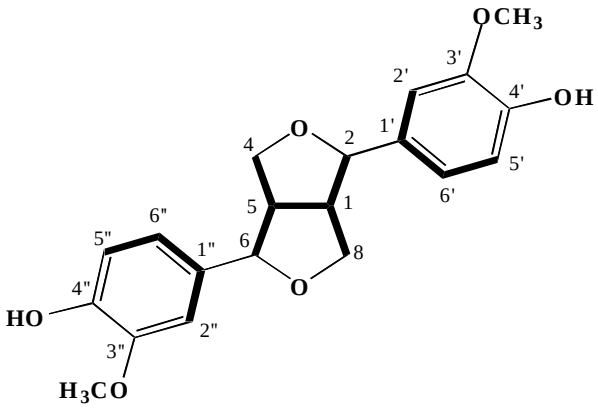

The bold lines show the connectivities from ^{1}H,^{1}H-COSY spectrum of compound IX

The HMBC spectral data (Fig. 9.7) of compound **IX** are very informative, concerning the assembly of the gross structure of **IX** by showing the ^{1}H, ^{13}C long range correlations of H–C-1 (or H–C-5) to C-1′ (or C-1″) and C-6 (or C-2); H–C-2 (or H–C-6) to C-1′ (or C-1″), C-2′ (or C-2″), C-6′ (or C-6″), C-5 (or C-1), and C-8 (or C-4); H–C-4 (or H–C-8) to C-1 (or C-5), and C-6 (or C-2); H–C-2′ (or H–C-2″) to C-4′ (orC-4″); H–C-5′ (or H–C-5″) to C-1′ (or C-1″), and C-3′ (or C-3″);

H–C-6′ (or H–C-6″) to C-2′ (or C-2″), and C-4′ (or C-4″); and the OMe-3′ H-atoms (or the OMe-3″ H-atoms) to C-3′ (or C-3″).

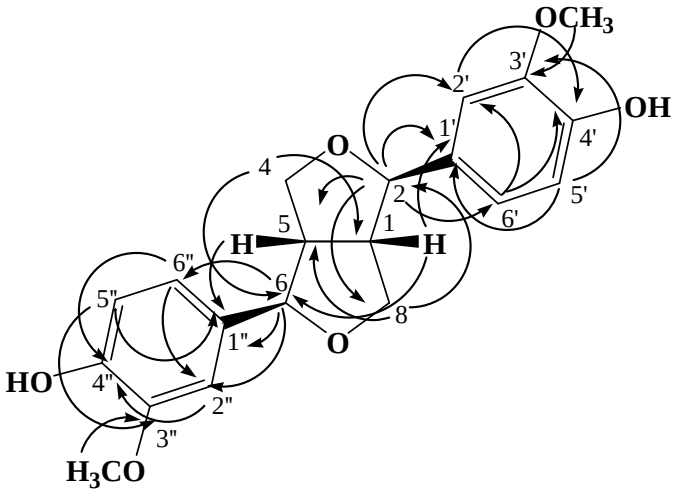

The curved arrows show HMBC correlations of compound IX

The NOESY spectrum (Fig 9.9) of compound **IX** shows cross peaks between H–C-1 (or H–C-5) and H–C-6′ (or H–C-6″); H–C-2 (or H–C-6) and CH_2-4 (or CH_2-8); the OMe-3′ H-atoms (or the OMe-3″ H-atoms) and H–C-2′ (or H-C-2″).

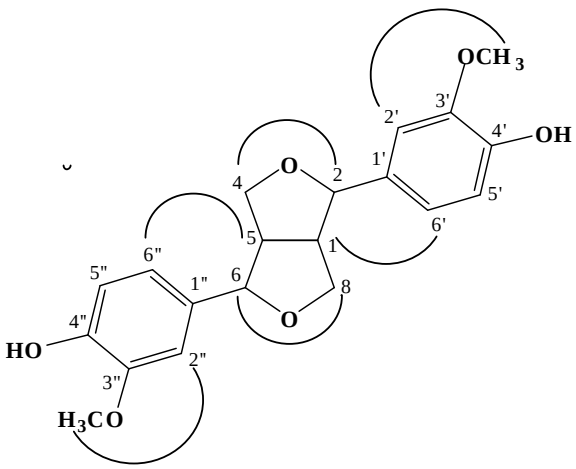

The curved lines show NOESY correlations of compound IX

Based upon these spectral data, compound **IX** is identified as pinoresinol, which was previously isolated from *Forsythia intermedia* (Rahman, Dewick, Jackson, and Lucas, 1990), *Fagraea racemosa* (Okuyama, Suzumura, and Yamazaki, 1995), and *Magnolia fargesii* (Miyazawa, Kasahara, and Kameoka, 1992). The ^{1}H- and ^{13}C-NMR spectral data of compound **IX** are in good agreement with those reported in the literature for pinoresinol (Miyazawa, et al., 1992), which are shown in Table 4.9. However, compound **IX** exhibits a specific rotation $[\alpha]_D^{24}$ (*c* = 0.99 in MeOH) of +61.63^{o}, while pinoresinol is reported to have a specific rotation $[\alpha]_D^{20}$ (*c* = 0.10 in MeOH) of +72^{o} (Okuyama, et al, 1995).

4.9.2 Biological activities

Compound **IX** exhibits antimalarial activity with IC_{50} value of 3.40 μg/mL and antimycobacterial activity *Mycobacterium tuberculosis* H37Ra with MIC value of 200 μg/mL. However, it is inactive at 20 μg/mL towards KB and BC cell lines and inactive at 50 μg/mL against *Candida albicans*.

Table 4.9 The ^{1}H-and ^{13}C-NMR spectral data of compound IX (at 500 and 125 MHz, respectively) and pinoresinol, in $CDCl_3$ (*J* in Hz).

	δ (ppm)			
	Compound IX		**Pinoresinol**	
	^{1}H	**^{13}C**	**^{1}H**	**^{13}C**
H–C-1	3.12 (*m*)	54.18	3.10 (*m*)	54.10
H–C-5	3.12 (*m*)	54.18	3.10 (*m*)	54.10
H–C-2	4.75 (*d*, *J* = 4.20)	85.94	4.74 (*d*, *J* = 5.00)	85.80
H–C-6	4.75 (*d*, *J* = 4.20)	85.94	4.74 (*d*, *J* = 5.00)	85.80
CH_2-4ax	3.80 (*d*, *J* = 7.00, 3.41)	71.71	3.87 (*dd*, *J* = 9.00, 4.00)	71.60
CH_2-4eq	4.24 (*m*)	71.71	4.24 (*dd*, *J* = 9.00, 7.00)	71.60
CH_2-8ax	3.80 (*d*, *J* = 7.00, 3.41)	71.71	3.87 (*dd*, *J* = 9.00, 4.00)	71.60
CH_2-8eq	4.24 (*m*)	71.71	4.24 (*dd*, *J* = 9.00, 7.00)	71.60
C-1′	–	132.93	–	132.90
C-1″	–	132.93	–	132.90
H–C-2′	6.95 (*s*)	108.74	6.94 (*s*)	108.60
H–C-2″	6.95 (*s*)	108.74	6.94 (*s*)	108.60
C-3′	–	146.81	–	146.70
C-3″	–	146.81	–	146.70
C-4′	–	145.33	–	145.20
C-4″	–	145.33	–	145.20
H–C-5′	6.85 (*m*)	114.39	6.88 (*m*)	114.30
H–C-5″	6.85 (*m*)	114.39	6.88 (*m*)	114.30
H–C-6′	6.82 (*m*)	119.03	6.82 (*m*)	118.90
H–C-6″	6.82 (*m*)	119.03	6.82 (*m*)	118.90
MeO–C-3′	3.91 (*s*)	56.01	3.90 (*s*)	55.90
MeO–C-3″	3.91 (*s*)	56.01	3.90 (*s*)	55.90

4.10 Compound X (naucledal, a known compound)

4.10.1 Structure elucidation

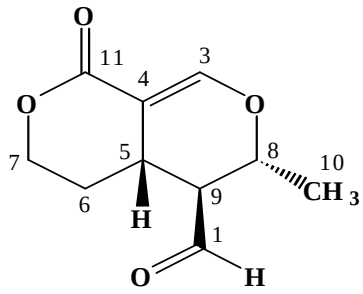

X

(Arbitrary atom numbering)

Compound **X** was obtained as yellow amorphous solid from the root extract of *F. fragrans*. The molecular formula $C_{10}H_{12}O_4$ is established by the ESI-TOF mass spectrum (Fig. 10.1), with the exact mass at *m/z* 219.0623 ($[M + Na]^+$, 219.0633 calculated for $[C_{10}H_{12}O_4 + Na]^+$).

The infrared spectrum (Fig. 10.2) of compound **X** shows absorption peaks (ν_{max}) at 3019 cm^{-1}(C–H stretching), 1704 cm^{-1}(C=O stretching of cyclic ester), 1475 cm^{-1}(C–H stretching of $–CH_2$), 1216 cm^{-1}(C–O–C stretching), and 772 cm^{-1} (C–O–C stretching). The UV-Vis spectrum (Fig. 10.3) of compound **X** shows absorption peaks (λ_{max}) at 203 and 247 nm.

The ^{1}H-NMR spectral data (Fig. 10.4) of compound **X** reveals signals of two adjacent methylene groups at δ_H 1.61-2.15 ppm (*m*) for CH_2-6 and 4.43-4.45 ppm (*m*) for CH_2-7, a methyl group at 1.50 ppm (*d*, *J* = 6.34 Hz) for CH_3-10, four methine groups at 2.38 ppm (*td*, *J* = 10.25 and 2.91 Hz) for H–C-9, 2.95 ppm (*tq*, *J* = 12.41 and 1.52 Hz) for H–C-5, 4.22 ppm (*dq*, *J* = 14.41 and 4.42 Hz) for H–C-8, and 7.80 ppm (*d*, *J* = 2.03 Hz) for H–C-3, and an aldehydic H-atom at 9.90 ppm (*d*, *J* = 1.89 Hz) for H–C(-1)=O.

The ^{13}C-NMR spectrum (Fig. 10.5) of compound **X** exhibits 10 signals, which are classified by DEPT and HMQC spectra (Figs. 10.5 and 10.6) as five methines, two methylenes, one methyl, and two quaternary carbon atoms. The downfield C-1 signal at δ_C 200.48 ppm is correlated to an aldehydic H-atom in the HMQC spectrum. The downfield C-11 signal at δ_C 165.00 ppm together with the IR absorption peak at 1704 cm^{-1} indicates the presence of an ester carbonyl group. In addition, the methylene CH_2-7 signal at δ_C 67.73 ppm and the H–C-8 signal at δ_C 73.12 ppm are of oxygenated sp^3 carbon atoms.

The ^{1}H,^{1}H-COSY spectrum (Fig. 10.8) of compound **X** exhibits the connectivities as shown below, revealing the connection from H–C(-1)=O to CH_3-10 through H–C-9 and H–C-8, and from H–C(-1)=O to CH_2-7 through H–C-9, H–C-5 and H–C-6.

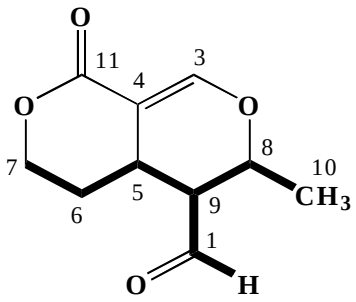

The bold lines show the connectivities from ^{1}H,^{1}H-COSY spectrum of compound X

The HMBC spectrum (Fig. 10.7) of compound **X** conclusively establishes the gross structure of **X** by exhibiting the correlations of H–C(-1)=O to C-5; H–C-3 to C-8 and C-11; H–C-5 to C-3; CH_2-7 to C-5 and C-11; and H–C-9 to C-6, and C-10.

The NOESY spectrum of compound **X** (Fig. 10.9) shows the

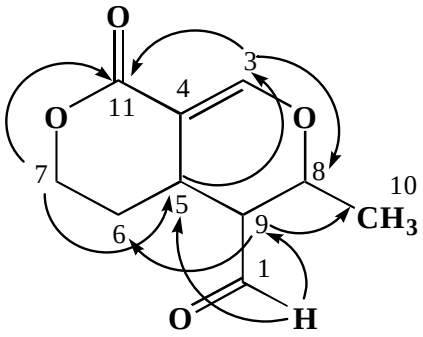

The curved arrows show HMBC correlations of compound X

correlation between H–C-5 and H–C-8, which confirms the *cis* relationship between them.

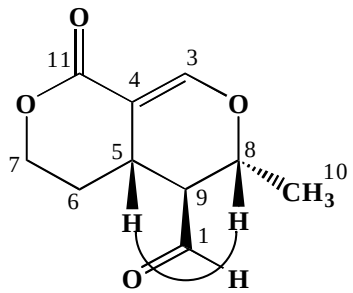

The curved lines show NOESY correlations of compound X

On the basis of these spectral data, together with the specific rotation $[\alpha]_D^{24}$ (c = 0.40 in MeOH) of –19.29^o of compound **X**, it is identified as (–)-naucledal, which was previously isolated from the bark of *Nauclea diderrichii* (Purdy and Mclean, 1977). Comparision of the ^{1}H-NMR spectral data of **X** with those reported in the literature (Purdy and Mclean, 1977) is shown in Table 4.10.

Table 4.10 The ^{1}H- and ^{13}C-NMR spectral data of compound X (at 500 and 125 MHz, respectively) and naucledal in $CDCl_3$ (*J* in Hz).

	δ (ppm)			
	Compound X		**Naucledal**	
	^{1}H	**^{13}C**	**^{1}H**	**^{13}C**
H–C(-1)=O	9.90 (*d*, *J* = 1.89)	200.48	9.90 (*d*, *J* = 2.80)	–
H–C-3	7.80 (*d*, *J* = 2.03)	155.83	7.73 (*d*, *J* = 2.0)	–
C-4	–	103.35	–	–
H–C-5	2.95 (*tq*, *J* = 12.41 and 1.52)	31.49	2.96 (*qd*, *J* = 12.00, 11.00, 4.00, and 2.00)	–
CH_2(a, b)-6	1.61-2.15 (*m*)	27.32	1.90-2.10 (*m*)	–
CH_2(a, b)-7	4.43-4.45 (*m*)	67.73	4.30-4.60 (*m*)	–
H–C-8	4.22 (*dq*, *J* = 14.41 and 4.42)	73.12	4.20 (*dq*, *J* = 10.00 and 6.00)	–
H–C-9	2.38 (*td*, *J* = 10.25 and 2.91)	55.70	2.36 (*td*, *J* = 11.00, 10.00, and 2.80)	–
Me-10	1.50 (*d*, *J* = 6.34)	19.32	1.44 (*d*, *J* = 6.00)	–
C-11	–	165.00	–	–

4.10.2 Biological activities

Compound **X** exhibits cytotoxicity towards NCI-H187 with IC_{50} value of 18.94 μg/mL, but is inactive towards the KB and BC cell lines at 20 μg/mL. It also demonstrates mild antimycobacterial activity against *Mycobacterium tuberculosis* H37Ra with MIC value of 200 μg/mL. However, it is inactive *in vitro* against the malarial parasite *Plasmodium falciparum* (at 20 μg/mL).

4.11 Compound XI (gentiogenal, a known compound)

4.11.1 Structure elucidation

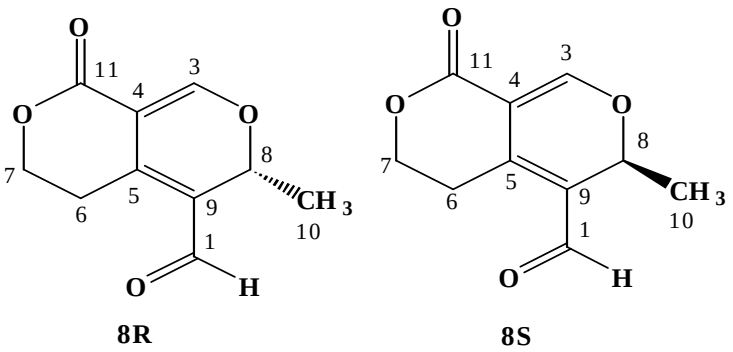

XI

(Arbitrary atom numbering)

Compound **XI** was obtained as yellow viscous liquid from the fruit extract of *F. fragrans*. The molecular formula $C_{10}H_{10}O_4$ is established by the ESI-TOF mass spectrum (Fig. 11.1), with the exact mass at *m/z* 195.0663 ($[M + H]^+$**,** 195.0657 calculated for $[C_{10}H_{10}O_4 + H]^+$.

The infrared spectrum (Fig. 11.2) of compound **XI** shows absorption peaks (ν_{max}) at 3022 cm^{-1} (C–H stretching), 1715 cm^{-1} (C=O stretching of cyclic ester), 1427 cm^{-1} (C–H stretching of $–CH_2$), 1215 cm^{-1} (C–O–C stretching), and 756 cm^{-1} (C–O–C stretching). The UV-Vis spectrum (Fig. 11.3) of **XI** shows absorption peaks (λ_{max}) at 206, 260, and 338 nm.

Information from the ESI-TOF and ^{1}H-NMR spectral data (Fig. 11.4) clearly indicates that compound **XI** is a derivative of naucledal (compound **X**). Analysis of the ^{1}H-NMR spectrum reveals the replacement of two methine H-atoms in **X** with a C-5–C-9 double bond in **XI**.

The ^{13}C-NMR spectrum (Fig. 11.5) of compound **XI** exhibits 10

signals, which are classified by DEPT and HMQC spectral data (Figs. 11.5 and 11.6) as two methines, two methylenes, one methyl, one aldehydic carbon atom, and four quaternary carbon atoms. The downfield C-1 signal at δ_C 189.44 ppm correlates to the aldehydic H signal at δ_H 9.20 ppm. The downfield C-11 signal at δ_C 163.98 ppm, together with the IR absorption peak at 1715 cm^{-1} indicates the presence of a carbonyl of cyclic ester. The downfield shift for C-5 at δ_C 171.74 ppm may be rationalized on the basis of electron withdrawing effect from two O-atoms through C-3–C-4 and C-1–C-9 bonds. The methylene CH_2-7 signal at δ_C 63.76 ppm and the methine H–C-8 signal at δ_C 74.16 ppm indicate that each of them is attached to an O-atom.

The $^1H,^1H$-COSY spectrum (Fig. 11.8) of compound **XI** exhibits the correlations between H–C-8 and Me-10; and CH_2-6 and CH_2-7.

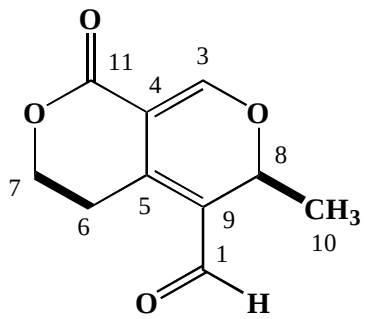

The bold lines show the connectivities from $^1H,^1H$-COSY spectrum of compound XI

The HMBC spectrum (Fig. 11.7) of compound **XI** is useful for the assembly of the gross structure of **XI** by showing the following correlations: H–C-1 to C-8 and C-9; H–C-3 to C-8; CH_2-6 to C-4; CH_2-7 to C-11; H–C-8 to C-9; and Me-10 to C-3.

Based upon these spectral data, compound **XI** it is identified as gentiogenal, which was previously isolated from *Blackstonia perfoliata* (Gentianacea)

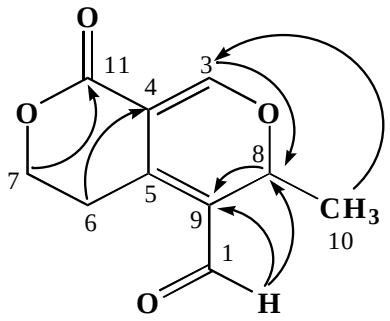

The curved arrows show HMBC correlations of compound XI

(Van der Sluis, Van der Nat, Spek, Ikeshiro, and Labadie, 1983). Since compound **XI** has the specific rotation $[\alpha]_D^{24}$ (*c* = 1.23 in MeOH) of –6.03°, which is close to zero, it may be in the form of racemic mixture, as previously suggested by Van der Sluis, et al., 1983. The ^{1}H- and ^{13}C-NMR spectral data of **XI**, compared to those reported (Van der Sluis, et al., 1983), are shown in Table 4.11. It should be noted that the assignment of C-3 and C-5 is exchanged (different from the previous assignment by Van der Sluis, et al. 1983), based upon the HMQC and HMBC spectral data (Figs. 11.6 and 11.7).

4.11.2 Biological activities

Compound **XI** exhibits cytotoxicity towards NCI-H187 with IC_{50} value of 5.06 μg/mL, but is inactive towards the KB and BC cell lines at 20 μg/mL. It also demonstrates mild antimycobacterial activity against *Mycobacterium tuberculosis* H37Ra with MIC value of 50 μg/mL, while it is inactive against K1 malarial parasite strain (*Plasmodium falciparum*) at 20 μg/mL.

Table 4.11 The ^{1}H- and ^{13}C-NMR spectral data of compound XI (at 500 and 125 MHz, respectively) and gentiogenal in $CDCl_3$ (*J* in Hz).

	δ (ppm)			
	Compound XI		**Gentiogenal**	
	^{1}H	**^{13}C**	**^{1}H**	**^{13}C**
H–C(-1)=O	9.20 (*s*)	189.44	9.88 (*s*)	185.70
H–C-3	7.26 (*s*)	135.40	7.95 (*s*)	163.30
C-4	–	101.15	–	103.90
C-5	–	171.74	–	142.70
CH_2-6	2.70 (*m*)	27.57	3.09-3.11 (*t*, *J* = 4.9)	22.60
CH_2-7	4.43 (*t*, *J* = 6.28)	63.76	4.43-4.44 (*t*, *J* = 4.9)	65.10
H–C-8	5.58 (*q*, *J* = 6.53)	74.16	5.64 (*q*, *J* = 6.5)	73.10
C-9	–	129.22	–	120.20
Me-10	1.43 (*d*, *J* = 6.54)	20.57	1.39 (*d*, *J* = 6.5)	19.80
C-11	–	163.98	–	163.90

4.12 Compound XII (sweroside, a known compound)

4.12.1 Structure elucidation

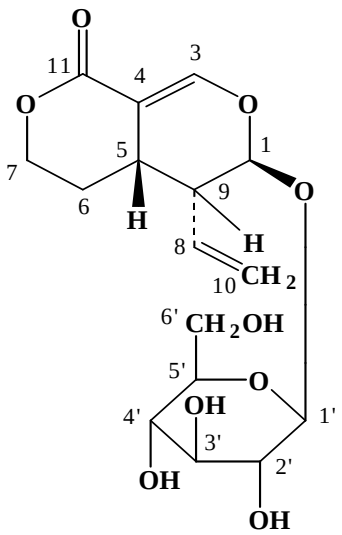

XII (Arbitrary atom numbering)

Compound **XII** was obtained as yellow viscous liquid from the stem extract of *F. fragrans*. The molecular formula $C_{16}H_{22}O_9$ is established by the ESI-TOF mass spectrum (Fig. 12.1), with the exact mass at *m/z* 381.1170 ($[M + Na]^+$, 381.1162 calculated for $[C_{16}H_{22}O_9 + Na]^+$).

The infrared spectrum (Fig. 12.2) of compound **XII** shows absorption peaks (ν_{max}) at 3405 cm^{-1} (broad, O–H stretching), 3021 cm^{-1} (C–H stretching), 1615 cm^{-1} (C=O stretching of carbonyl group), and 1215 cm^{-1} and 757 cm^{-1} (C–O–C stretching). The UV-Vis spectrum (Fig. 12.3) of compound **XII** shows absorption peaks (λ_{max}) at 205 and 243 nm.

The ^{1}H- and ^{13}C-NMR spectra (Figs. 12.4 and 12.5) of compound **XII** reveals characteristics of iridoid, particularly at δ_H 7.45 ppm (*d*, *J* = 2.54 Hz) for H–C-3, between 1.63-1.78 ppm for CH_2-6, and between 4.30-4.40 ppm for CH_2-7. The ^{1}H- and ^{13}C-NMR spectral data also demonstrate signals of a sugar unit at δ_H 3.23-4.70 ppm.

The ^{13}C-NMR spectrum (Fig. 12.5) of compound **XII** exhibits 16 signals, which are classified by DEPT and HMQC spectral data (Figs. 12.5 and 12.6) as ten methines, four methylenes, and two quaternary carbon atoms. The downfield methine H–C-3 signal at δ_C 151.13 ppm reveals the attachment to an sp^3 oxygen atom of a partial structure =CH–O–, while the downfield H–C-1 signal at δ_C 96.19 ppm is of an acetal carbon atom. The downfield C-11 signal at δ_C 164.46 ppm, together with the IR absorption peak at 1615 cm^{-1} indicates the presence of a carbonyl group of cyclic ester.

The ^{1}H,^{1}H-COSY spectrum (Fig. 12.8) of compound **XII** exhibits the connectivity from H–C-1′ through CH_2-6′ of the sugar unit. It also reveals partial

structures from H–C-1 through H–C-9, H–C-8, and CH_2-10, and through H–C-9, H–C-5, CH_2-6, and CH_2-7.

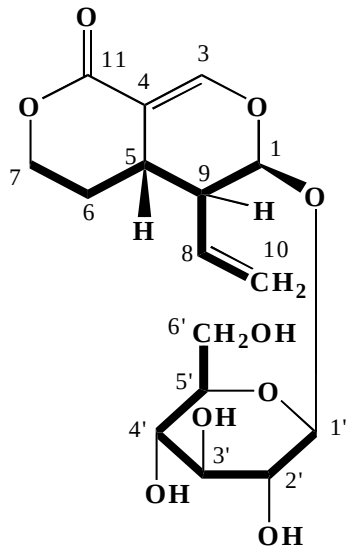

The bold lines show the connectivities from ^{1}H,^{1}H-COSY spectrum of compound XII

The HMBC spectrum (Fig. 12.7) of compound **XII** conclusively reveals the gross molecular structure of **XII** by exhibiting the following correlations: H–C-1 to C-1′, C-3, C-5, and C-8; H–C-3 to C-11; H–C-5 to C-3, and C-8; CH_2-6 to C-9; CH_2-7 to C-5, and C-11; and H–C-9 to C-4, and C-10.

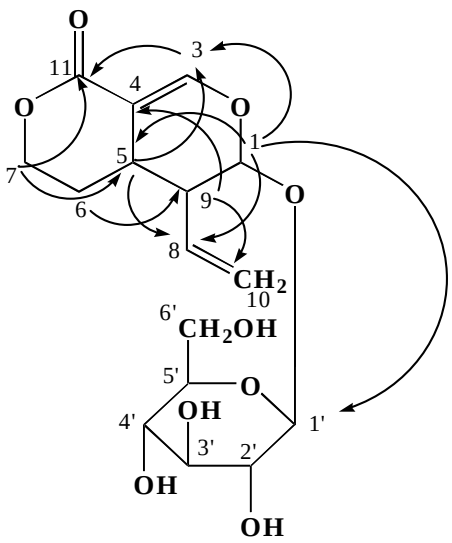

The curved arrows show HMBC correlations of compound XII

The NOESY spectrum (Fig. 12.9) of compound **XII** indicates the correlations between H–C-5 and CH_2-7 ax; H–C-9 and CH_2-10; and CH_2-6′ and H–C-4′.

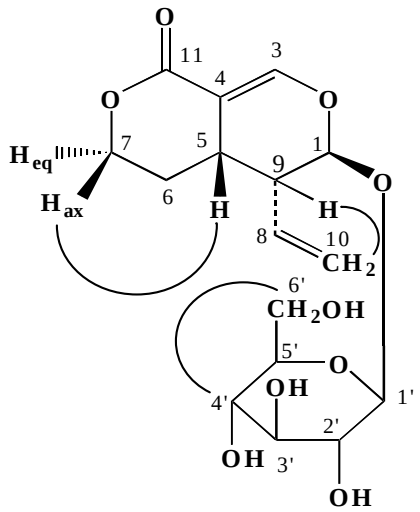

The curved lines show NOESY correlations of compound XII

On the basis of these spectral data, compound **XII** is identified as (–)-sweroside, which was previously isolated from *Lonicera caerulea* (Machida, Asano, and Kikuchi, 1995), and *Tabernaemontana psorocarpa* (Van beek, Lankhorst, Verpoorte, and Baerheim Svendsen, 1982). The specific rotation $[\alpha]_D^{25}$ (c = 0.90 in MeOH) of –205.68^o of compound **XII** is similar to that of (–)-sweroside ($[\alpha]_D^{20}$ = –224^o in MeOH, Van der Sluis and Labadie, 1981). The ^{1}H- and ^{13}C-NMR spectral data of compound **XII**, compared to those reported (Machida, et al., 1995) are shown in Table 4.12.

Table 4.12 The ^{1}H- and ^{13}C-NMR spectral data of compound XII (at 500 and 125 MHz, respectively) in acetone-d_6 and sweroside in CD_3OD (*J* in Hz).

	δ (ppm)			
	Compound XII		**Sweroside**	
	^{1}H	**^{13}C**	**^{1}H**	**^{13}C**
H–C-1	5.50 (*d*, *J* = 1.7)	96.19	–	97.90
H–C-3	7.45 (*d*, *J* = 2.54)	151.13	–	153.90
C-4	–	105.30	–	106.00
H–C-5	3.12 (*m*)	27.33	–	28.40
CH_2-6, ax	1.78 (*dt*, *J* = 13.67, 2.36)	24.90	–	25.90
CH_2-6, eq	1.63 1.63 (*qd*, *J* = 12.96 and 4.29)	24.75	–	25.90
CH_2-7, ax	4.30 (*td*, *J* = 11.75 and 2.17)	67.64	–	69.70
CH_2-7, eq	4.40 (*dq*, *J* = 11.10 and 2.14)	67.66	–	69.70
H–C-8	5.55 (*dt*, *J* = 9.97 and 17.13)	132.56	–	133.30
H–C-9	2.68 (*qd*, *J* = 4.10 and 1.40)	42.46	–	43.80
CH_2-10, a	5.25 (*dd*, *J* = 10.28 and 1.92)	119.62	–	120.80
CH_2-10, b	5.32 (*dd*, *J* = 17.17 and 1.81)	119.62	–	120.80
C-11	–	164.46	–	168.50
H–C-1′	4.70 (*d*, *J* = 7.83)	98.49	–	99.70
H–C-2′	3.23 (*t*, *J* = 8.41)	73.64	–	74.70
H–C-3′	3.38 (*dd*, *J* = 8.17 and 6.76)	77.13	–	78.40
H–C-4′	3.44 (*t*, *J* = 8.74)	70.59	–	71.50
H–C-5′	3.34 (*q*, *J* = 9.04)	76.77	–	77.90
CH_2-6′, a	3.85 (*d*, *J* = 11.97)	61.93	–	62.70
CH_2-6′, b	3.65 (*t*, *J* = 7.15)	61.93	–	62.70

4.12.2 Biological activities

Compound **XII** demonstrates mild anti-Herpes simplex virus type 1 (anti-HSV-1) activity with more than 35-50% inhibition at IC_{50} value of 1.2 ± 0.3 μg/mL. However, it is inactive towards Vero (at 50 μg/mL), NCI-H187, KB and BC (at 20 μg/mL) cell lines, and *Mycobacterium tuberculosis* H37Ra (at 200 μg/mL).

4.13 Compound XIII

4.13.1 Structure elucidation

Due to the limited amount of compound **XIII** isolated, the molecular structure of this compound could not be elucidated. Its IR, UV-Vis, ^{1}H-NMR, ^{13}C-NMR, HMQC, HMBC, ^{1}H,^{1}H-COSY, and NOESY spectra are shown in Figs. 13.1-13.8, respectively.

4.13.2 Biological activities

Due to the limited amount of compound **XIII** isolated, the biological activities of this compound were not evaluated.

CHAPTER V

CONCLUSION

Chemical exploration of the CH_2Cl_2 extract of the roots of *Bauhinia saccocalyx* led to the identification of four new bibenzyls, bauhinol A-D (compounds **I**-**IV**), together with two known bibenzyls (compounds **V**-**VI**).

Bauhinol A (compound **I**) exhibits significant cytotoxicity against NCI-H187, BC, and KB cell lines with IC_{50} value of 3.4, 2.7, and 4.5 μg/mL, respectively. Bauhinol B (compound **II**) possesses cytotoxicity against NCI-H187 (IC_{50} = 1.1 μg/mL) and BC (IC_{50} = 9.7 μg/mL) cell lines, but is inactive towards the KB cell line (at 20 μg/mL). Bauhinol B also demonstrates mild antifungal activity against *Candida albicans* with IC_{50} value of 28.9 μg/mL. Bibenzyl **VI** is active against NCI-H187 (IC_{50} = 14.1 μg/mL) and BC (IC_{50} = 4.0 μg/mL) cell lines, but is inactive (at 20 μg/mL) towards the KB cell line. Bibenzyl **VI** also exhibits mild antifungal activity against *Candida albicans* with IC_{50} value of 11.7 μg/mL. Bibenzyls **I**, **II**, and **VI** show mild antimycobacterial activity with MIC values of 50, 25, and 25 μg/mL, respectively, but they are inactive (at 20 μg /mL) against the malarial parasite *Plasmodium falciparum*. While bauhinol A (**I**) is inactive against COX-1 and COX-2, compound **II** and **VI** inhibit both COX-1 and COX-2 with IC_{50} values of 9.0 and 2.5 μg/mL, respectively for COX-1, and 1.3 and 1.8 μg/mL, respectively for COX-2. These IC_{50} values are comparable to those of the standard drug, aspirin. Biological activities of bibenzyl **III** and **V** were not evaluated due to the limited amount of

samples isolated, whilst the bioactivities of **IV** could not be obtained due to its instability in the test systems.

The CH_2Cl_2 extract of *F. fragrans* was purified by Sephadex LH-20 and HPLC to yield four known compounds: pinoresinol (**IX**) from the stem bark, naucledal (**X**) from the roots, gentiogenal (**XI**) from the fruits, and sweroside (**XII**) from the stems. Pinoresinol (**IX**) exhibits antimalarial activity against the K1 malarial parasite strain (*Plasmodium falciparum*) with IC_{50} value of 3.4 μg/mL and antitubercular activity against *Mycobacterium tuberculosis* (H37Ra) with MIC value of 200 μg/mL. However, Pinoresinol (**IX**) is inactive at 20 μg/mL towards the KB and BC cell lines, and shows no antifungal activity against *Candida albicans.* Naucledal (**X**) exhibits cytotoxicity towards NCI-H187 with IC_{50} value of 18.94 μg/mL) and demonstrates mild antitubercular activity with MIC value of 200 μg/mL), but is inactive at 20 μg/mL towards the KB and BC cell lines and the malarial parasite. Gentiogenal (**XI**) exhibits cytotoxicity towards NCI-H187 with IC_{50} value of 5.06 μg/mL and also demonstrates mild antitubercular activity with MIC value of 50 μg/mL, but is inactive at 20 μg/mL towards the KB and BC cell lines and the malarial parasite. Sweroside (**XII**) demonstrates mild anti-HSV-1 activity with more than 35-50% inhibition at IC_{50} value of 1.2 ± 0.3 μg/mL, but is inactive against Vero (at 50 μg/mL), NCI-H187, KB and BC (at 20 μg/mL) cell lines, and *Mycobacterium tuberculosis* (H37Ra, at 200 μg/mL).

REFERENCES

REFERENCES

สมาคมพ่อค้ายา กรุงเทพฯ. (2521). **ตำราหลักวิชาแพทย์แผนโบราณ สาขาเภสัชกรรม.** กรุงเทพ ฯ: ห้างหุ้นส่วนจำกัดคุณทินอักษรกิจ.

สมาคมโรงเรียนแพทย์แผนโบราณ สำนักวัดพระเชตุพนวิมลมังคลาราม. (2521). **ประมวลสรรพคุณยาไทย (ภาคหนึ่ง) ว่าด้วยพฤษชาติ วัตถุธาตุ และสัตว์วัตถุนานาชนิด.** กรุงเทพฯ: ไพศาลศิลป์การพิมพ์.

Achenbach, H., Stocker, M., and Constenla, M. A. (1988). Flavonoid and other constitutents of *Bauhinia manca*. **Phytochemistry.** 27 (6): 1835-1841.

Anjaneyulu, A. S. R., Raghava Reddy, A. V., and Reddy, D. S. K. (1984). A new dibenzo(2,3-6,7)oxepin derivative from *Bauhinia racemosa* Lamk. **Tetrahedron.** 40 (21): 4245-4252.

Anjaneyulu, A. S. R., Raghava Reddy, A. V., Reddy, D. S. K., Cameron, T. S., and Roe, S. P. (1986). Racemosol: a novel tetracyclic phenol from *Bauhinia racemosa* Lamk. **Tetrahedron.** 42 (9): 2417-2420.

Bhakuni, D. S., Dhar, M. L., Dhar, M. M., Dhawan, B. N., and Mehrotra, B. N. (1968). Screening of Indian plants for biological activity: Part 2. **Indian Journal of Experimental Biology.** 7: 250-262.

Asakawa, Y., Hashimoto, T., Takikawa, K., Tori, M., and Ogawa, S. (1991). Prenyl bibenzyls from the liverwort *Radula kojana*. **Phytochemistry**, 30 (1): 219-234.

Bhakuni, D. S., Dhar, M. L., Dhar, M. M., Dhawan B. N., and Mehrotra, B. N. (1968). Screening of Indian plants for biological activity: Part 2. **Indian Journal of Experimental Biology.** 7: 250-262.

Cambie, R. C., Rickard, C. E. F., Lal, A. R., and Tanaka, N. (1990). Chemistry of Fijian plants. V. constituents of *Fagracea gracilipes* A. Gray. **Chemical and Pharmaceutical Bulletin.** 38 (7): 1857-1861.

Cannell, R. J. P. (1998). **Natural products isolation.** New Jersey: Humana Press.

Collins, L. and Franzblau, S. G. (1997). Microplate alamar blue assay versus BACTEC 460 system for high-throughput screening of compounds against *mycobacterium tuberculosis* and *mycobacterium avium*. **Antimicrobial agents and chemotherapy.** 41 (5); 1004-1009.

Cuendet, M., Hostettmann, K., Potterat, O., and Dyatmiko, W. (1997). Iridoid glucosides with free radical scavenging properties from *Fagraea blumie.* **Helvetica Chimica Acta.** 80 (4): 1144-1152.

Dalziel, J. M. (1948). **The Useful Plants of West Tropical Africa.** The Crown Agents for Oversea Governments and Administration. London.

Damasceno, D. C., Volpato, G. T., Calderon Ide, M., Aguilar, R., and Rudge, M. V. (2004). Effect of *Bauhinia forficata* extract in diabetic pregnant rats: maternal repercussions. **Phytomedicine.** 11 (2-3): 196-201.

Desjardins, R. E., Canfield, C. J., Haynes, J. D., and Chulay, J. D. (1979). Quantitative assessment of antimalarial activity *in vitro* by a semiautomated microdilution technique. **Antimicrobial agents and chemotherapy.** 16 (6): 710-718.

Duret, S. and Paris, R. R. (1977). Nepalese plants. V. The flavonoid of several species of *Bauhinia: B. valhii, B. variegata* and *B. malabarica* (Leguminosae). **Plant Medicinal Phytother.** 11: 213.

Flora of SUT. (2004). *Bauhinia saccocalyx.* [On-line]. Available: http://flora.sut.ac.th

Gonzalez-Mujica, F., Motta, N., Marquez, A. H., and Capote-Zulueta, J. (2003). Effects of *Bauhinia megalandra* aqueous leaf extract on intestinal glucose absorption and uptake by enterocyte brush border membrane vesicles. **Fitoterapia.** 74: 84-90.

Grosvenor, P. W., Gothard, P. K., Mc.William, C., Supriono, A., and Gray, D. O. (1995). Medicinal plants from Riau province, Sumatra, Indonesia. Part 1: User. **Journal of Ethnopharmacology.** 45: 75-95.

Grosvenor, P. W., Supriono, A., and Gray, D. O. (1995). Medicinal plants from Riau province, Sumatra, Indonesia. Part 2: antibacterial and antifungal activity. Journal of Ethnopharmacology. **45: 97-111.**

Hanawa, F., Yamada, T., and Nakashima, T. (2001). Phytoalexins from *Pinus strobus* bark infected with pinewood nematode, *Bursaphelenchus xylophilus.* **Phytochemistry.** 57: 223-228.

Hawser, S. P., Norris, H., Jessup, C. J., and Ghannoum, M. A. (1998) Comparison of a 2,3-bis(2-methoxy-4-nitro-5-sulfophenyl)-5-[phenylamino)carbonyl]-2*H*-tetrazolium hydroxide (XTT) colorimetric method with the standardized National Committee for Clinical Laboratory Standards method of testing clinical yeast isolates for susceptibility to antifungal agents. **Journal of Clinical Microbiology**. 36 (5): 1450-1452.

Holdsworth, D. and Sakulas, H. (1986). Medicinal plants of the Morobe province. **International Journal of Crude Drug Research.** 24 (1): 31-40.

Hong, L. T. and Mohd, A. R. (1983). Anti-fungal properties of methanol extractives from some tropical hardwoods. **The Malaysian Forester.** 46 (1): 138-139.

Iribarren, A. M. and Pomilio, A. B. (1987). Sitosterol 3-α-D-xyluronofuranoside from *Bauhinia candicans.* **Phytochemistry.** 26 (3): 857-858.

Iwagawa, T., Kawasaki, J., Hase, T., Sako, S., Okubo, T., Ishida, M., and Kim, M. (1990). An acylated flavonol glycoside from *Lasiobema japonica.* **Phytochemistry.** 29 (3): 1013-1014.

Jagdish Kumar, R., Krupadanam, G. L. D., and Srimannarayana, G. (1990). Phenolic constituents from the pods of *B. vahlii*. **Fitoterapia.** 61 (5): 475-476.

Kirtikara, K., Morham, S. G., Raghow, R., Laulederkind, S. J., Kanekura, T., Goorha, S., and Ballou, L. R. (1998). Compensatory prostaglandin E_2 biosynthesis in cyclooxygenase 1 or 2 null cells. **Journal of Experimental Medicine.** 16; 187 (4): 517-523.

Kittakoop, P., Kirtikara, K., Tanticharoen, M., and Thebtaranonth, Y. (2000). Antimalarial preracemosols A and B, possible biogenetic precursors of racemosol from *Bauhinia malabarica* Roxb. **Phytochemistry.** 55: 349-352.

Kittakoop, P., Nonpichai, S., Thongon, N., Charoenchai, P., and Thebtaranonth, Y. (2004). Bauhinoxepins A and B: new antimycobacterial Dibenzo[b,f]oxepins from *Bauhinia saccocalyx.* **Helvetica Chimica Acta.** 87: 175- 179.

Kun-anake, A., and Ragvatin, C. (1976). Bitter glucoside from leaves of Kan-grau. **Department of Medical Sciences Bulletin.** 18 (1): 1-11.

Kuo, Y., Yeh. M., and Huang, S. (1998). A Novel 6-butyl-3-hydroxyflavanone from heartwood of *Bauhinia purpurea.* **Phytochemistry.** 49 (8): 2529-2530.

Leaman, D. J., Arnason, J. T., Yusuf, R., Sangat-Roemantyo, H., Soedjito, H., Angerhofer, C. K., and Pezzuto, J. M. (1995). Malaria remedies of the Kenyah of the Apo Kenyah, East Kalimantan, Indonesian Borneo: A quantitative assessment of local consensus as an indicator of biological efficacy. **Journal of Ethnopharmacology.** 49 (1): 1-16.

Machida, K., Asano, J., and Kikuchi, M. (1995). Caeruleosides A and B, bis-iridoid glucosides from *lonicera caerulea.* **Phytochemistry.** 39 (1): 111-114.

Maillard, M. P., Recio-Iglesias, M., Saadou, M., Stoeckli-Evans, H., and Hostettmann, K. (1991). Novel antifungal tetracyclic compounds from *Bauhinia rufescens* Lam. **Helvetica Chimica Acta.** 74: 791-799.

Meyre-Silva, C., Yunes, R. A., Delle Monsche, F., Santos, A. R. S., Schmeling, L. O., De Maria Gadotti, V., Liz, F., and Cechinel-Filho, V. (2001). Phytochemical and pharmacological analysis of *Bauhinia microstachya* (Raddi) Macrb (Leguminosae). **Zeitschrift fur Naturforschung.** 56 (11-12): 939-942.

Miyazawa, M., Kasahara, H., and Kameoka, H. (1992). Phenolic lignans from flower buds of *Magnolia fargesii*. **Phytochemistry.** 31 (10): 3666-3668.

Natarajan, P. N., Wan, Alfred S. C., and Zaman, V. (1974). Antimalarial, antiamoebic and toxicity tests on gentianine. **Planta Medica.** 25: 258-260.

Okuyama, E., Suzumura, K., and Yamazaki, M. (1995). Pharmacologically active components of Todopon Puok (*Fagraea racemosa)*, A medicinal plant from Borneo. **Chemical and Pharmaceutical Bulletin.** 43 (2): 2200-2204.

Ostraff, M., Anitono, K., Nicholson, A., and Booth, G. M. (2000). Traditional Tongan cures for morning sickness and their mutagenic/toxicological evaluations. **Journal of Ethnopharmacology.** 71: 201-209.

Prabhakar, P., Gandhidasan, R., Raman, P. V., Krishnasamy, N. R., and Nandudi, S. (1994). De-*O*-Methylracemosol: a tetracyclic 2,2-dimethylchroman from the roots of *Bauhinia racemosa*. **Phytochemistry.** 36 (3): 817-818.

Prakash, A., and Khosa, R. (1976). Chemical studies on *Bauhinia racemosa*. **Current Surgery (Science direct).** 45: 705.

Purdy, J. and Mclean, S. (1977). Constituents of *Nauclea diderrichii*. Part IX. Conversion of sweroside to naucledal and 3-epinaucledal. **Canadian Journal of Chemistry.** 55: 4233-4237.

Qasim, M. A., Roy, S. K., Kamil, M., and Ilyas, M. (1987). A new glycosyl flavone from *Fagraea obovata* Wall. **Journal of Phytochemistry.** 26 (10): 2871-2872.

Rahman, M. M. A., Dewick, P. M., Jackson, D. E., and Lucas, J. A. (1990). Lignans of *Forsythia intermedia*. **Phytochemistry.** 29 (6): 1971-1980.

Silva, K. L., Biavatti, M. W., Leite, S. N., Yunes, R. A., Delle Monache, F., and Cechinel Filho, V. (2000). Phytochemical and pharmacognositc investigation of *Bauhinia forficata* Link (Leguminosae). **Zeitschrift fur Naturforschung.** 55 (5-6): 478-480.

Simonsen, H. T., Nordskjold, J. B., Smitt, U. W., Nyman, U., Palpu, P., and Joshi, P. (2001). In vitro screening of Indian medicinal plants for antiplasmodial activity. **Journal of Ethnopharmacology.** 74: 195-204.

Singh, Y. N., Ikahihifo, T., Panuve, M., and Slatter, C. (1984). Folk medicine in Tonga. **Journal of Ethnopharmacology.** 12: 305-329.

Skehan, P., Storeng, R., Scudiero, D., Monks, A., McMahon, J., Vistica, D., Warren, J. T., Bokesch, H., Kenney, S., and Boyd, M. R. (1990). New colorimetric

cytotoxicity assay for anticancer-drug screening. **Journal of the National Cancer Institute.** 82 (13): 1107-1112.

Smitinand, T. (2001). **Thai Plant Names**. (rev. ed.). Royal forest department.

Smitinand, T., and Lasen, K. (1984). **Flora of Thailand.** 4 (1): 20-21. The TISTR Press.

Sosa, S., Braca, A., Altinier, G., Della Loggia, R., Morelli, I., and Tubaro, A. (2002). Topical anti-inflammatory activity of *Bauhinia tarapotensis* leaves **Phytomedicine.** 9 (7): 646-653.

Sultana, S., Ilyas, M., Kamil, M., and Shaida, W. A. (1985). Chemical investigation of *Bauhinia vahlii* Linn. (Leguninoceae). **Journal of Indian Chemical society.** 62 (4): 337-338.

Tang, X. Y., Yuan, C. P., Zhang, Z. H., and Zhou, M. H. (1992). Chemical constituents of *Bauhinia hupehara* craib. **Zhongguo Zhongyao Zazhi.** 17 (10): 613-615.

Trager, W. and Jensen, J. B. (1976). Human malaria parasites in continuous culture. **Science.** 193 (4254): 673-675.

Van beek, T. A., Lankhorst, P. P., Verpoorte, R., and Baerheim Svendsen, A. (1982). Isolation of the secoiridoid-glucoside sweroside from *Tabernaemontana Psorocarpa.* **Journal of Medicinal Plant Research.** 44: 30-31.

Van der Sluis, W. G., Van der Nat, J. M., Spek, A. L., Ikeshiro, Y., and Labadie, R. P. (1983). Gentiogenal, a conversion product of gentiopicrin (gentiopicroside). **Journal of Medicinal Plant Research.** 49: 211-215.

Van der Sluis, W. G. and Labadie, R. P. (1981). Secoiridoids and Xanthones in the Genus *Centaurium*. **Journal of Medicinal Plant Research.** 41: 221-231.

Wall, M. E., Wani, M. C., Huehes, T. J., and Taylor, H. (1988). Plant antimutagenic Agent, 1. General bioassay and isolation procedures. **Journal of Natural Products.** 51 (5): 866-873.

Wan, A. S. C., Macko, E., and Douglas, B. (1972). Pharmacological investigations of gentianine from *Fagraea fragrans* Roxb. **Asian Journal of Medicine.** 8: 334-335.

Wongsatit, C., et al. (1996). **Medicinal Plants in Siri Ruckhachati Garden** (2nd ed.). Amarin printing.

Yadava, R. N. and Reddy, V. M. (2003). Anti-inflammatory activity of a novel flavonol glycoside from the *Bauhinia variegata Linn.* **Natural Product Research.** 17 (3): 165-169.

APPENDIX

APPENDIX

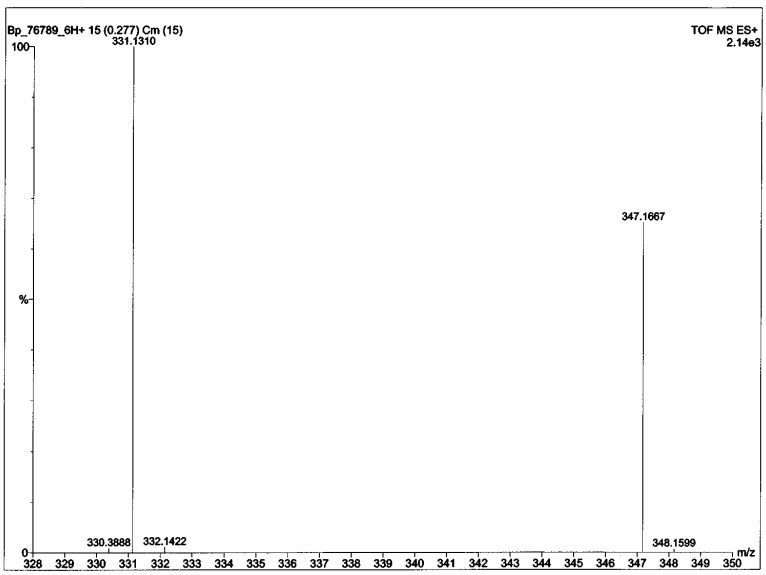

Figure 1.1 Mass spectrum of compound **I**

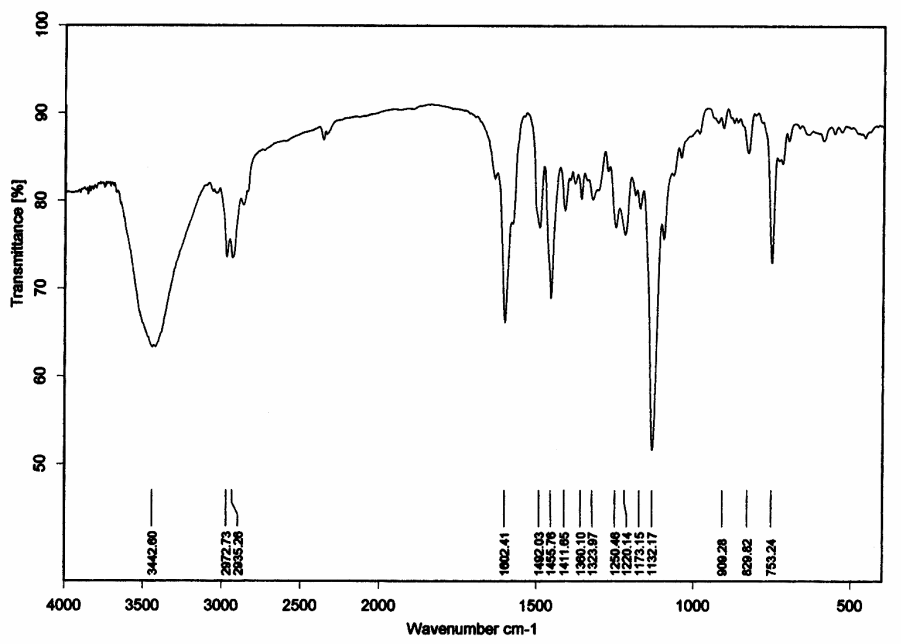

Figure 1.2 IR spectrum of compound **I**

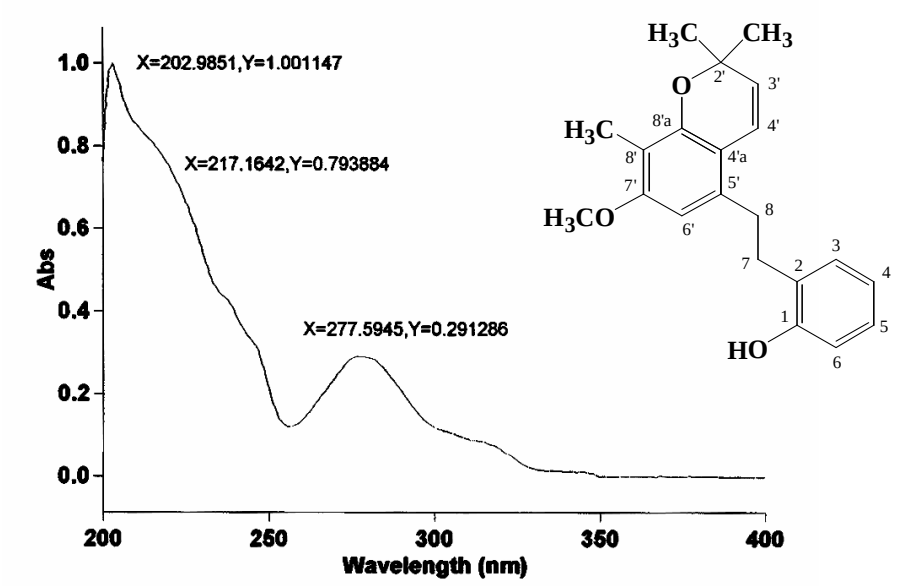

Figure 1.3 UV-Vis spectrum of compound **I**

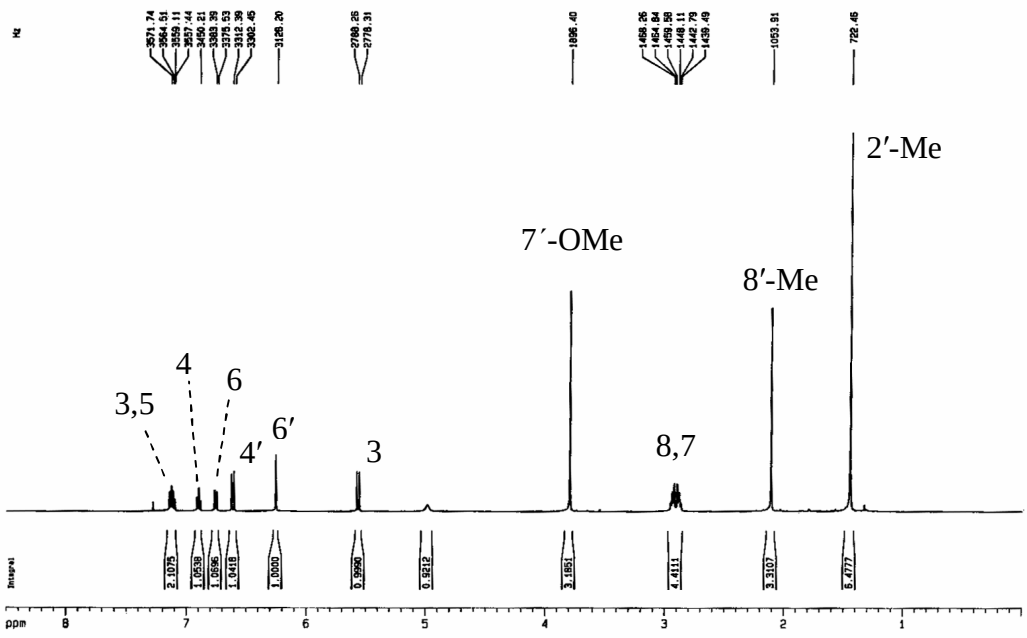

Figure 1.4 500 MHz ^{1}H-NMR spectrum of compound **I** in $CDCl_3$

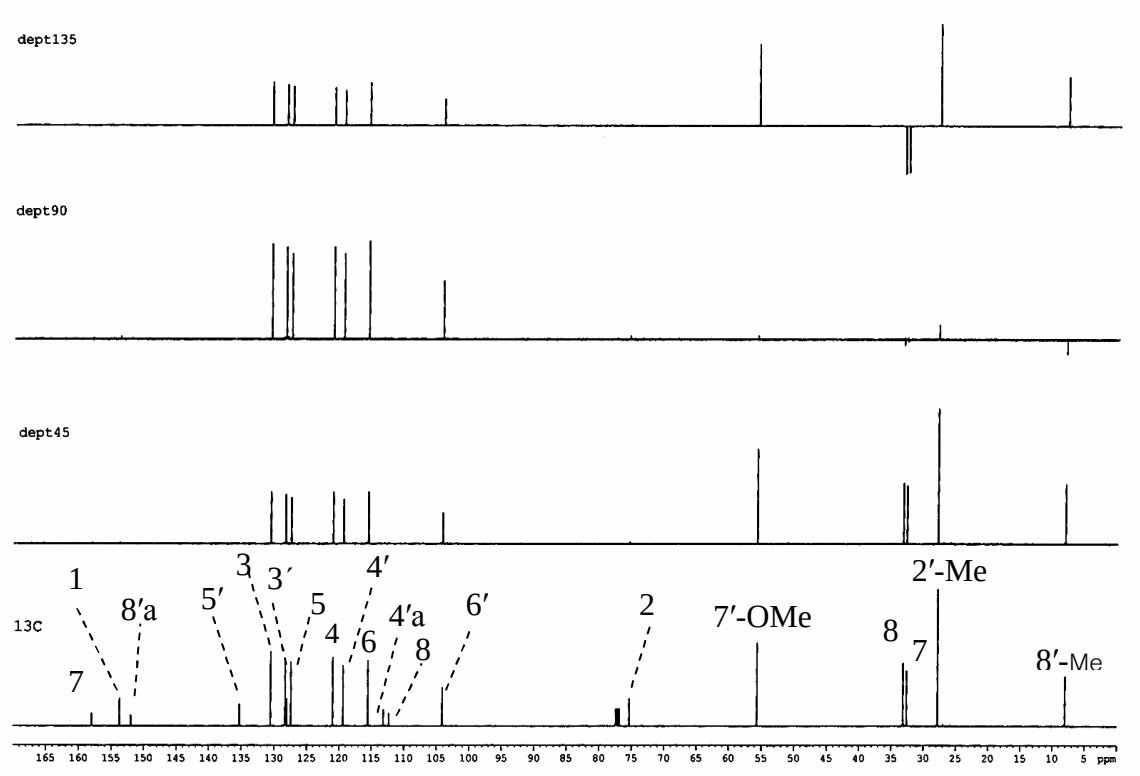

Figure 1.5 ^{13}C-NMR and DEPT spectra of compound **I** in $CDCl_3$

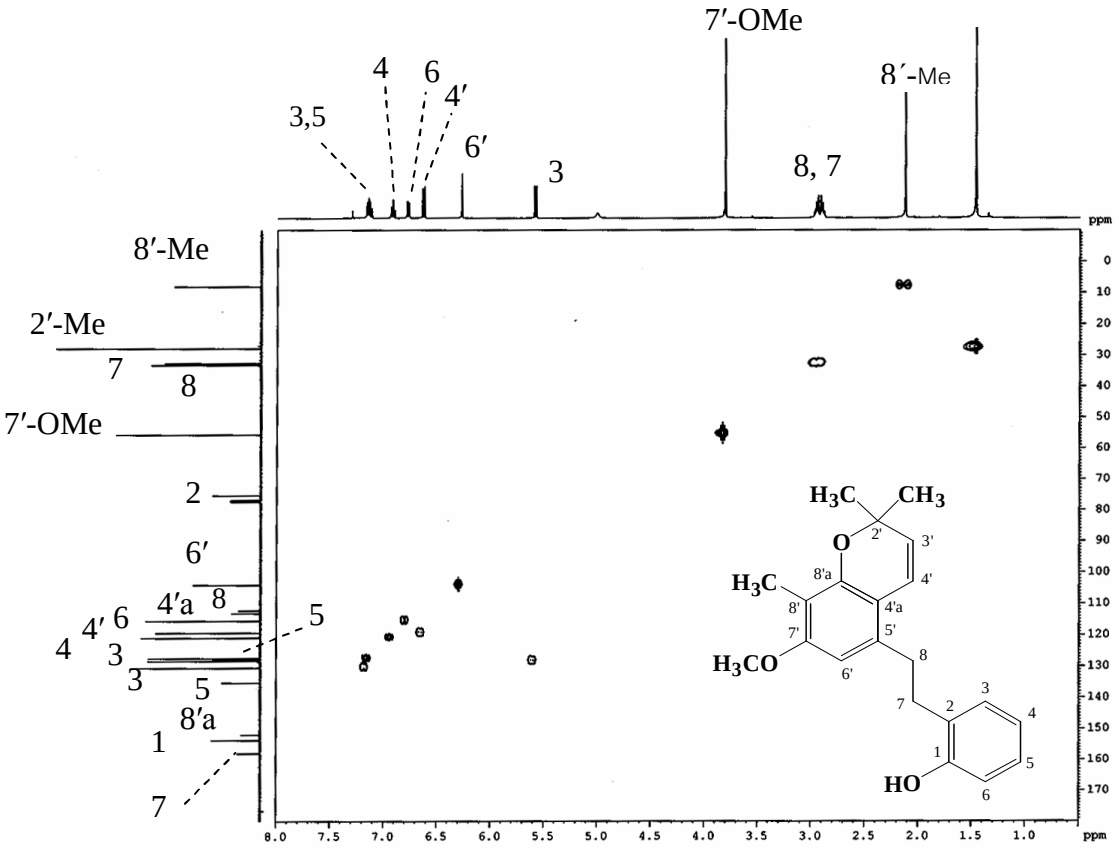

Figure 1.6 HMQC spectrum of compound **I** in $CDCl_3$

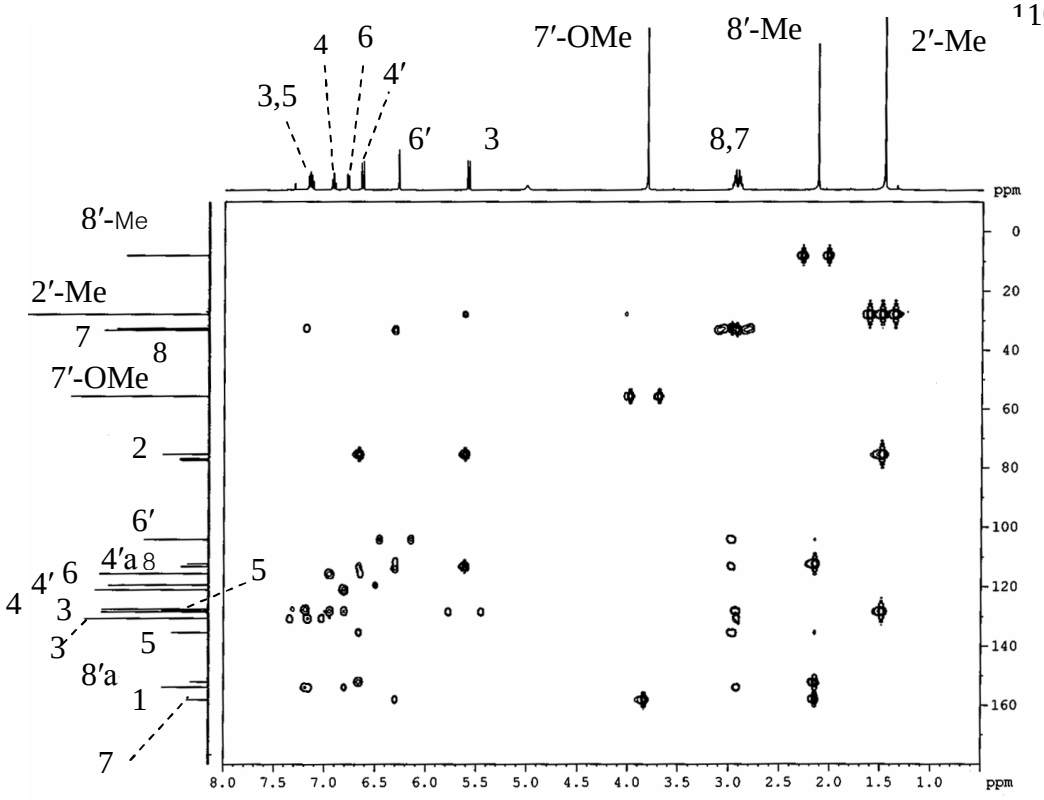

Figure 1.7 HMBC spectrum of compound **I**

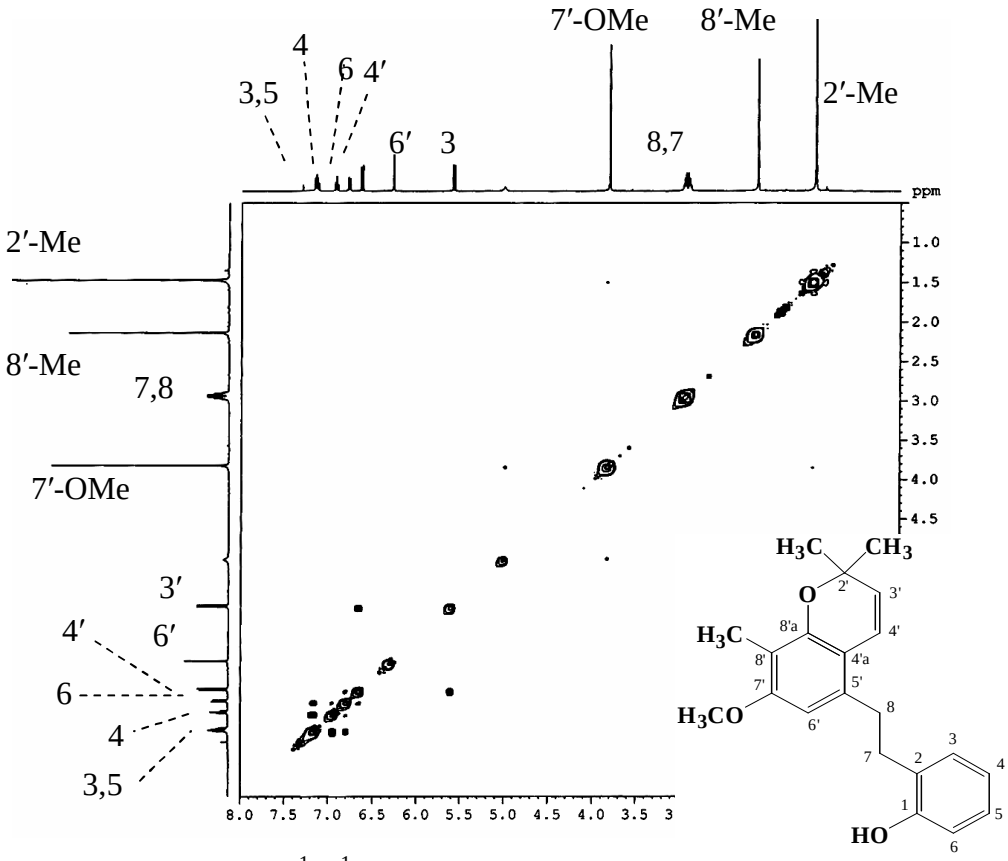

Figure 1.8 ^{1}H,^{1}H-COSY spectrum of compound **I**

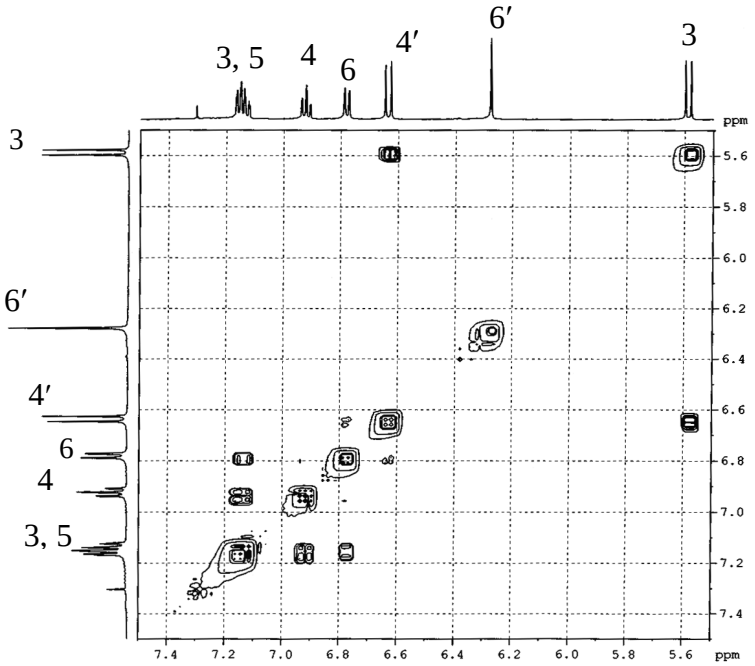

Figure 1.8a Expansion of Fig. 1.8

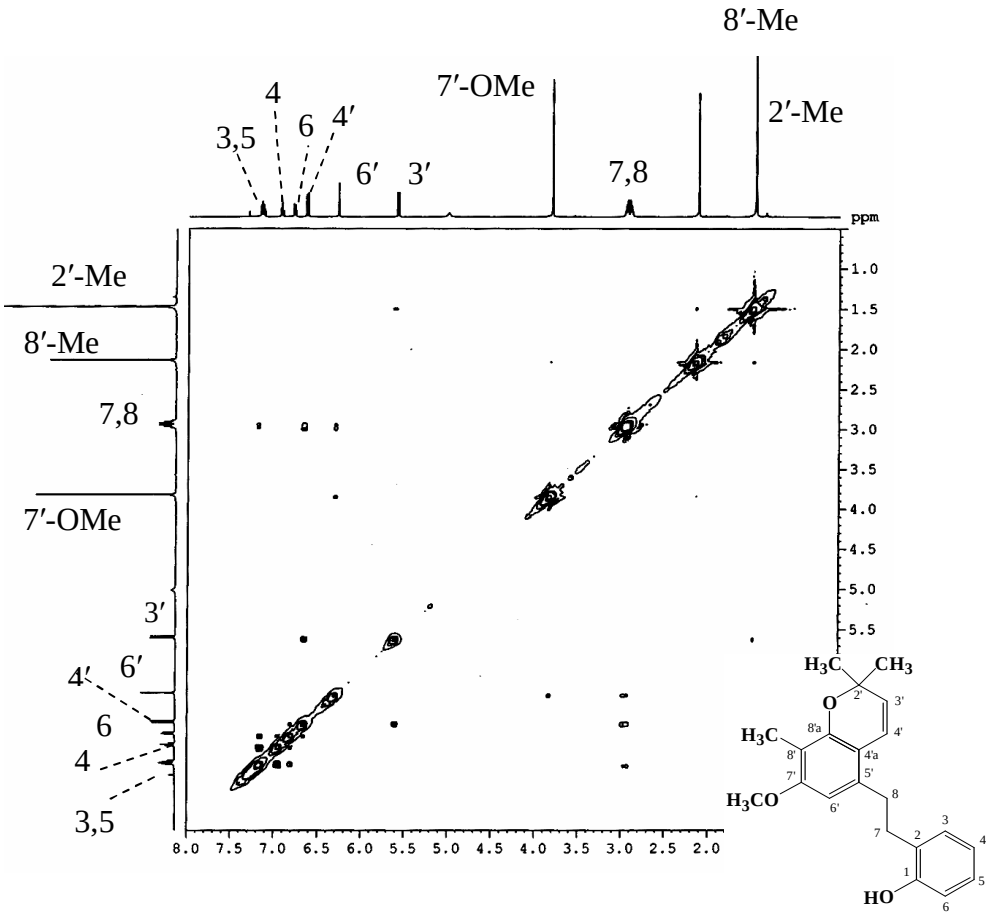

Figure 1.9 NOESY spectrum of compound **I**

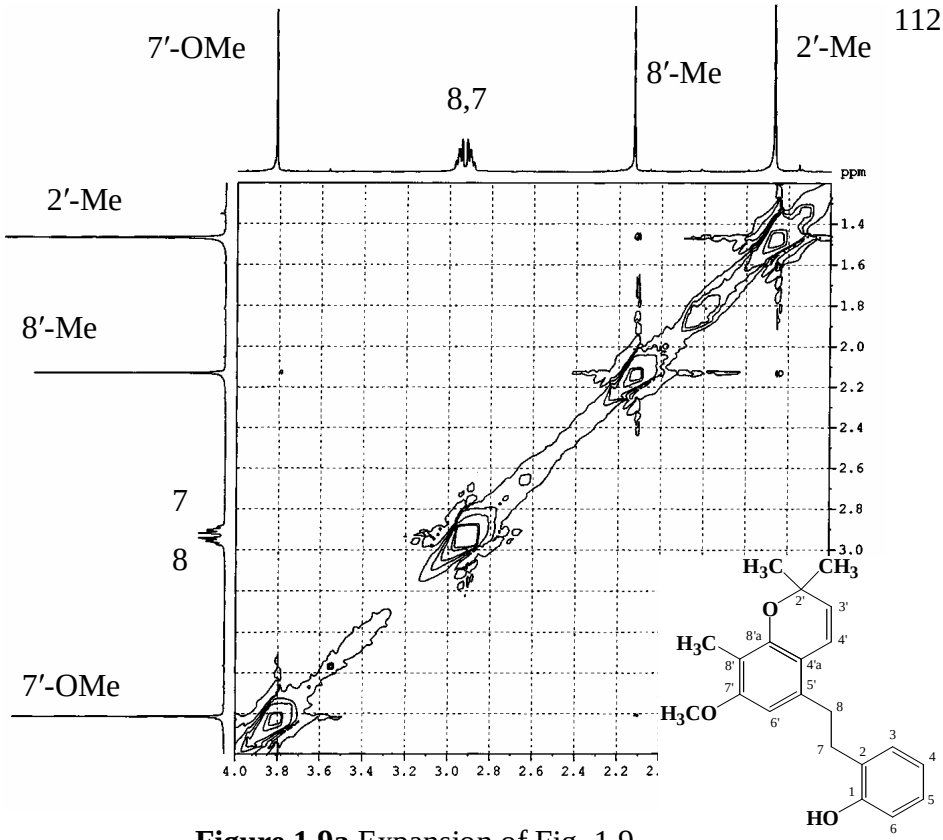

Figure 1.9a Expansion of Fig. 1.9

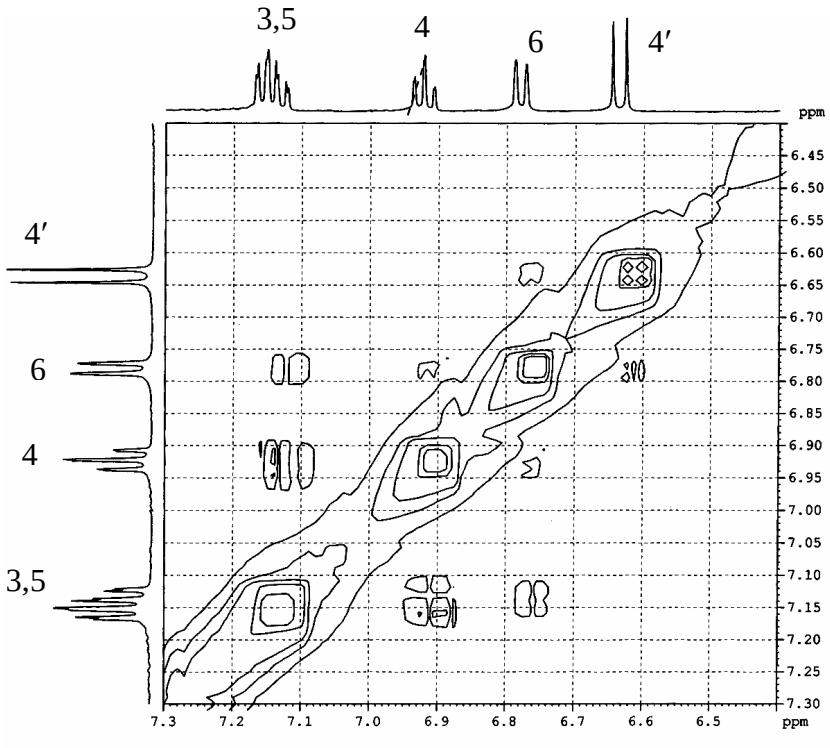

Figure 1.9b Expansion of Fig. 1.9

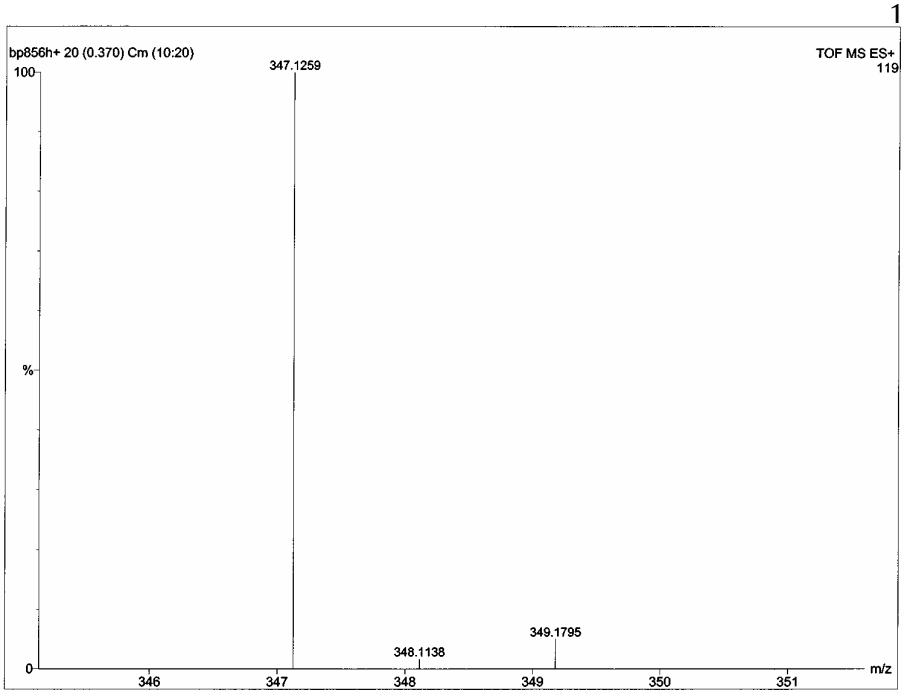

Figure 2.1 Mass spectrum of compound **II**

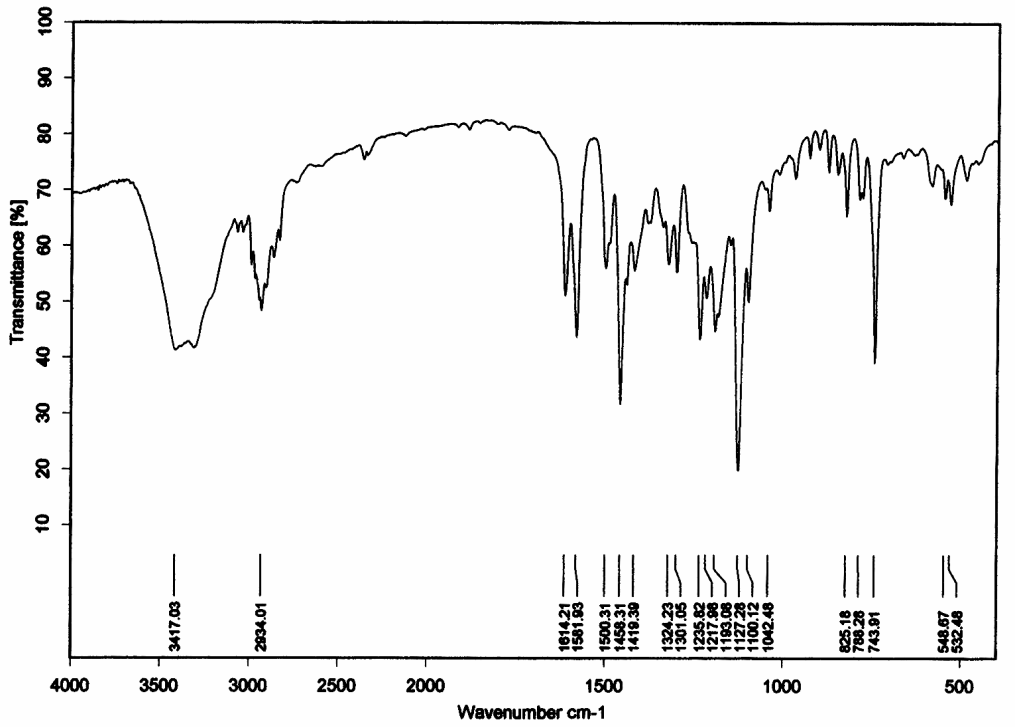

Figure 2.2 IR spectrum of compound **II**

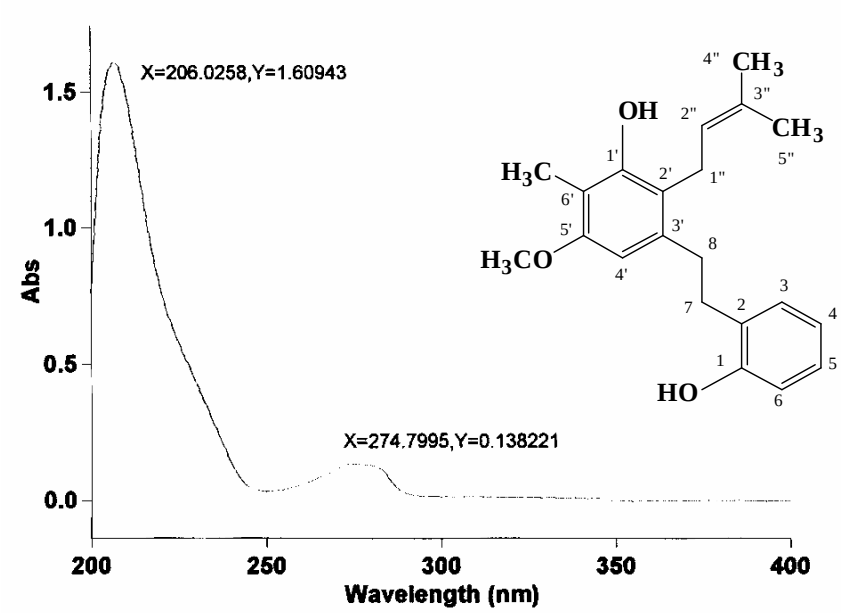

Figure 2.3 UV-Vis spectrum of compound **II**

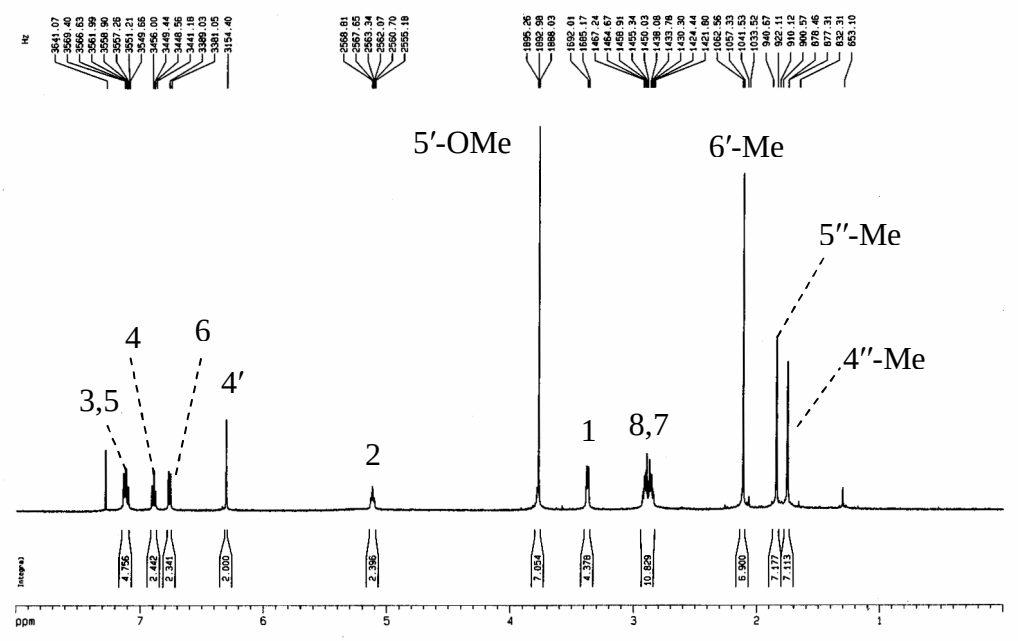

Figure 2.4 500 MHz ^{1}H-NMR spectrum of compound **II** in $CDCl_3$

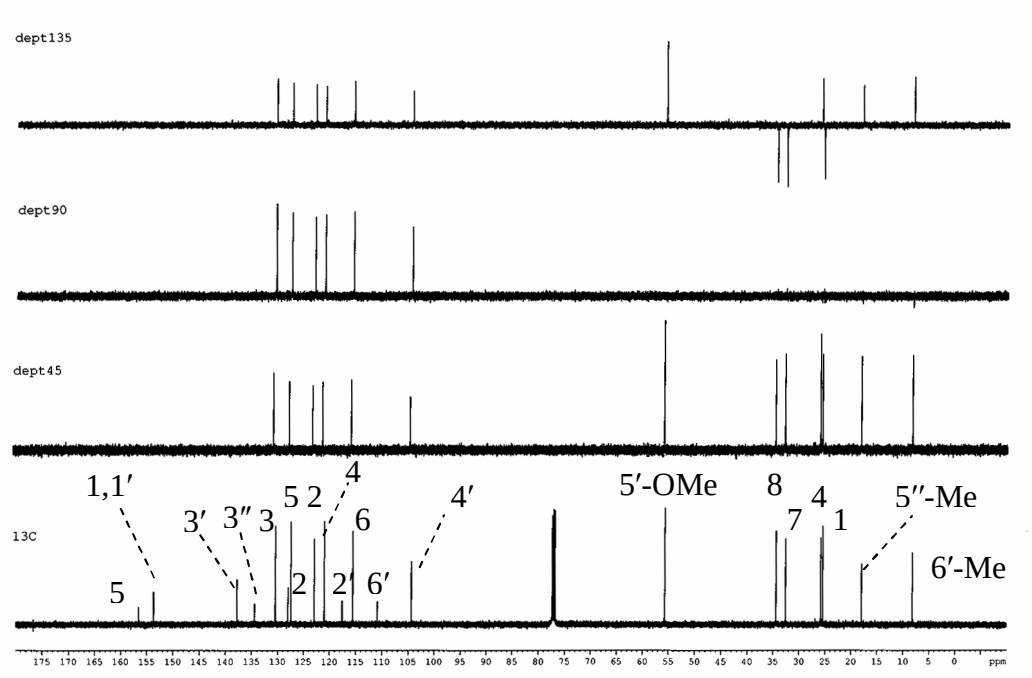

Figure 2.5 ^{13}C-NMR and DEPT spectra of compound **II** in $CDCl_3$

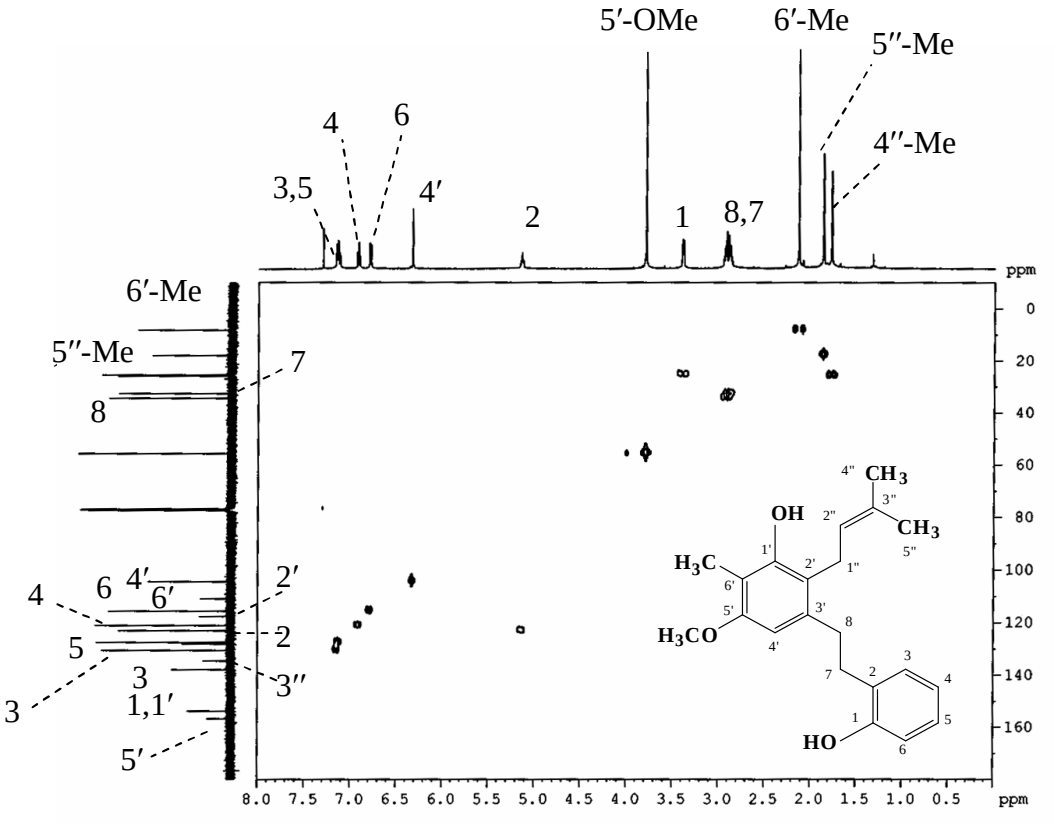

Figure 2.6 HMQC spectrum of compound **II**

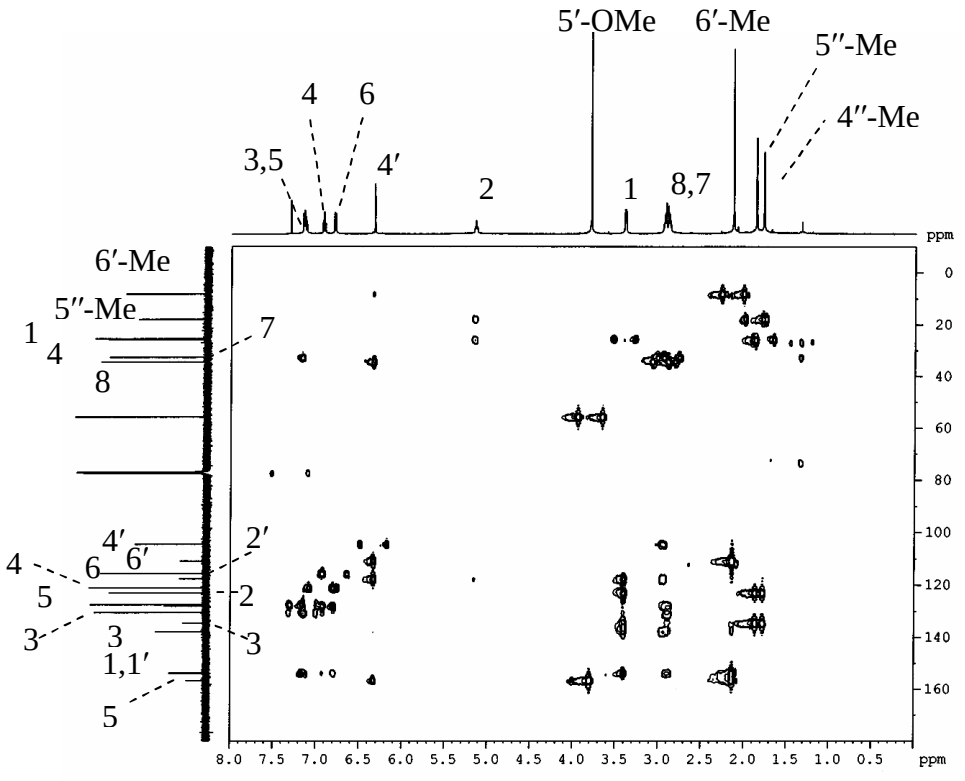

Figure 2.7 HMBC spectrum of compound **II**

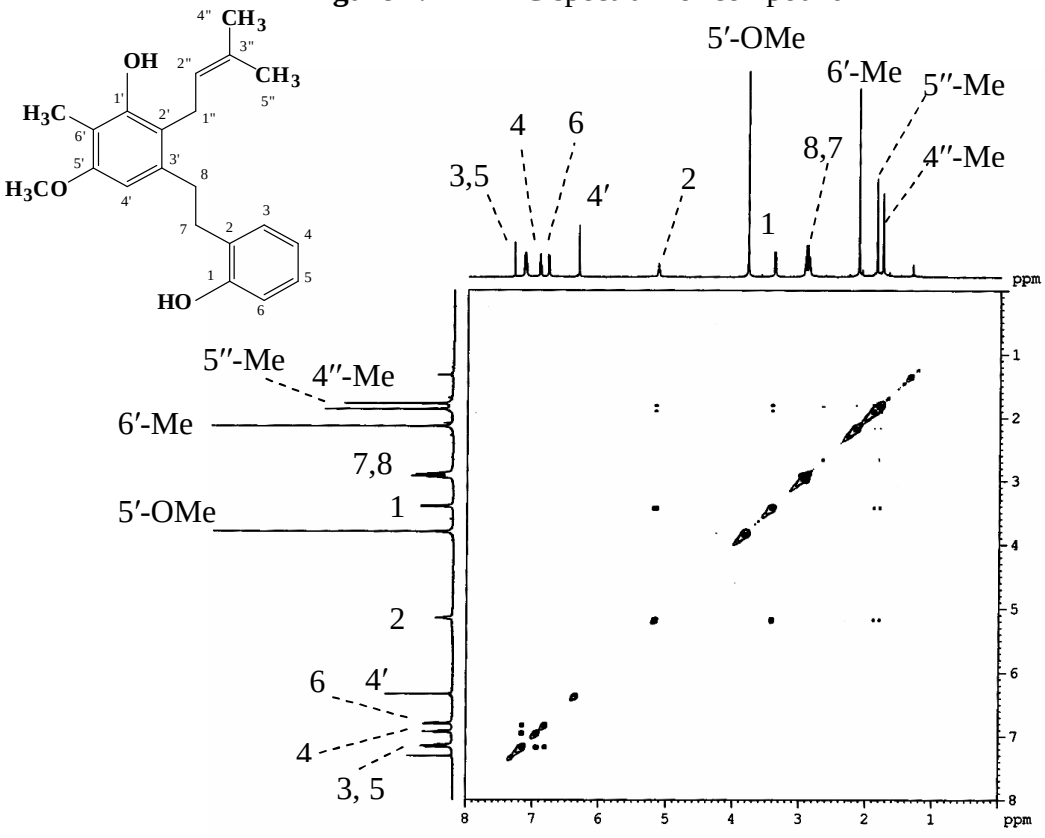

Figure 2.8 ^{1}H,^{1}H-COSY spectrum of compound **II**

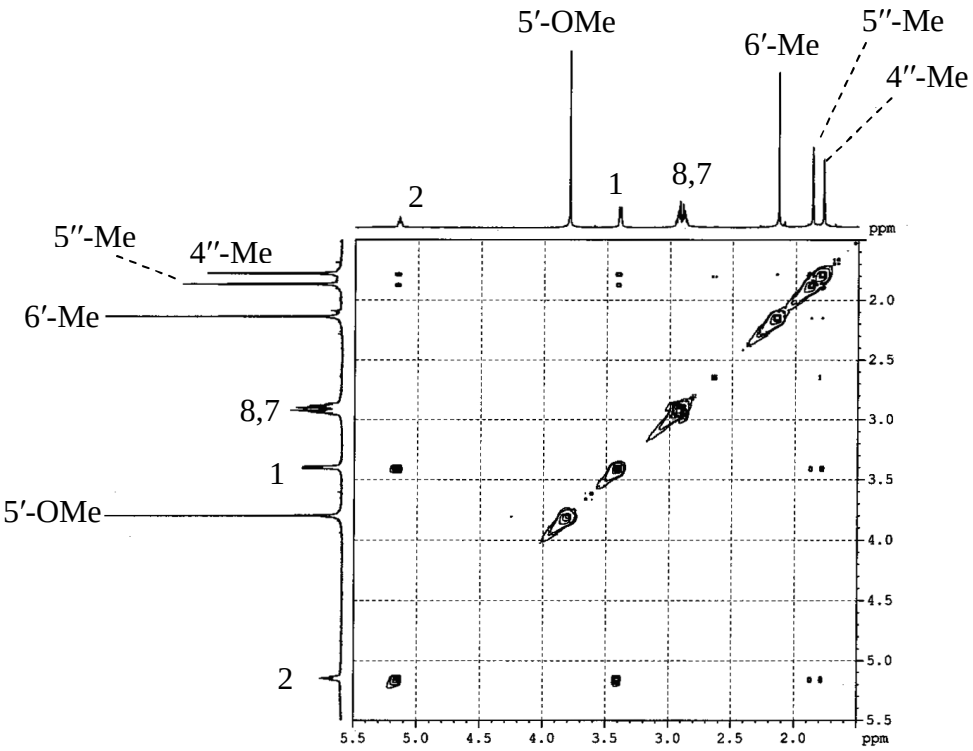

Figure 2.8a Expansion of Fig. 2.8

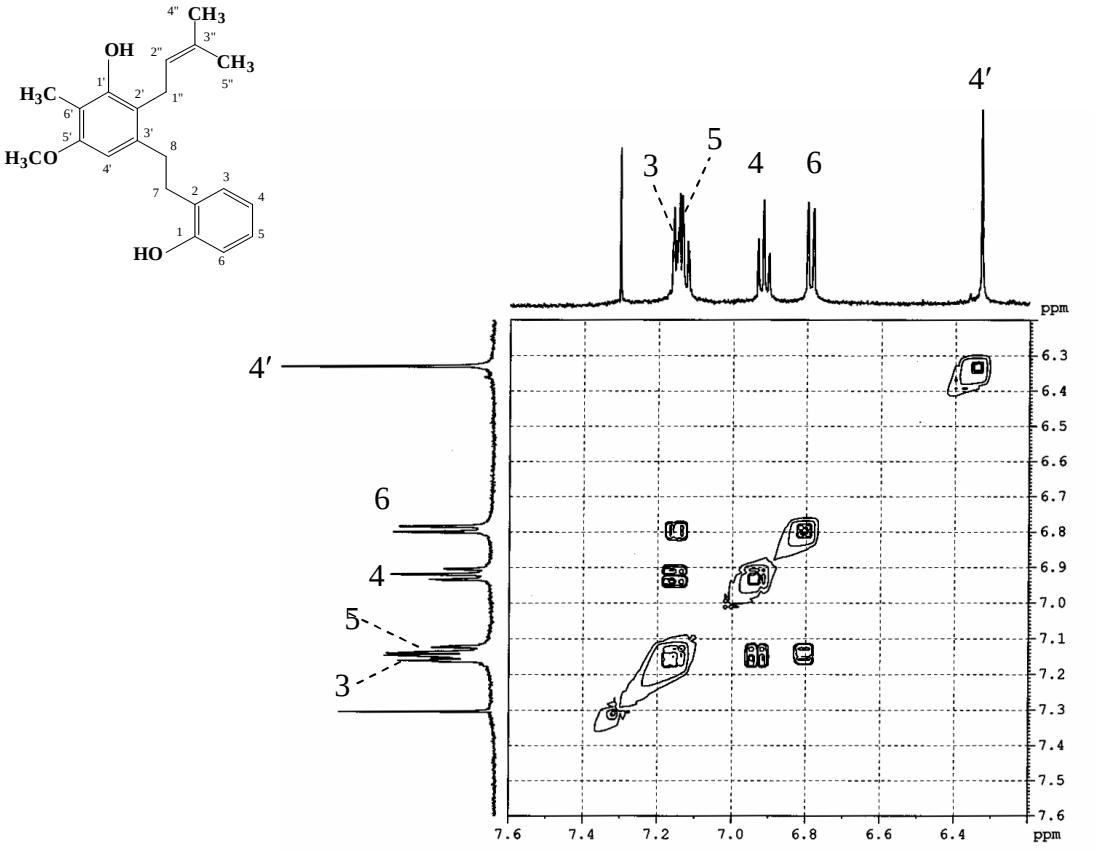

Figure 2.8b Expansion of Fig. 2.8

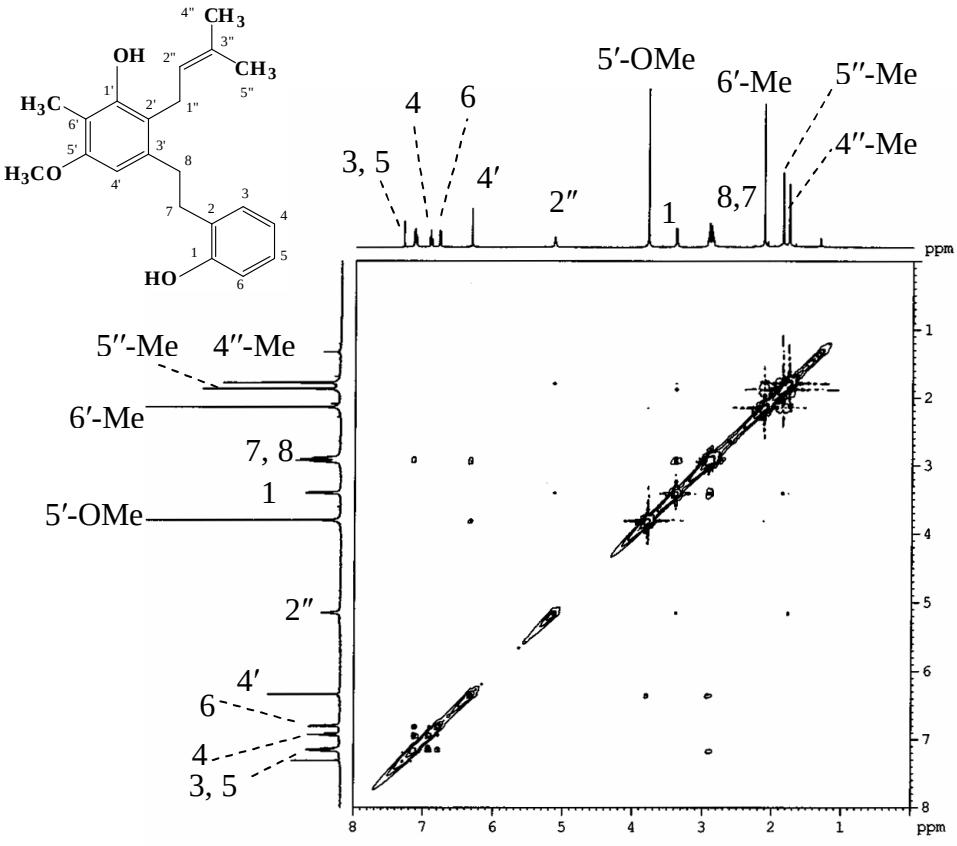

Figure 2.9 NOESY spectrum of compound **II**

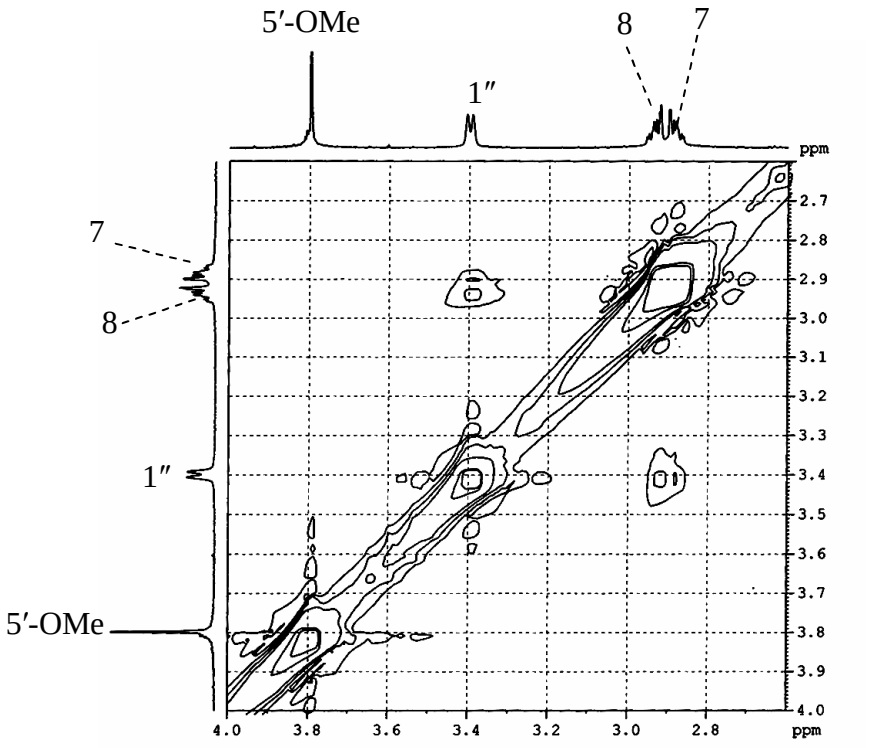

Figure 2.9a Expansion of Fig. 2.9

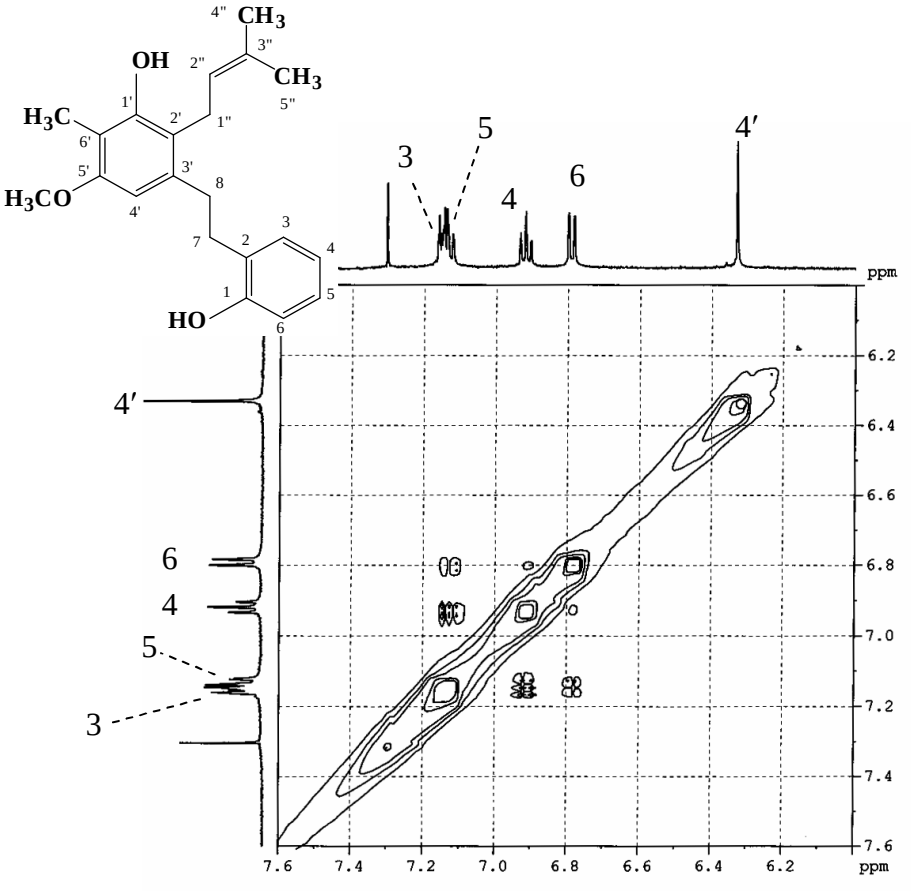

Figure 2.9b Expansion of Fig. 2.9

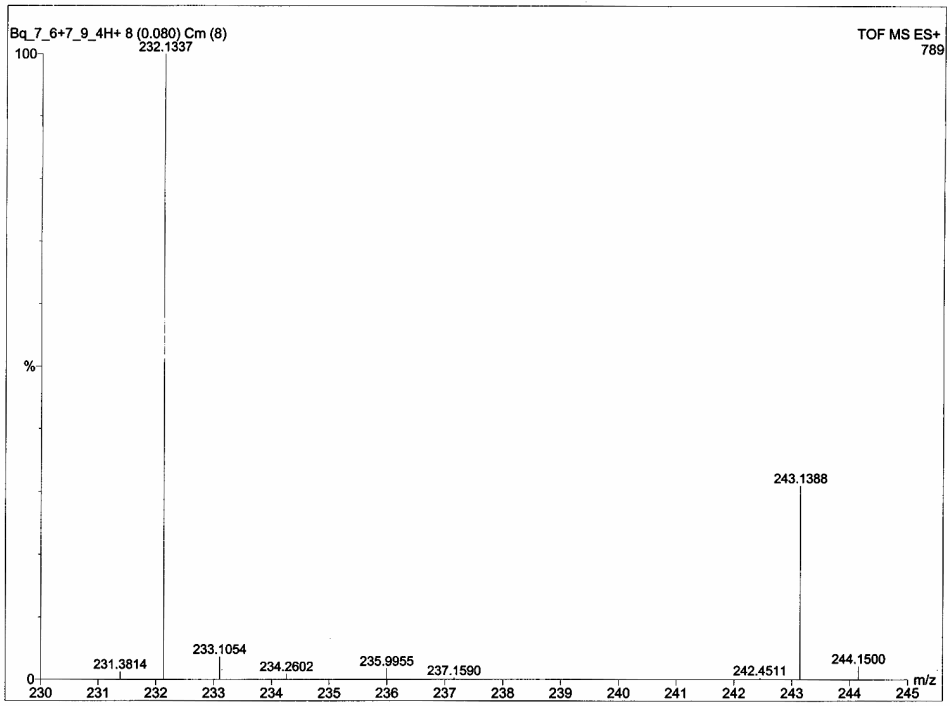

Figure 3.1 Mass spectrum of compound **III**

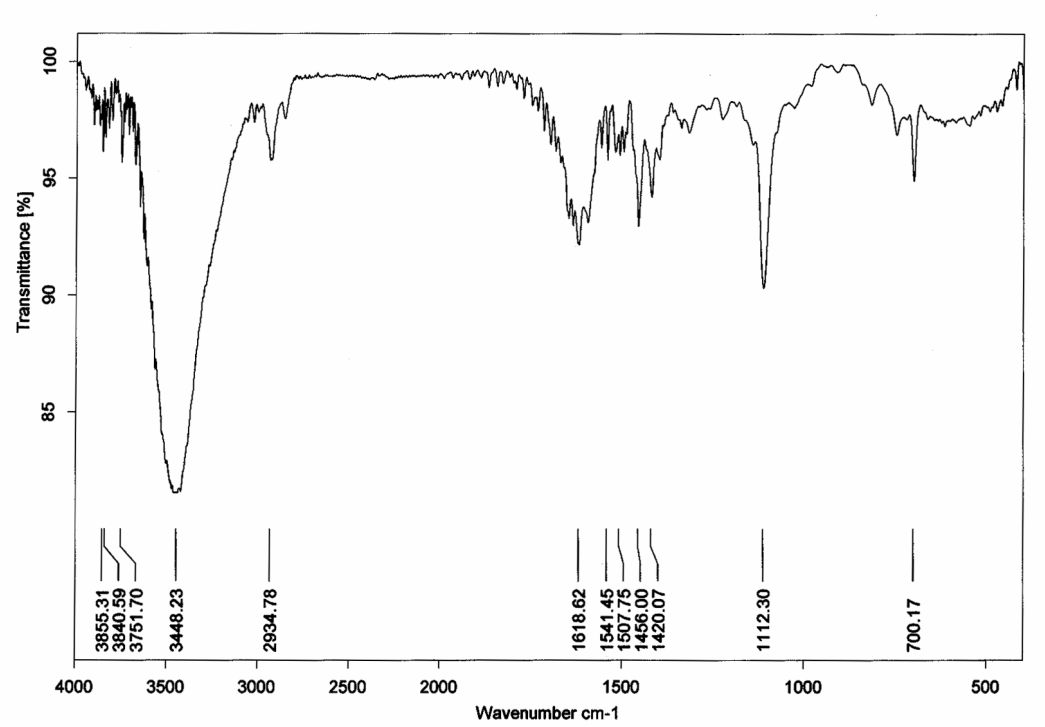

Figure 3.2 IR spectrum of compound **III**

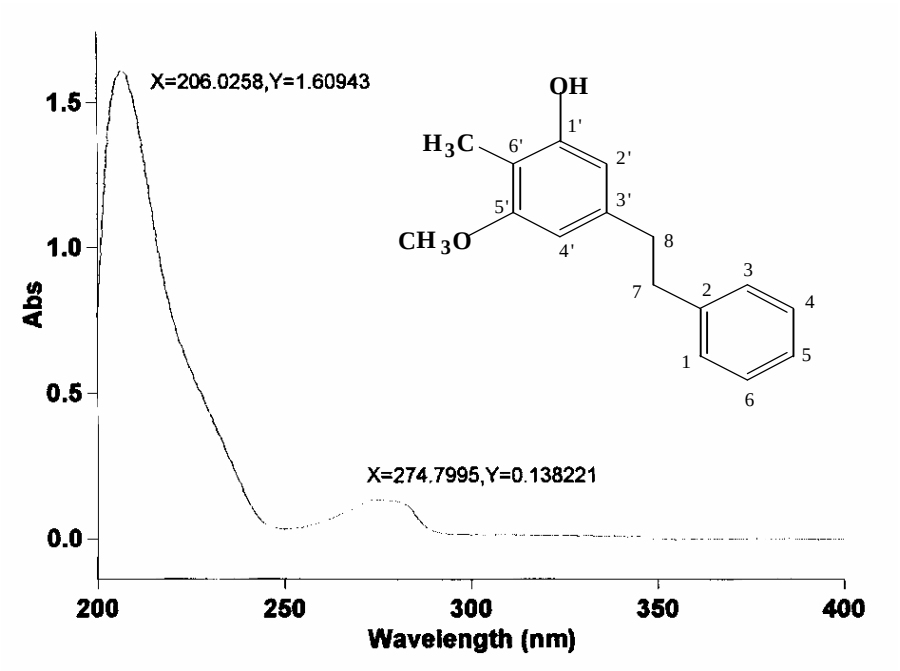

Figure 3.3 UV-Vis spectrum of compound **III**

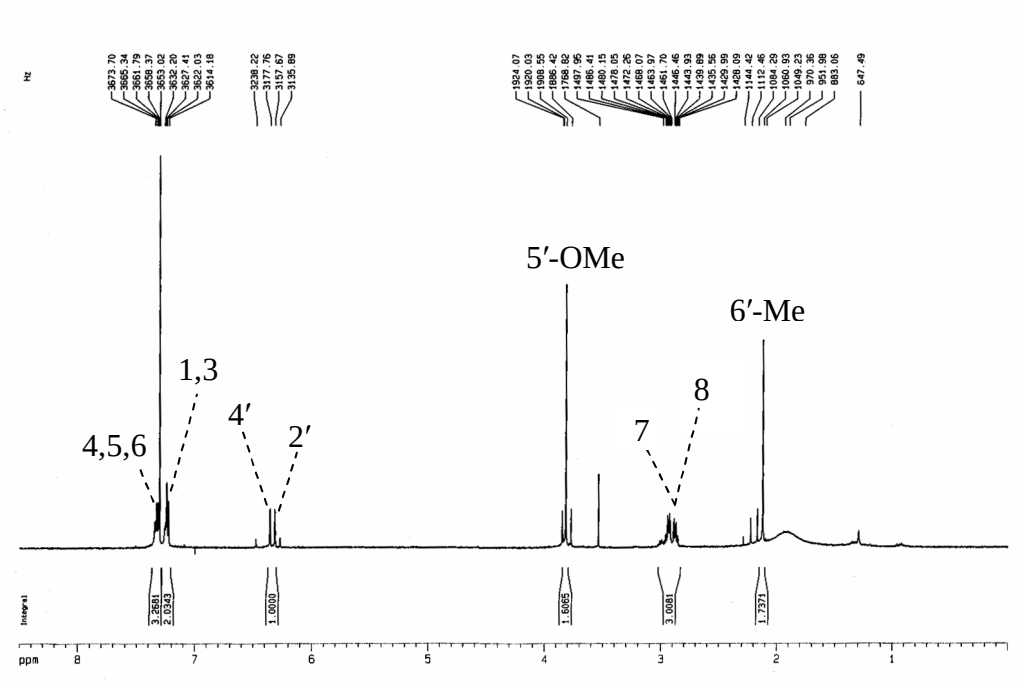

Figure 3.4 500 MHz ^{1}H-NMR spectrum of compound **III** in $CDCl_3$

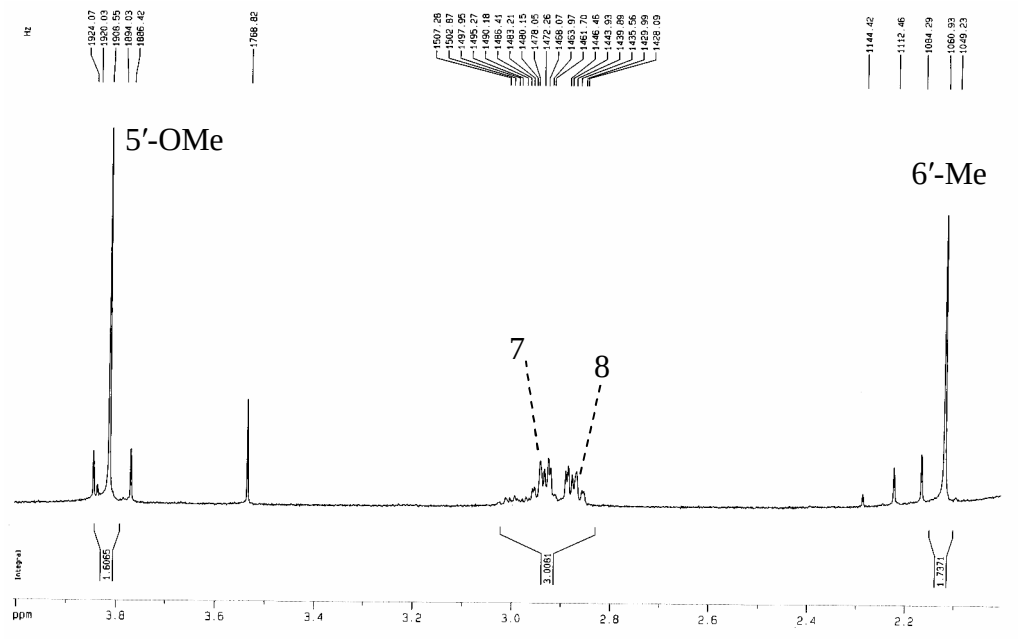

Figure 3.4a Expansion of Fig. 3.4

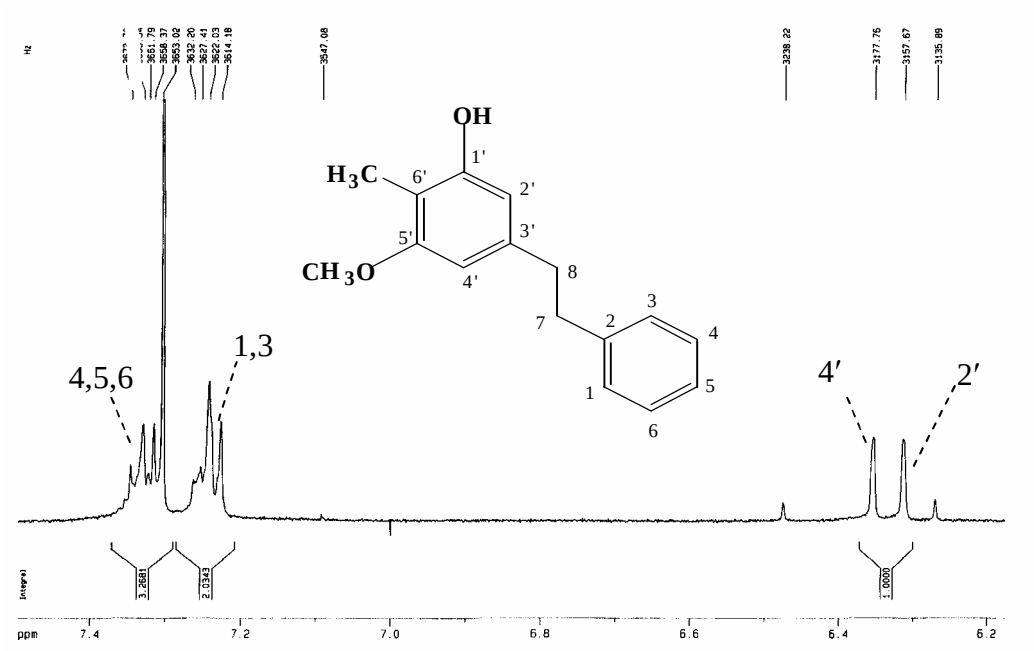

Figure 3.4b Expansion of Fig. 3.4

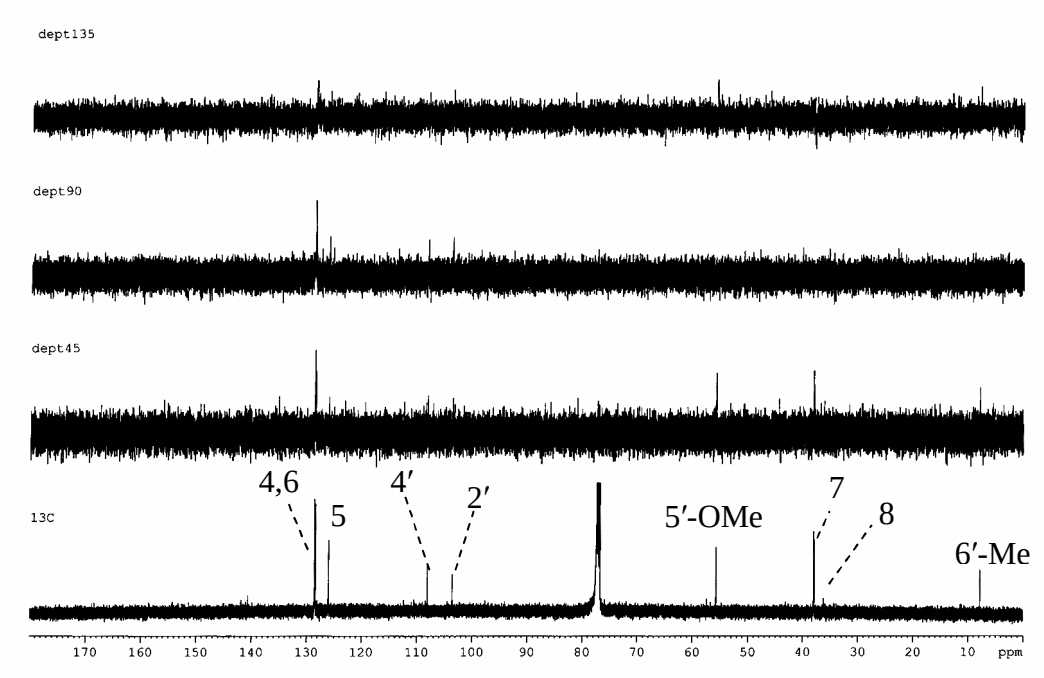

Figure 3.5 ^{13}C-NMR and DEPT spectra of compound **III** $CDCl_3$

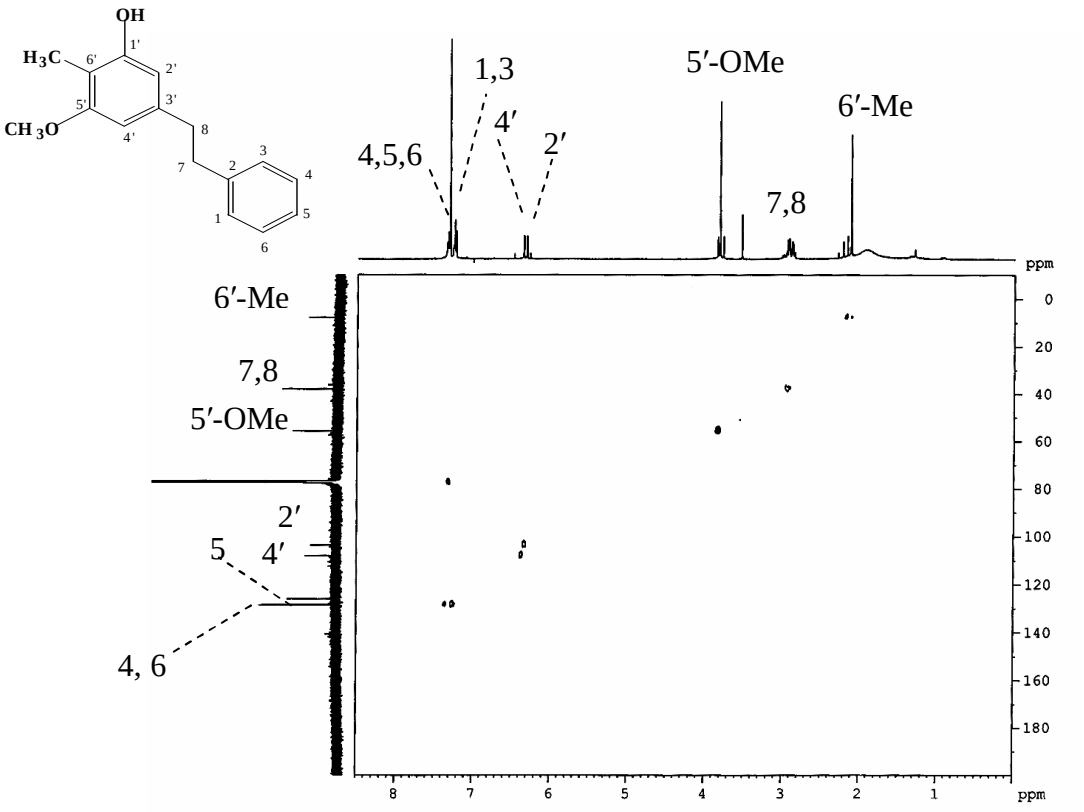

Figure 3.6 HMQC spectrum of compound **III**

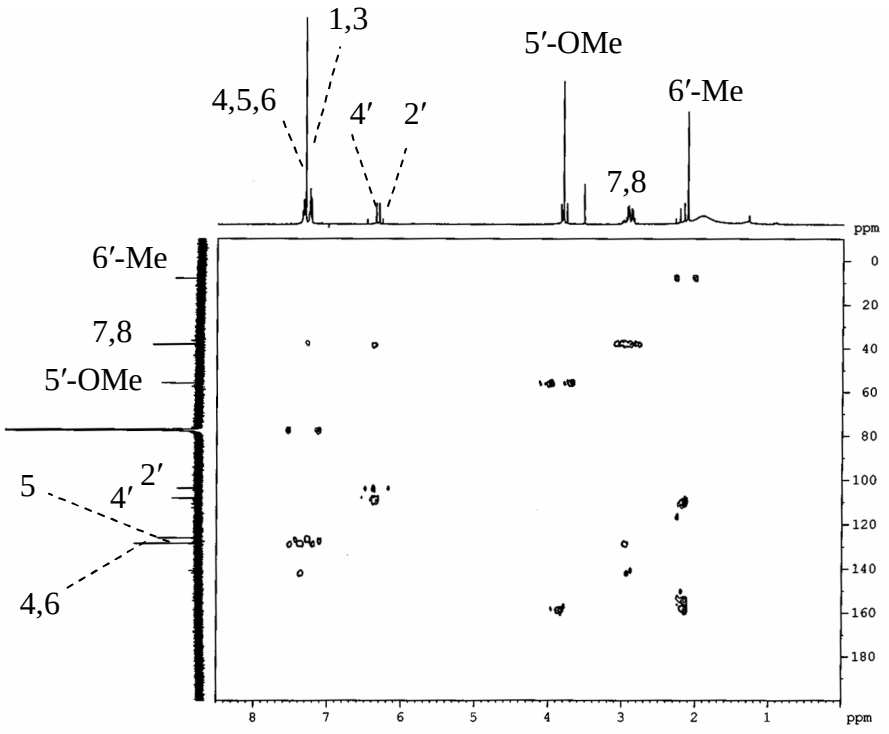

Figure 3.7 HMBC spectrum of compound **III**

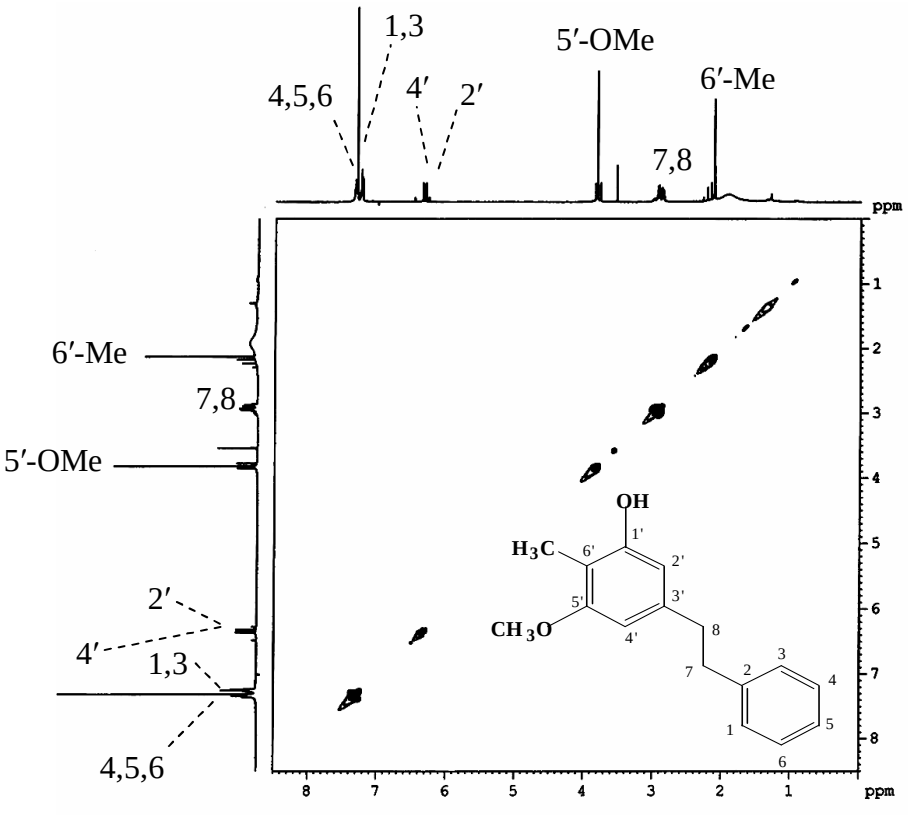

Figure 3.8 ^{1}H,^{1}H-COSY spectrum of compound **III**

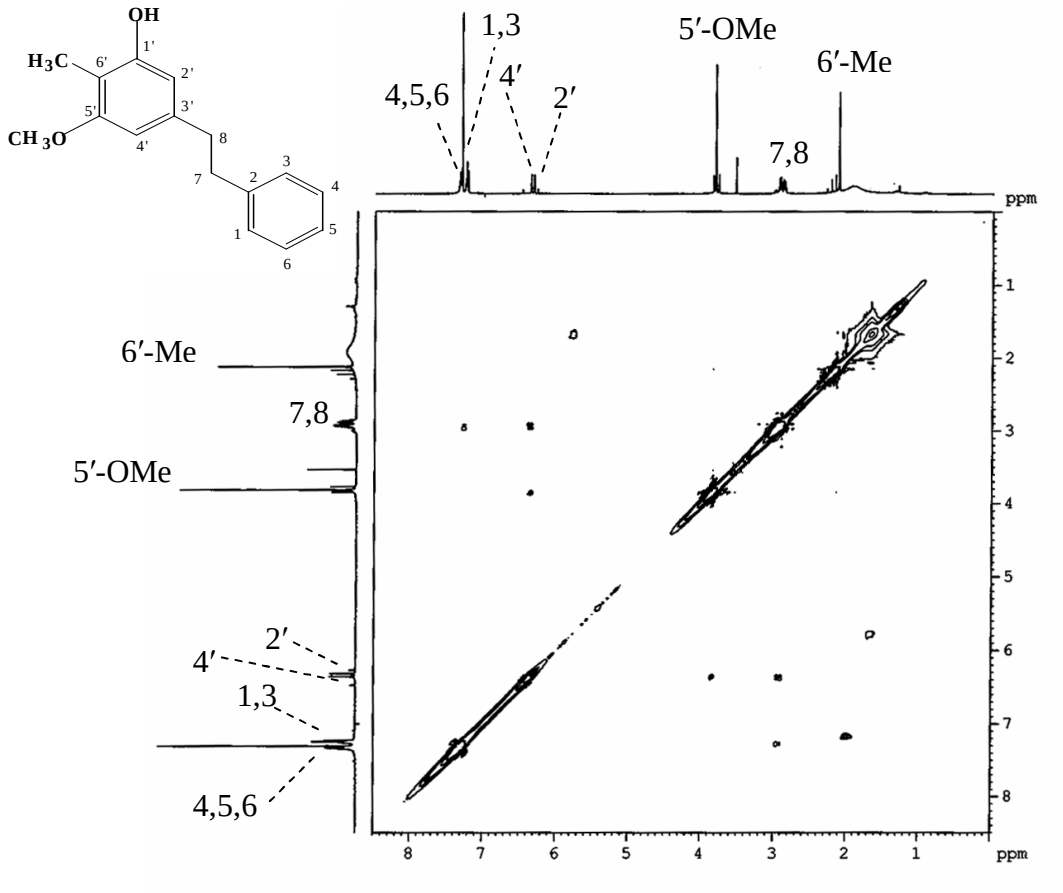

Figure 3.9 NOESY spectrum of compound **III**

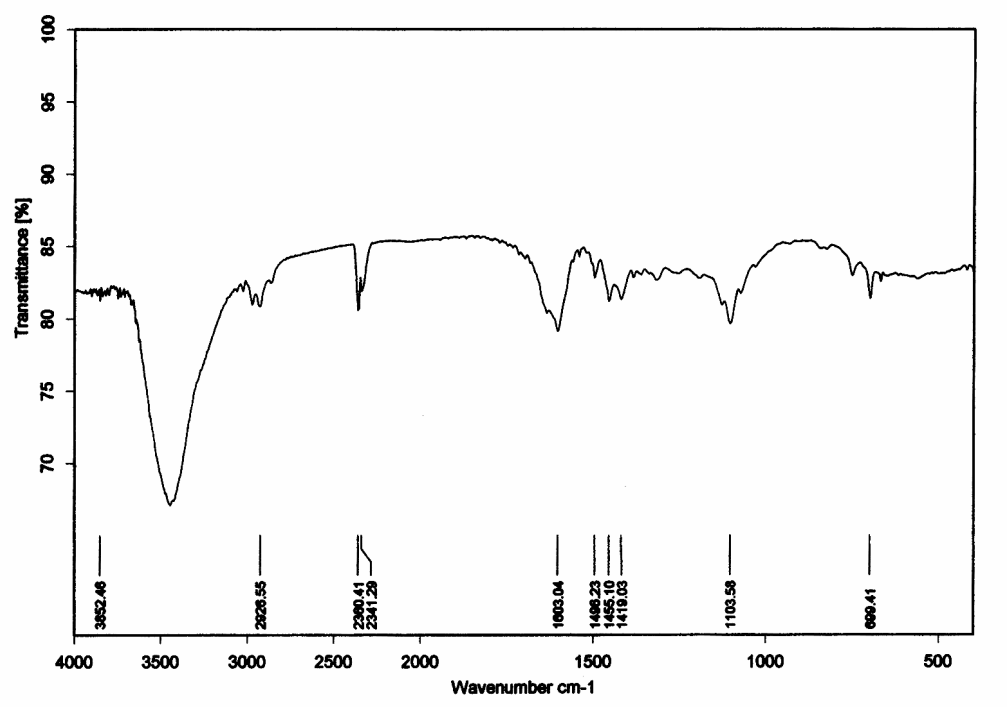

Figure 4.1 IR spectrum of compound **IV**

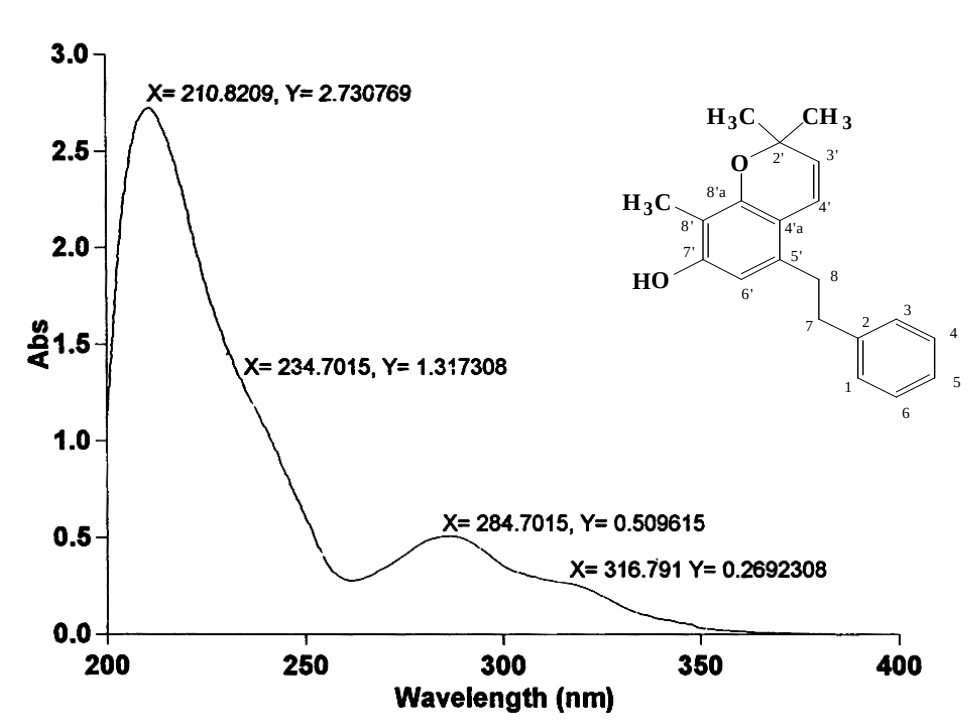

Figure 4.2 UV-Vis spectrum of compound **IV**

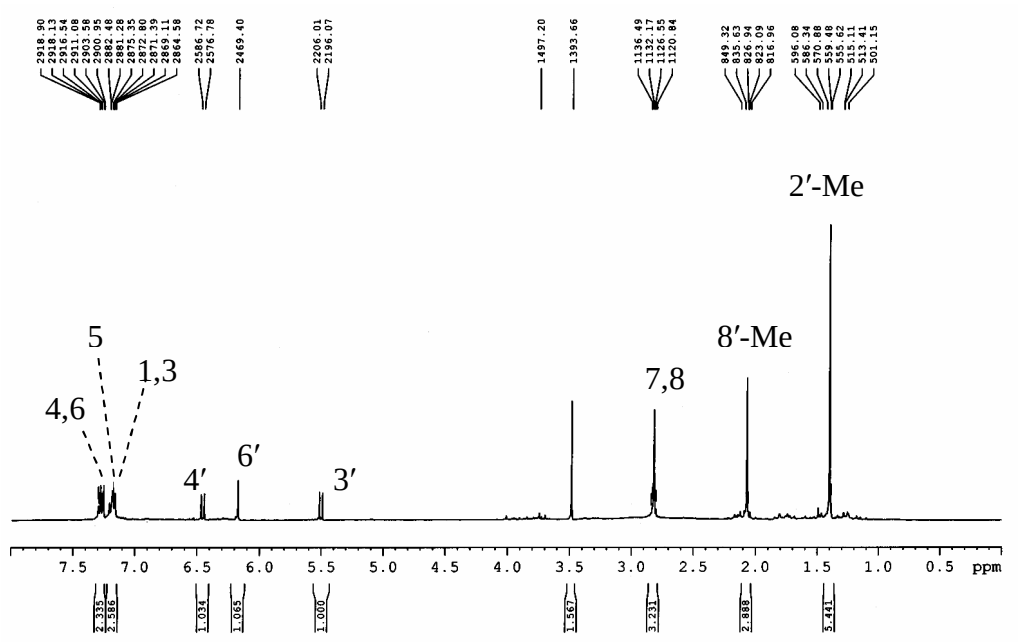

Figure 4.3 400 MHz ^{1}H-NMR spectrum of compound **IV** in $CDCl_3$

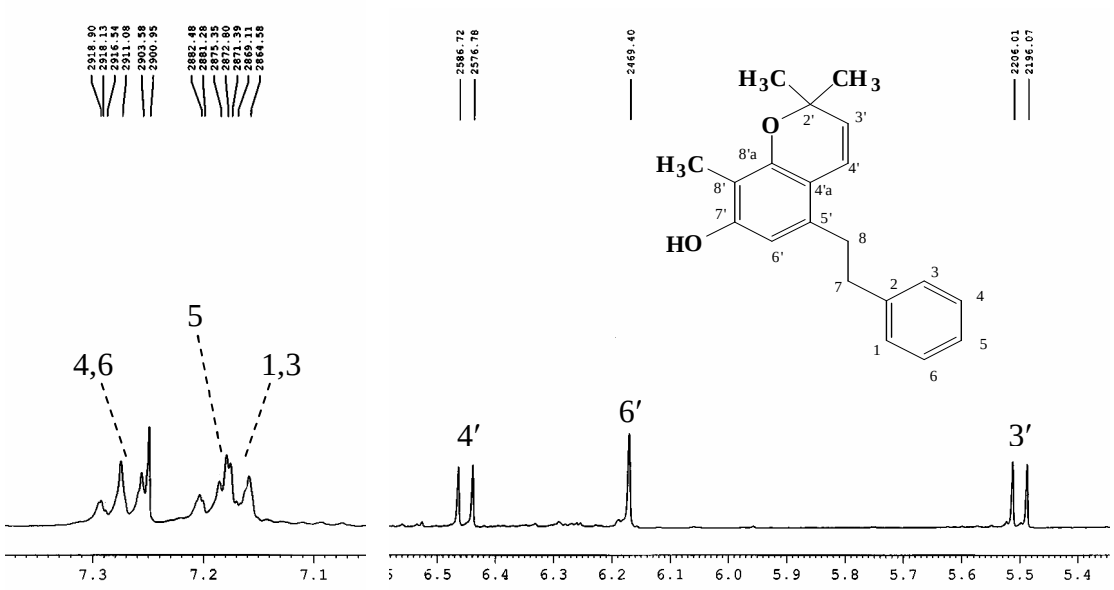

Figure 4.3a Expansion of Fig. 4.3

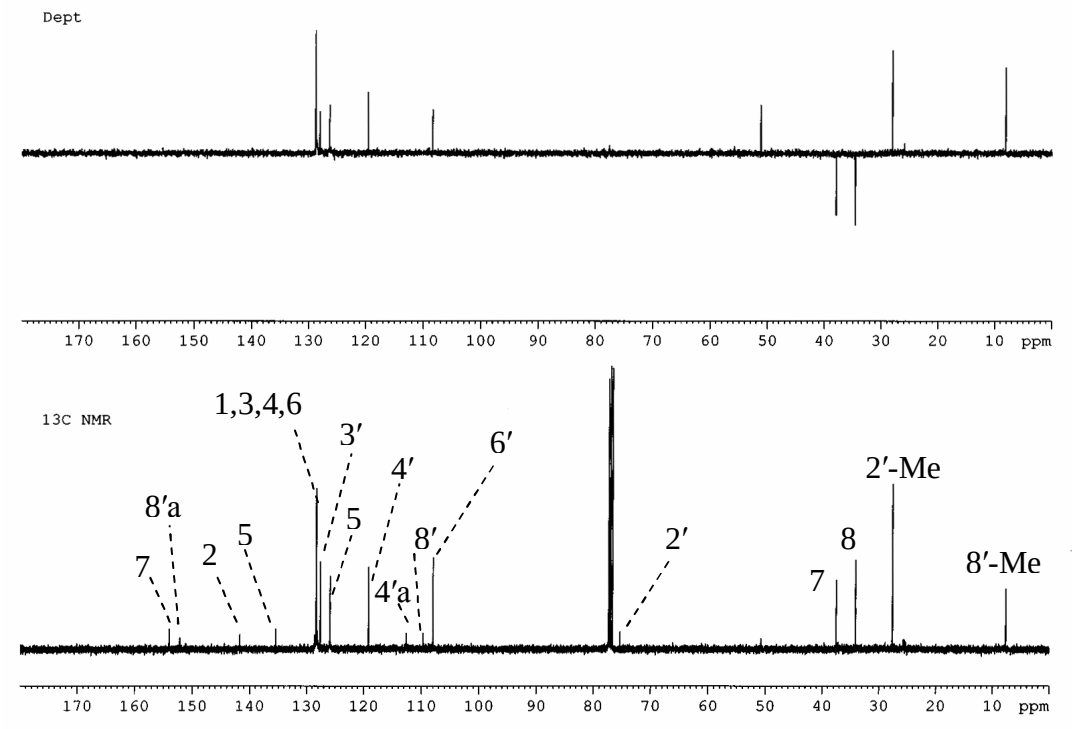

Figure 4.4 ^{13}C-NMR and DEPT spectra of compound **IV** in $CDCl_3$

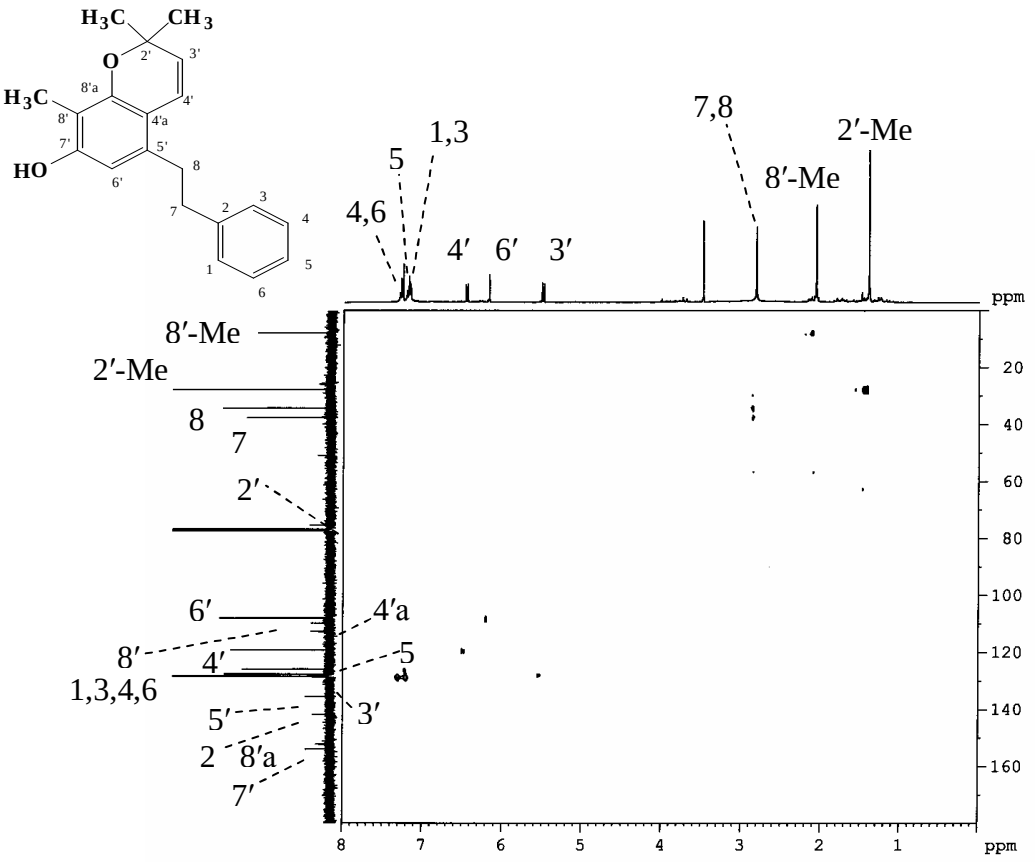

Figure 4.5 HMQC spectrum of compound **IV**

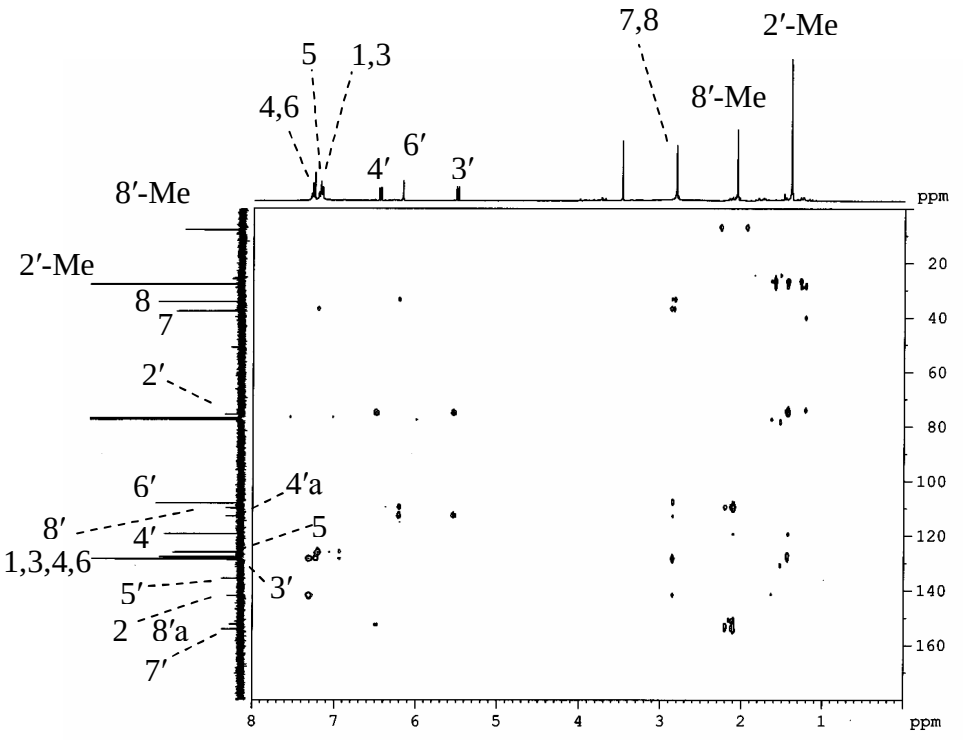

Figure 4.6 HMBC spectrum of compound **IV**

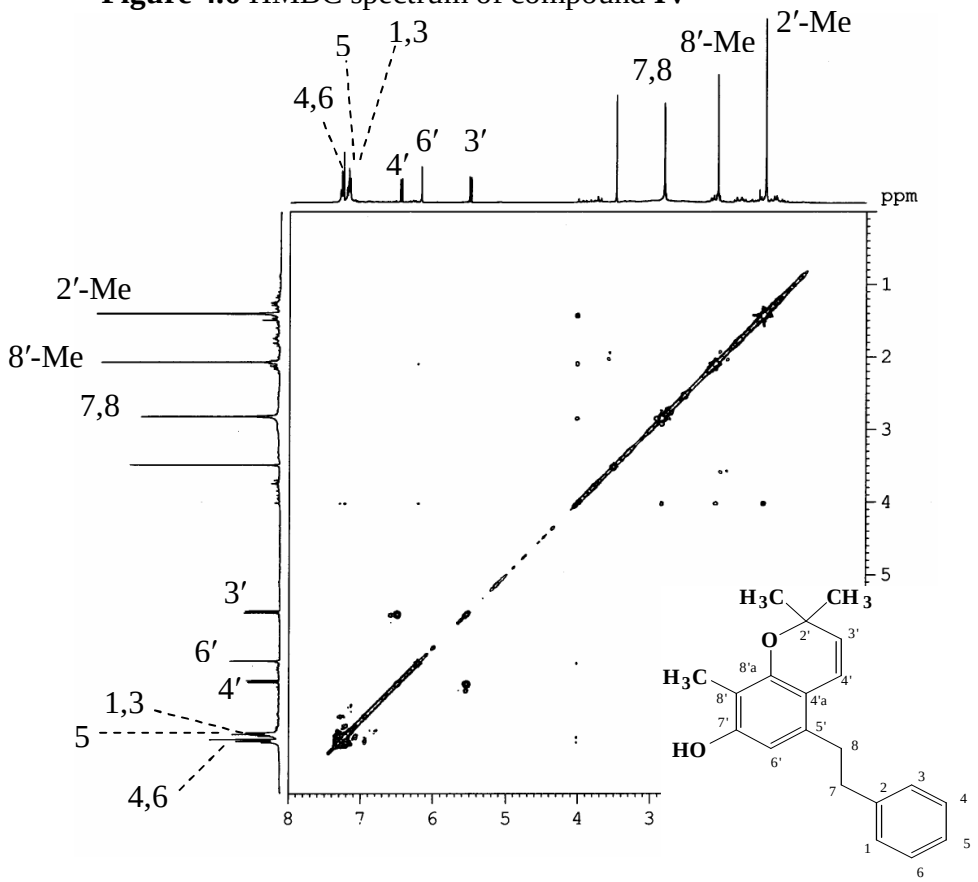

Figure 4.7 ^{1}H,^{1}H-COSY spectrum of compound **IV**

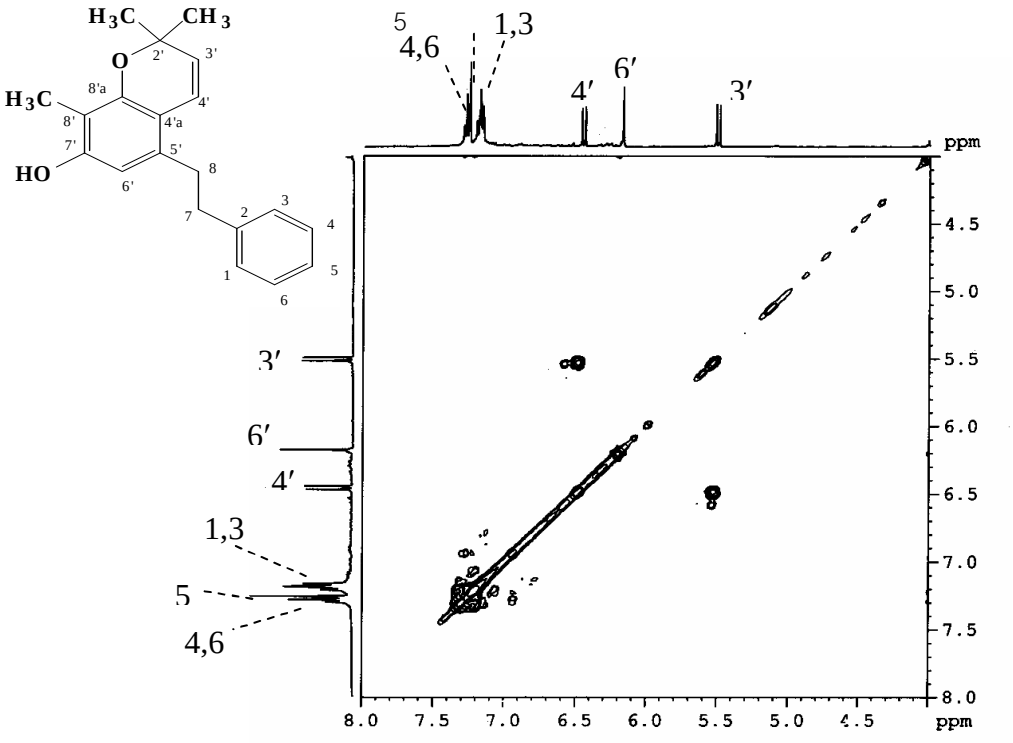

Figure 4.7a Expansion of Fig. 4.7

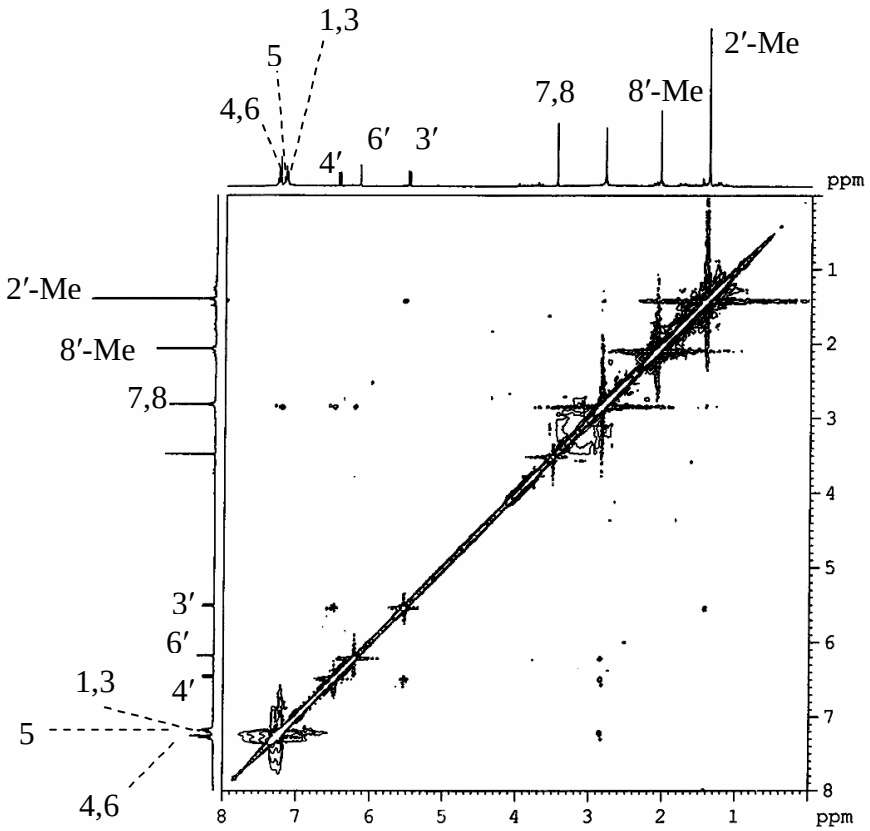

Figure 4.8 NOESY spectrum of compound **IV**

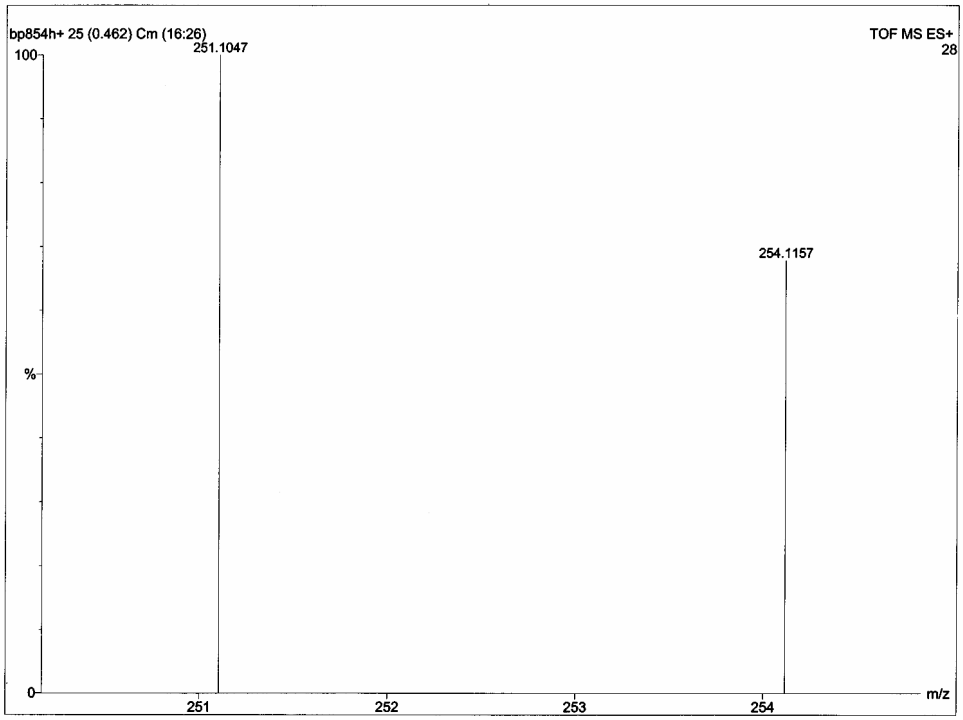

Figure 5.1 Mass spectrum of compound **V**

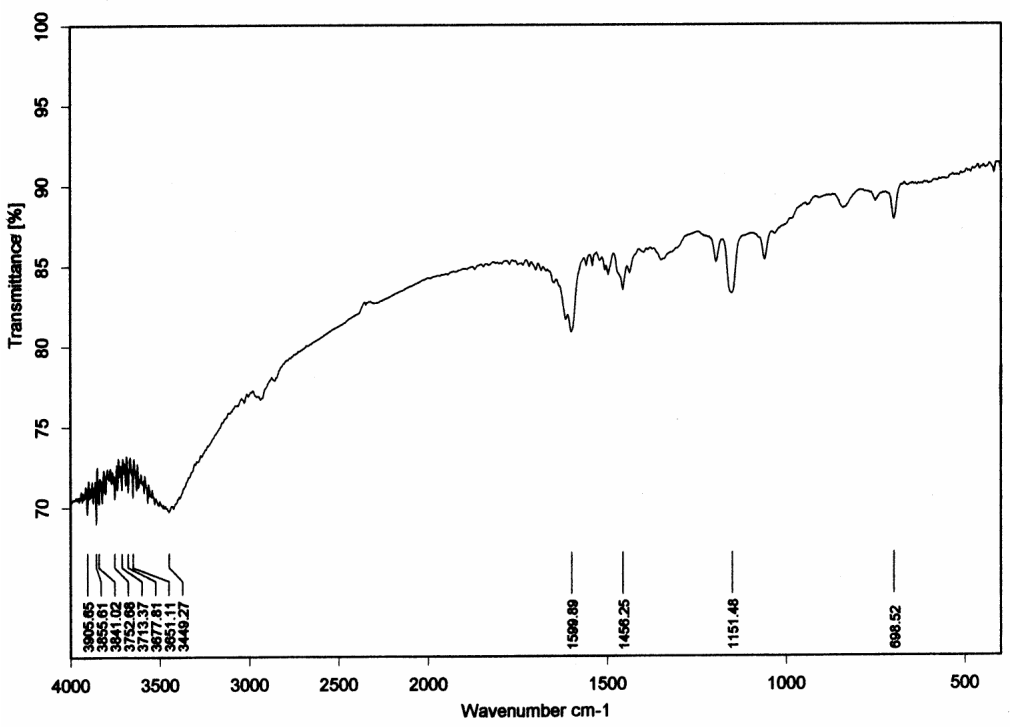

Figure 5.2 IR spectrum of compound **V**

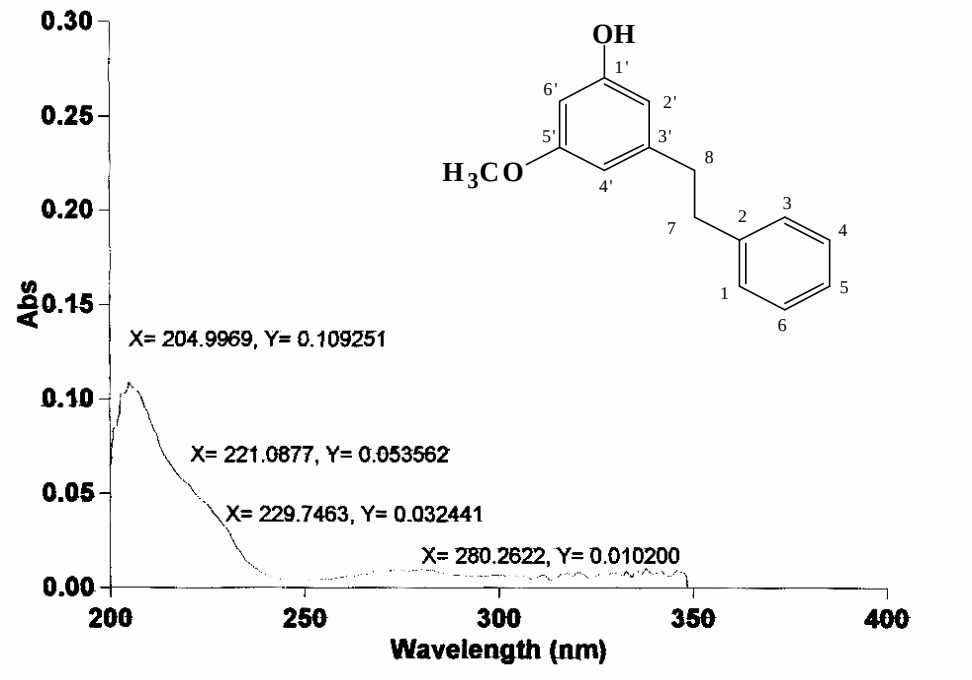

Figure 5.3 UV-Vis spectrum of compound **V**

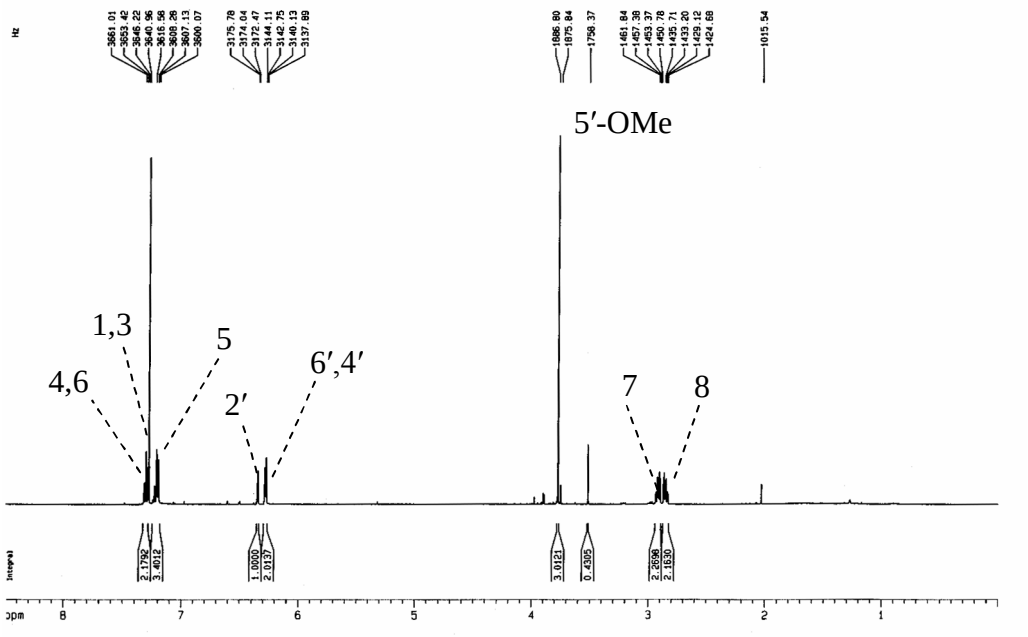

Figure 5.4 500 MHz ^{1}H-NMR spectrum of compound **V** in $CDCl_3$

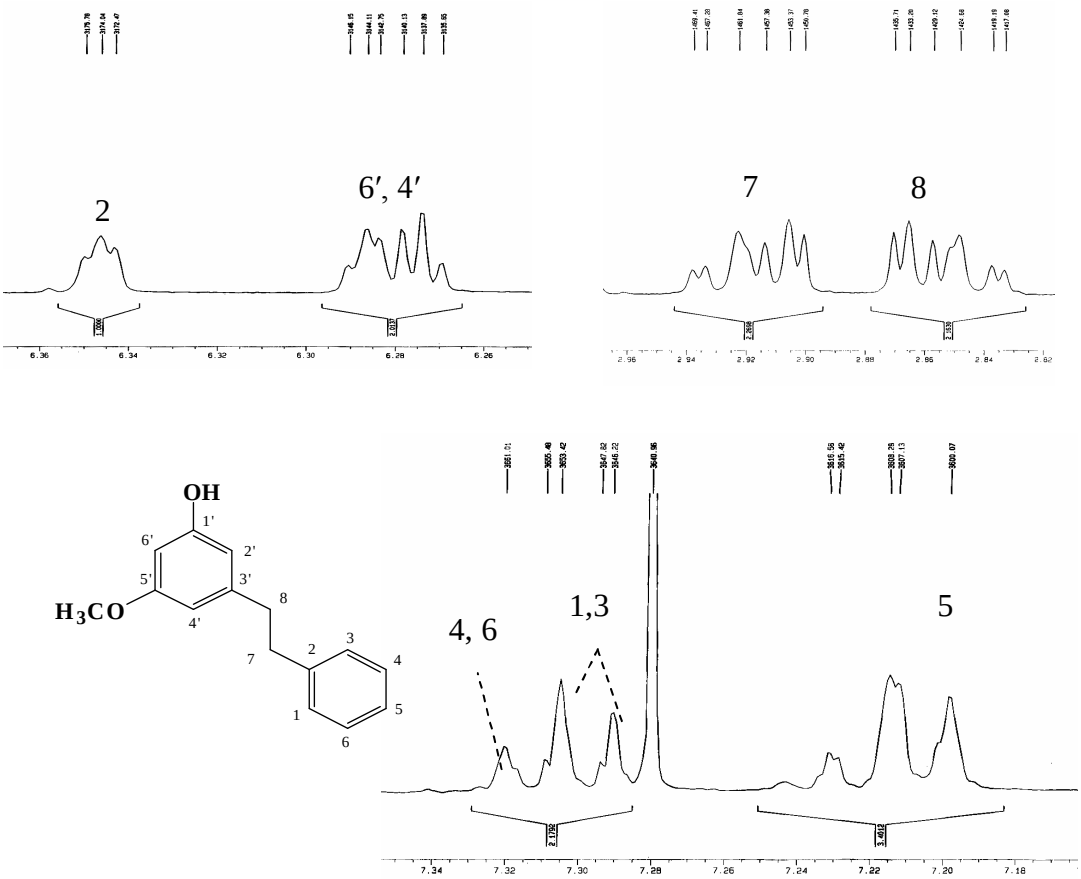

Figure 5.4a Expansion of Fig.5.4

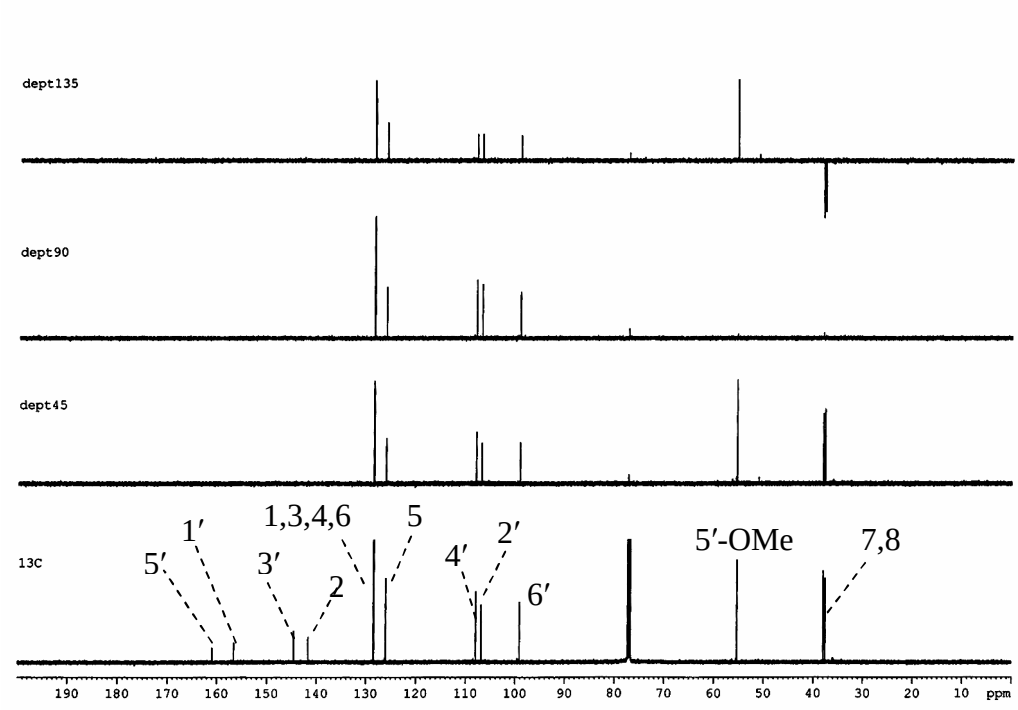

Figure 5.5 ^{13}C-NMR and DEPT spectra of compound **V** in $CDCl_3$

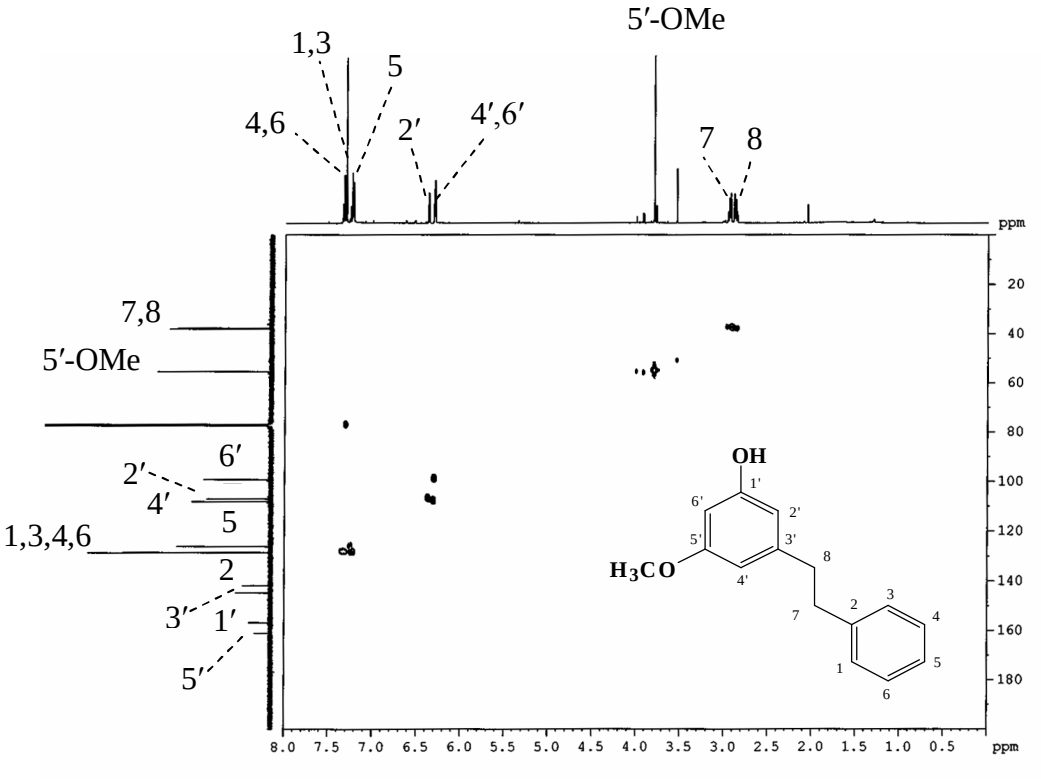

Figure 5.6 HMQC spectrum of compound **V**

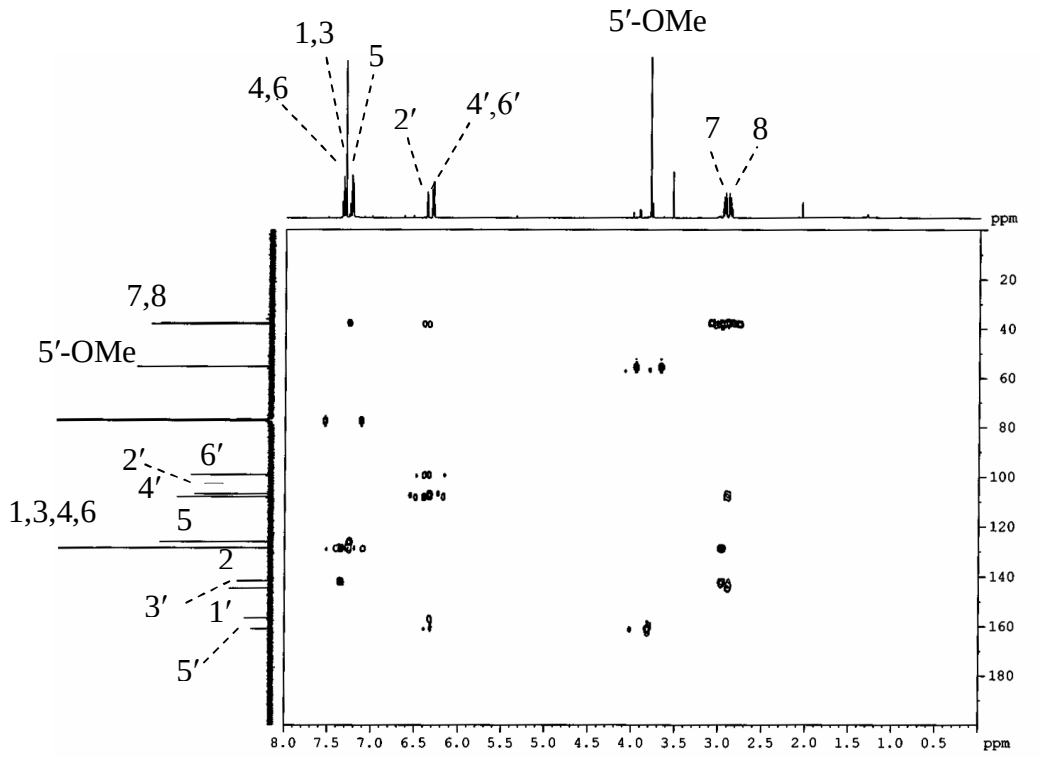

Figure 5.7 HMBC spectrum of compound **V**

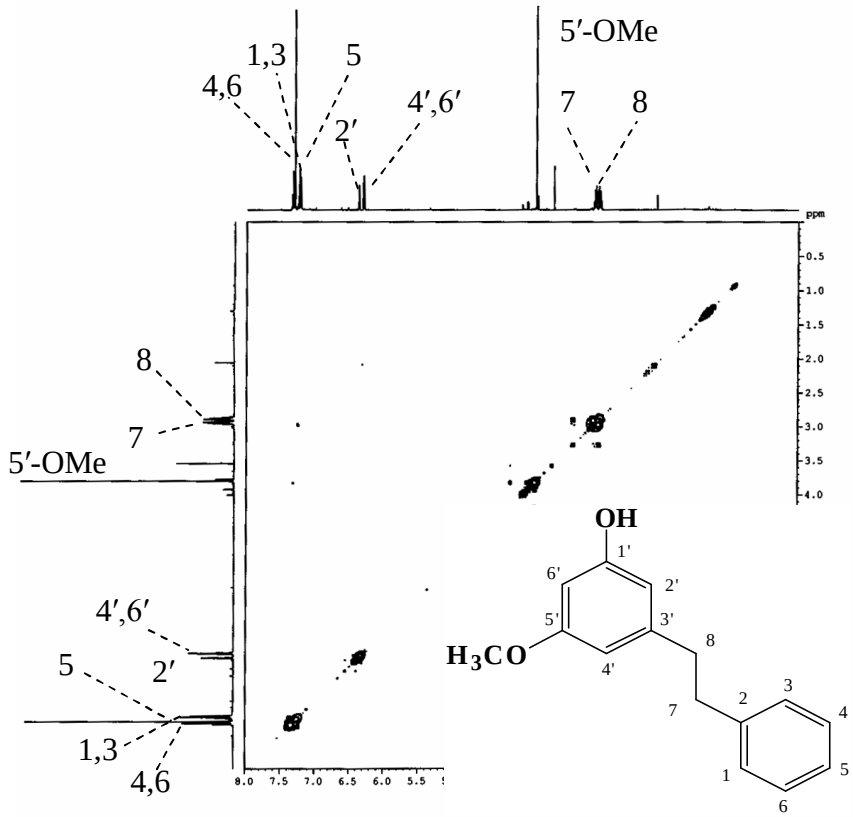

Figure 5.8 $^{1}H,^{1}H$-COSY spectrum of compound **V**

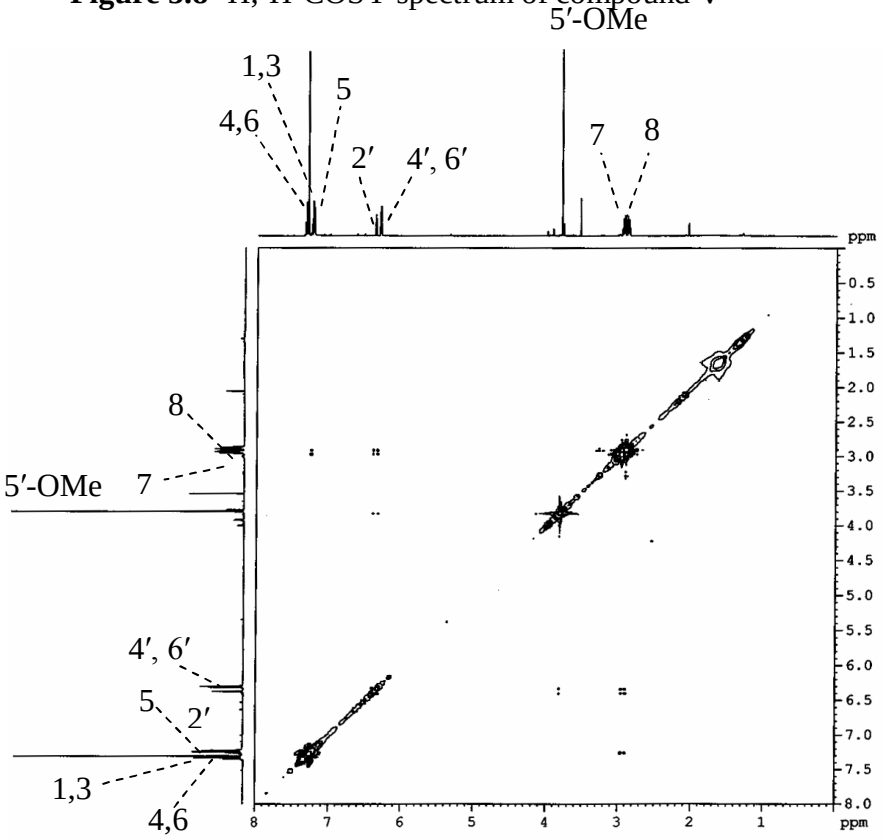

Figure 5.9 NOESY spectrum of compound **V**

136

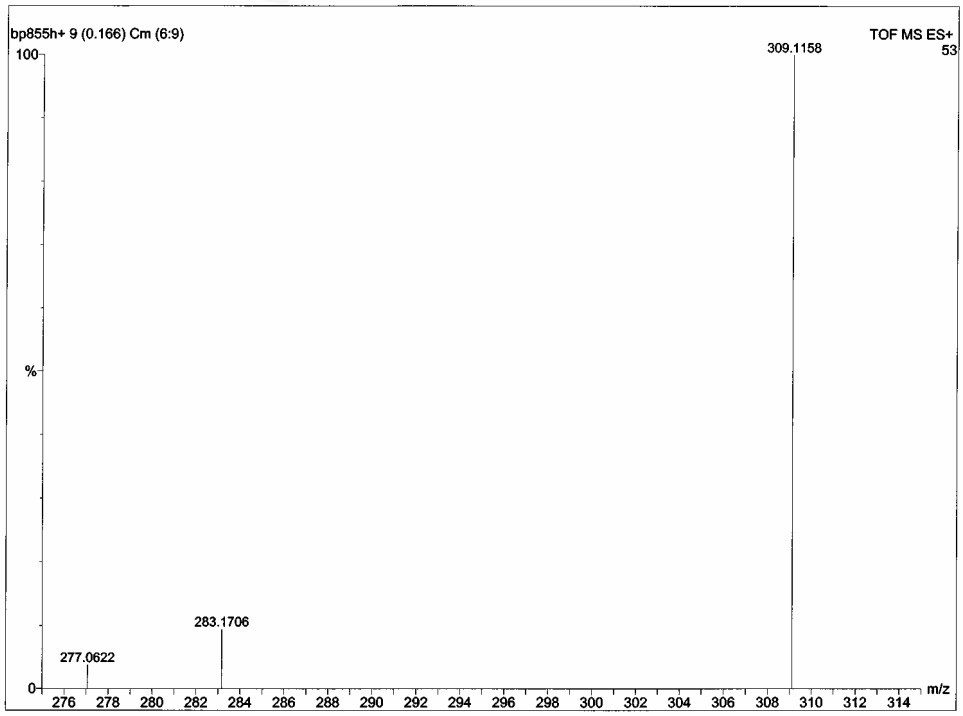

Figure 6.1 Mass spectrum of compound **VI**

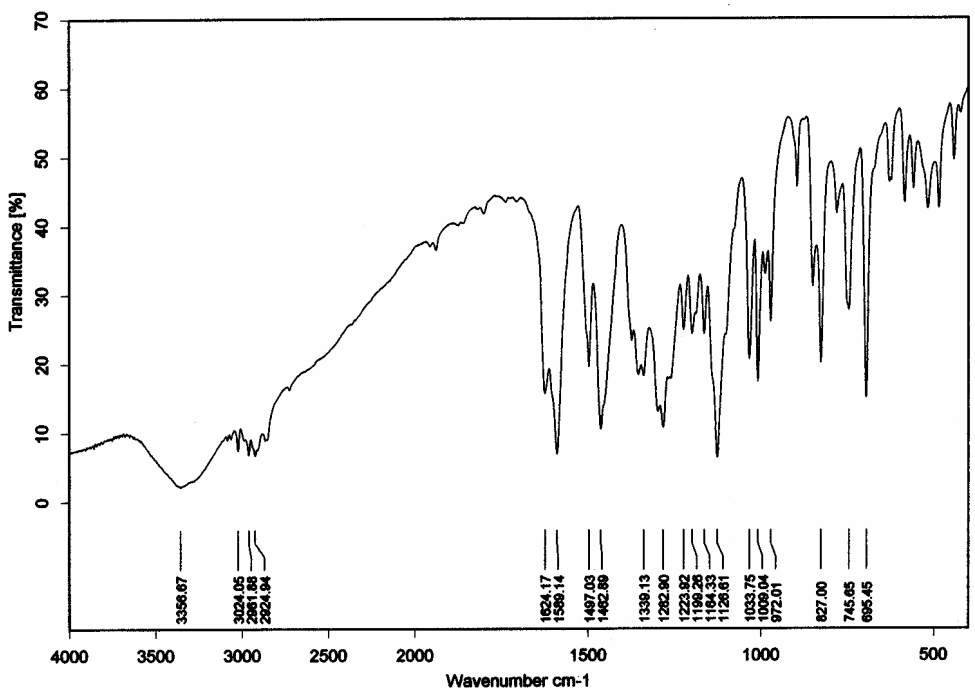

Figure 6.2 IR spectrum of compound **VI**

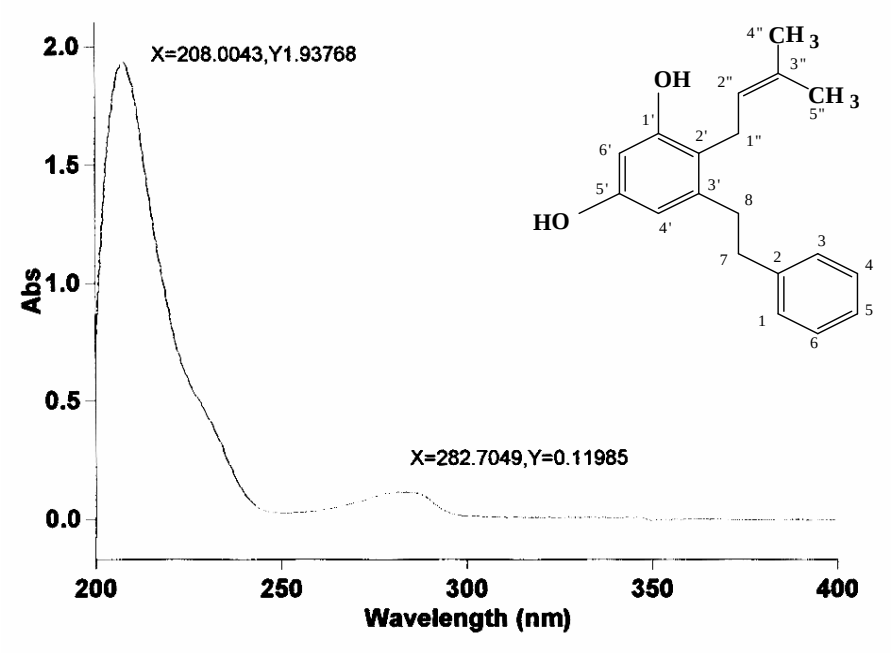

Figure 6.3 UV-Vis spectrum of compound **VI**

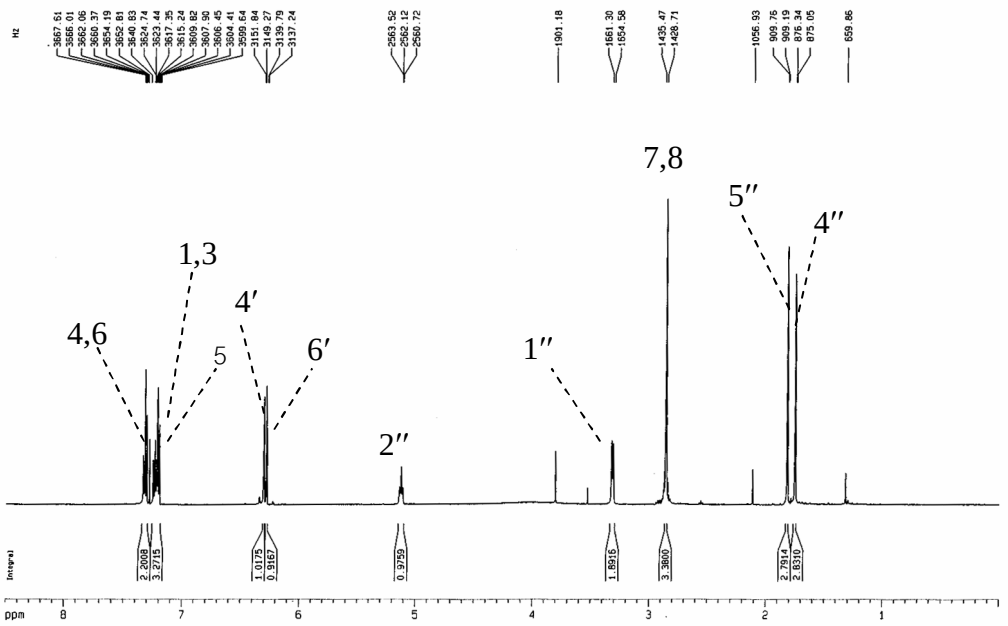

Figure 6.4 500 MHz ^{1}H-NMR spectrum of compound **VI** in $CDCl_3$

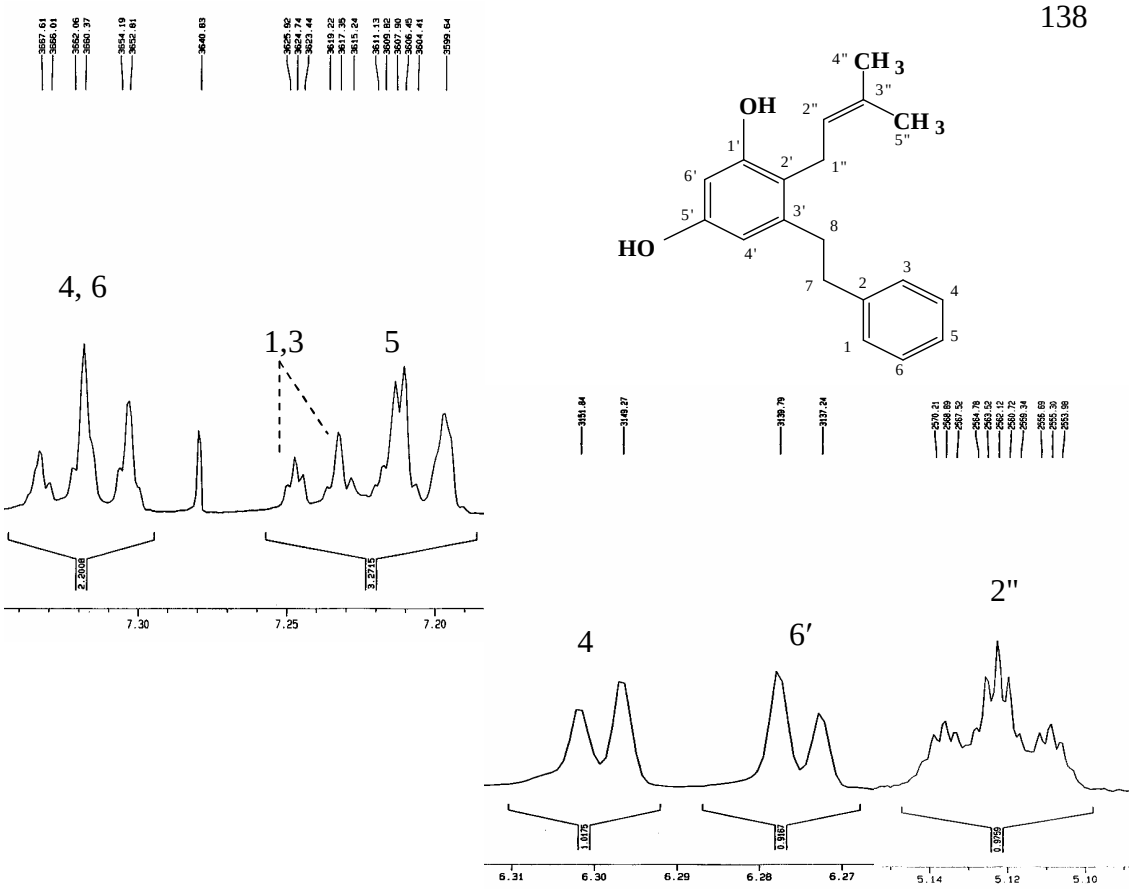

Figure 6.4a Expansion of Fig.6.4

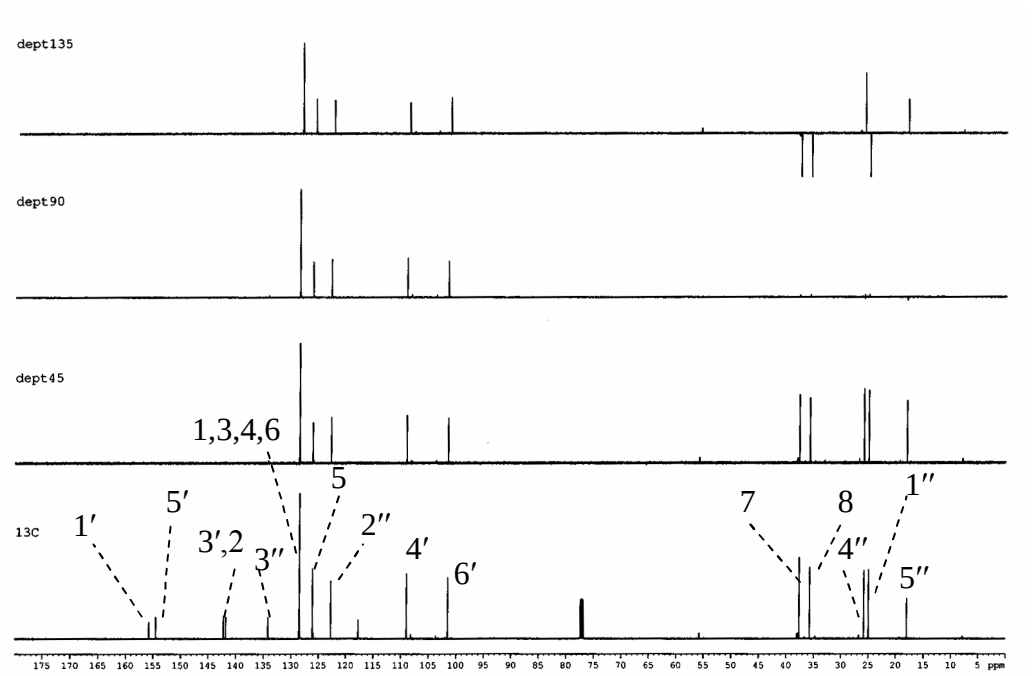

Figure 6.5 ^{13}C-NMR and DEPT spectra of compound **VI** in $CDCl_3$

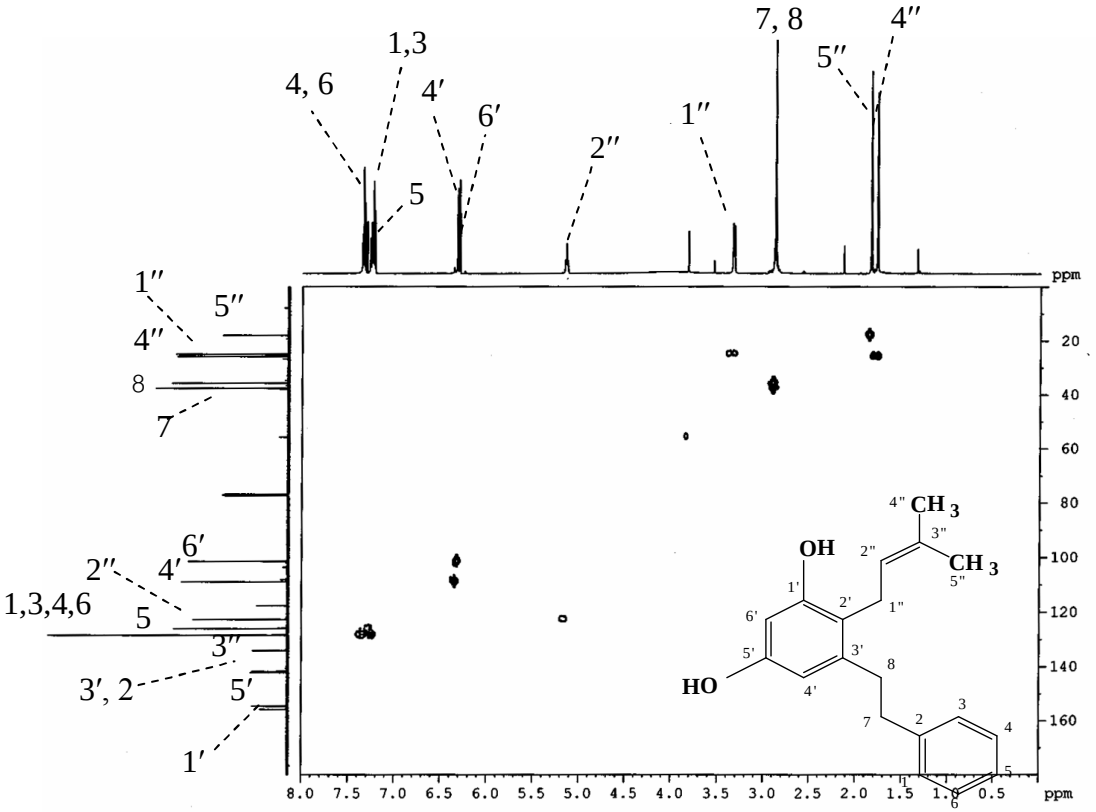

Figure 6.6 HMQC spectrum of compound **VI**

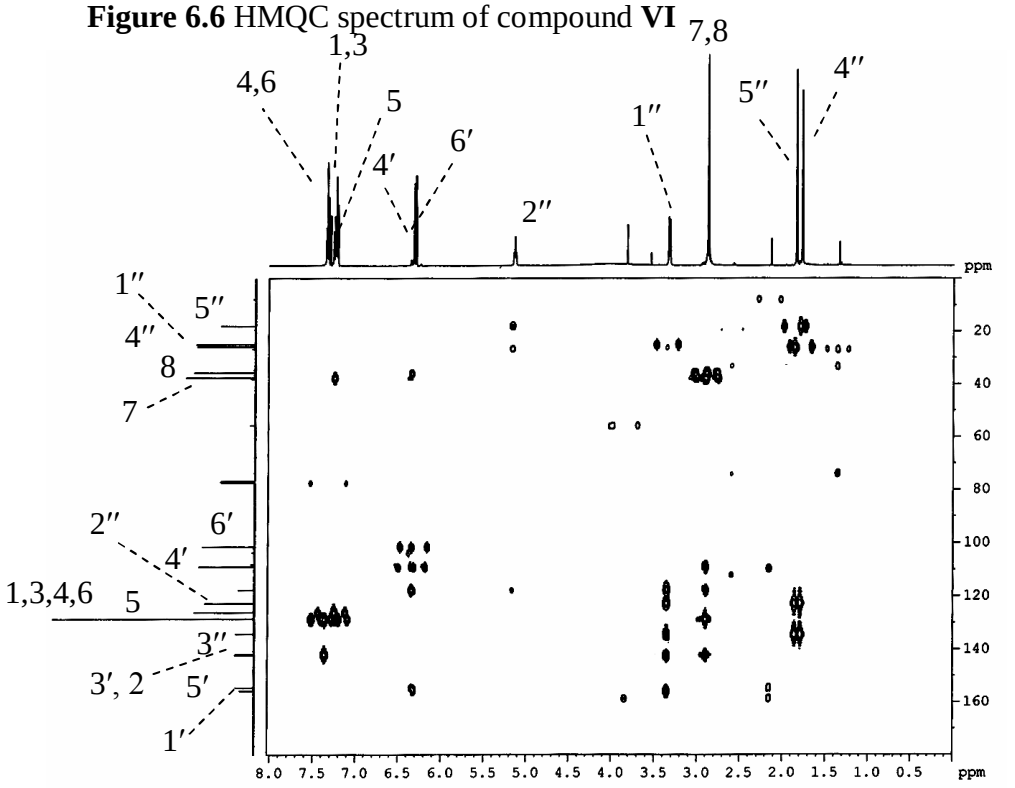

Figure 6.7 HMBC spectrum of compound **VI**

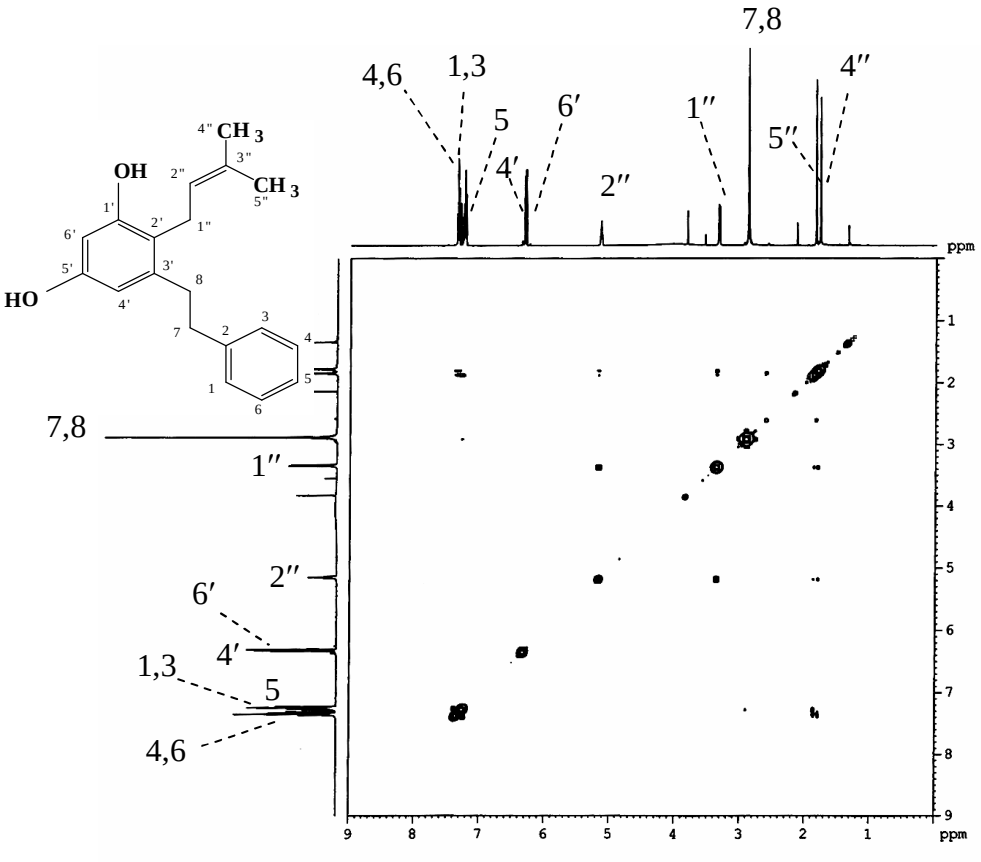

Figure 6.8 ^{1}H,^{1}H-COSY spectrum of compound **VI**

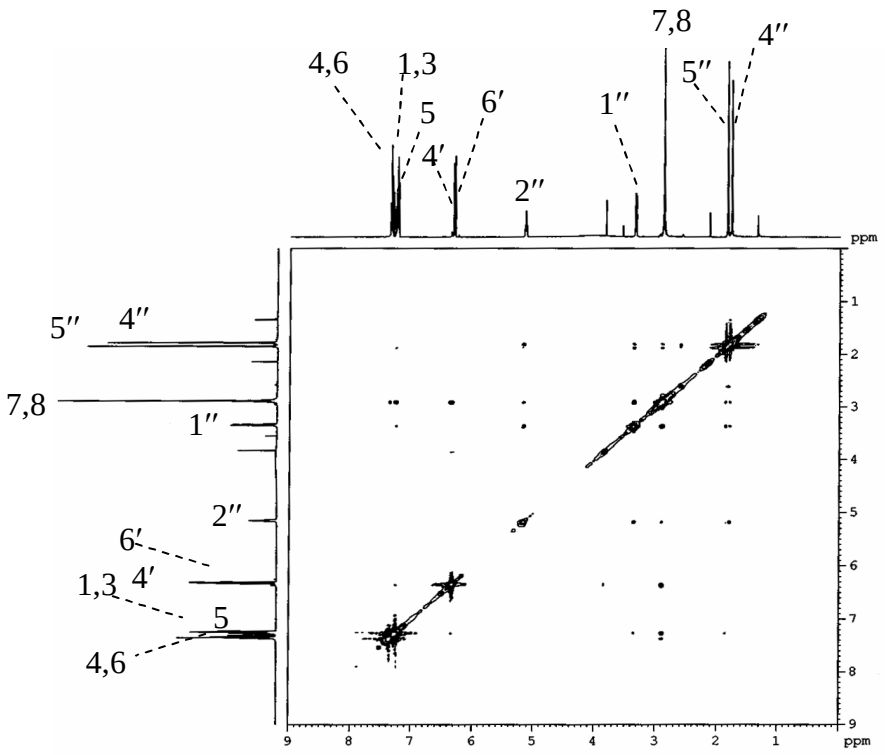

Figure 6.9 NOESY spectrum of compound **VI**

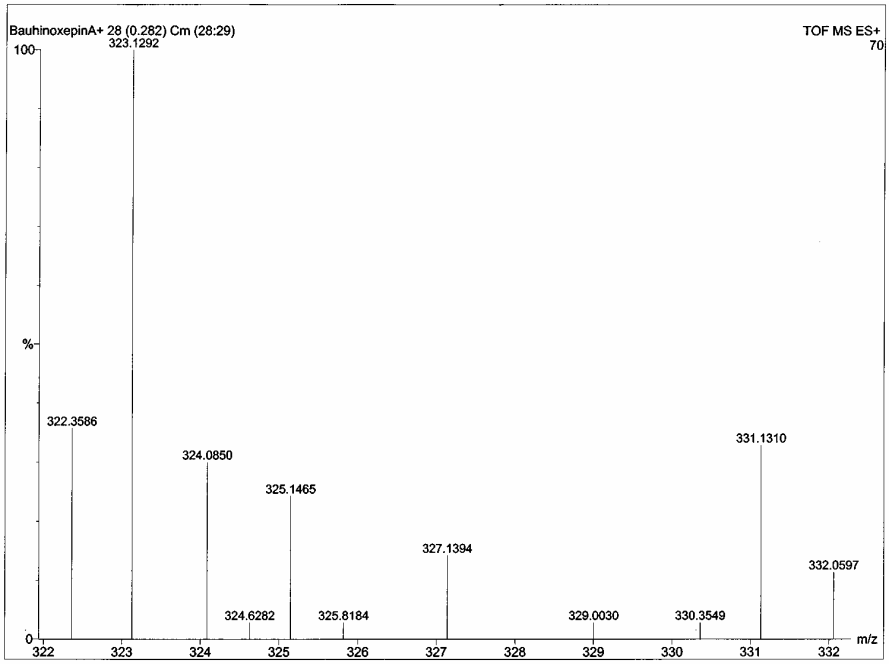

Figure 7.1 Mass spectrum of compound **VII**

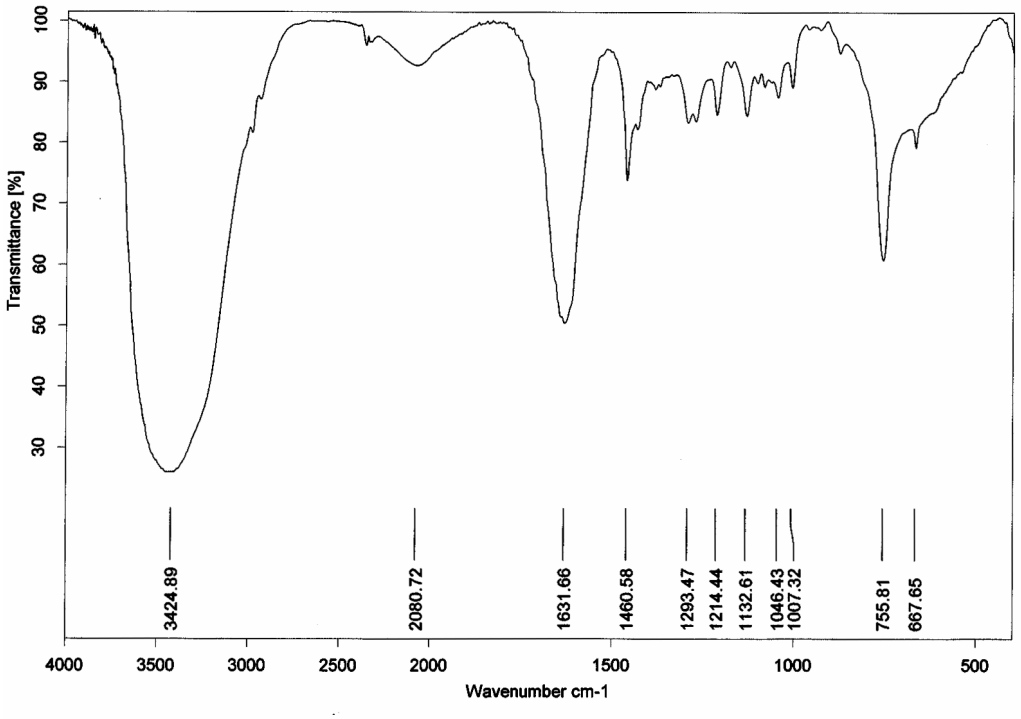

Figure 7.2 IR spectrum of compound **VII**

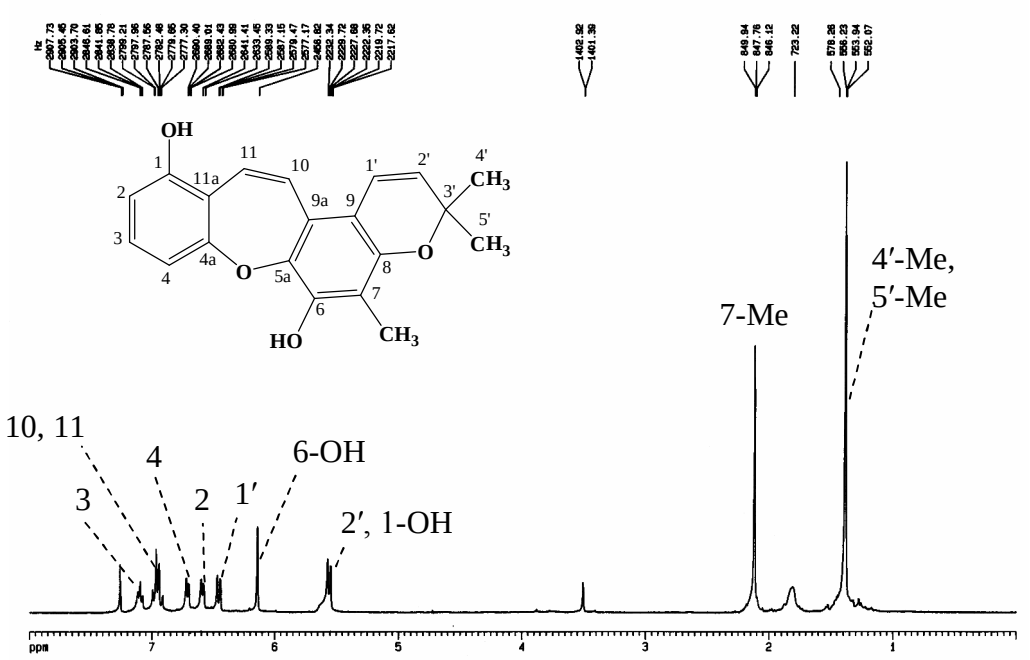

Figure 7.3 500 MHz ^{1}H-NMR spectrum of compound **VII** in $CDCl_3$

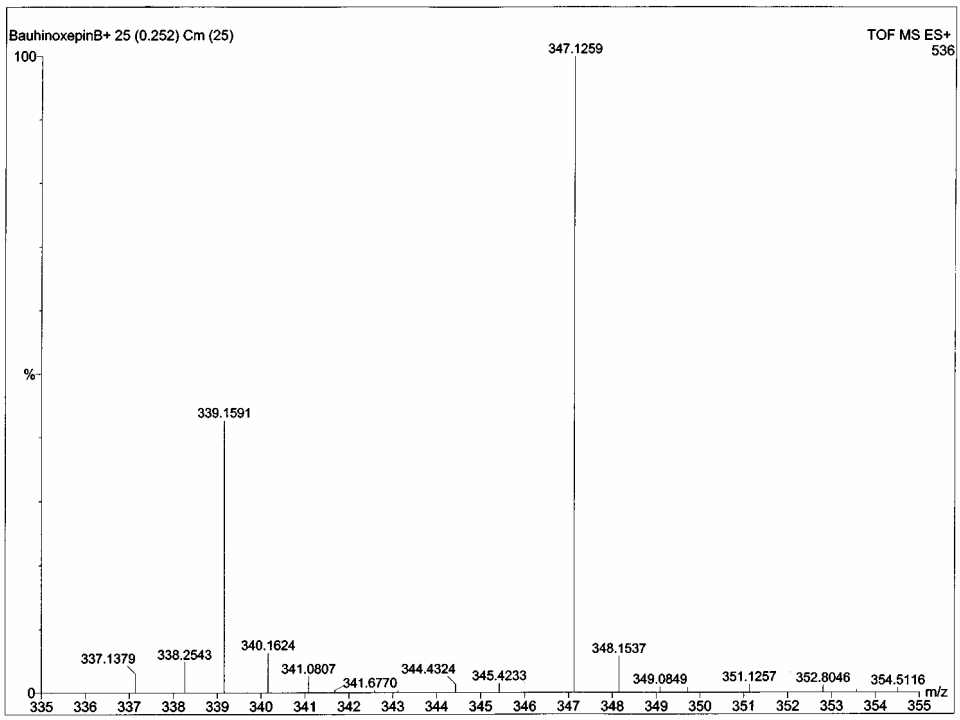

Figure 8.1 Mass spectrum of compound **VIII**

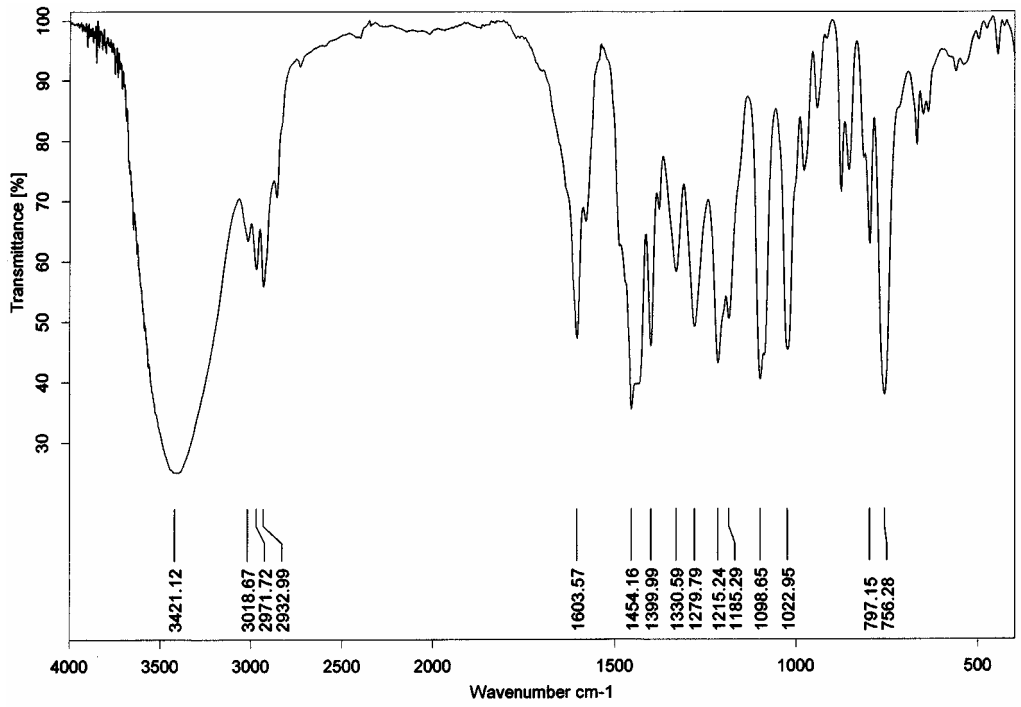

Figure 8.2 IR spectrum of compound **VIII**

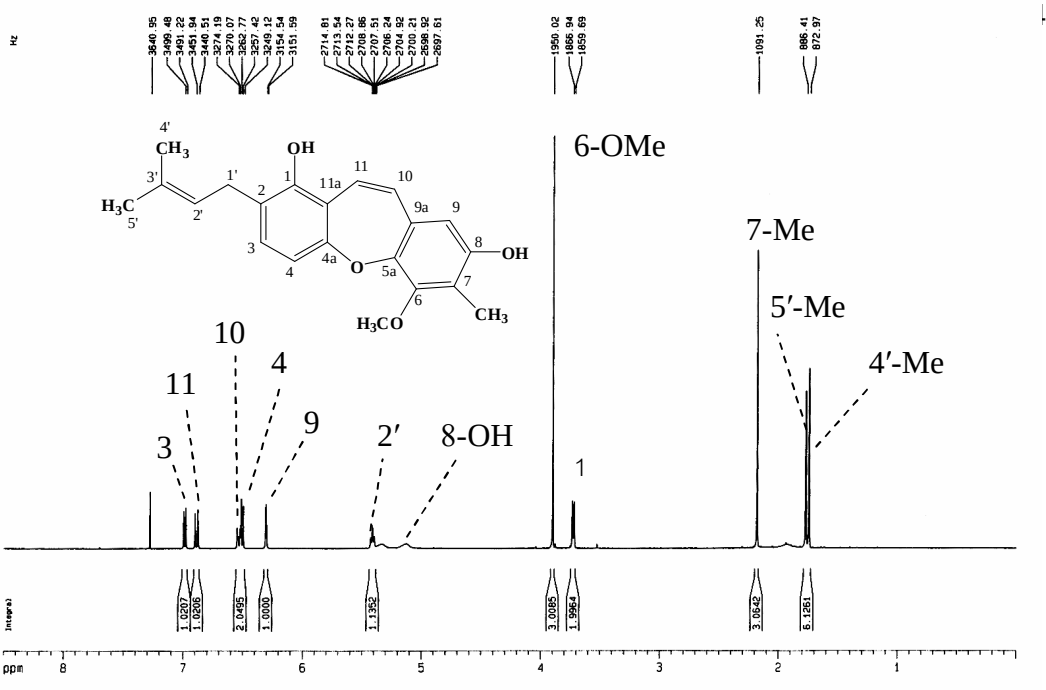

Figure 8.3 500 MHz ^{1}H-NMR spectrum of compound **VIII** in $CDCl_3$

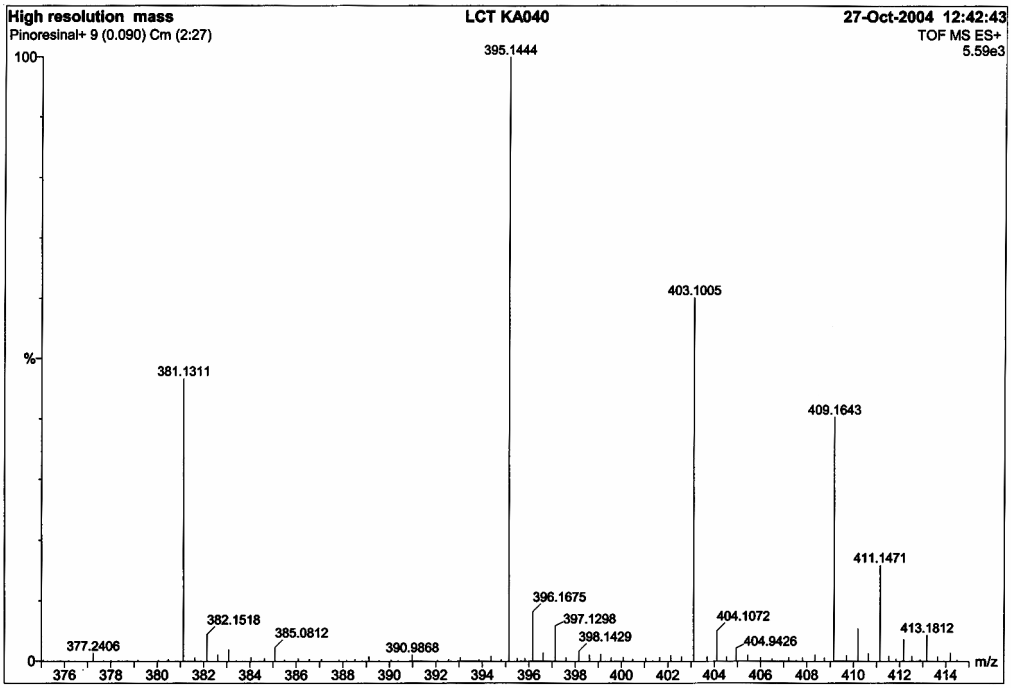

Figure 9.1 Mass spectrum of compound **IX**

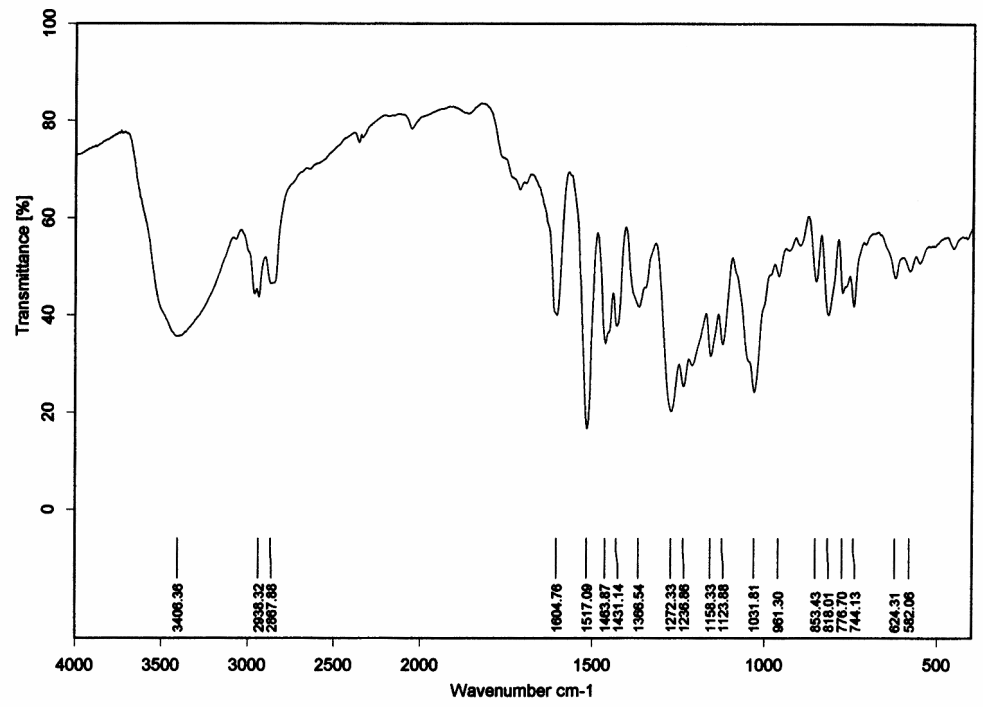

Figure 9.2 IR spectrum of compound **IX**

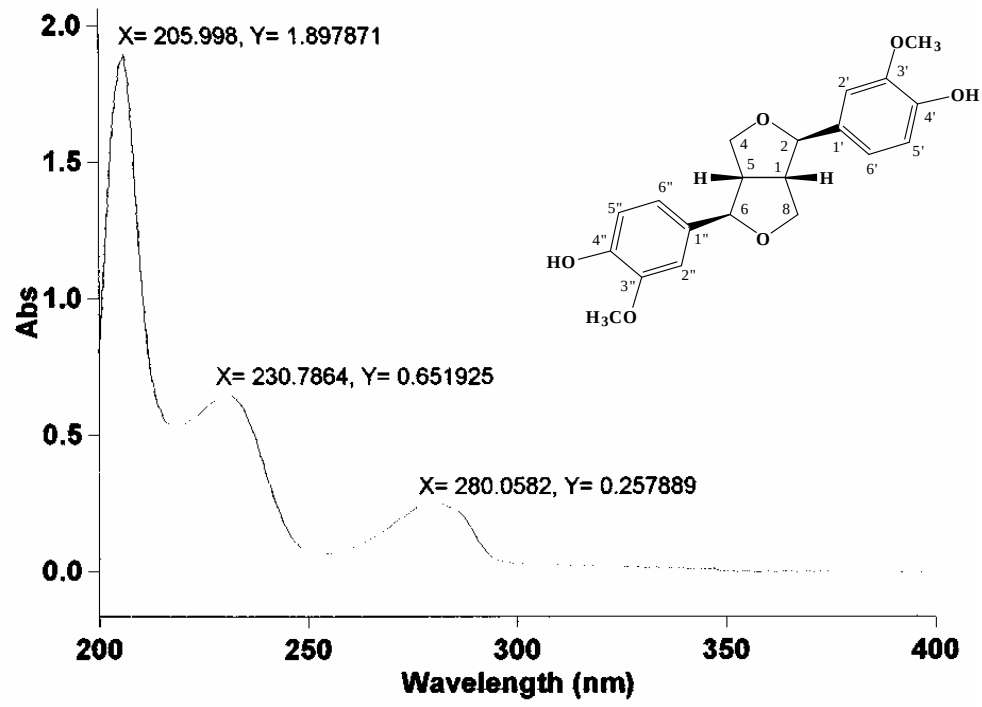

Figure 9.3 UV-Vis spectrum of compound **IX**

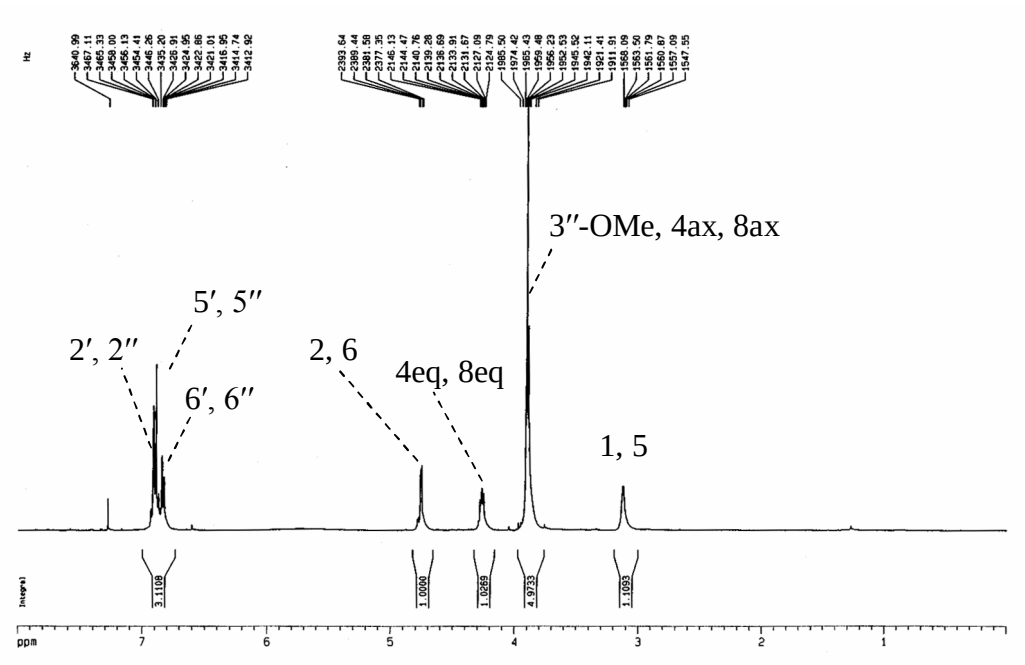

Figure 9.4 500 MHz ^{1}H-NMR spectrum of compound **IX** in $CDCl_3$

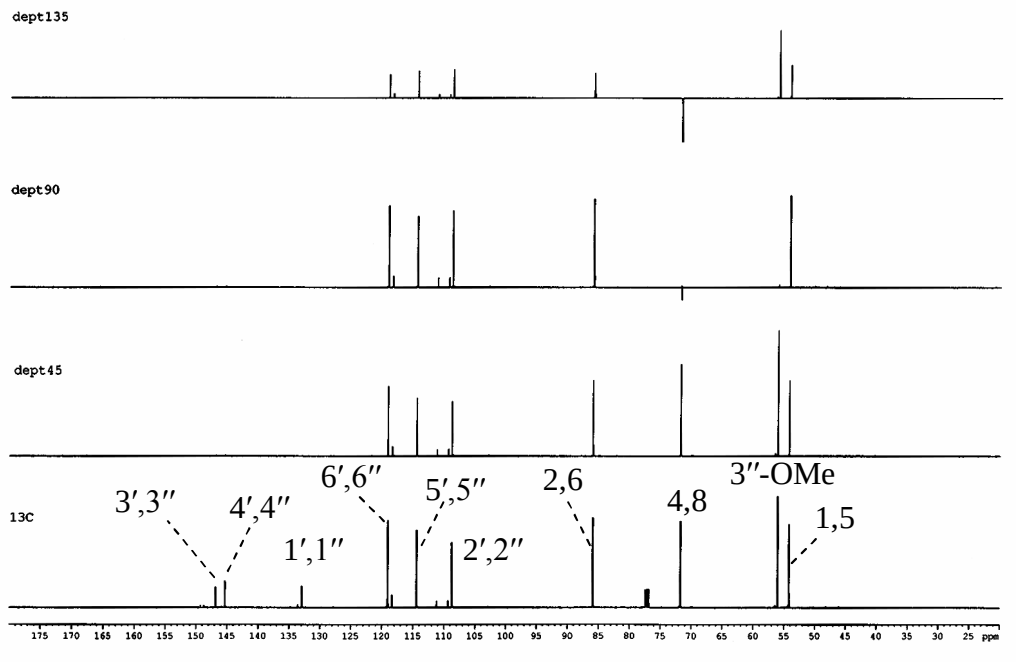

Figure 9.5 ^{13}C-NMR and DEPT spectra of compound **IX** in $CDCl_3$

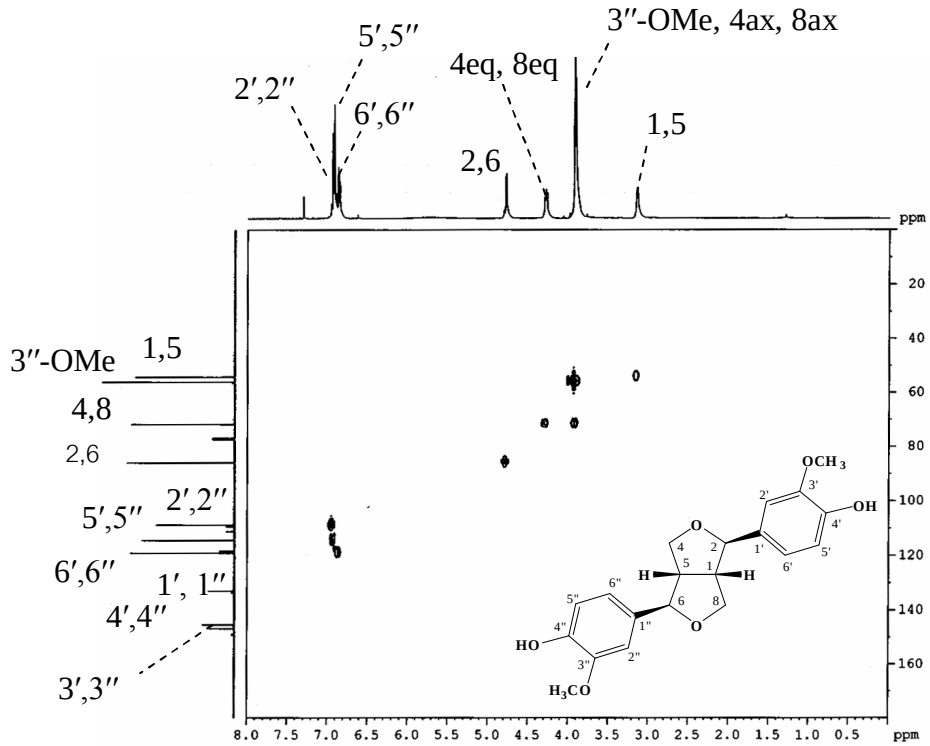

Figure 9.6 HMQC spectrum of compound **IX**

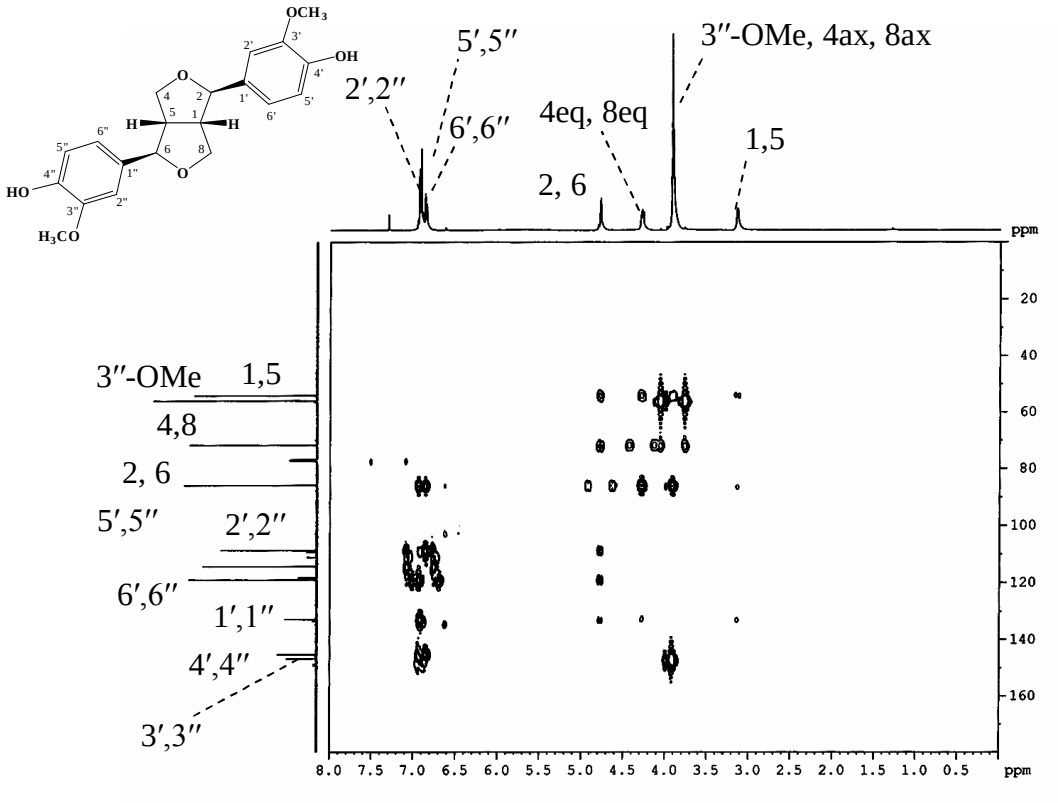

Figure 9.7 HMBC spectrum of compound **IX**

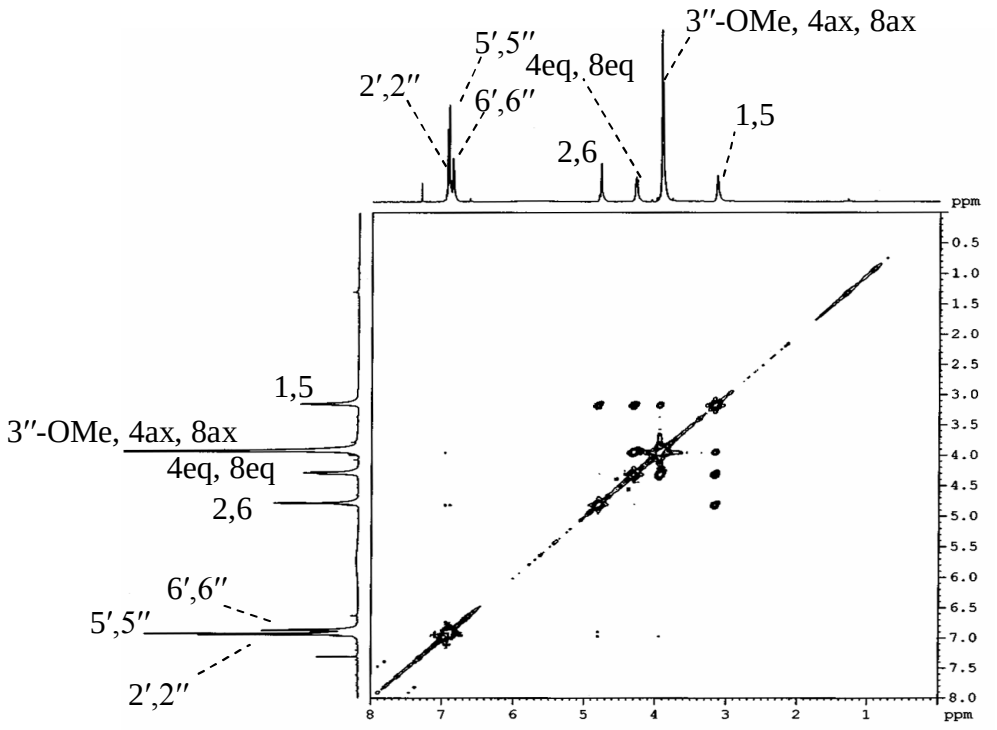

Figure 9.8 ^{1}H,^{1}H-COSY spectrum of compound **IX**

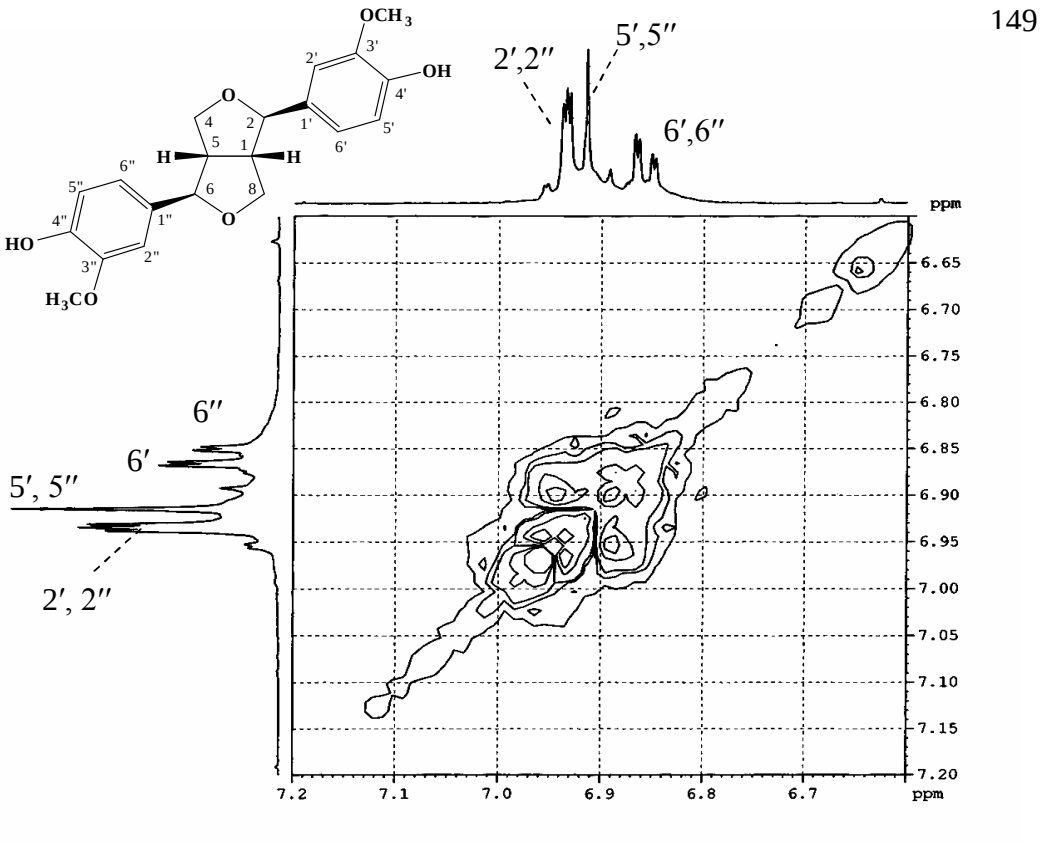

Figure 9.8a Expansion of Fig. 9.8

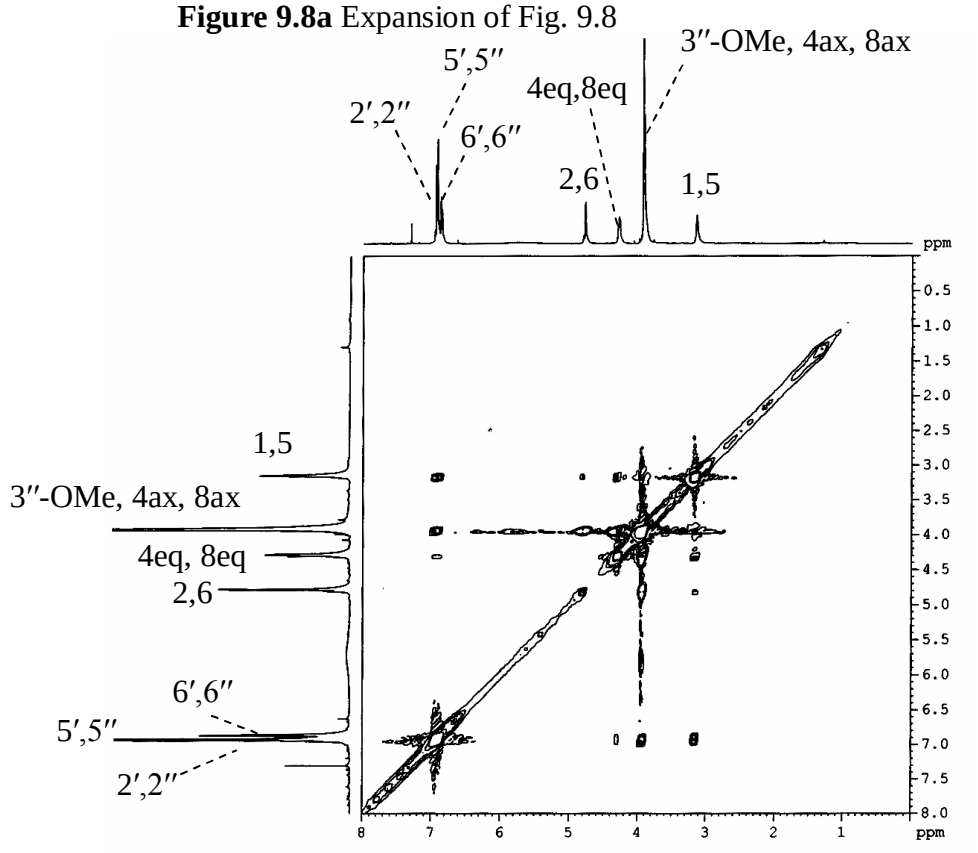

Figure 9.9 NOESY spectrum of compound **IX**

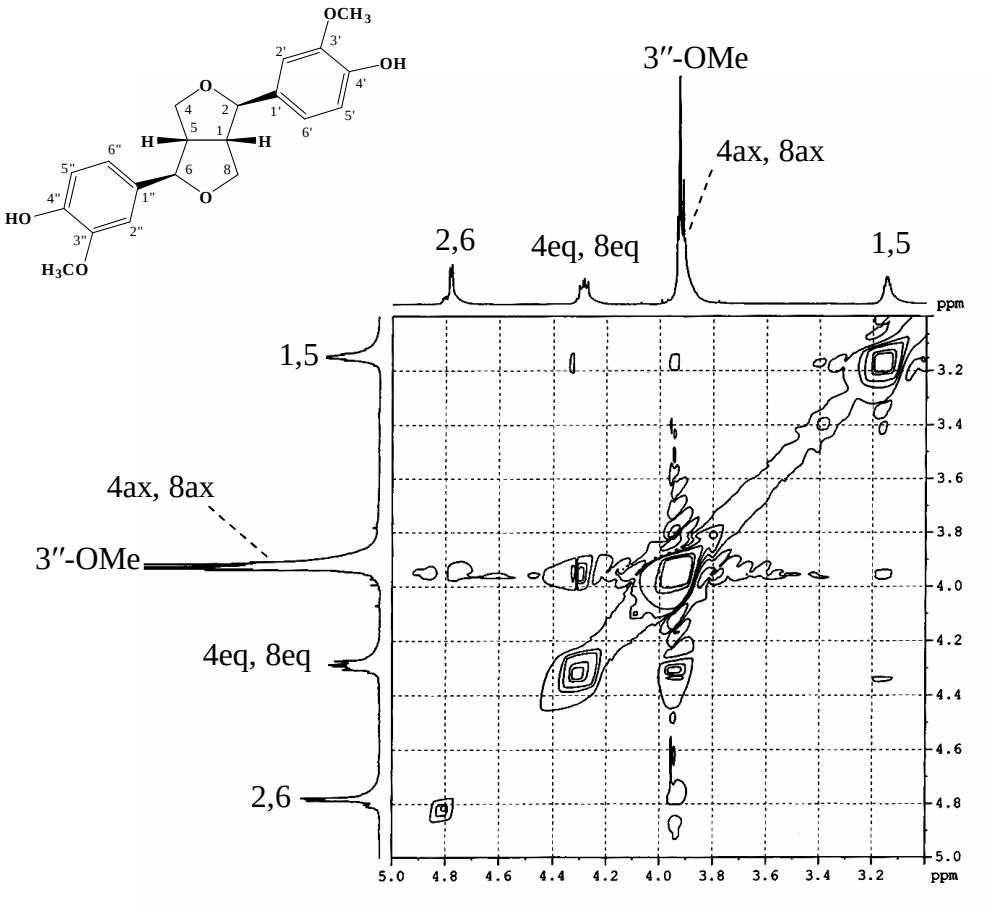

Figure 9.9a Expansion of Fig. 9.9

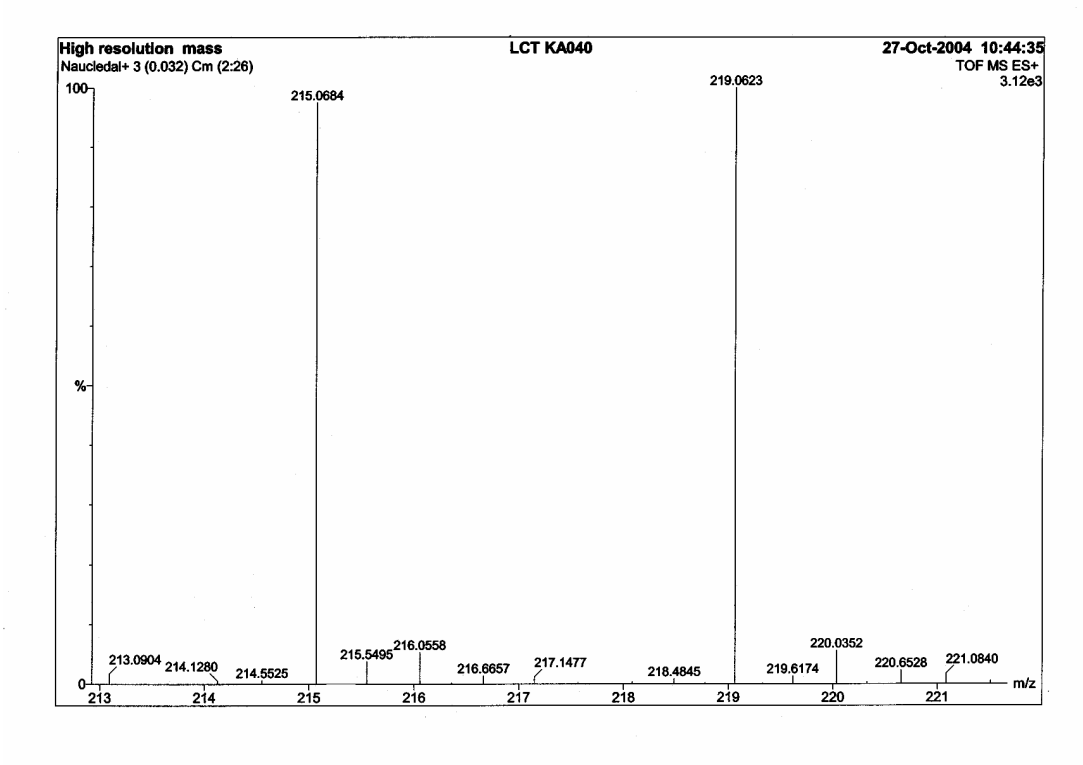

Figure 10.1 Mass spectrum of compound **X**

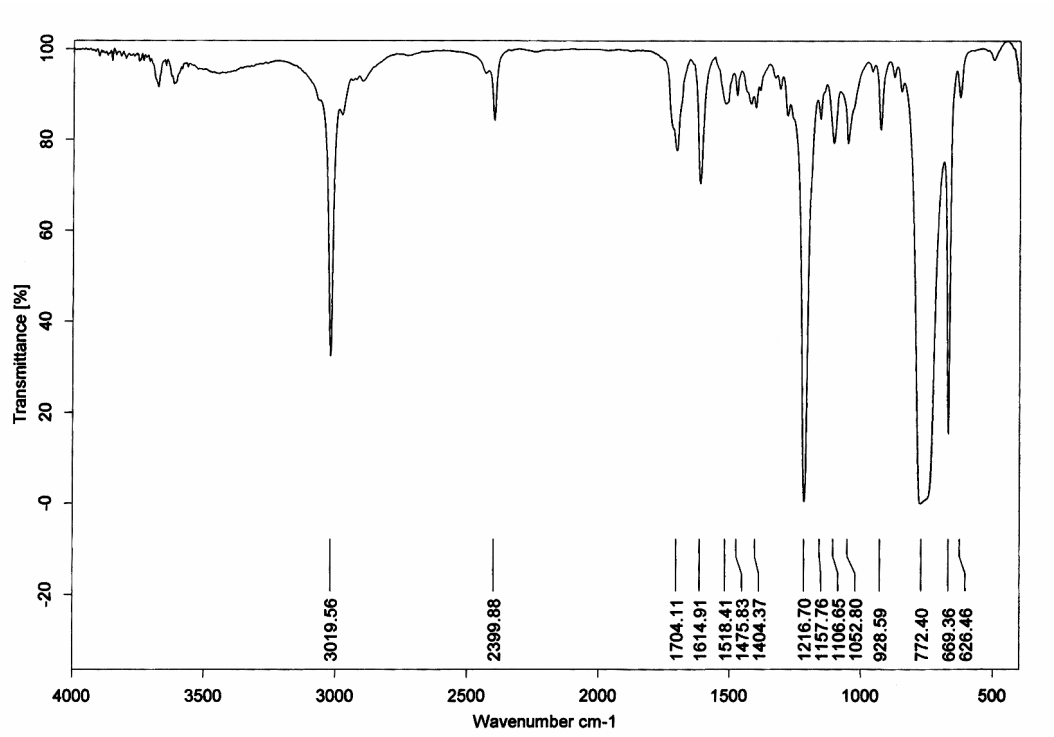

Figure 10.2 IR spectrum of compound **X**

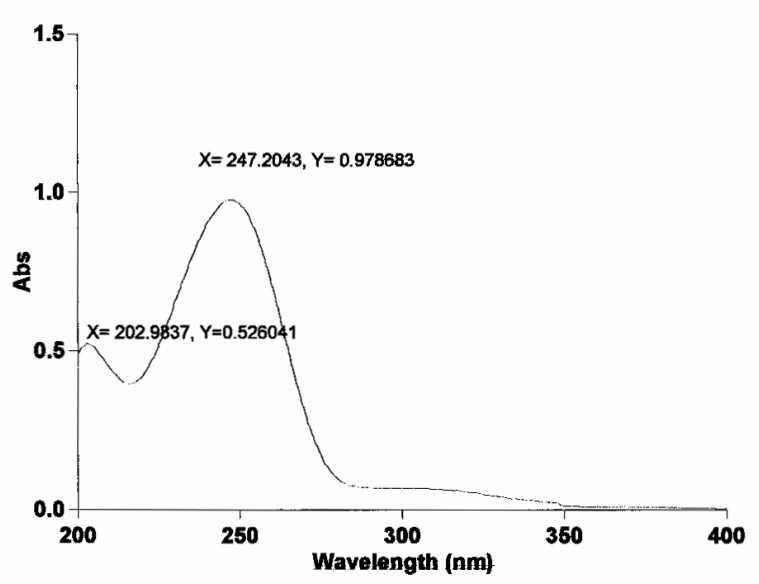

Figure 10.3 UV-Vis spectrum of compound **X**

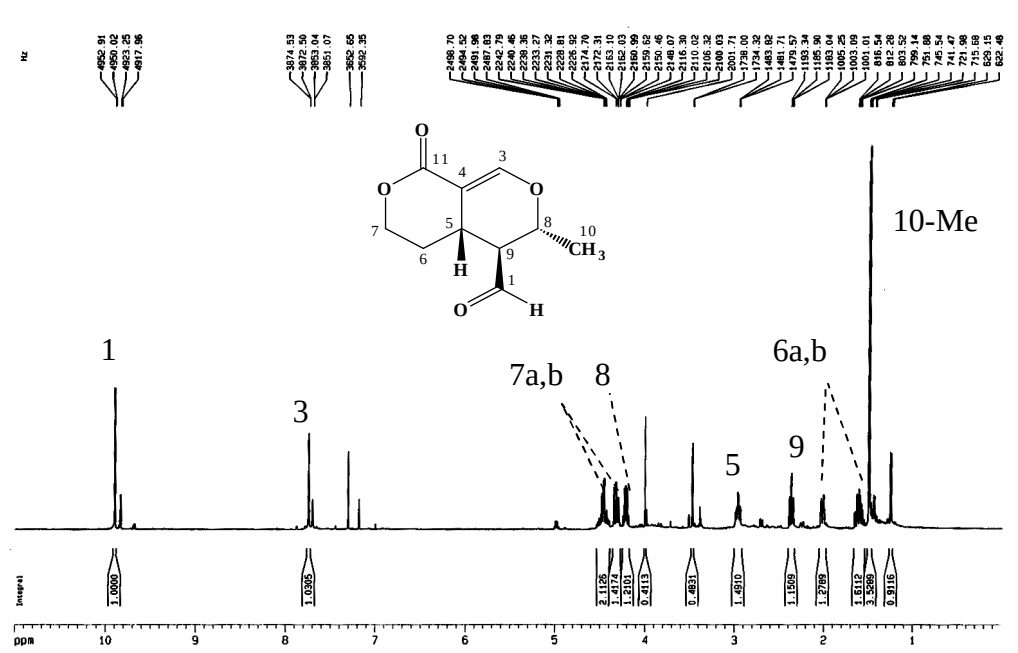

Figure 10.4 500 MHz ^{1}H-NMR spectrum of compound **X** in $CDCl_3$

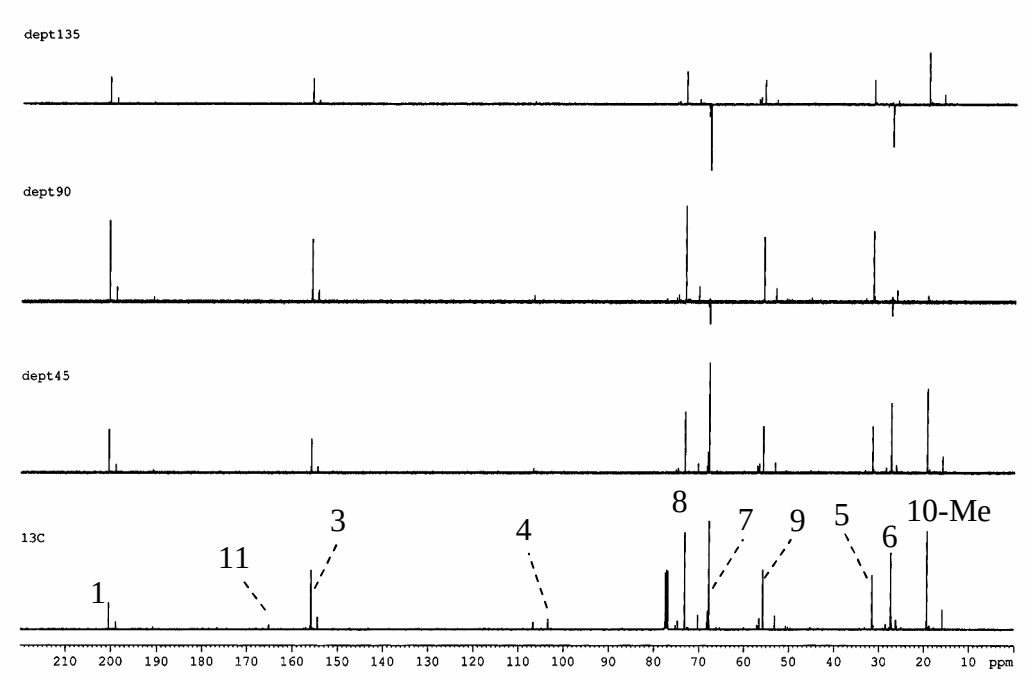

Figure 10.5 ^{13}C-NMR and DEPT spectra of compound **X** in $CDCl_3$

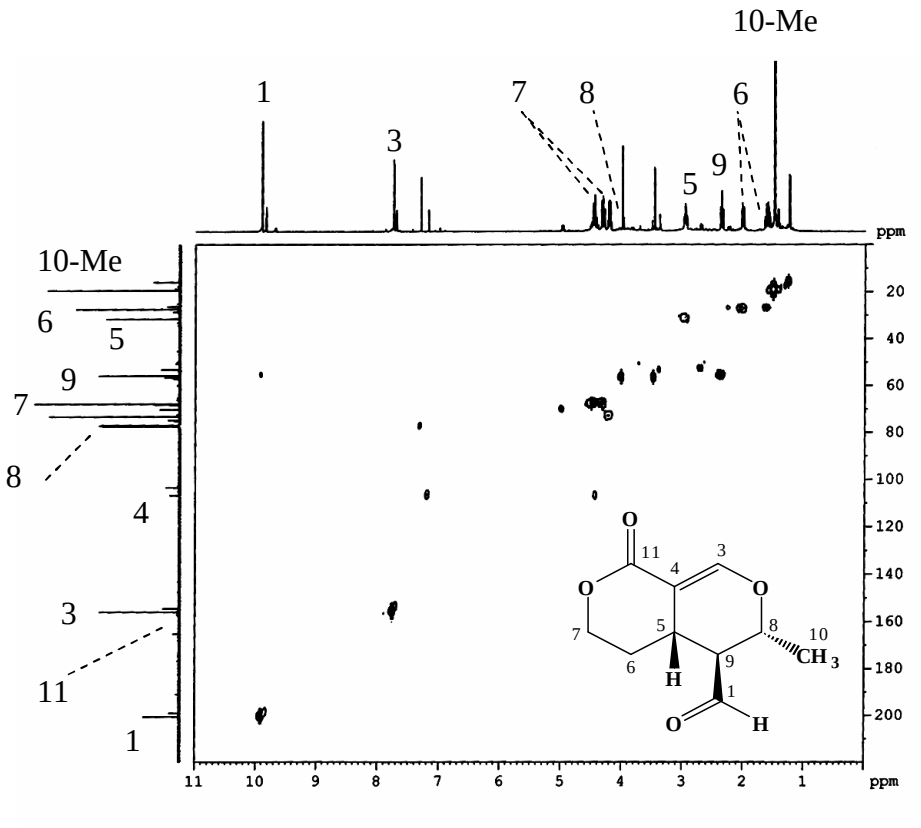

Figure 10.6 HMQC spectrum of compound **X**

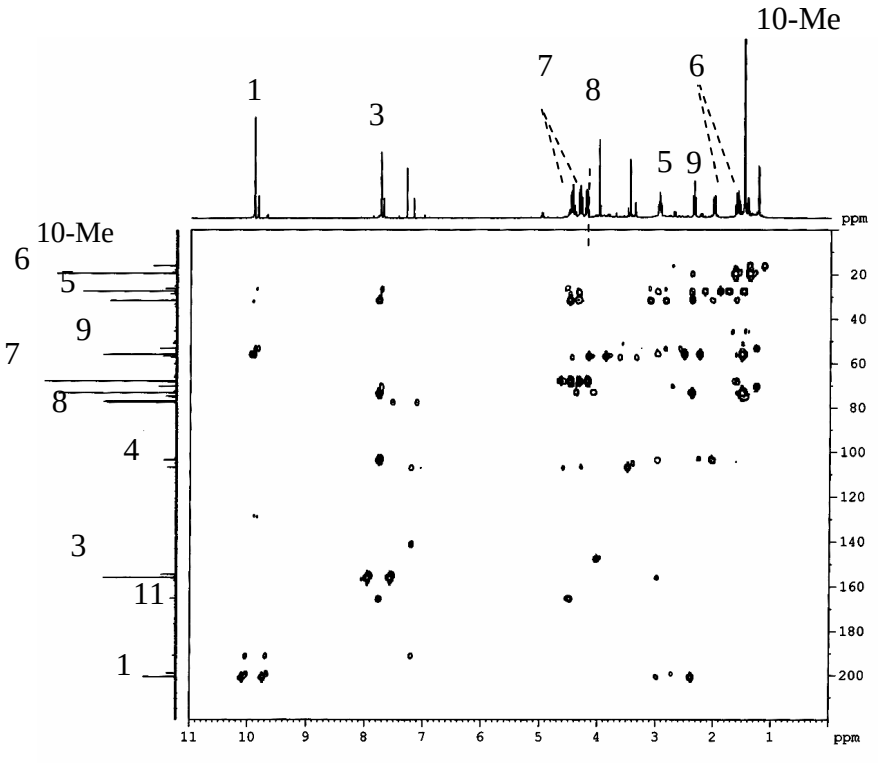

Figure 10.7 HMBC spectrum of compound **X**

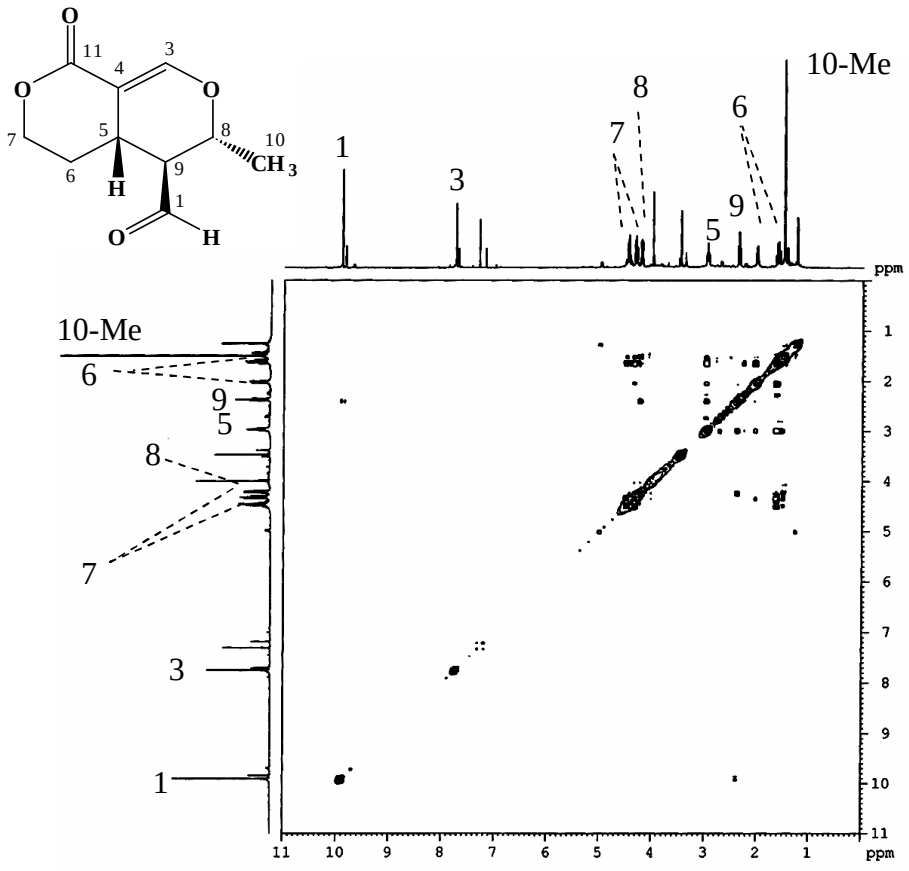

Figure 10.8 ^{1}H,^{1}H-COSY spectrum of compound **X**

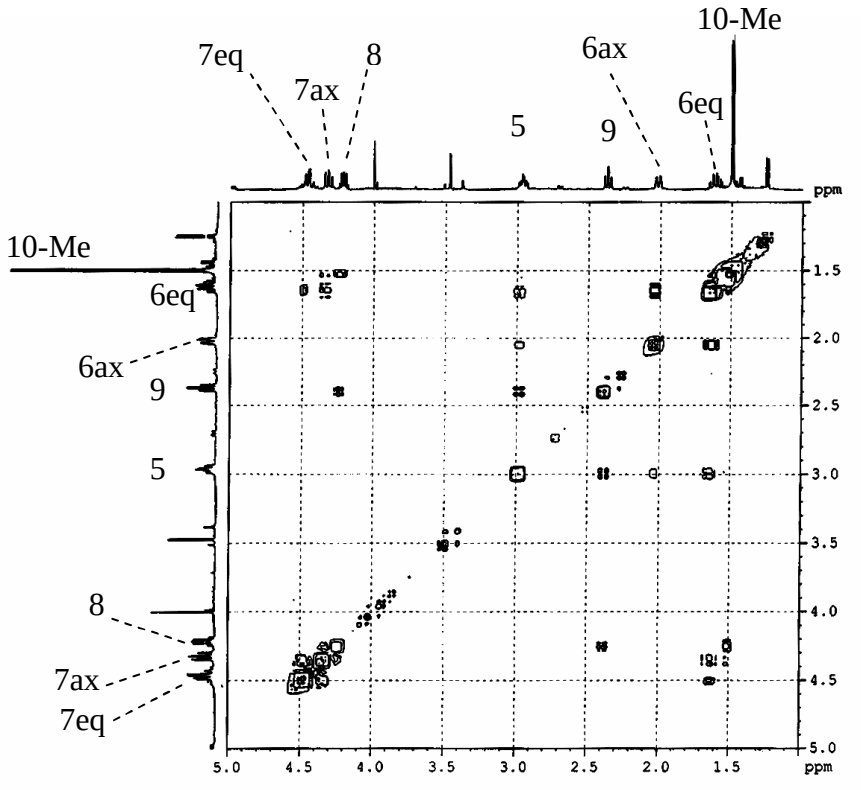

Figure 10.8a Expansion of Fig.10.8

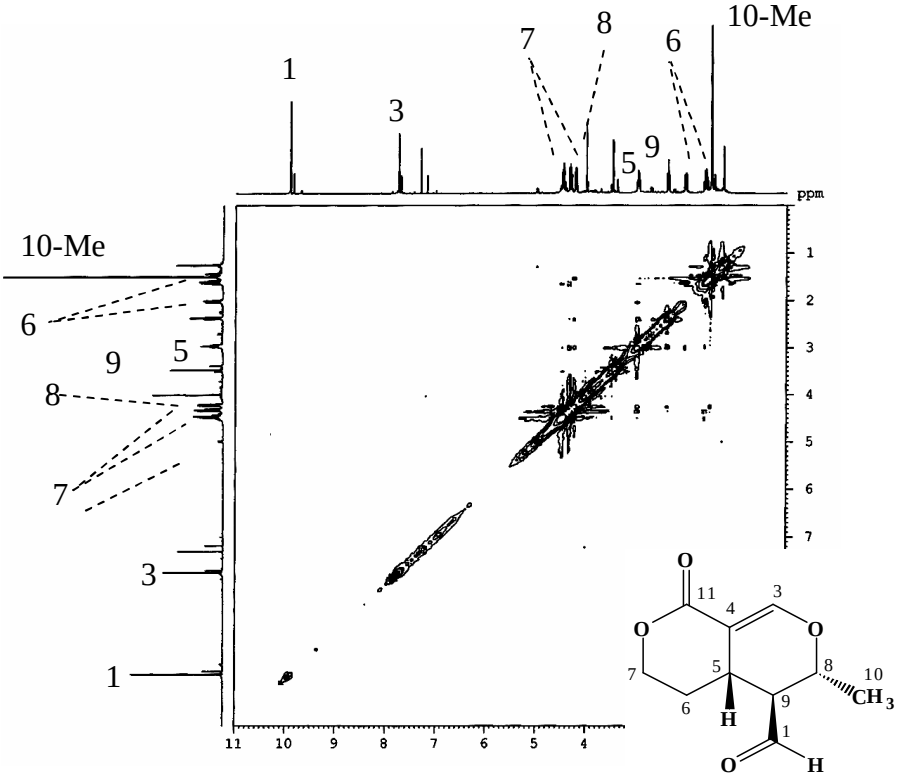

Figure 10.9 NOESY spectrum of compound **X**

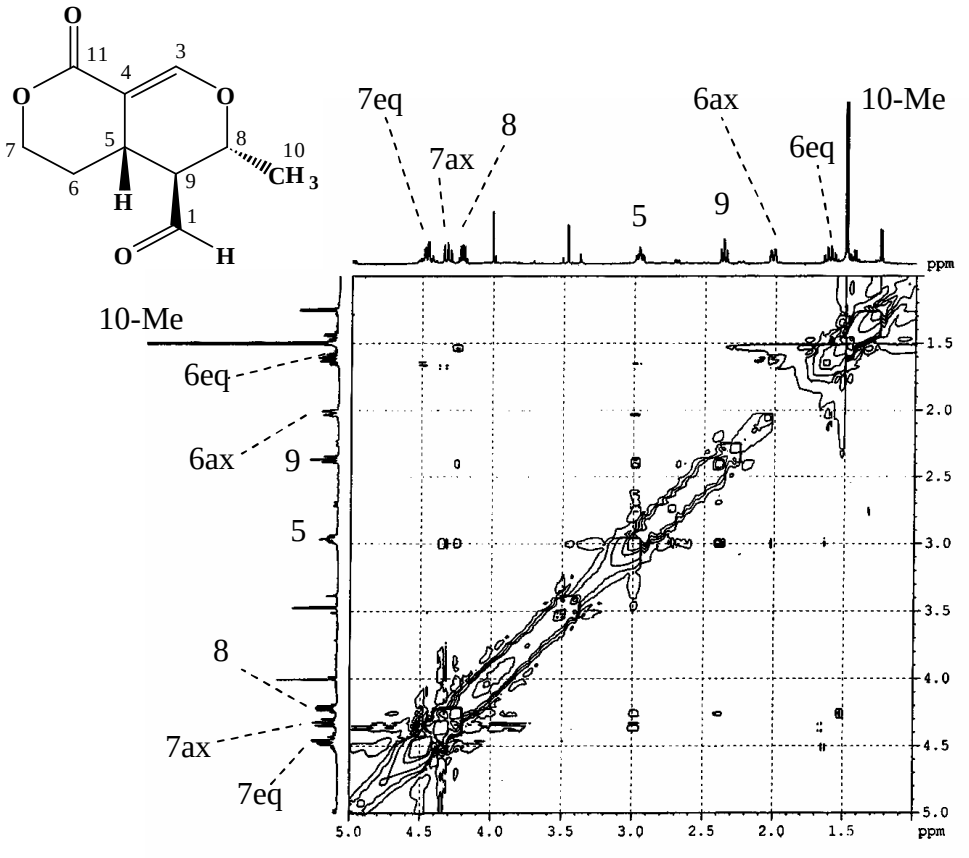

Figure 10.9a Expansion of Fig.10.9

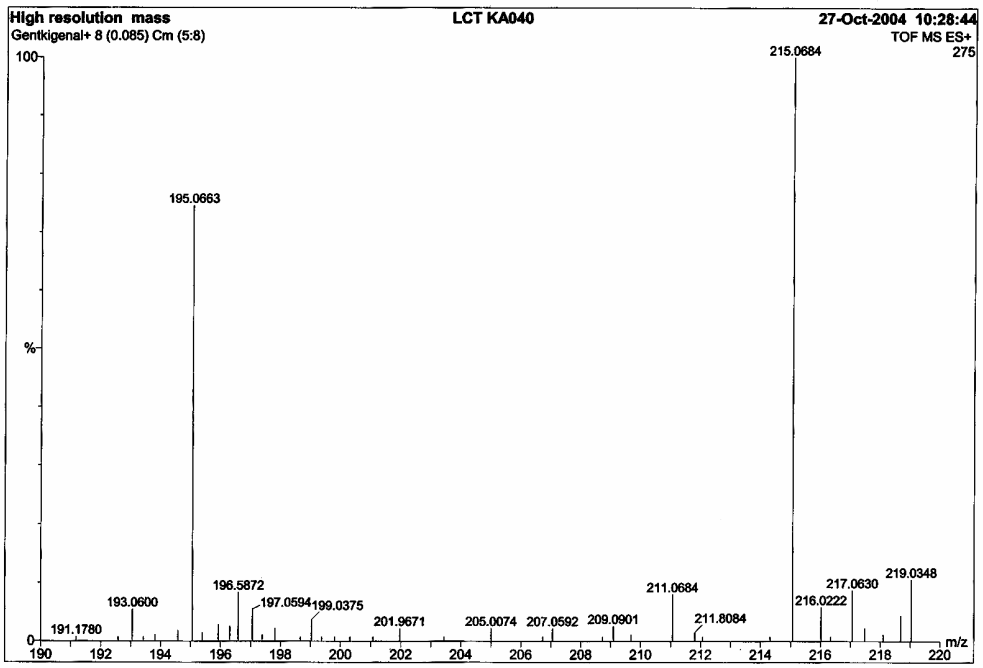

Figure 11.1 Mass spectrum of compound **XI**

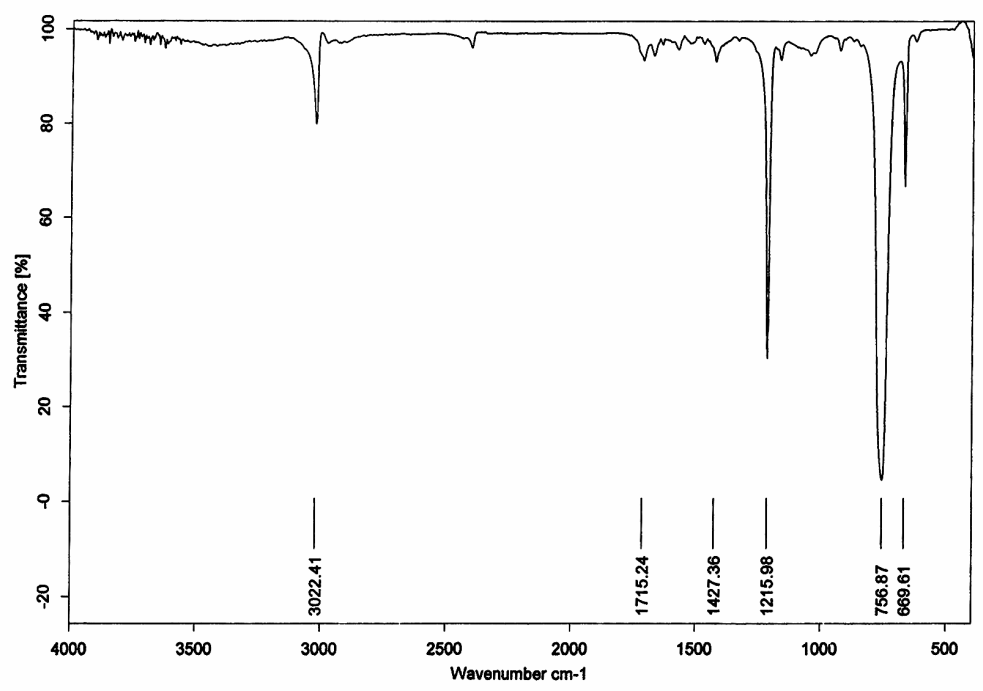

Figure 11.2 IR spectrum of compound **XI**

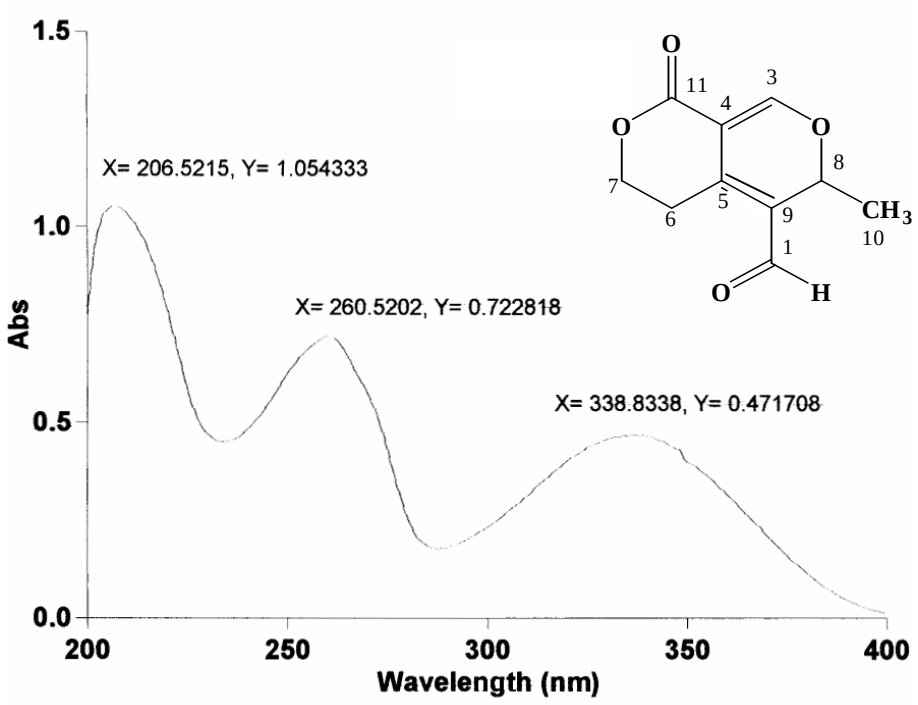

Figure 11.3 UV-Vis spectrum of compound **XI**

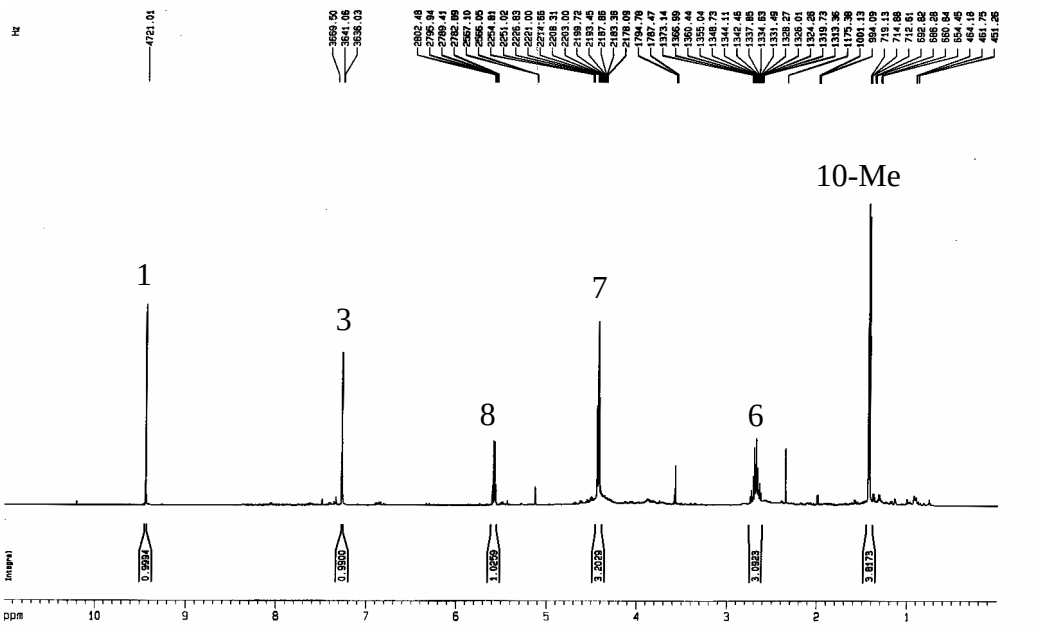

Figure 11.4 500 MHz ^{1}H-NMR spectrum of compound **XI** in $CDCl_3$

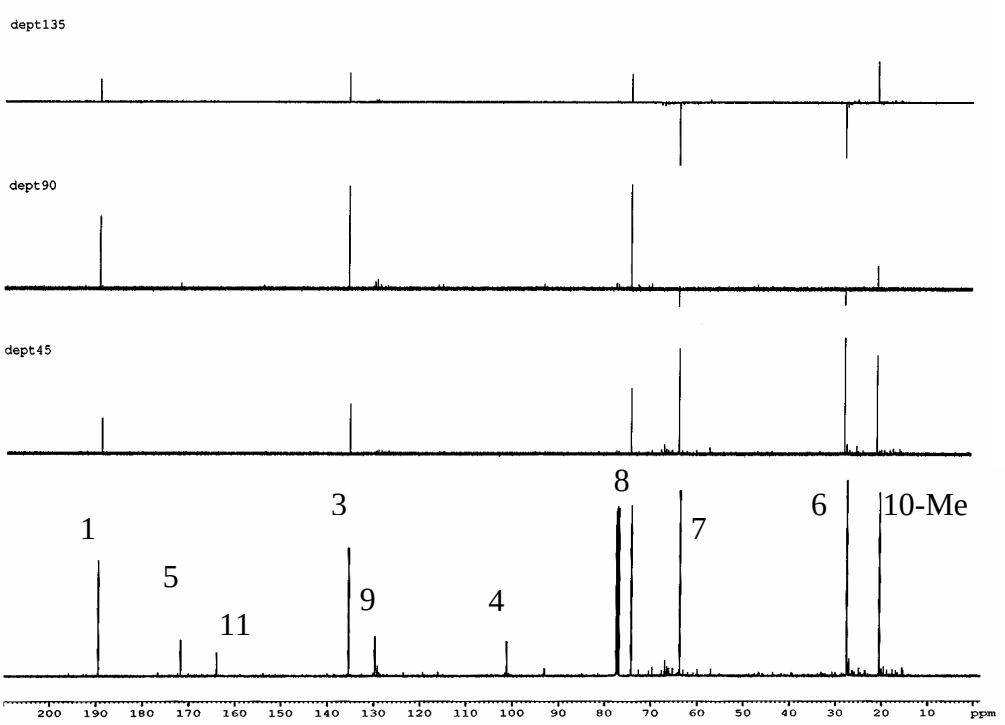

Figure 11.5 ^{13}C-NMR and DEPT spectra of compound **XI** in $CDCl_3$

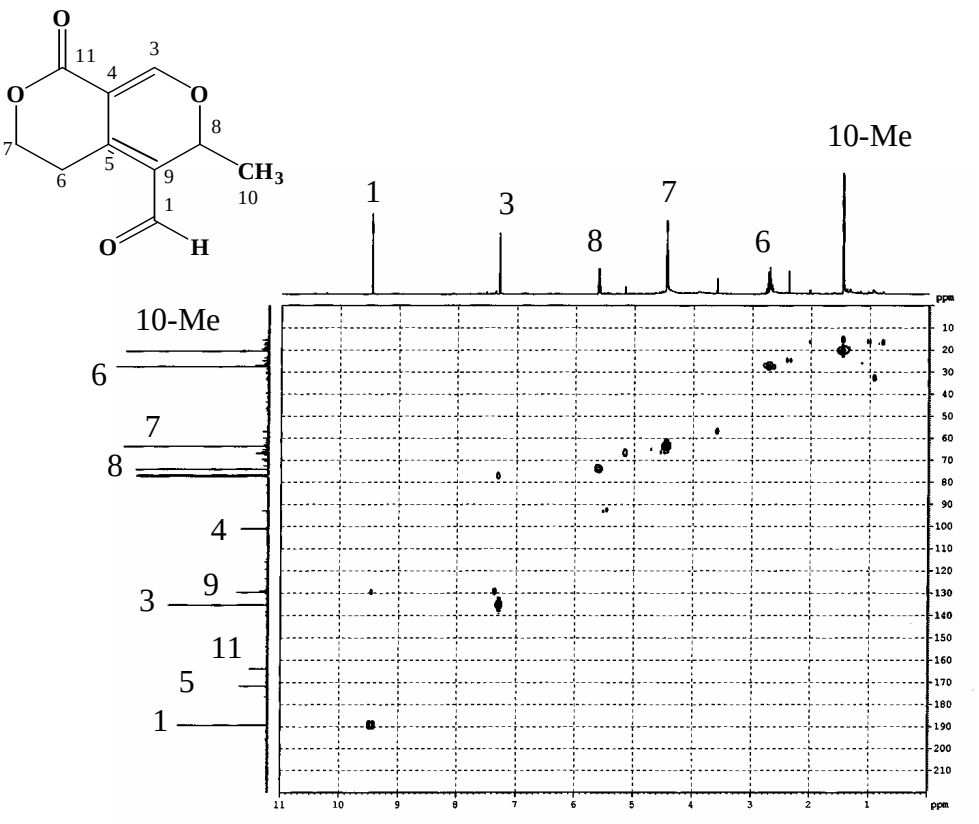

Figure 11.6 HMQC spectrum of compound **XI**

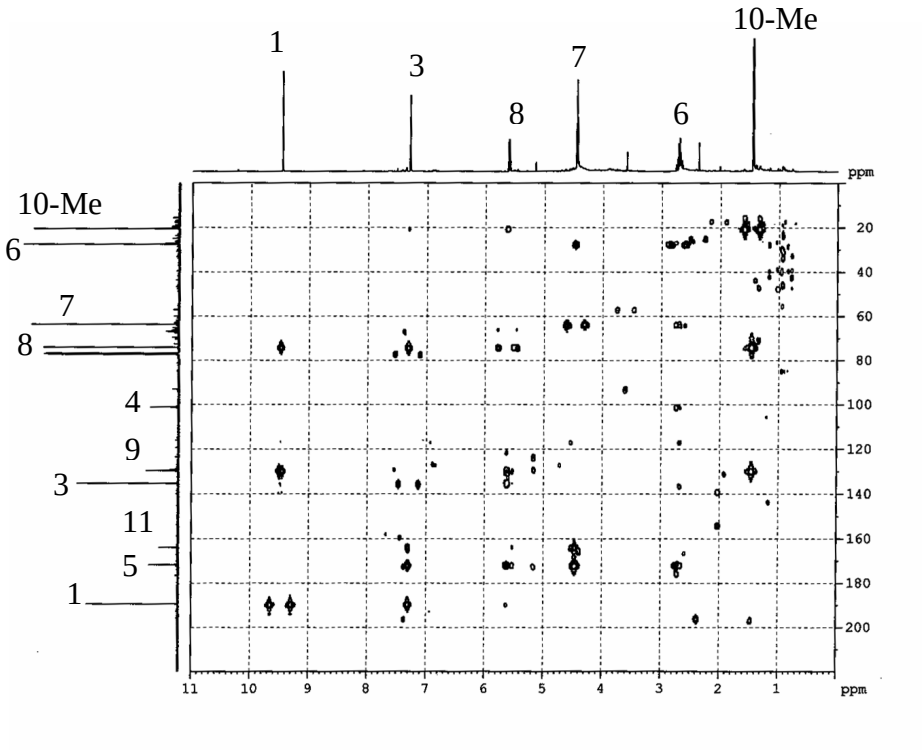

Figure 11.7 HMBC spectrum of compound **XI**

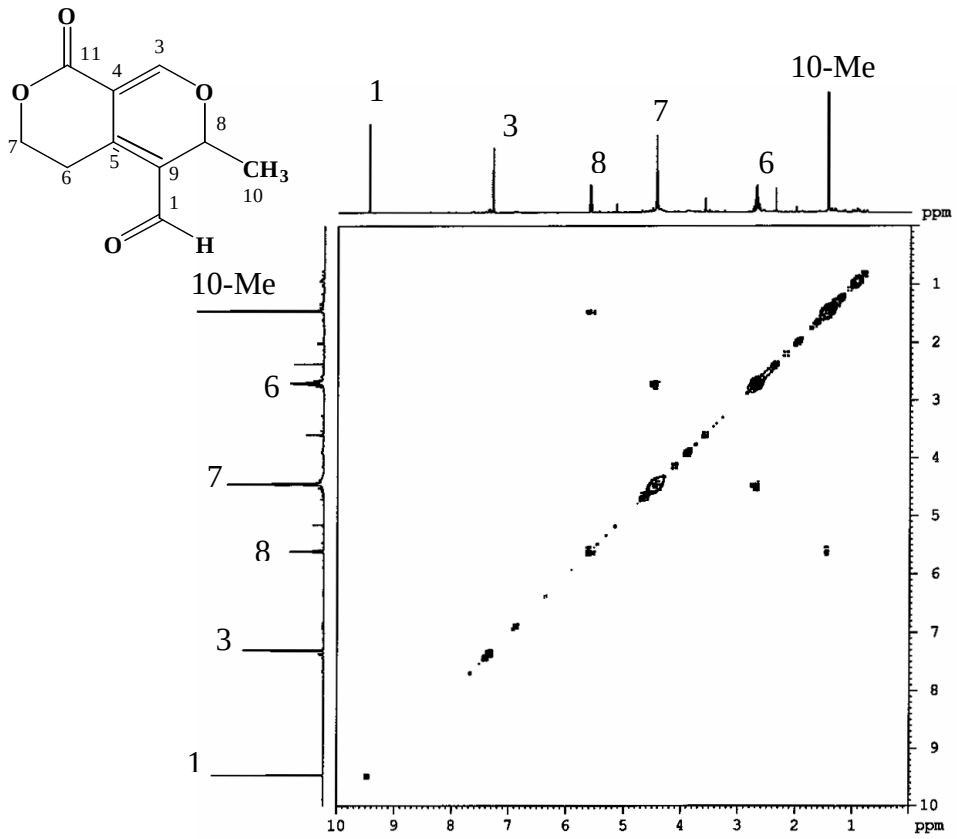

Figure 11.8 ^{1}H,^{1}H-COSY spectrum of compound **XI**

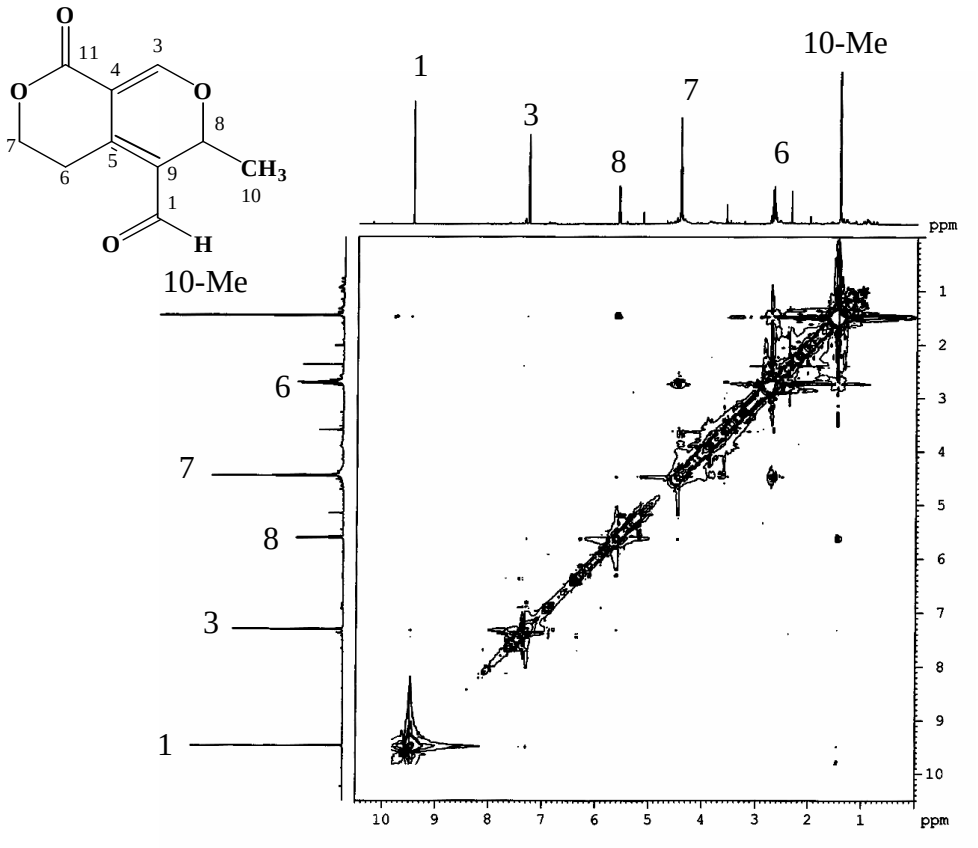

Figure 11.9 NOESY spectrum of compound **XI**

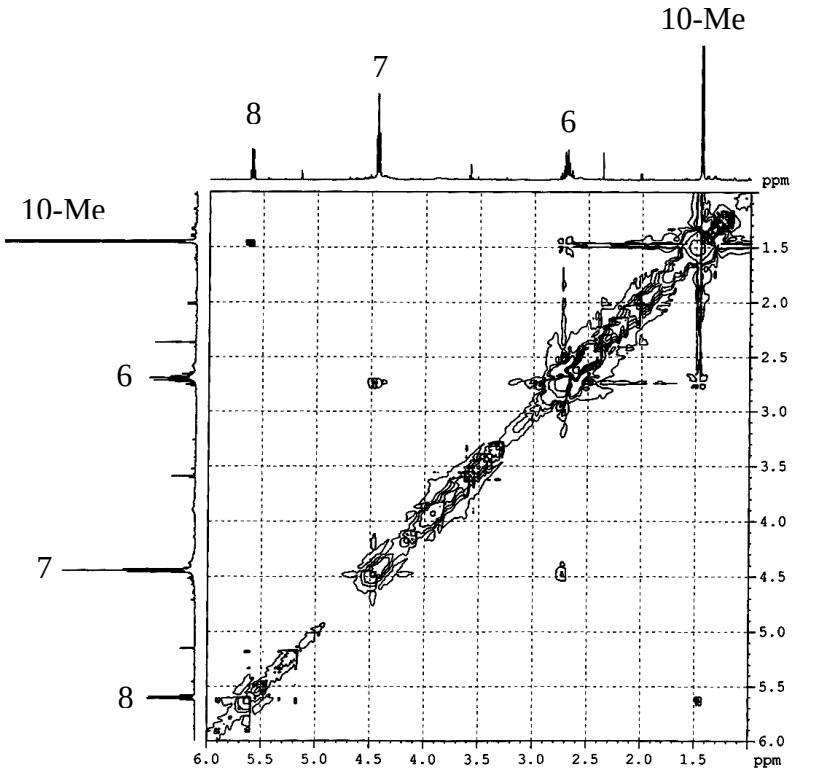

Figure 11.9a Expansion of Fig.11.9

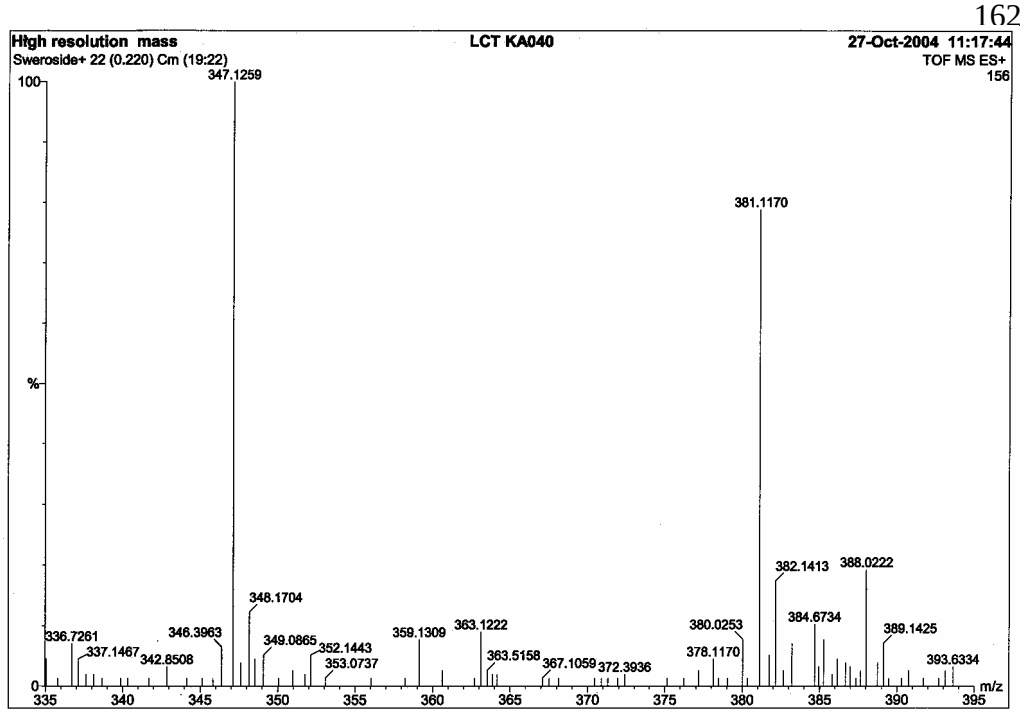

Figure 12.1 Mass spectrum of compound **XII**

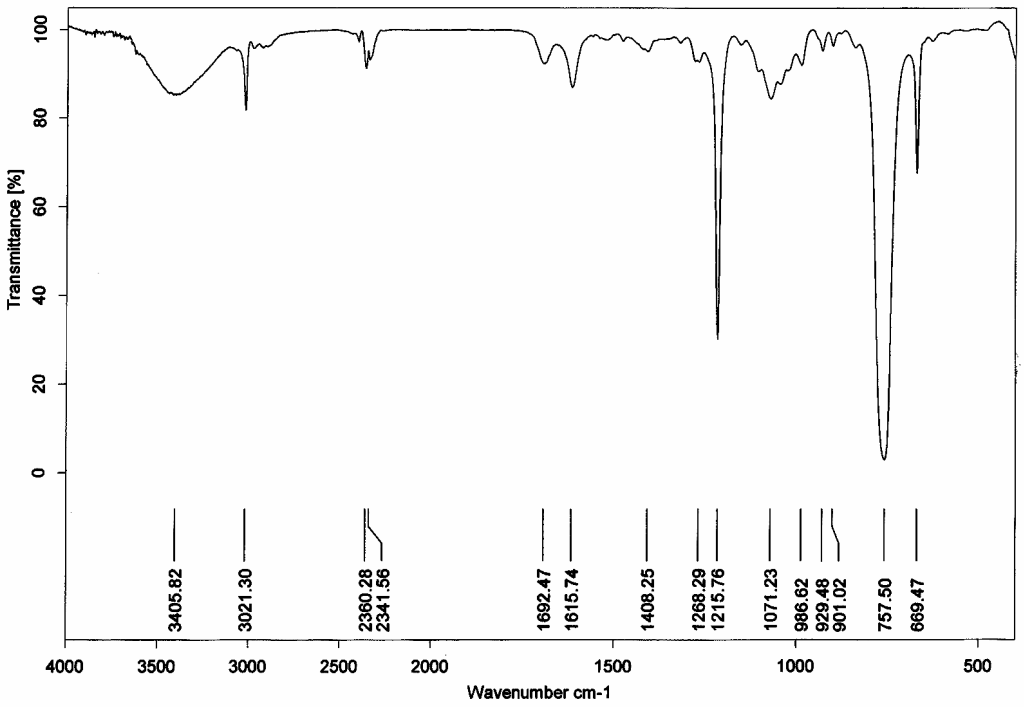

Figure 12.2 IR spectrum of compound **XII**

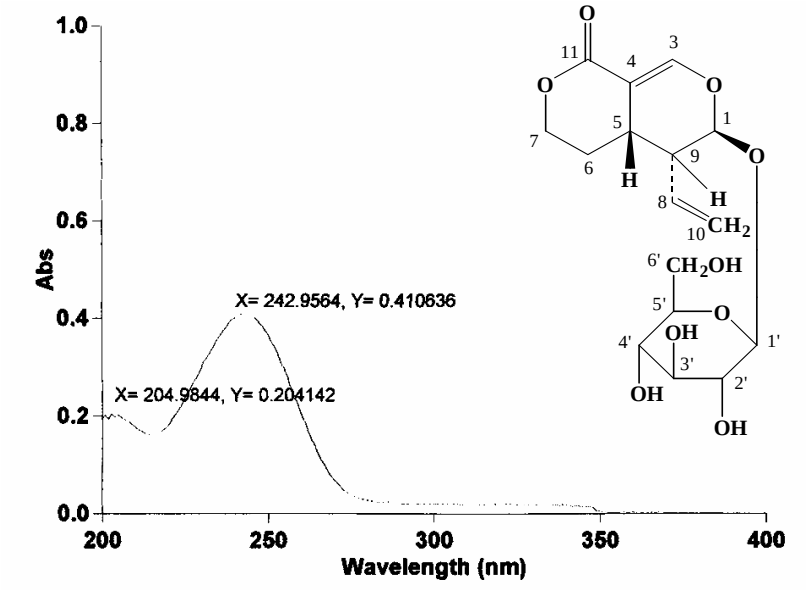

Figure 12.3 UV-Vis spectrum of compound **XII**

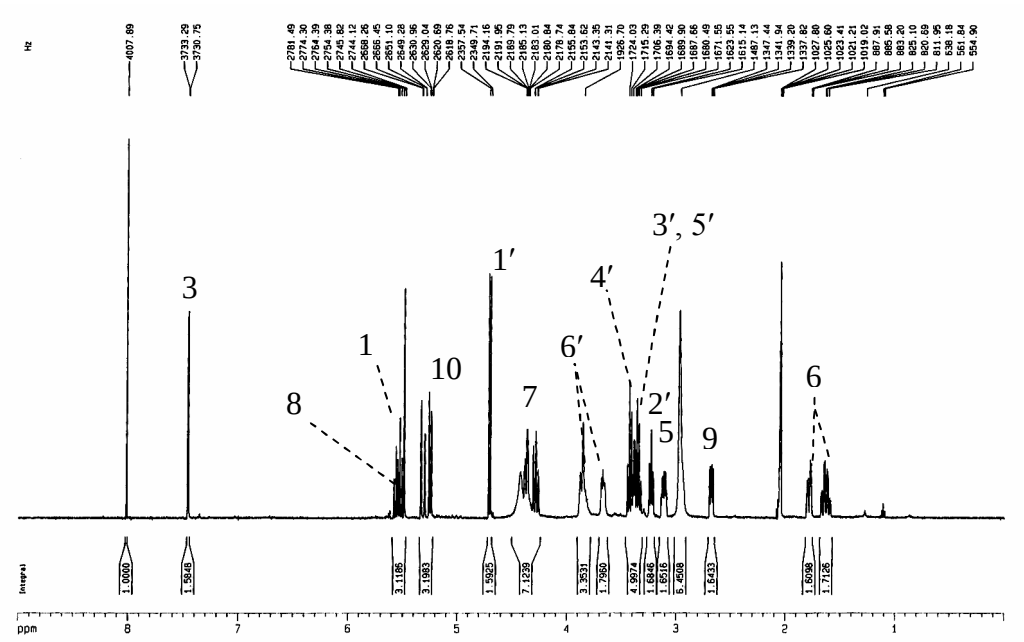

Figure 12.4 500 MHz ^{1}H-NMR spectrum of compound **XII** in acetone-d_6

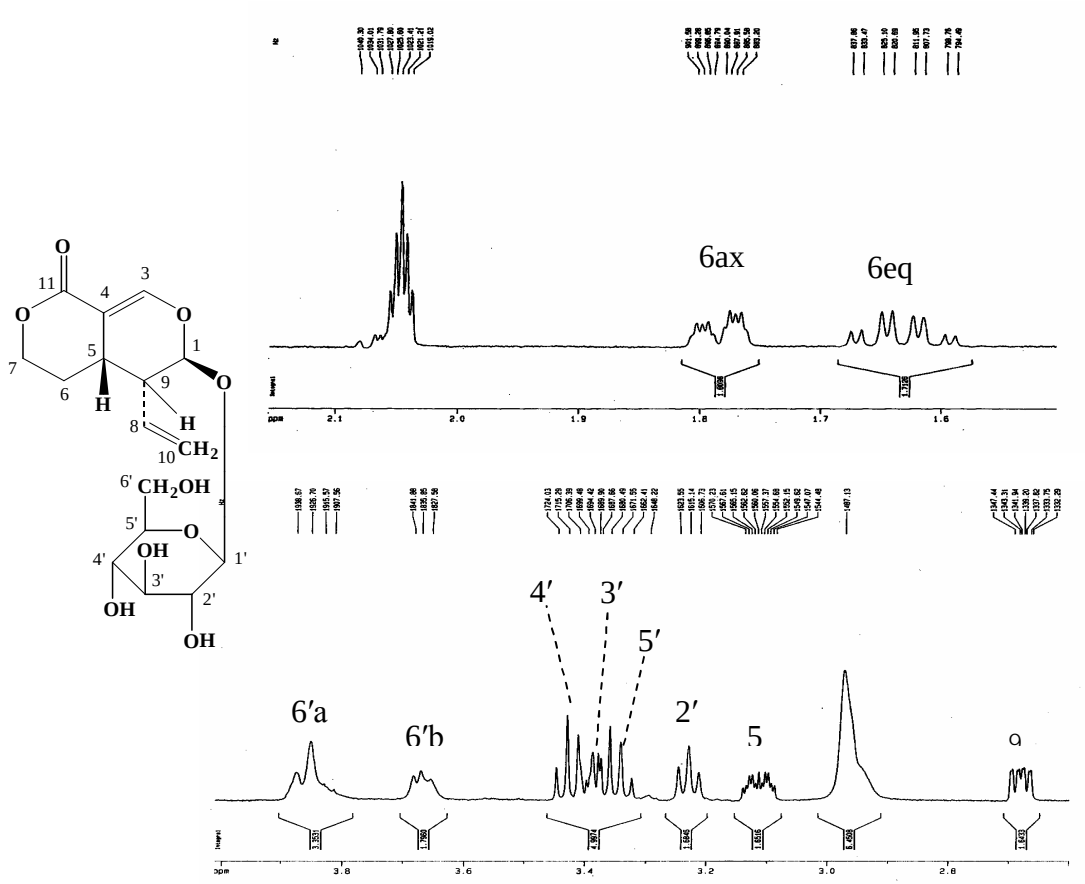

Figure 12.4a Expansion of Fig.12.4

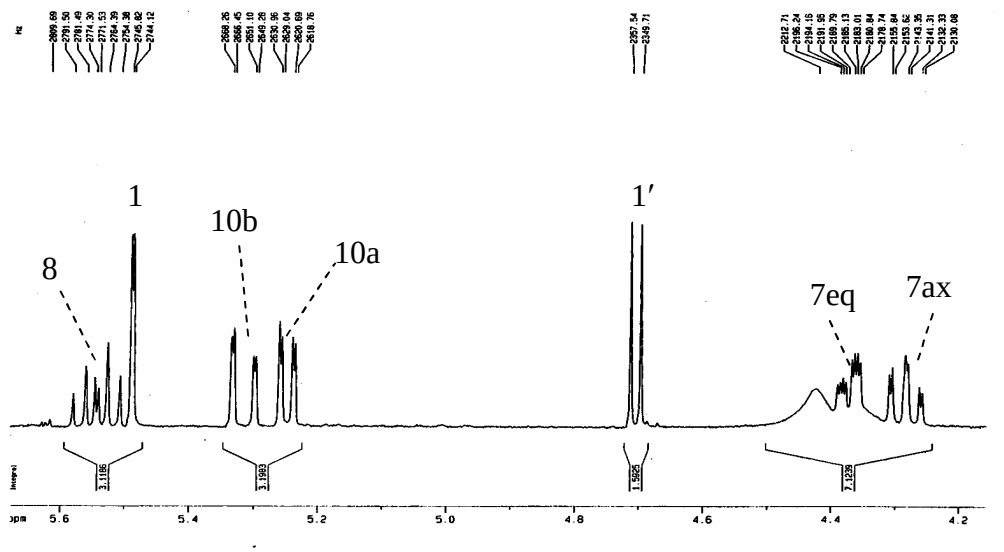

Figure 12.4b Expansion of Fig.12.4

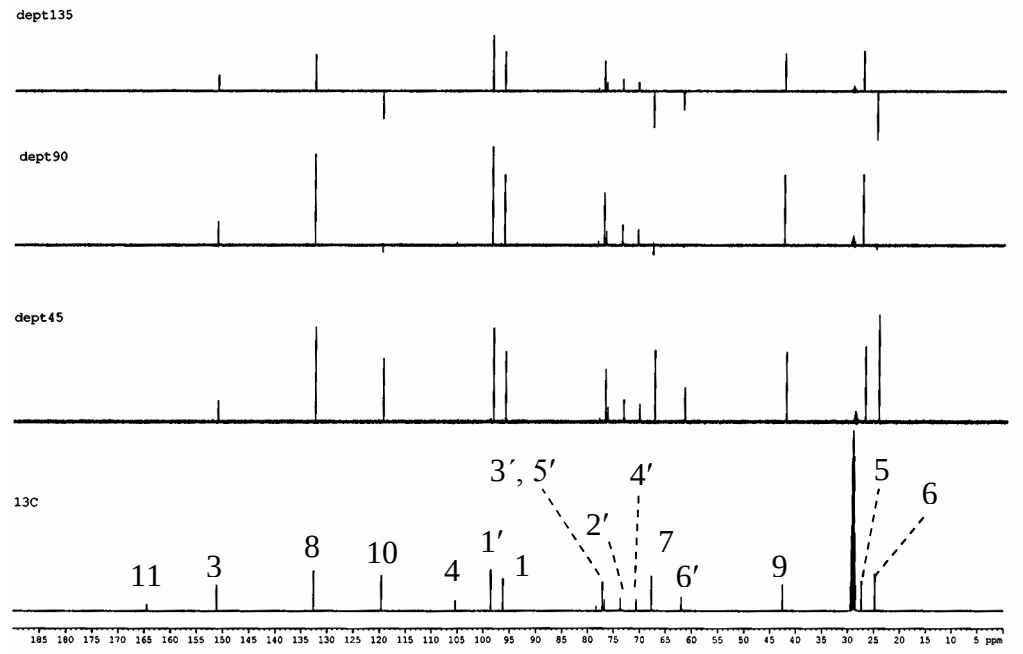

Figure 12.5 ^{13}C-NMR and DEPT spectra of compound **XII** in acetone-d_6

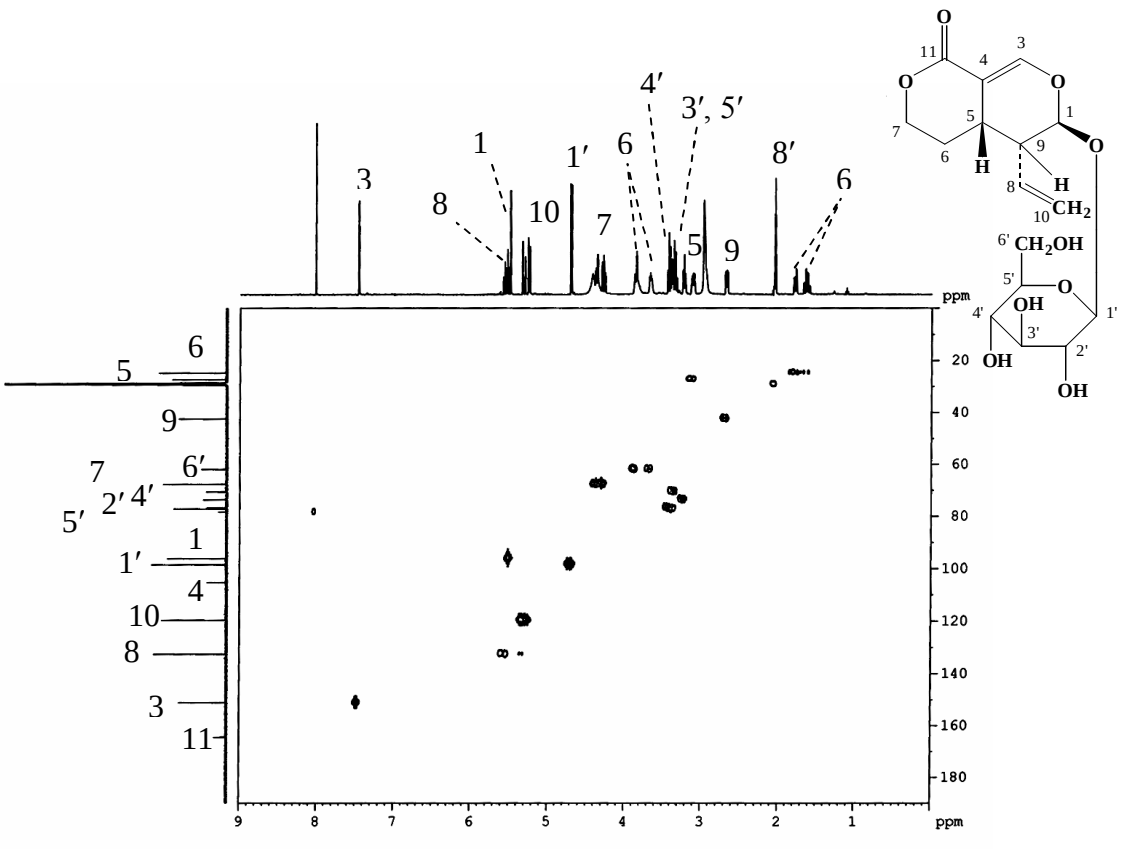

Figure 12.6 HMQC spectrum of compound **XII**

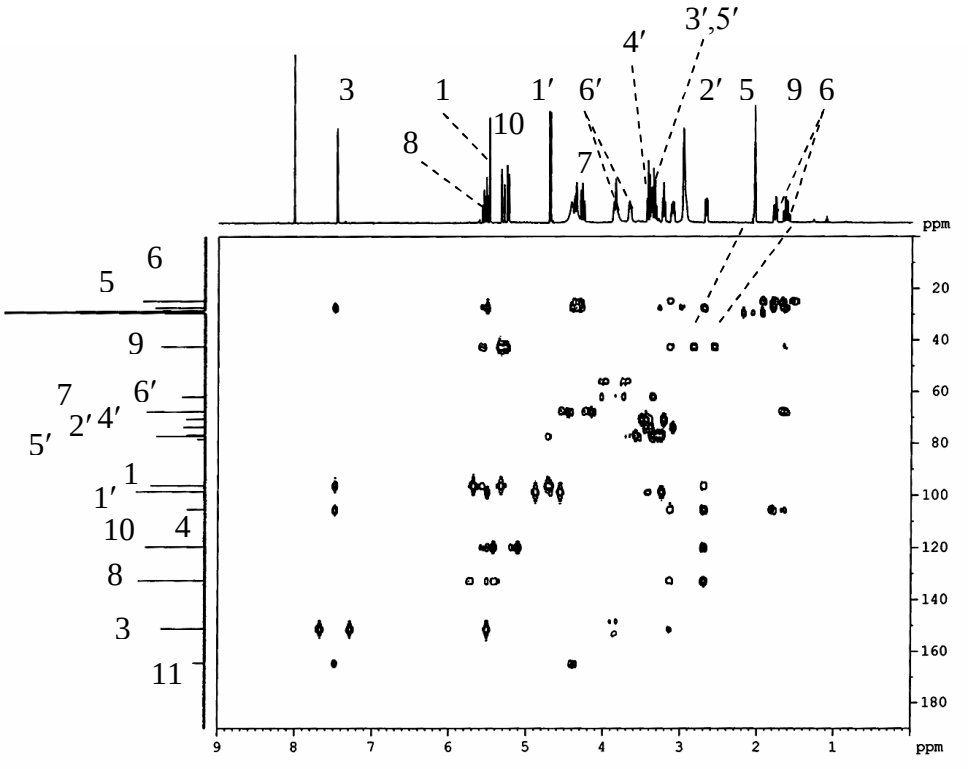

Figure 12.7 HMBC spectrum of compound **XII**

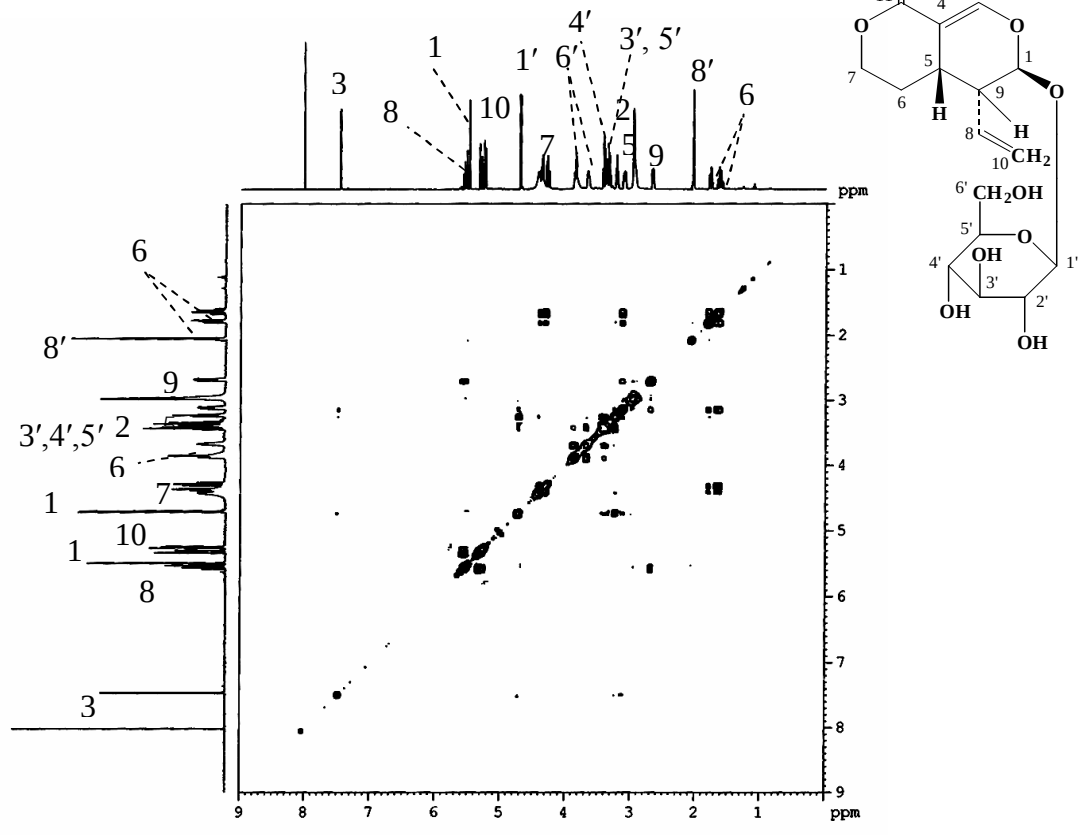

Figure 12.8 ^{1}H,^{1}H-COSY spectrum of compound **XII**

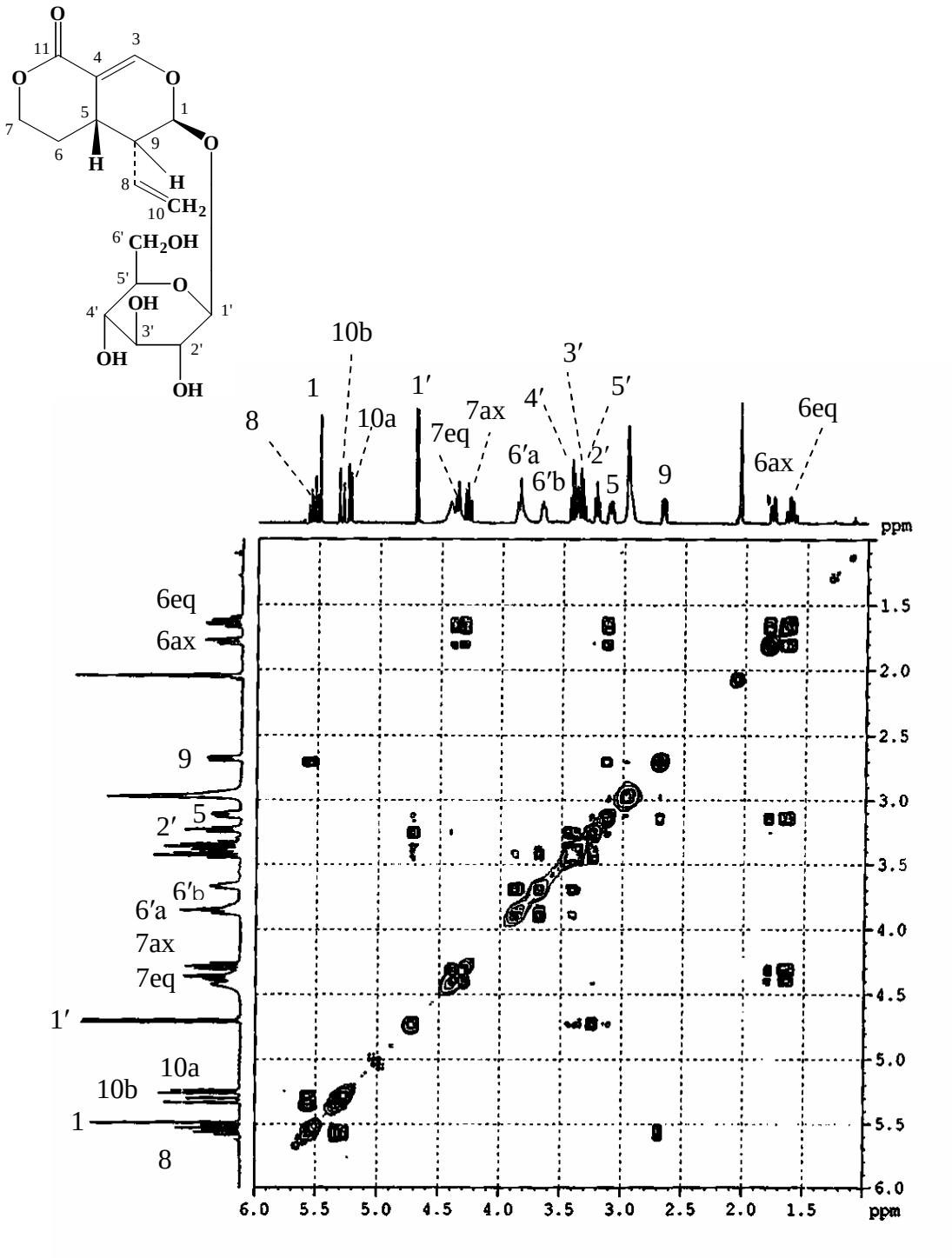

Figure 12.8a Expansion of Fig.12.8

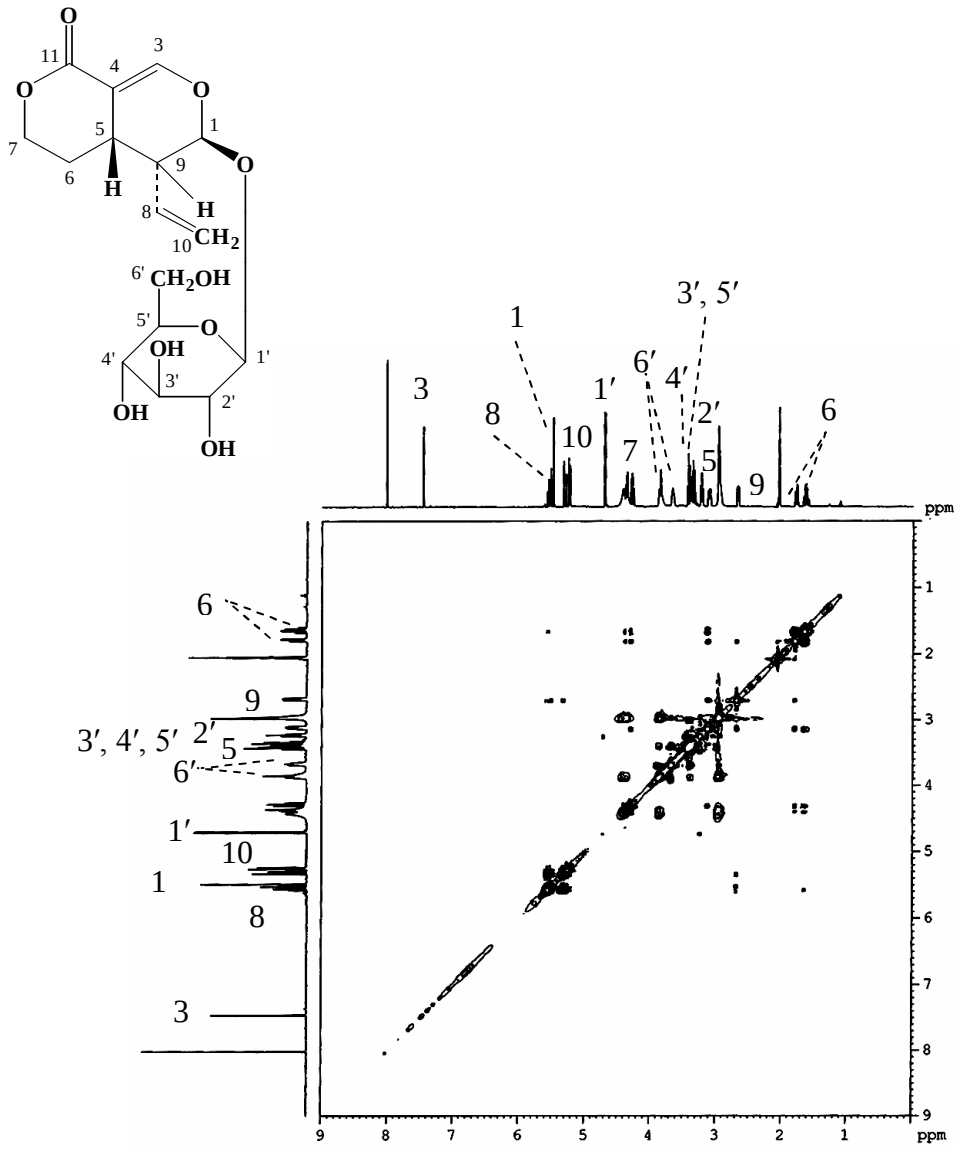

Figure 12.9 NOESY spectrum of compound **XII**

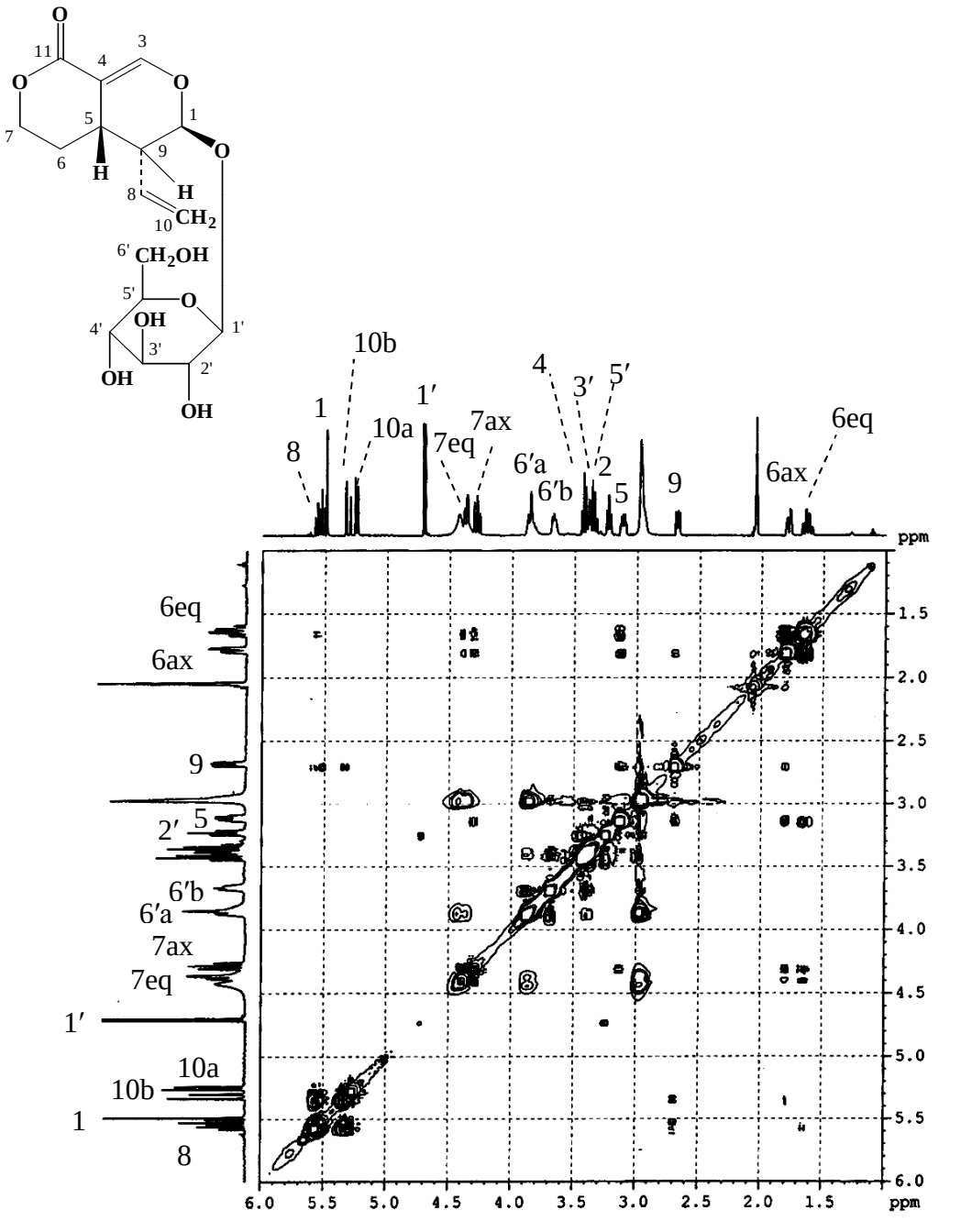

Figure 12.9a Expansion of Fig.12.9

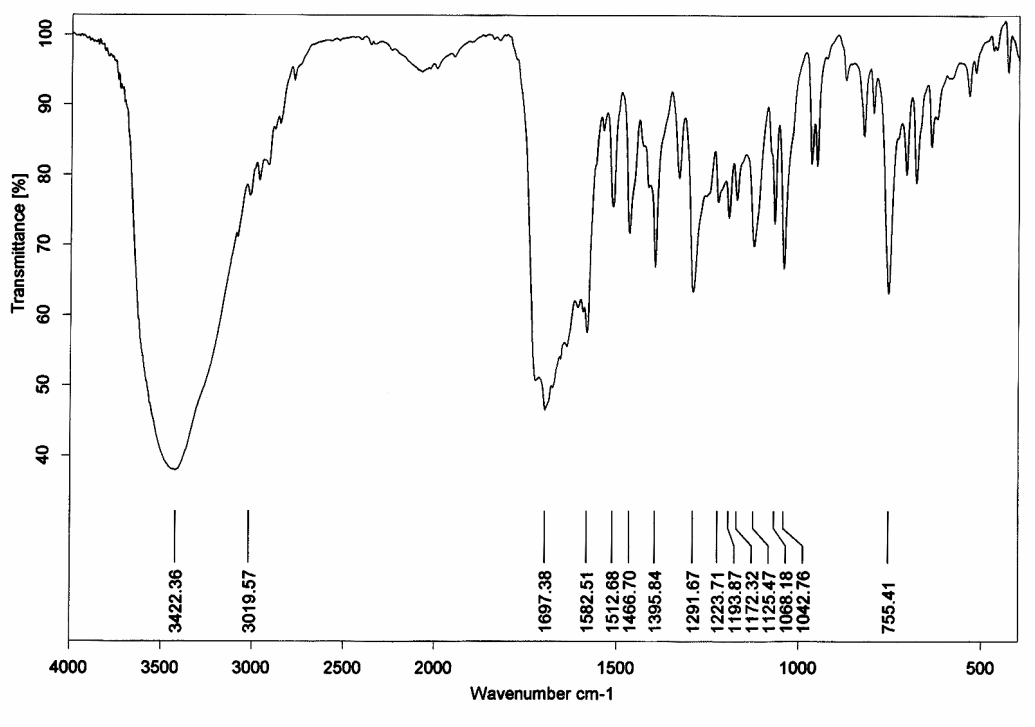

Figure 13.1 IR spectrum of compound **XIII**

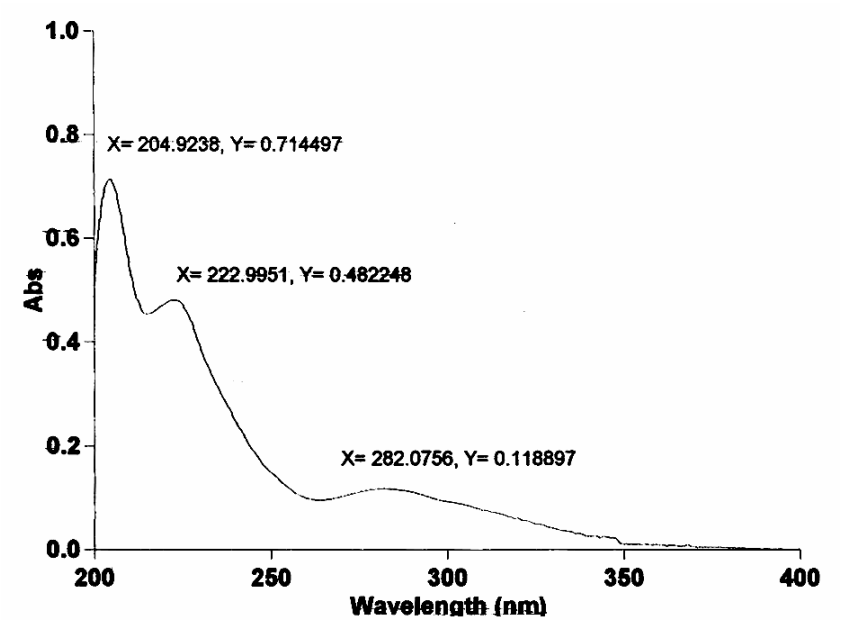

Figure 13.2 UV-Vis spectrum of compound **XIII**

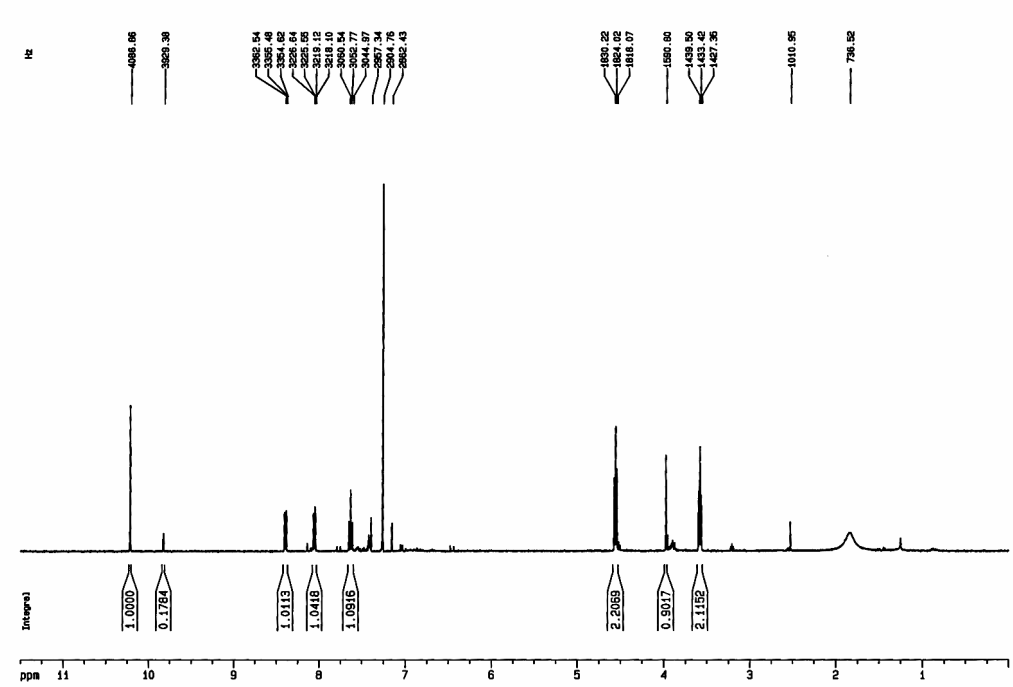

Figure 13.3 500 MHz ^{1}H-NMR spectrum of compound **XIII** in $CDCl_3$

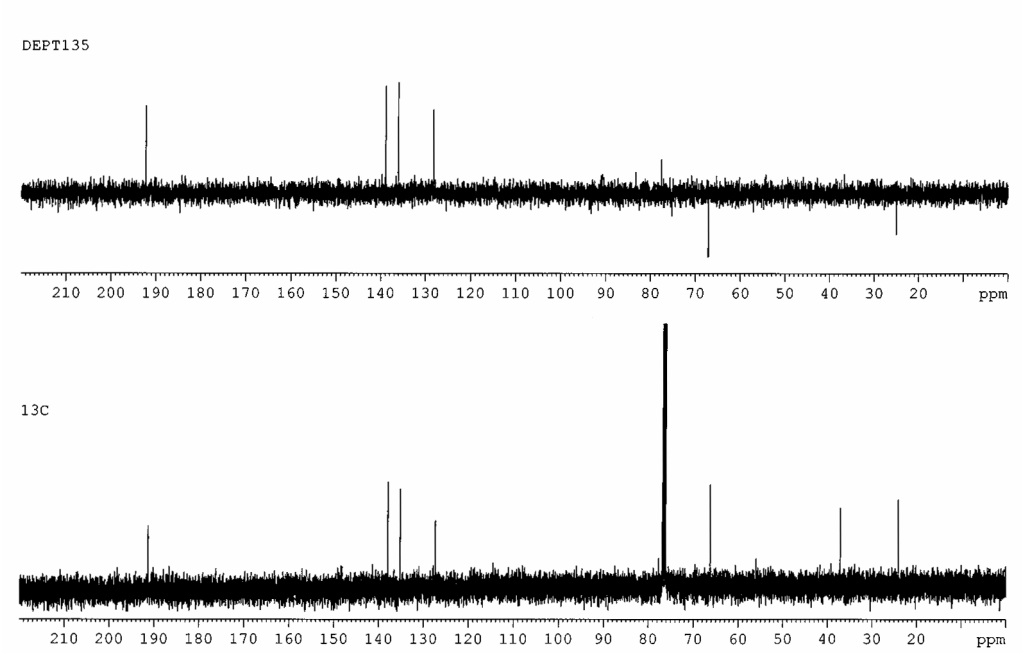

Figure 13.4 ^{13}C-NMR and DEPT spectra of compound **XIII** in $CDCl_3$

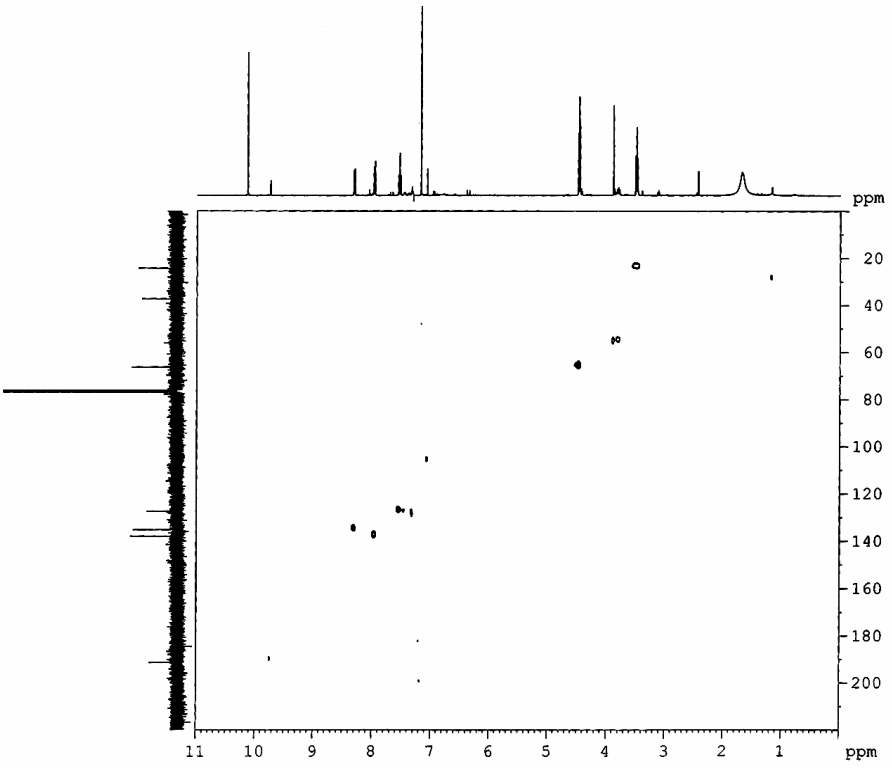

Figure 13.5 HMQC spectrum of compound **XIII**

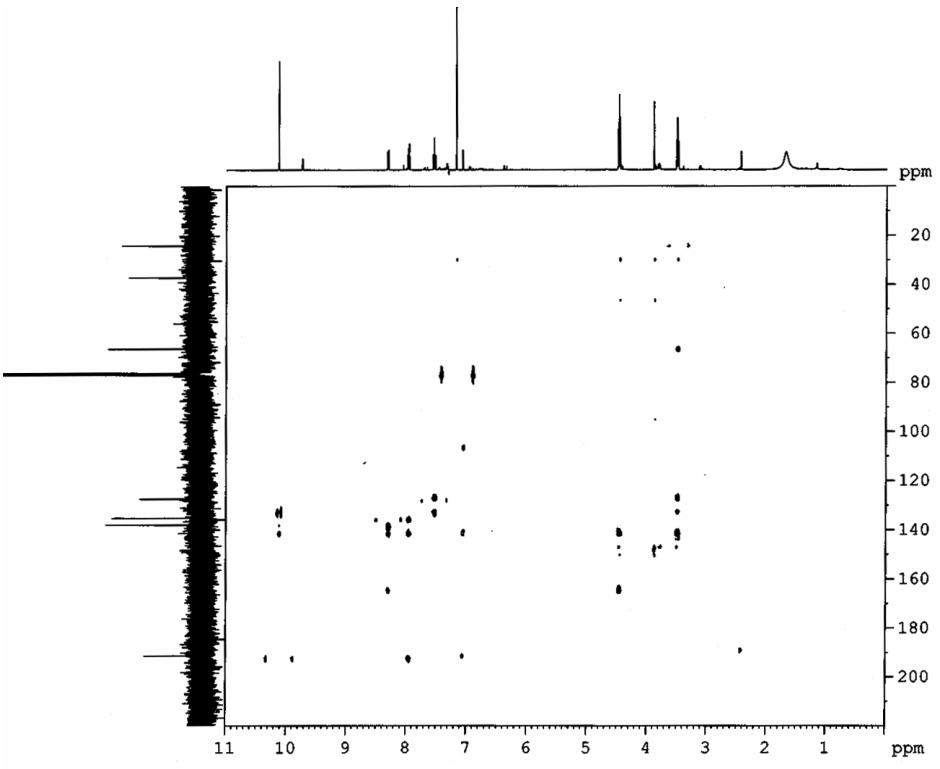

Figure 13.6 HMBC spectrum of compound **XIII**

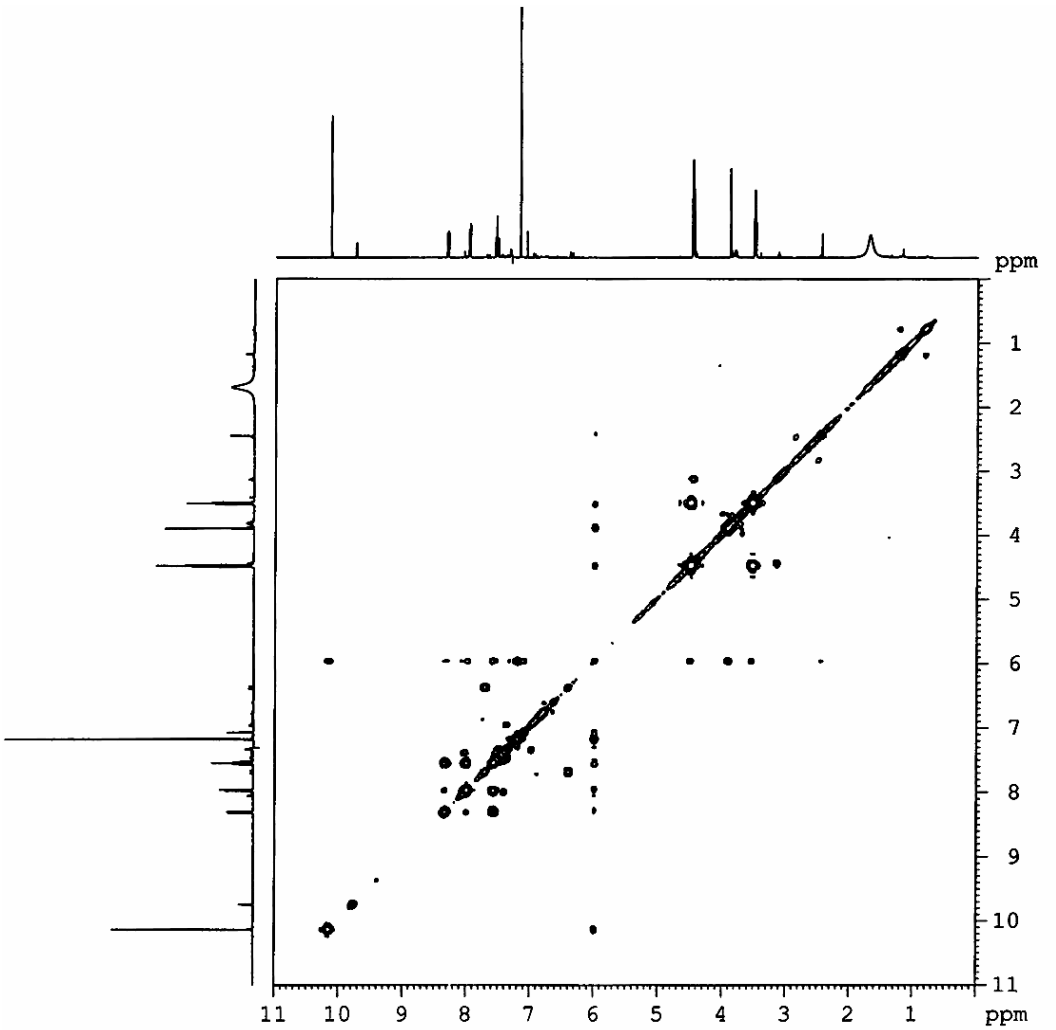

Figure 13.7 ^{1}H,^{1}H-COSY spectrum of compound **XIII**

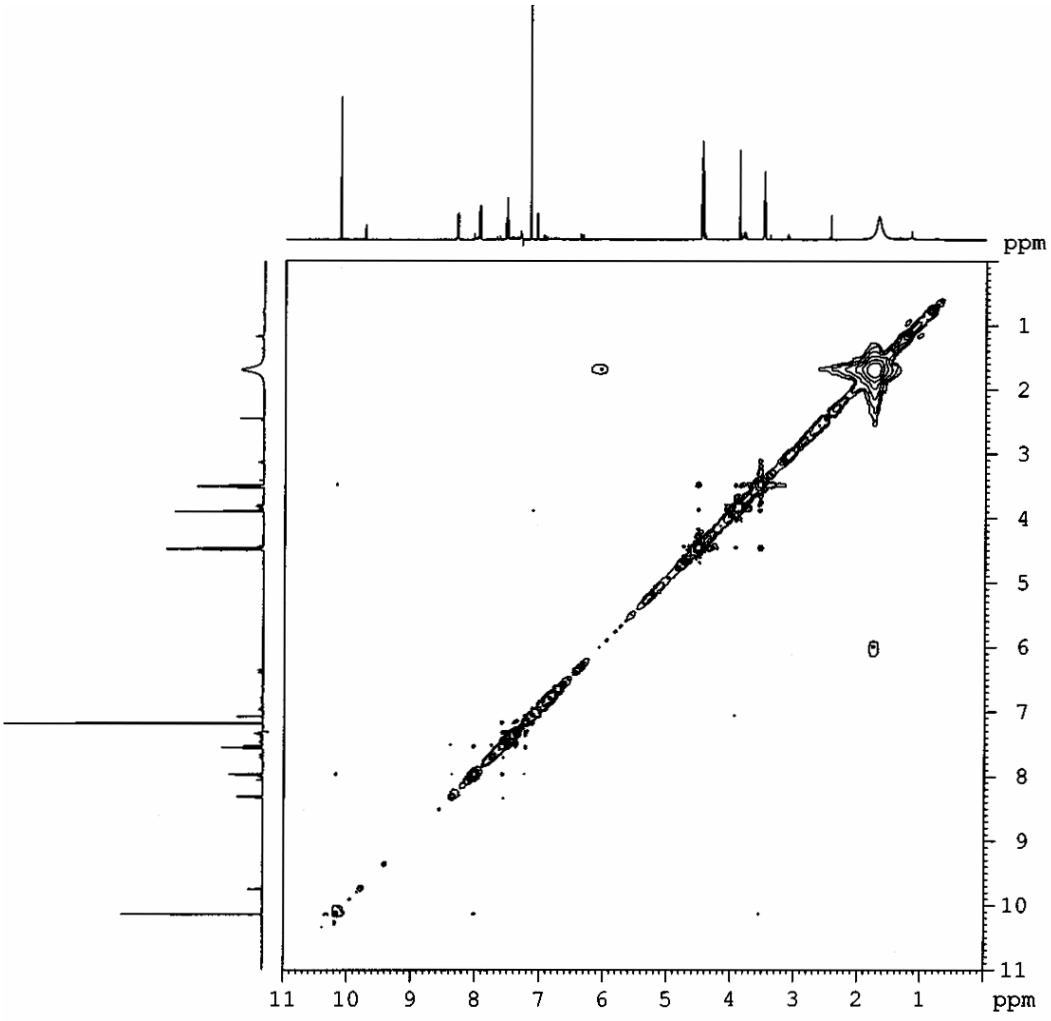

Figure 13.8 NOESY spectrum of compound **XIII**

CURRICULUM VITAE

NAME Miss Samneang Apisantiyakom

PLACE OF BIRTH Bangkok, Thailand

INSTITUTIONS ATTENDED Ramkumhang University, 1980-1985

Bachelor of Science (Chemistry)

Chulalongkorn University, 1990-1992

Master's degree (Organic Chemistry)

Suranaree University of Technology

2000-2004

Doctor of Philosophy (Organic Chemistry)

PRESENT Rajabhat Valayalongkorn University.

Phahonyothin Rd, Patumthani province.

13180 Thailand.

a_samneang@yahoo.com